

# **Cancer Immunotherapy Requires Interferon- dependent Senescence Induction**

**Dissertation**

der Mathematisch-Naturwissenschaftlichen Fakultät  
der Eberhard Karls Universität Tübingen  
zur Erlangung des Grades eines  
Doktors der Naturwissenschaften  
(Dr. rer. nat.)

vorgelegt von  
Dipl. Biol. Ellen Brenner  
aus Stuttgart

Tübingen  
2021

Gedruckt mit Genehmigung der Mathematisch-Naturwissenschaftlichen Fakultät der  
Eberhard Karls Universität Tübingen.

Tag der mündlichen Qualifikation:	17.11.2021
Dekan:	Prof. Dr. Thilo Stehle
1. Berichterstatter:	Prof. Dr. Martin Röcken
2. Berichterstatter:	Prof. Dr. Hans-Georg Rammensee
3. Berichterstatter:	Prof. Dr. Karsten Mahnke

# Versicherung an Eides Statt

Hiermit erkläre ich an Eides statt, dass ich die vorliegende wissenschaftliche Arbeit „Tumor-Immuntherapie benötigt Interferon-abhängige Seneszenz Induktion“ eigenständig, ohne unerlaubte Hilfe und nur unter Verwendung der angegebenen Hilfsmittel angefertigt habe. Alle sinngemäß und wörtlich übernommenen Textstellen aus Veröffentlichungen oder aus anderweitigen fremden Äußerungen habe ich als solche kenntlich gemacht.

Tübingen, den 17.11.2021

Ellen Brenner

# Danksagung

Prof. Dr. Martin Röcken danke ich für das unermüdliche Interesse und die Korrektur meiner Arbeit und seine brennende Leidenschaft für die Forschung. Ich danke für meine wissenschaftliche Ausbildung, die Möglichkeit selbst Mitarbeiter zu betreuen und die Laborpraxis frei zu gestalten. Ich danke für Ausflüge, die gemeinsamen Feiern und Erfolgsmomente.

Prof. Dr. Hans-Georg Rammensee danke ich für die Begutachtung meiner Doktorarbeit. Ich bin dankbar für die Zeit im Graduiertenkolleg des SFBs 685, die damit verbundenen Treffen waren ein stimmiger, motivierender, zielorientierter Start in meine Doktorarbeit.

Prof. Dr. Thomas Wieder danke ich für die Durchsicht meiner Doktorarbeit und die erfolgreiche Zusammenarbeit an Manuskripten, Reviews und Anträgen. Danke für die Unterstützung auf meinem Weg zur Doktorarbeit.

Dr. Heidi Braumüller danke ich für die Betreuung zu Beginn dieser Doktorarbeit und den familiären Umgang im Labor und im Team.

Barbara Schörg, Dr. Manfred Kneilling und Prof. Dr. Bernd Pichler danke ich für die Zusammenarbeit am Manuskript für Nature Communications. Ebenso danke ich Prof. Dr. Ralph Mocikat, Dr. Fathima Ahmetlic, Nadine Homberg, die unsere Arbeit mit einem weiteren Modell bereichert haben. Birgit Fehrenbacher mit Team danke ich für die exzellente und freundliche Zusammenarbeit bei der großen Aufgabe der histologischen Aufarbeitung unserer Versuche. Dr. Heike Niessner und Dr. Tobias Sinnberg danke ich für die Zusammenarbeit an Patientenmaterial und und Dr. Franz Joachim Hilke bin ich dankbar für Zusammenarbeit bei der genetische Analyse der Proben.

Ich danke für die finanzieller Förderung meiner Arbeit und der Förderung meines Arbeitsumfeldes durch die Deutschen Krebshilfe (109037, 110662, 110664), die Wilhelm Sander-Stiftung (2012.056.3) und die Deutsche Forschungsgemeinschaft (SFB 685, SFB TRR 156/2).

Susanne Weidemann danke ich für ihr gewissenhaftes Arbeiten, ihre Hilfsbereitschaft und Organisation, Tatkräftigkeit und Einfallsreichtum. Ich konnte mich immer auf sie verlassen und bin dankbar für unser Team. Die Freude mit ihr zu arbeiten ist ein

emotionaler Grund an der Universität Tübingen zu bleiben. Besonderer Dank an meine weiteren Kolleginnen Katharina Böhm, Nadine Simon, Britta Bauer und Viola Galinat. Sie haben meine Doktorarbeit zu einem glücklichen Lebensabschnitt gemacht. Das freundschaftliche Arbeitsklima, die gegenseitige Unterstützung, die vielen hilfreichen, fachlichen Gespräche sind wesentliche Zutaten für den Erfolg dieser Arbeit.

Ich danke Kirsten Deinert, Dr. Jürgen Brück, Julia Holstein, Prof. Dr. Birgit Schitteck, Dr. Corinna Kosnopfel, Dr. Daniela Beck, Dr. Susanne Kaesler und Ulrike Schmidt für die freundschaftliche Unterstützung bei der Arbeit und die schöne gemeinsame Freizeit.

Dr. Heike Niessner, Lorenzo Hohmann, Katharina Böhm und Andrea Voit danke ich für das Gegenlesen dieser Arbeit.

Dr. Yuliya Skabytska hat mich mit ihrem Arbeitseifer und ihrer Effektivität inspiriert und sich Respekt erarbeitet. Aus diesem Respekt ist eine tiefe Freundschaft entstanden für die ich sehr dankbar bin.

Ich danke Andrea Voit, Gabriele Larsen und Madlene Egetemeir dafür, dass sie auf mich achtgeben.

Martial Herbst danke ich, dass er mich mit Zuversicht und Gelassenheit umsorgt, dass er mir Trost und Wärme spendet und mich bestens auf meinem Weg unterstützt.

Lothar Brenner danke ich dafür, dass er mir die Sicherheit gegeben hat zu studieren und in die universitäre Forschung einzusteigen. Mein Vater gab mir das Motto mit auf den Weg, dass Veränderung durch Erkenntnis entsteht.

Brigitte Brenner danke ich für ihre immerwährende Hilfsbereitschaft und Unterstützung meiner Ziele. Meine Mutter war meine Modeberatung auf jedem Kongress wofür ich dankbar bin.

Heike Niessner ist die beste Wegbegleiterin die ich mir wünschen kann. Mit ihr habe ich mein Studium angefangen und mit dem Dank für ihre allumfassende Freundschaft möchte ich diese kumulative Dissertation beginnen.

*„Man soll auf alles achten, denn man kann alles deuten.“*

DAS GLASPERLENSPIEL  
HERMANN HESSE

# Zusammenfassung

Zentrale Ziele dieser Dissertation waren die Entwicklung einer innovativen Immuntherapie zur Behandlung von Krebspatienten, die Gewinnung von Erkenntnissen über die verantwortlichen Mechanismen der Immunreaktionen, sowie die Bestimmung der entscheidenden Faktoren für deren Wirksamkeit.

Diese Forschungsarbeit zum Thema „Tumor-Immuntherapie benötigt Interferon-abhängige Seneszenz Induktion“ begann vor dem Durchbruch der Immuntherapie mit monoklonalen Antikörpern zur Immuncheckpoint Blockade (ICB). Der Ansatz bestand darin, mit tumorantigenspezifischen CD4<sup>+</sup> Typ1-T-Helferzellen (T<sub>H</sub>1) eine aktive, antitumorale Immunantwort im Tumormicroenvironment hervorzurufen. Das Ziel war die T<sub>H</sub>1-basierte Immuntherapie als adoptiven Transfer zur Behandlung von immunkomprimierte Patienten in die Klinik zu bringen. Dieser Ansatz wurde in einem murinen Modell eines nicht immunogenen Tumors, dem RIP-Tag2 (RT2)-Modell, etabliert. RT2-Mäuse entwickeln in der zehnten Lebenswoche Inselzellkarzinome und sterben etwa in Woche 14 an einer Hypoglykämie. Während etablierte Behandlungsmethoden mit Chemotherapie oder Angiogeneseinhibitoren das Leben der Mäuse kaum verlängerten, bewirkte eine präventive Immuntherapie mit Transfer von Tag2-spezifischer T<sub>H</sub>1-Zellen zwei Erfolge: Erstens verlängerte sich die Lebenserwartung, die Hälfte aller Mäuse lebten für über 30 Wochen. Zweitens kontrollierten die T<sub>H</sub>1-Zellen die Tumore, ohne eine Zerstörung der Inselzellen zu induzieren und ohne Diabetes zu verursachen. Die resultierende Fragestellung war, wie T<sub>H</sub>1-Zellen die Verbesserung der Lebenserwartung von RT2-Mäusen ohne zellvermittelte Zytotoxizität durch professionelle Killerzellen und ohne jegliches Anzeichen einer Zerstörung des Tumors bewirken können. Die daraus entstandene Publikation „T-helper-1-cell cytokines drive cancer into senescence“ zeigte, dass die löslichen Faktoren Interferon- $\gamma$  (IFN- $\gamma$ ) und Tumor-Nekrose-Faktor (TNF) von T<sub>H</sub>1-Zellen durch Aktivierung des Zellzyklus-Kontrollpunktes p16<sup>Ink4a</sup> das Tumorstadium blockierte. Dies wurde als Zytokin-induzierte Seneszenz (CIS) definiert **(1)**. Diese Erkenntnis aus der Krebstherapie mit T<sub>H</sub>1 Zellen wurde anschließend in der Arbeit „Changing T-cell enigma“ diskutiert, da bisher die Funktion von T-Zellen in der Zerstörung von Tumorzellen gesehen wurde und fast alle neuen Therapieansätze darauf abzielten diese Zytotoxizität zu optimieren **(2)**. Diese

Studie führte zu der Hypothese, dass CIS als ein allgemeiner Mechanismus der Wachstumskontrolle von Krebserkrankungen angesehen werden kann. Wir diskutierten dies bei der Behandlung des Melanoms in der Publikation „Immunotherapy of melanoma: efficacy and mode of action“ **(3)**, und „Cytokine-induced senescence for cancer surveillance“ **(4)**. Diesen Zellzyklus-Kontroll-Mechanismus bestätigten wir in der humanen Mammakarzinom Zelllinie MCF-7 und der humanen Rhabdomyosarkom Zelllinie A-204 unter Einbeziehung des Gen-regulierenden Argonautenprotein 2 (Ago2) „Nuclear translocation of argonaute 2 in cytokine-induced senescence“ **(5)**. Nach Erscheinen von klinischen Studien mit immun-modulierenden Antikörpern zur Reaktivierung der endogenen Immunität, diskutierten wir unsere Befunde der Seneszenz in Tumorzellen im Kontext der ICB Therapie im Review „Immune checkpoint blockade therapy“ **(6)**. Therapieresistenz ist das Hauptproblem der Immuntherapien mittels ICB, weshalb wir die Bedeutung der Seneszenzinduktion nach ICB Behandlung über Interferon-Signalwege untersuchten, um die damit verbundenen Resistenzmechanismen zu verstehen. Die Studie „Cancer immune control needs senescence induction by interferon-dependent cell cycle regulator pathways in tumours“ **(7)** zeigte die zentrale Rolle des IFN- $\gamma$ -Signalweges in den Tumoren für die Wachstumskontrolle mittels Seneszenz. Die Bedeutung von Mutationen im IFN- $\gamma$ -Signalweg und den Zellzyklus-Kontrollpunkten bei der Resistenz gegenüber Immuntherapie war ein Schwerpunkt der Arbeit.

Zusammenfassend zeigen diese Daten, dass Interferon-dominierte Immunantworten in Tumorzellen über den Mechanismus der Seneszenz das Wachstum von Tumorzellen langfristig verhindert.



# Summary

The key objectives of this thesis were to develop an immunotherapy to treat patients suffering from cancer, to gain knowledge about the mechanisms underlying the anti-cancer immune responses, and to establish factors critical for an effective therapeutic response.

The topic “Cancer Immunotherapy Requires Interferon-dependent Senescence Induction” started before the breakthrough in immunotherapy with immune checkpoint blockade (ICB). At that time, our approach was to induce an active immunoreaction against tumors with tumor antigen-specific CD4<sup>+</sup> T helper 1 (T<sub>H</sub>1) cells. The ultimate goal was to bring T<sub>H</sub>1 adoptive transfer immunotherapy into the clinics as a treatment strategy for immunocompromised patients. This approach was established in a murine model of a non-immunogenic tumor, the RIP-Tag2 (RT2) model. RT2 mice develop islets cancers at week ten of life and die at around week 14 from hypoglycemia. While established treatment methods with chemotherapy or angiogenesis inhibition hardly prolonged the life of these mice, early immunotherapy with transferring Tag2-specific T<sub>H</sub>1 cells provided two key observations: First, extended life expectancy, half of all mice lived for more than 30 weeks. Second, T<sub>H</sub>1 cells controlled the tumors without inducing islets cell destruction and without causing diabetes. We focused on the question how T<sub>H</sub>1 cells can cause such an improvement of the life expectancy of RT2-mice without cell-mediated cytotoxicity by professional killer cells and without detectible signs of tumor destruction. The resulting publication “T-helper-1-cell cytokines drive cancer into senescence” reveals that the soluble factors interferon- $\gamma$  (IFN- $\gamma$ ) and tumor necrosis factor (TNF) secreted by T<sub>H</sub>1 cells controlled tumor cell growth in RT2-cancers and a variety of other murine and human cancers by activation of the cell cycle checkpoint p16<sup>Ink4a</sup> **(1)**. We propose a new strategy of cancer therapy in “Changing T-cell enigma” by postulating that tumor cell senescence induced by CD4<sup>+</sup> T cells is a key function in controlling tumor growth in addition to the function of T cells in killing tumor cells **(2)**. Our study leads to the hypothesis that cytokine-induced senescence (CIS) can be seen as a general mechanism involved in the growth control of cancers. We subsequently discuss this for the treatment of melanomas with ICB in “Immunotherapy of melanoma: efficacy and mode of action” **(3)**. Moreover, CIS seems to be of crucial importance for a long-lasting tumor control as outlined in

“Cytokine-induced senescence for cancer surveillance” **(4)**. We confirmed this mechanism of CIS in human breast cancer cell line MCF-7 and human rhabdomyosarcoma cell line A-204, which involves the gene regulating argonaute proteins (Ago) in our study “Nuclear translocation of argonaute 2 in cytokine-induced senescence” **(5)**. When clinical studies with immunomodulating antibodies showed that reactivation of endogenous immunity can induce a regression and stable growth arrest in metastases, we discuss that CIS could play an important role also in ICB therapy of human cancers in the review “Immune checkpoint blockade therapy” **(6)**. Therapy resistance is the main issue of immunotherapies using ICB. Thus, we investigate the importance of CIS during ICB in animal models and in ICB-treated patients. The data uncovers important associated resistance mechanisms, which we analyze in the study “Cancer immune control needs senescence induction, by interferon-dependent cell cycle regulator pathways in tumours” **(7)**.

Collectively, these results demonstrate that in mice and in humans, interferon-mediated signals in cancer cells prevent tumor growth by inducing a long-lasting growth arrest, called senescence.

# Contents

<b>Versicherung an Eides Statt</b> .....	<b>3</b>
<b>Danksagung</b> .....	<b>4</b>
<b>Zusammenfassung</b> .....	<b>7</b>
<b>Summary</b> .....	<b>9</b>
<b>Contents</b> .....	<b>11</b>
<b>Publications</b> .....	<b>13</b>
<b>Personal Contributions</b> .....	<b>14</b>
<b>Abbreviations</b> .....	<b>15</b>
<b>1. Introduction</b> .....	<b>19</b>
1.1 Cancer Growth and Cancer Evasion Mechanisms.....	19
1.1.1 Cancer Development and Progression .....	19
1.1.2 Immunoediting .....	20
1.2 Cancer Immunotherapies.....	21
1.2.1 Immune Checkpoint Blockade Therapy.....	21
1.2.2 Adoptive T cell Transfer.....	23
1.2.3 Cytokine Therapy.....	24
1.2.4 IFN- $\gamma$ Therapy.....	25
1.2.5 TNF Therapy.....	26
1.2.6 Combined Effects of IFN- $\gamma$ and TNF .....	27
1.2.7 Mode of Action.....	27
1.3 Cellular Senescence.....	29
1.3.1 Modes of Senescence Induction.....	29
1.3.2 Senescence Marker .....	30
1.3.3 Senescence in ICB Therapies .....	31
1.4 Project Outline.....	32

<b>2. Results and Discussion .....</b>	<b>33</b>
2.1 Immunotherapy with AT and AT/ICB Controls Cancer Cells .....	34
2.1.1 RT2 Mice with AT of T <sub>H</sub> 1 Cells is Dependent on the T <sub>H</sub> 1 Cell Cytokines .....	35
2.1.2 <i>Stat1</i> -dependent Control of Advanced Malignant Insulinomas with AT/ICB Therapy .....	35
2.2 Immunotherapy with AT and AT/ICB Induce Senescence in Cancer Cells .....	37
2.2.1 Characterization of Cancer Control after Immunotherapy <i>in vitro</i> .....	37
2.2.2 Characterization of Cancer Control Mechanisms <i>in vivo</i> .....	38
2.3 T <sub>H</sub> 1 Cell Cytokine Induced Senescence in Cancer Cells .....	40
2.3.1 <i>Stat1</i> /IFN- $\gamma$ -dependent Senescence Induction in Cancer Cells.....	40
2.3.2 <i>Tnfr1</i> /TNF-dependent Senescence Induction in Cancer Cells .....	40
2.3.3 Senescence Induction in Cytokine-dependent Cancer Immunotherapy .....	41
2.3.4 <i>Cdkn2a</i> -dependent Senescence Induction in Cancer Cells.....	41
2.4 Tumor Intrinsic Conditions for Efficient Immunotherapy.....	42
2.4.1 Efficient Responses in Mice with Ectopic Insulinomas using ICB Therapy .....	42
2.5 CIS is Required for Efficient ICB Therapy of $\lambda$ -MYC Lymphomas .....	43
2.5.1 IFN- $\gamma$ -dependent Senescence Induction in $\lambda$ -MYC Lymphomas .....	43
2.5.2 p21 <sup>Cip1</sup> -dependent Senescence Induction in $\lambda$ -MYC Lymphomas.....	44
2.6 CIS is Required for Efficient ICB Therapy of Human Melanoma Metastases.....	45
<b>Figures.....</b>	<b>48</b>
<b>Figures Appendix .....</b>	<b>49</b>
<b>Tables.....</b>	<b>54</b>
<b>Tables Appendix .....</b>	<b>55</b>
<b>References.....</b>	<b>56</b>
<b>Appendix.....</b>	<b>68</b>
1. Publications .....	68

# Publications

- (1) T-helper-1-cell cytokines drive cancer into senescence (2013). H. Braumüller, T. Wieder, E. Brenner, S. Assmann, M. Hahn, M. Alkhaled, K. Schilbach, F. Essmann, M. Kneilling, C. Griessinger, F. Ranta, S. Ullrich, R. Mocikat, K. Braungart, T. Mehra, B. Fehrenbacher, J. Berdel, H. Niessner, F. Meier, M. Van Den Broek, H. U. Häring, R. Handgretinger, L. Quintanilla-Martinez, F. Fend, M. Pesic, J. Bauer, L. Zender, M. Schaller, K. Schulze-Osthoff, M. Röcken. **Nature** 494(7437): 361-365.
- (2) Changing T-cell enigma (2013). T. Wieder, H. Braumüller, E. Brenner, L. Zender, M. Röcken. **Cell Cycle** 12(19): 3146-3153.
- (3) Immuntherapie des Melanoms: Wirksamkeit und Wirkungsmechanismen (2016). Immunotherapy of melanoma: efficacy and mode of action (2016). T. Wieder, E. Brenner, H. Braumüller, M. Röcken. *Journal der Deutschen Dermatologischen Gesellschaft* 14(1): 28-36/7.
- (4) Cytokine-induced senescence for cancer surveillance (2017). T. Wieder, E. Brenner, H. Braumüller, O. Bischof, M. Röcken. **Cancer and Metastasis Reviews** 36(2): 357-365
- (5) Nuclear translocation of argonaute 2 in cytokine-induced senescence (2018). M. Rentschler, Y. Chen, J. Pahl, L. Soria-Martinez, H. Braumüller, E. Brenner, O. Bischof, M. Röcken, T. Wieder. **Cellular Physiology and Biochemistry** 51(3): 1103-1118.
- (6) Immune checkpoint blockade therapy (2018). T. Wieder, T. Eigentler, E. Brenner, M. Röcken. **Journal of Allergy and Clinical Immunology** 142(5): 1403-1414.
- (7) Cancer immune control needs senescence induction by interferon-dependent cell cycle regulator pathways in tumours (2020). E. Brenner, B. F. Schorg, F. Ahmetlic, T. Wieder, F. J. Hilke, N. Simon, C. Schroeder, G. Demidov, T. Riedel, B. Fehrenbacher, M. Schaller, A. Forschner, T. Eigentler, H. Niessner, T. Sinnberg, K. S. Bohm, N. Homberg, H. Braumüller, D. Dauch, S. Zwirner, L. Zender, D. Sonanini, A. Geishauser, J. Bauer, M. Eichner, K. J. Jarick, A. Beilhack, S. Biskup, D. Docker, D. Schadendorf, L. Quintanilla-Martinez, B. J. Pichler, M. Kneilling, R. Mocikat, M. Röcken. **Nature communications** 11(1): 1335

# Personal Contributions

**(1)** For the study “T-helper-1-cell cytokines drive cancer into senescence” most of the work was done by H. Braumüller. E. Brenner supported the experiments of Figure 1a, b. H. Braumüller, and E. Brenner conducted the experiments Suppl. Fig. 1b and Figure 4a, b together. E. Brenner planned and analyzed the experiments of Suppl. Fig. 15, designed the experiments for Suppl. Table 1, Suppl. Table 2, and assisted in their implementation. M. Röcken directed the project.

**(2)** For the review “Changing T-cell enigma” most of the work was done by T. Wieder. E. Brenner was involved in the literature research and structuring of the manuscript. M. Röcken directed the project.

**(3)** For the review “Immunotherapy of melanoma: efficacy and mode of action” most of the work was done by T. Wieder. E. Brenner was involved in the literature research, structuring of the manuscript and created the illustrations for the review. M. Röcken directed the project.

**(4)** For the review “Cytokine-induced senescence for cancer surveillance” most of the work was done by T. Wieder. E. Brenner was involved in the literature research and structuring of the manuscript. M. Röcken directed the project.

**(5)** For the study “Nuclear translocation of argonaute 2 in cytokine-induced senescence”. E. Brenner supervised the experiments Figure 1e and Figure 2c, g. T. Wieder directed the project.

**(6)** For the review “Immune checkpoint blockade therapy”. E. Brenner was involved in the writing of the manuscript and created the illustrations Fig. 1, Fig. 2 and Fig. 3a of the review. M. Röcken directed the project.

**(7)** For the study “Cancer immune control needs senescence induction by interferon-dependent cell cycle regulator pathways in tumours”. E. Brenner developed the concept together with M. Röcken and T. Wieder. E. Brenner performed and analyzed the experiments of Figure 1, Figure 2, Figure 3, Figure 5b, Figure 7, Figure 10d-e, Suppl. Fig. 4, Suppl. Fig. 5b-c, Suppl. Fig. 11c-e, Suppl. Fig. 14, of which all immunofluorescence data were generated in collaboration with B. Fehrenbacher. M. Röcken directed the project.

# Abbreviations

A-204	<i>human rhabdomyosarcoma</i>
ADCC	<i>antibody-dependent cellular cytotoxicity</i>
Ago	<i>argonaute protein 2</i>
APCs	<i>antigen presenting cells</i>
AT	<i>adoptive T-cell transfer</i>
<i>CCND1/2/3</i>	<i>cyclin D1/2/3</i>
<i>CCNE1</i>	<i>cyclin E1</i>
CDK	<i>cyclin-dependent kinase</i>
CDK4/6	<i>cyclin dependent kinases CDK4/6</i>
CDKi	<i>cyclin dependent kinase inhibitor</i>
CIS	<i>cytokine-induced senescence</i>
CNVs	<i>copy number variations</i>
COLO-205	<i>human colon cancer</i>
CTLA-4	<i>cytotoxic T-lymphocyte-associated protein 4</i>
CTLs	<i>cytolytic CD8<sup>+</sup> T cells</i>
DD	<i>death domain</i>
DDR	<i>DNA damage response</i>
DISC	<i>death-inducing signaling complex</i>
DNA-PK	<i>DNA-dependent protein kinase</i>
DSB	<i>DNA double-strand breaks</i>
FADD	<i>FAS-associated death domain protein</i>
FDA	<i>Food and Drug Administration</i>
GAS	<i>interferon gamma-activated sequence</i>
h	<i>hours</i>
HLA	<i>human leukocyte antigen</i>
HOP-62	<i>human lung cancer</i>
ICB	<i>immune checkpoint blockade</i>
IFNGR1	<i>interferon gamma receptor 1</i>
IFNGR2	<i>interferon gamma receptor 2</i>

IFN- $\alpha$	<i>interferon alpha</i>
IFN- $\gamma$	<i>interferon gamma</i>
IL	<i>interleukin</i>
<i>IL2rg</i> <sup>-/-</sup>	<i>interleukin 2 receptor common gamma chain knockout</i>
INDELS	<i>small insertions and deletions</i>
IRF9	<i>interferon regulatory factor 9</i>
ISRE	<i>interferon-stimulated response element</i>
Jak1	<i>janus kinase 1</i>
Jak2	<i>janus kinase 2</i>
JNK	<i>JUN N-terminal kinase</i>
LAG-3	<i>lymphocyte activation gene-3</i>
M1	<i>type I macrophages</i>
M2	<i>type II macrophages</i>
mAbs	<i>monoclonal antibodies</i>
MALME-3M	<i>human malignant melanoma</i>
MAPK	<i>mitogen-activated protein kinase</i>
<i>MDM2/4</i>	<i>MDM2/4 proto-oncogene</i>
MDSCs	<i>myeloid derived suppressor cells</i>
MHC	<i>major histocompatibility complex</i>
<i>MYC</i>	<i>MYC proto-oncogene</i>
NF- $\kappa$ B	<i>nuclear factor-kappaB</i>
NK	<i>natural killer</i>
NSG	<i>NOD–scidIL2rg</i> <sup>-/-</sup>
OIS	<i>oncogene-induced senescence</i>
OVCAR-5	<i>human ovarian cancer</i>
p	<i>passage</i>
p21 <sup>Cip1</sup>	<i>cyclin-dependent kinase inhibitor p21<sup>Cip1</sup></i>
p53	<i>tumor suppressor gene p53</i>
PD-1	<i>programmed cell death protein 1</i>
PD-L1	<i>programmed cell death-ligand 1</i>
PI3K	<i>phosphoinositide 3-kinases</i>
PTEN	<i>phosphatase and tensin homolog</i>



PyVmT	<i>polyomavirus middle T antigen</i>
RIP	<i>rat insulin 1 promotor</i>
RT2	<i>RIP-Tag2</i>
RT2. <i>Cdkn2a</i> <sup>-/-</sup>	<i>Cdkn2a knockout β-cancer cells</i>
RT2.CRISPR- <i>Cdkn2a</i>	<i>Cdkn2a-specific CRISPR/Cas9 transfected β-cancer cell line</i>
s.c.	<i>subcutaneously</i>
<i>scid</i>	<i>severe combined immune deficiency</i>
SAHF	<i>senescence-associated heterochromatic foci</i>
SASP	<i>Senescence-associated secretory phenotype</i>
SA-β-gal	<i>Senescence-associated beta-galactosidase</i>
<i>shp16-p19</i>	<i>Cdkn2a-specific shRNA transfected β-cancer cell line</i>
shRNA	<i>short hairpin RNA</i>
SNB-75	<i>cancer cells from the central nervous system</i>
SNVs	<i>somatic mutations</i>
SSF-295	<i>cancer cells from the central nervous system</i>
STAT1	<i>signal transducer and activator of transcription 1</i>
<i>Stat1</i> <sup>-/-</sup>	<i>signal transducer and activator of transcription 1 knockout mice</i>
STAT2	<i>signal transducer and activator of transcription 2</i>
Suppl. Fig.	<i>Supplementary Figure</i>
TAA	<i>tumor-associated antigens</i>
Tag2	<i>simian virus 40 large T antigen 2</i>
TCR	<i>T-cell receptor</i>
T <sub>H</sub> 1	<i>typ1-T helper cells</i>
TILs	<i>tumor-infiltrating lymphocytes</i>
TIS	<i>therapy-induced senescence</i>
TMB	<i>tumor mutational burden</i>
TNF	<i>tumor necrosis factor</i>
TNFR1	<i>tumor necrosis factor receptor 1</i>
<i>Tnfr1</i> <sup>-/-</sup>	<i>tumor necrosis factor receptor 1 knockout mice</i>
TNFR2	<i>tumor necrosis factor receptor 2</i>
TRAF	<i>TNFR-associated factor</i>
Tregs	<i>regulatory T cells</i>

$\beta$ 2M

*$\beta$ 2-microglobulin*

$\beta$ -cancer

*pancreatic insulin-producing tumors of RT2 mice*

$\gamma$ H2AX

*gamma histone variant H2AX*

# 1. Introduction

The aim of this thesis was to make a relevant contribution to the understanding of immunomodulatory therapeutic approaches in the treatment of cancer. Here references are made to the essential aspects of my publications **Publications (1-7)**.

This research is based on an established T<sub>H</sub>1 cell therapy **(8)** in a murine model of endogenous pancreatic insulin-producing tumors ( $\beta$ -cancer) of RT2 mice **(9, 10)**. The mechanisms underlying this successful therapy were investigated. The research further based on insights into the modulation of T cells of immune responders by either IFN- $\gamma$  producing T<sub>H</sub>1 cells or interleukin-4 (IL-4) producing T<sub>H</sub>2 cells **(11-14)**. Analyzed are the role of T<sub>H</sub>1 cells for a cancer immunotherapy, which is able to regulate and control the cancer growth. Here the scientific background of cancer formation, the use of the immune system for therapeutic approaches, and what is known about the underlying mechanisms is presented.

## 1.1 Cancer Growth and Cancer Evasion Mechanisms

Cancer cells manifest different organizing principles that enable the growth and metastatic spread of cancer cells. Hanahan and Weinberg defined these capabilities as “hallmarks of cancer” including the ability of tumor cells and their microenvironment to sustain proliferative signaling, evade growth suppressors, trigger evasion of immune responses, promote replicative immortality, induce inflammation, activate invasion and metastasis, induce angiogenesis, set genomic instability, resist cell death, and reprogram energy metabolism **(15, 16)**. Different tumor entities can be considered as role models to study the hallmarks of cancer and to develop general treatment options.

### 1.1.1 Cancer Development and Progression

One of the first mouse models to investigate the “hallmarks of cancer” was the pancreatic neuroendocrine RIP-Tag2 tumor where the rat insulin I promoter (RIP) is used to regulate the transcription of the oncoprotein simian virus 40 large T antigen 2 (Tag2) **(9)**. Whereas the tumor driver is expressed in all  $\beta$ -cells of the pancreas, only a minority of the islet develop into adenocarcinomas, suggesting that further genetic aberrations are required for cancer development and progression. During multistep tumorigenesis,

protein expression and DNA content of the  $\beta$ -cells showed alterations, indicating that not only the overall tumor burden, but also the tumor mutational burden (TMB) increases over time **(7, 17)**. Additional tumor types with a high frequency of somatic mutations such as melanomas, lung cancer and colorectal cancer are candidates for therapeutic approaches with immunotherapy **(18)**.

### 1.1.2 Immunoediting

The natural tumor control is part of the immune systems recognition of foreign pathogens. The control of precancerous or cancerous cells is termed cancer immunosurveillance. Cancer cells can evolve if they escape the elimination of the immune system known as immunoediting that also limit cancer immunotherapy **(19, 20)**. Tumor cells can hide from the immune system by many mechanisms. Among these mechanisms is the absence of tumor antigen expression, the loss of human leukocyte antigen (HLA) expression, defects in antigen processing, and expression of inhibitory receptors, for examples inhibitory receptors that prevent killing by natural killer (NK) cells **(21)**. Alterations in distinct signaling pathways like the mitogen-activated protein kinase (MAPK) pathway or loss of the protein phosphatase and tensin homolog (PTEN) expression, and subsequent enhancement of phosphoinositide 3-kinases (PI3K) signaling can lead to accelerated cancer growth. Cancer immune evasion also involves factors of the tumor microenvironment such as regulatory T cells (Tregs), myeloid derived suppressor cells (MDSCs), type II macrophages (M2), and accessory molecules inhibiting immune responses **(22)**. These regulators of the immune system are named “immune checkpoints” are surface proteins like programmed cell death 1 (PD-1) and its ligand (PD-L1). The discovery of their blockade, which enables or enhances immune responses against tumors, revolutionized cancer immunotherapy. ICB therapy operates through reverting the T cells anergy and establishing effective anti-tumor immune responses **(19, 20)**.

Many melanoma cell lines resist apoptosis induction in response to cytokine stimuli like IFN **(23)** or in response to other proapoptotic stimuli due to an impaired apoptotic signaling cascade **(24)**. Therefore, they have lost a key mechanism needed to clear damaged cells by destruction. Yet, cells that resist apoptosis-induction may still be vulnerable for the stress response pathway of cellular senescence that induces permanent

cell-cycle arrest **(25)**. However, not many studies address the significance of cellular senescence as an important control mechanism of anticancer immunity.

## 1.2 Cancer Immunotherapies

Cancer immunotherapies can target immunogenic antigens that are naturally processed and presented by cancers. Immunotherapy strategies can overcome negative immune signaling via the use of blocking monoclonal antibodies (mAbs) or adoptive T-cell transfer (AT) **(26)**. Further immune activating strategies via CD28 co-stimulatory signals can restore the production of IL-2, IL-6, and in particular IFN- $\gamma$  **(27)**. Moreover, cancer immunotherapy may also include the administration of various cytokines, such as IFN- $\alpha$  or TNF **(28, 29)**. The presence of immune responses can in addition be used as a prognostic factor predicting the efficacy of a cancer treatment **(30-32)** and to discriminate *hot tumors*, tumors with immune cell infiltration, and *cold tumors*, tumors without immune cell infiltration **(33)**.

### 1.2.1 Immune Checkpoint Blockade Therapy

Melanoma and other cancer types frequently show immune cell infiltrates, tumor-infiltrating lymphocytes (TILs), in conjunction with cancer regression, suggesting that the immune system can recognize tumor-associated antigens (TAA) **(26, 33-37)**. TILs can not only induce cancer regression, but also long-term disease control **(38-40)**.

Immune checkpoint proteins like PD-1 and its ligand PD-L1 have their peak expression on immune cells during the contraction phase of immune responses **(41)**. This ensures the decline of the expansion of the immune cells. PD-L1 can also be expressed on immunogenic tumor cells and promote immune evasion as it inhibits cytotoxic T cells **(42)**. ICB therapy is the first immunotherapy that improved the long-term outcome of patients with solid cancer. Therefore, it was named “Breakthrough of the Year” by Science in 2013 **(43)**. The first approved therapeutic by the Food and Drug Administration (FDA) was ipilimumab in 2011 targeting the immune checkpoint cytotoxic T-lymphocyte associated antigen 4 (CTLA-4) for the treatment of melanoma. Followed by the anti-PD-1 mAbs pembrolizumab and nivolumab in 2014. **Table 1** summarizes the ICB mAbs used to analyze the mode of action of IFN- $\gamma$  in cancer immunotherapy.

**Table 1. Immune checkpoints used in this study and their clinical description.**

Immune checkpoint	CTLA-4	PD-1		PD-L1		LAG-3
<b>Synonym</b>	CD152	CD279		CD274, B7-H1		CD223
<b>Drug</b>	Ipilimumab	Pembrolizumab	Nivolumab	Atezolizumab	Avelumab	Relatlimab
<b>Expression</b>	T cells	activated T cells		cancer cells, T cells, dendritic cells, macrophages		T cells
<b>Respective ligands</b>	CD80 (B7-1), CD86 (B7-2)	CD274 (PD-L1), CD273 (PD-L2)		CD 279 (PD-1)		CD74 (MHC-II)
<b>Approved</b>	25.03.2011	04.09.2014	22.12.2014	18.05.2016	09.05.2017	pending
<b>Drug</b>	YERVOY	KEYTRUDA	OPDIVO	TECENTRIQ	BAVENCIO	(BMS-986016)
<b>Company</b>	BMS	Merck	BMS	Genentech	EMD Serono	BMS

James P. Allison and Tasuku Honjo were awarded “The Nobel Prize in Physiology or Medicine 2018” for their discovery of the immunological checkpoint receptors CTLA-4 and of PD-L1, as these discoveries allowed the development of the first broad effective cancer immunotherapy **(19, 20, 44, 45)**.

Ipilimumab induces an objective response in many tumor types, including melanoma **(46-48)**, lung cancer **(49-51)**, and prostate cancer **(52, 53)**, in a small, but significant number of patients. Serious, generally manageable, adverse events are among others colitis, hepatitis, hypophysitis, type I diabetes or myocarditis. This side effects are T cell mediated autoimmune diseases. Besides its inhibition of negative immune regulation, CLTA-4 blockade modulates the T cell population frequencies, resulting in unusual T cell population such as T<sub>H</sub>1-like CD4<sup>+</sup> T cells **(54, 55)**.

Tumor-infiltrating T cells are the primary PD-1 expressing cells in cancers. PD-L1 is induced after T cell stimulation via antigen presentation by antigen presenting cells (APCs) in the presence of IFN- $\gamma$  **(56)**. This mechanism of immune inhibition is part of adaptive immune resistance and protects against autoimmune diseases **(57)**.

Lymphocyte activation gene-3 (LAG-3) is expressed on activated CD4<sup>+</sup> and on CD8<sup>+</sup> T cells, Tregs, and NK cells. LAG-3 is a CD4 homolog that binds to the major histocompatibility complex (MHC) class II molecules. LAG-3 proteins, like PD-L1 and MHC class II molecules, are induced by stimulation of T cells and modulated by soluble factors **(58, 59)**.

As LAG-3 and PD-1 have a synergistically role to prevent autoimmunity, treatment of cancer patients with anti-LAG-3 and anti-PD-L1 mAbs appears to be a promising approach to enhance anti-tumor immune responses **(57)**. Combined therapy in mice show higher efficacy in preventing tumor recurrence in melanoma as compared to monotherapy **(60)**. Further preclinical studies using TAA-specific T cells in combination with the blockade of LAG-3 and PD-1/PD-L1 interaction reveal a highly efficient anti-cancer regime. Both, anti-LAG-3 and anti-PD-L1 mAbs, show reawakening of TAA-specific T cells to a greater extent than blockade with either of the mAbs **(61)**. Overall, combinational therapy approaches seem to increase the effectiveness of immunotherapy **(62-64)**.

### 1.2.2 Adoptive T cell Transfer

Studies on AT preferentially focus on TAA with recognized by CD8<sup>+</sup> cytolytic T cells (CTLs). Therapy with autologous *ex vivo* expanded CTLs has been successfully applied in patients after immunodepletion **(65)**. This approach achieved good responses in the therapy of metastatic melanoma **(66-68)**. Identification of target antigens recognized by CTLs enabled the development of therapeutic approaches to enhance cellular antitumor immunity **(69)**. AT of activate T cells can directly elicit an antitumor immune response. Durable responses can be achieved with engineered T cells that express the T-cell receptor (TCR) for the HLA\*0201 epitope of the cancer testis gene NY-ESO-1 **(70)**, an approach that targets tumor neoantigens **(26)**.

Somatic gene mutations of cancer cells provide a basis for individualized immunotherapies with T cells. However, immunotherapies can fail to respond if mutations are present in the IFN- $\gamma$  signaling, antigen processing, or antigen presentation genes **(71)**. Cancer resistance or non-responsiveness to immunotherapies is further exacerbated by additional suppressive immune checkpoints in the tumor microenvironment. A combination of AT with ICB is a promising therapeutic approach to maintain immunity to tumors in an activated state that counteracts the immunosuppressive microenvironment.

Other promising options of tumor immunotherapy are combinations of AT with cytokines, such as IL-2, in patients with metastatic melanoma **(28, 29)**, or stimulation of APC to present TAA to CD4<sup>+</sup> T cells.

Tumor immunotherapy with TAA-specific CD4<sup>+</sup> T cells arrests tumor growth (1, 2). The therapeutic T cells migrate to the tumor-draining lymph nodes and directly to the tumors and act via their cytokines IFN- $\gamma$ - and TNF in the tumor microenvironment (8, 72, 73).

### 1.2.3 Cytokine Therapy

The presence of immune cells within tumors can predict clinical outcome (28, 30). Besides their direct contact-dependent effector function, they secrete cytokines that enhance cellular immune responses (Figure 1).

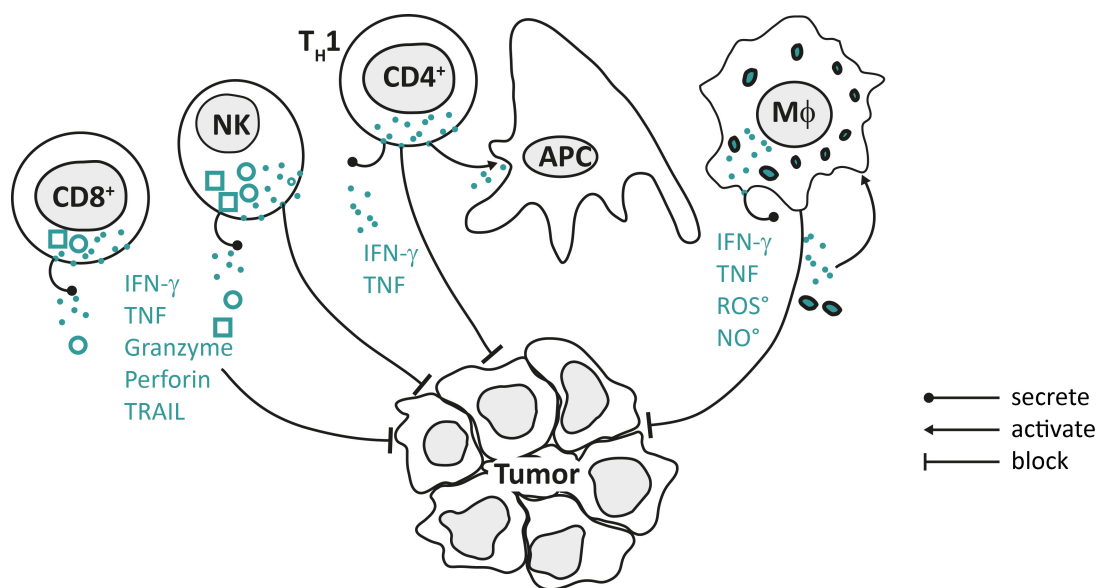


**Figure 1. Cytokine therapy as soluble anticancer immunity.**

After stimulation, cellular effector cells secrete soluble factors to target tumor cells. CD8<sup>+</sup> T cells and NK cells secrete IFN- $\gamma$ , TNF, granzyme, perforin, and TRAIL. CD4<sup>+</sup> T<sub>H</sub>1 cells secrete IFN- $\gamma$  and TNF. Type I macrophages (M1) secrete ROS and NO. The humoral immunoreaction targets tumor cells to control tumor cell proliferation, induces tumor cell apoptosis, improves tumor antigen presentation and inhibits angiogenesis.

Inflammatory responses likely evolved as a defense mechanism against infection and as a repair mechanism for wound healing (74). Secretion of the acute-phase protein TNF in the absence of IFN, as in chronic inflammation and wound healing, may promote proliferation and differentiation of cells (8, 75). Chronic inflammations are therefore relevant risk factor. Approximately 25% of the global cancer burden is caused by infections and chronic inflammation. Chronic release of low doses of TNF seems to play a key role in inflammation-induced cancer (76, 77).

IL-2 is approved by the FDA for the treatment of melanoma and renal cell carcinoma. Treatment of melanoma patients with recombinant IL-2 was the first



successful immunotherapy in humans **(78-80)**. IL-2 has been further developed for the combination with AT or vaccination using the melanocyte protein PMEL, also known as gp100 **(81, 82)**. Currently, its clinical application is largely reduced due to the efficacy of ICB therapy of metastatic melanoma **(46, 48, 83, 84)**.

Similarly, the indication for the administration of interferon alpha (IFN- $\alpha$ ), which had been approved as adjuvant therapy for high risk malignant melanoma, have been reduced **(85-91)**.

This work focuses on the T<sub>H</sub>1 cytokines IFN- $\gamma$  and TNF with their outstanding importance in cancer control **(1, 7, 8)**. Therefore, the therapeutic effects of the cytokines IFN- $\gamma$  and TNF, as well as their combination, are presented separately below.

#### 1.2.4 IFN- $\gamma$ Therapy

For cancer ICB therapy, the IFN- $\gamma$  gene signature has been shown to be essential for a clinical response **(32, 71)**. Combination of ICB therapy with oncolytic virotherapy was shown to increase IFN- $\gamma$ -based immunity in advanced melanoma which in turn led to improved clinical response **(92)**. IFN- $\gamma$  may additionally contribute to tumor therapy due to its antiangiogenic effects on tumor vessel formation **(93)**. On the other side, persistent IFN- $\gamma$  signaling, has opposing effects compared to short-term IFN- $\gamma$  signaling as it promotes chronic infection and can induce T cell dysfunctions and resistance to ICB therapy **(94)**.

Cellular responses to the cytokine IFN- $\gamma$  are mediated by binding as a dimer to the receptor chains interferon gamma receptor 1 (IFNGR1) and interferon gamma receptor 2 (IFNGR2). Thereby the Janus kinases Jak1 and Jak2 are activated by phosphorylation and then phosphorylate the IFNGR1 chain, which recruits the signal transducer and activator of transcription 1 (STAT1). The JAK-STAT pathway leads to translocation of STAT1 homodimers to the nucleus, binding to the promoter interferon-gamma-activated sequence (GAS) and increased expression of IFN- $\gamma$  inducible genes. STAT1 can also interact with signal transducer and activator of transcription 2 (STAT2), interferon regulatory factor 9 (IRF9), and induce the interferon-stimulated response element promoter (ISRE) **(95)**.

To analyze the role of IFN- $\gamma$  signaling for the therapeutic effect of the AT therapy with TAA-specific T<sub>H</sub>1-cells, the homozygous STAT1 knockout phenotyp (*Stat1*<sup>-/-</sup>, 129S6/SvEv-*Stat1*<sup>tm1Rds</sup>) developed by Robert D. Schreiber was bred into C3HeB/FeJ

mice to generate the required genetic background. *Stat1*<sup>-/-</sup> mice are unable to initiate transcription of IFN- $\gamma$ -inducible genes, and IFN- $\alpha$ -inducible genes, but show normal responses to IL-6 and IL-10. Due to the loss of IFN signaling, *Stat1*<sup>-/-</sup> mice are sensitive to viral infection and intracellular microbial pathogens **(96)**, and more susceptible to tumor formation induced by chemical stress or loss of the tumor suppressor gene p53 (p53) **(97)**, or the cyclin-dependent kinase inhibitor p21<sup>Cip1</sup> (p21<sup>Cip1</sup>) **(98)**.

Finally, C3H/FeJ-*Stat1*<sup>tm1Rds</sup> mice were crossbred with RT2 mice to generate an IFN-dependent cancer model.

### 1.2.5 TNF Therapy

TNF is described as a factor that connects infection and cancer regression, more precisely as an endotoxin-inducing factor able to induce hemorrhagic necrosis of tumors in certain animal models **(99)**. TNF is secreted by T cells, macrophages, NK cells, B cells, neutrophils, fibroblasts, and keratinocytes **(28)**. TNF has been studied as a system therapy in humans with cancer, but treatment options are limited by severe side effects of the cytokine, ranging from influenza-like symptoms to the development of life-threatening symptoms of shock.

TNF-receptor signaling is precisely regulated and decides whether cells survive or go into apoptosis or regulated necrosis **(100-102)**. In brief, TNF binds to two receptors of the TNF receptor superfamily, the surface receptors tumor necrosis factor receptor 1 (TNFR1) and tumor necrosis factor receptor 2 (TNFR2). Most tissues constitutively express TNFR1, whereas expression of TNFR2 is expressed on immune cells.

The first cell fate after TNF binding signals via a crosstalk of TNFR1 and TNFR2 which promotes via complex I binding cell survival through nuclear factor- $\kappa$ B (NF- $\kappa$ B) activation. NF- $\kappa$ B activation leads to the transcription of antiapoptotic factors such as cFLIP, XIAP, Bcl-2, Bcl-X<sub>L</sub> and others. Complex I consists of TRADD, RIPK1, TRAF2 or TRAF5 and cIAP. RIPK1 further modulates the signaling via activating the MAPK and JUN N-terminal kinase (JNK) pathway **(100-102)**.

The second cell fate following TNF stimulation is apoptosis, and for this, caspase activation is required. TNFR1 contains the protein-protein interaction domain (death domain (DD)), which binds other DD-containing proteins and couples the death receptors to caspase activation and apoptosis. TNFR1 is also a potent activator of gene expression via indirect recruitment of members of the TNFR-associated factor (TRAF) family, while

TNFR2 lacks a DD-domain and directly recruits TRAF2. The modulation of RIPK1 via deubiquitinating enzymes enables TRADD, RIP1, and TRAF2 to move to the cytosol. FAS-associated death domain protein (FADD) and pro-caspase-8 bind to this cytosolic complex and form complex II, or death-inducing signaling complex (DISC). Pro-caspase 8 then forms a homodimer and autocatalytically cleaves its pro-domains. The initiator caspase-8 cleaves downstream executor caspases, like caspase-3, -6, and -7 that modify proteins ultimately responsible for programmed cell death **(100-102)**.

The third cell fate after TNF stimulation is necroptosis, it occurs after formation of complex II when pro-caspase-8 cannot be activated. This stress response then leads to receptor-mediated swelling of the cell and rupture of the cell membrane **(100-102)**.

*Tnfr1*<sup>-/-</sup> mice yield normal T cells. *Tnfr1*<sup>-/-</sup> mice have an increased sensitivity to viral infections and intracellular pathogens. Since the animals are kept under specific-pathogen-free conditions, the defect has no influence on their life expectancy. However, the absence of TNFR signaling largely abolishes the TNF response. To analyze the role of TNF-dependent signaling for the therapeutic effect of the immunotherapy, the homozygous TNFR1 knockout phenotyp (*Tnfr1*<sup>-/-</sup>) **(103)** was backcrossed to C3HeB/FeJ and crossbred with RT2 mice.

### 1.2.6 Combined Effects of IFN- $\gamma$ and TNF

IFN- $\gamma$  and TNF in combination for the treatment of tumors have synergistic effects on cytostatic control or cytotoxic killing of tumor cells **(104-106)**. An important issue in cancer control is the appropriate dosage finding and delivery to provide efficient control and overcome therapy resistance. To prevent side effects, the cytokines IFN- $\gamma$  and TNF were administered, together in a study with the chemotherapeutic melphalan, by isolated limb perfusion in patients with melanoma metastases. This cytokine-based therapy is relatively well tolerated with a high local response rate **(107)**. Targeted administration of the cytokines is achieved by using T<sub>H</sub>1 cells as carrier **(1, 7, 8)**. Preclinical study of a tumor kinase inhibitor with adoptively transferred T cells shows that IFN- $\gamma$  and TNF enhances the effect and induce cell cycle arrest in tumor cells **(108)**.

### 1.2.7 Mode of Action

The mechanisms of the body to overcome a cancer disease can act through apoptosis, necroptosis or necrosis to kill the cancer cells. Cytolysis, mainly mediated by

CTL and NK cells. In addition, senescence induction is an additional mechanism leading to durable control of cancer growth (1, 7, 109). If all these mechanisms fail, tumor escapes from the immune responses, and start growing (Figure 2).

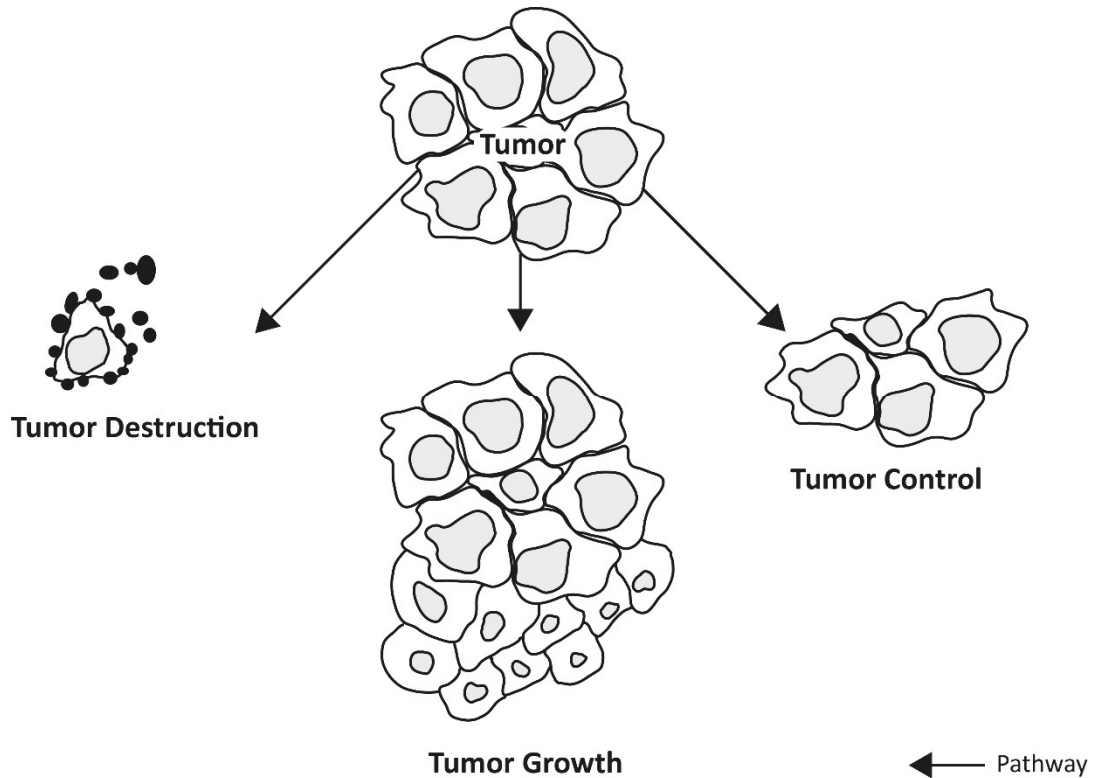


**Figure 2. Tumor responses to cancer immunotherapies.**

A developing tumor can either be destroyed via cytolysis, apoptosis, necrosis, necroptosis, or show resistance and continues to grow, or can be controlled via senescence by the anticancer immunity. The fate of the tumor depends on the immune composition and the signal transmission within the tumor cell.

The topic of escape mechanisms is above described in the **Chapter 1.1**. The mechanisms of tumor immune control are summarized in review (3) **Figure 3**. First, CD8<sup>+</sup> T cells via cytolysis, second receptor-mediated induction of apoptosis, third the NK cell-mediated cytotoxicity, fourth antibody-dependent cellular cytotoxicity (ADCC), and fifth the induction of senescence are mechanisms to control tumor cells.

In this thesis, senescence could be elaborated as a key mechanism of immunotherapy via CD4<sup>+</sup> T<sub>H</sub>1 cells (1), and T<sub>H</sub>1 cells in combination with the application of ICB via blocking mAbs as an effective cancer therapy (7). Therefore, the mechanisms of senescence induction with special focus on CIS will be presented in the next chapter.

## 1.3 Cellular Senescence

In 1961, cellular or replicative senescence was first described as a permanent growth arrest of fibroblasts that divide about 50 times before becoming growth-arrested, a phenomenon also known as Hayflick limit **(110, 111)**. The physiological relevance of senescence mechanisms extends to tissue homeostasis in addition to aging and thus may play a significant role in the control of tumorigenesis.

### 1.3.1 Modes of Senescence Induction

The induction of replicative senescence is caused by the shortening of the telomeric ends of a linear chromosome, following persistent DNA damage response (DDR) signaling that lead to a stable growth arrest of the cell.

Physiological, programmed cellular senescence was found as a mechanism during mammalian embryonic development, which protects cells from apoptosis via p21-mediated senescence **(112, 113)**.

Oncogenic Ras induces accumulation of the tumor suppressor proteins p16<sup>Ink4a</sup> or p53, described as oncogene-induced senescence (OIS) **(114, 115)**.

Cytokine-induced senescence (CIS) triggers via IFN- $\gamma$  and TNF also the upregulation of the tumor suppressor proteins p16<sup>Ink4a</sup> *in vitro* and in tumors *in vivo* and can acts as a barrier to cancer progression **(1, 7, 8)**. In this thesis modes of senescence induction in the RT2 mice are studied. In RT2 mice  $\beta$ -cells transform into  $\beta$ -cancer cells through partial inactivation of Rb1 and p53 by viral Tag2. These tumor suppressor proteins are essential for maintaining the senescent state **(116)**. However, genetic changes like loss-of function mutations of p16<sup>Ink4a</sup> can reverse cellular senescence **(117, 118)**. Therapeutic approaches were studied with an antibody-cytokine fusion protein to deliver IL-12 into tumor tissue. The IL-12 stimulus differentiates CD4<sup>+</sup> T cells, which secretes IFN- $\gamma$  and TNF and induces cancer killing and cancer cell senescence in human rhabdomyosarcoma (A-204) cells *in vivo* in fully humanized NSG mice **(119)**. Senescence induction via AT with TAA-specific T<sub>H</sub>1 cells was detected via imaging methods *in vivo* **(120)**. IFN- $\gamma$  can induce p21-dependent senescence in human melanocytes **(121)**, and can act via oxidative stress, leading to DDR and subsequent cellular senescence **(122)**. IFN- $\gamma$  and CD4<sup>+</sup> T cells also establish a barrier against breast cancers by inducing senescence and apoptosis **(123)**, and in a melanoma model the loss of IFN signaling leads to a loss of senescence and further melanoma progression **(124)**.

Therapy-induced senescence (TIS) is established as direct senescence response of chemotherapy or small molecule inhibitor targeting the p16<sup>Ink4a</sup> and p53 tumor suppressor mechanisms **(125)**. Targeting the inhibition of the cyclin-dependent kinases CDK4 and CDK6 (CDK4/6) with substances like palbociclib, ribociclib, and abemaciclib is an established approach for the treatment of breast cancers **(126-130)**. Since 2015, palbociclib has the FDA approval for treatment of hormone receptor-positive, advanced-stage breast cancer patients. Application strategies were further developed to combine CDK4/6 inhibitors with MEK inhibitors to increase the effect of chemotherapy in pancreatic cancer **(131)**.

In melanocytic nevi, the common overexpression of BRAF<sup>E600</sup> leads to senescence **(132-135)**, which is associated with signs of DDR **(136, 137)**. Primary human melanomas, often carry the driver mutation BRAF<sup>V600E</sup> that results in permanent activation of the serin/threonin kinase associated with a loss of p16<sup>Ink4a</sup>. Treatment with specific BRAF-inhibitors mainly destroys the targeted melanoma cells, but can also restore senescence in part of the melanoma cells **(138)**.

### 1.3.2 Senescence Marker

Senescence, as a cellular condition of growth arrest cannot be distinguished from dormancy, quiescence, or terminal differentiation in tissues. Therefore, senescence-specific markers are needed to define senescence growth arrested cells.

In tissue cultures senescent cells differ from proliferating cells with their enlarged, irregular morphology **(139)**. Senescence-associated beta-galactosidase (SA-β-gal) between pH 5.5 and pH 6.0 is the gold standard marker to characterize senescent cells in tissue cultures and *in vivo* **(109, 111, 132, 140, 141)**. Because of its importance, we developed a method to quantify SA-β-gal in tissue slides **(7) Suppl. Fig. 2**.

Increased expression of the tumor suppressor protein Cdkn2a also known as p16<sup>Ink4a</sup> **(117, 118, 142, 143)**, as well as Cdkn1a also known as p21<sup>Cip1</sup> **(112, 113, 121)** are functional markers for senescence. They prevent the progression of the cell cycle as they suppress cyclin-dependent kinases (CDKs) and act as natural CDK inhibitors (CDKis) namely CDK4/CDK6 **(139)**. Suppression of CDK4/CDK6 results in a permanent dephosphorylation of Rb1, causing cell cycle arrest in the G1 phase, partly by suppressing E2F molecules. Further, proliferation capacity can be monitored as well as the proliferation marker Ki67 **(144)**.

Senescence-associated epigenetic histone modifications can be detected by increased pHP1 $\gamma$  or H3K9me3, which are markers for senescence-associated heterochromatic foci (SAHF) **(145, 146)**. A functional biomarker to address DDR is the phosphorylated histone variant H2AX ( $\gamma$ H2AX).

Moreover, senescent cells are highly metabolically active, and secrete pro-inflammatory cytokines, chemokines, growth factors, and proteases, known as senescence-associated secretory phenotype (SASP) **(147-152)**.

### 1.3.3 Senescence in ICB Therapies

From the first reports on ICB therapy in patients with advanced cancer **(46, 47, 83, 153)**, to the phase II to phase IV studies **(38-40, 48, 84, 154-156)**, to the present **(157)**, all studies have in common that in responder patients residual metastases remain. Mechanisms must exist that can control stable metastases in addition to tumor eradication. Senescence could be one mechanism **(3)**. Based on the clinical regression of metastases, the response to ICB therapy can be divided into two phases: the first phase of tumor regression; followed by a second phase of stable disease. Immunotherapy mediated senescence or apoptosis mechanisms within tumor cells thereby keeping tumor growth under control. We speculate that ICB therapy has an effect on immunoediting and converts the tumor into an equilibrium state of immune-mediated senescence called this process consolidation phase, probably in combination with apoptosis of cells that escape from senescence **(6) Figure 3c**.

## 1.4 Project Outline

### *Objectives*

Carcinogenesis results from the stepwise transformation of somatic cells growing inside an ordered system into cells with an autonomous growth pattern that increasingly ignores to their given rules of growing and functionary. This results in an invasive growth pattern and the capacity to settle at distinct sites by forming metastases. Melanoma is a particularly aggressive tumor disease that begins to metastasize at tumor thickness less than 1 mm and causes metastasis in about half of patients at  $\geq 4$  mm thickness. As cancer dissemination can occur very early during cancer development, almost all melanoma-associated deaths result from cancer metastases. Despite high public awareness leading to enormous investment in broad research, there has been almost no progress in the medical treatment of disseminated metastases from melanoma. The major breakthrough in the treatment of melanoma metastases occurred in 2011 with the introduction of immune checkpoint blockade (ICB) inhibitor targeting CTLA-4 into the clinic; followed by ICB inhibitors targeting PD-1 or PD-L1, and research on LAG-3 as promising target. Yet, about 50% of the patients with metastatic melanoma die from this disease.

### *Work program*

Develop a feasible, life-prolonging, quality-of-life-improving immunotherapy in mice; characterize the therapeutic outcome and the responsible mechanism; evaluate key cellular components, test transferability to other systems, and test relevant insights in the clinic.

### *Topic*

Both,  $T_H1$  cell therapy and ICB therapy result in IFN- $\gamma$ -dependent tumor cell senescence.



## 2. Results and Discussion

The focus of this thesis was to show the effectiveness of cancer immunotherapy with  $T_H1$  cells. Therefore, we studied the mechanism in pancreatic insulinomas from the RT2 mouse model during different stages of carcinogenesis. RT2 mice develop hyperplastic  $\beta$ -cells in islets at 5 weeks of age, from which angiogenic spontaneous insulin-secreting  $\beta$ -cells develop, resulting in declining blood glucose levels. The clinically relevant decrease in blood glucose levels begins around 10 weeks of life in RT2 mice. By 12 weeks of life, the mice have developed large tumors, leading to death from hypoglycemia between 13 and 14 weeks of life (**9, 10, 158**). Immunotherapy with genetically engineered tumor specific, viral activated CTLs can temporarily control the insulinoma of RT2 mice through  $\beta$ -cells killing. CTLs must be used with the awareness that significant side effects may occur due to cell destruction, such as in the case of  $\beta$ -cell destruction, the induction of autoimmune diabetes (**159**). Immunotherapy with  $T_H1$  cells showed even more promising strategy to control tumors in RT2 mice (**8**). Regarding to the multistage carcinogenesis, treatment of 5-7 weeks old RT2 mice are designed as prevention trials to test immunotherapies for their ability to contain the establishment of large tumors (**1, 7, 8**). Treatment of 10 week old mice are intervention trails on already diseased mice with established tumors to test the therapeutic outcome with normalization of the blood glucose levels and prolonged survival and to investigate mechanisms of ICB therapy (**7**). In order to generate an anticancer immune reaction, we generated autologous TAA-specific  $CD4^+$   $T_H1$  cells. **Figure 3** shows the scheme for priming and expansion of the therapeutic  $CD4^+$   $T_H1$  cells *in vitro* and the mode of action *in vivo* with combined ICB administration.

Freshly isolated  $\beta$ -cancer cells from RT2 mice are a tool to obtain insights in the tumor intrinsic signaling pathways by *in vitro* experiments and subsequent the determination of the responsible factors for senescence induction during immunotherapy. Further,  $\beta$ -cancer cells were used as engrafted tumors in wild type mice to analyze the role of the immune system during immunotherapy.

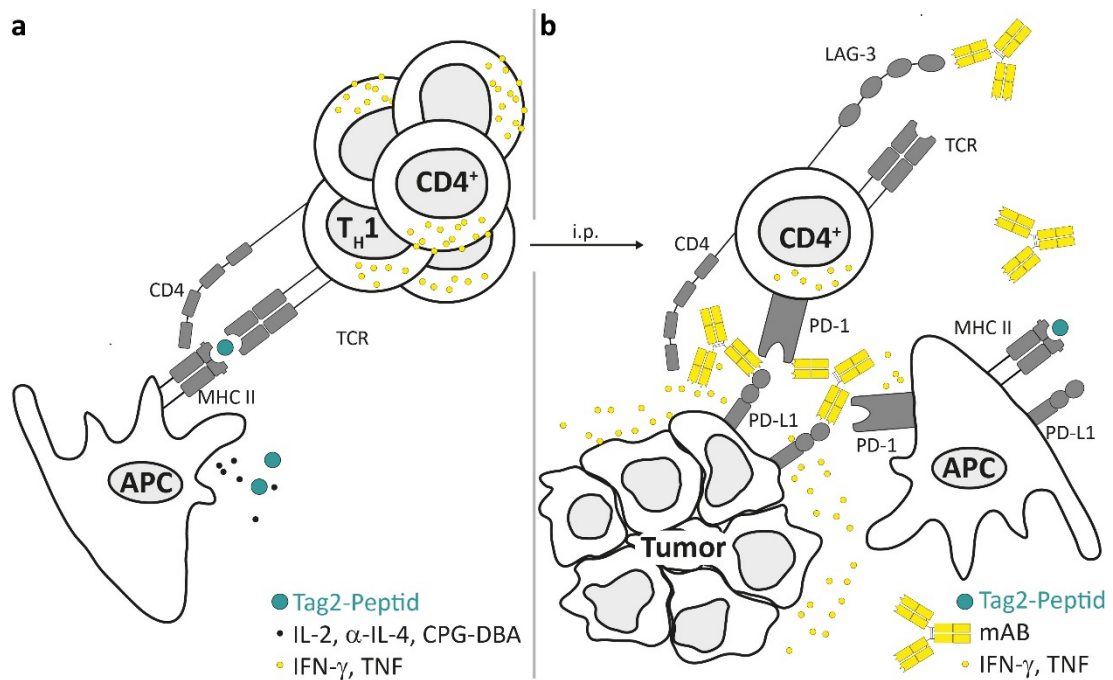


**Figure 3. AT/ICB therapy with CD4<sup>+</sup> T<sub>H</sub>1 cells, anti-PD-L1 mAbs, and anti-LAG-3 mAbs.**

**a**, *in vitro*: TAA-specific CD4<sup>+</sup> T cell priming in the presence of APC, Tag2-peptide, IL-2, anti-IL-4, and CPG-DNA to generate functional T<sub>H</sub>1 cells, followed by expansion of T<sub>H</sub>1 cells for AT therapy. **b**, *in vivo*: mode of action of combined i.p. AT/ICB therapy. T<sub>H</sub>1 cells migrate to the tumor and secrete IFN-γ and TNF. IFN-γ induces PD-1 expression and after ligation with PD-L1 the expression of cytokines reduces and T<sub>H</sub>1 cells become dysfunctional. In parallel, LAG-3 is expressed, which inhibits T cell function by ligation with MHC II. Treatment with ICB mAbs blocks these inhibitory mechanisms.

In addition, we investigated the role of senescence induction by immunotherapy in a B-cell lymphoma model. In this model, the human MYC oncogene acts as a tumor driver which is controlled by immunoglobulin-λ enhancers (160). This model was chosen for broad relevance to address different senescence mechanisms, respectively suppressor proteins. Finally, we translated our finding from bench to bedside and studied the role of senescence for efficient ICB of metastatic melanoma in patients.

## 2.1 Immunotherapy with AT and AT/ICB Controls Cancer Cells

RT2 tumors are immunologically *cold* tumors, as no functional TAA-specific T cells can be detected in the animals. Therefore, a weekly adoptive transfer of T-cells is necessary for prolonged antitumor immunotherapy (8, 159). Immunotherapy with Tag2-specific T<sub>H</sub>1 cells provided two important findings: First, half of the mice were alive after 30 weeks. Second, T cells controlled the tumors without inducing islet cell destruction and without causing diabetes (8).

### 2.1.1 RT2 Mice with AT of T<sub>H</sub>1 Cells is Dependent on the T<sub>H</sub>1 Cell Cytokines

As RT2 tumors are not expressing MHC II **(1) Suppl. Fig. 3**,  $\beta$ -cancer cells are not susceptible for T<sub>H</sub>1 cell mediated cancer cell killing. To test the role of the T<sub>H</sub>1 cell effector cytokines 6 week old RT2 mice, or RT2. *Tnfr1*<sup>-/-</sup> mice **(1) Suppl. Fig. 1** or RT2.*Stat1*<sup>-/-</sup> mice (unpublished data) were treated once a week by TAA-specific T<sub>H</sub>1 cells. The therapeutic approach started at early times of the carcinogenesis in a prevention trials as previous work showed that AT with TAA-specific T<sub>H</sub>1 cells prolongs the overall survival the earlier the therapy starts **(8)**. We measured the blood glucose level as therapeutic parameter. In RT2, AT with T<sub>H</sub>1 cells resulted in stabilization of the blood glucose level and prevention of the tumor outgrowth, whereas the blood glucose level from control-treated mice as well as from RT2.*Tnfr1*<sup>-/-</sup> mice or RT2.*Stat1*<sup>-/-</sup> mice decreased progressively. At 12 weeks of age, the control-treated and *Tnfr1*- or *Stat1*-deficient mice reached the termination criterion due to low blood glucose levels and the trial had to be aborted. The histological sections of the pancreas showed a control of the tumor burden in RT2 mice, while the mice with low blood glucose levels had loss in the pancreas architecture due to large insulinomas **(1) Suppl. Fig. 1**. The data suggested that the T<sub>H</sub>1 cell cytokines IFN- $\gamma$  and TNF leads to tumor control. The required presence of T<sub>H</sub>1 cells after AT in the surrounding of the  $\beta$ -cancer was prior detected via fluorescent labeled T<sub>H</sub>1 cells **(72)**. We stained the specific T-cell marker CD4 in paraffin sections of AT-treated RT2 mice and were thus able to detect the presence of T cells, predominantly in the tumor microenvironment **(1) Suppl. Fig. 2**. The data showed that T<sub>H</sub>1 cells are present in the microenvironment of  $\beta$ -cancers in RT2 mice and *Tnfr1*-deficient RT2 mice after AT therapy, but without controlling the tumor growth in *Stat1*- and *Tnfr1*-deficient RT2 mice. This suggests that the T<sub>H</sub>1 cell cytokines IFN- $\gamma$  and TNF are the effector molecules for the T<sub>H</sub>1 cell therapy.

### 2.1.2 *Stat1*-dependent Control of Advanced Malignant Insulinomas with AT/ICB Therapy

To analyze immunotherapy with T<sub>H</sub>1 cells after advanced tumor disease in an intervention trails we treated 10 week old RT2 mice bearing large insulinomas **(7) Suppl. Fig. 7a**. The presence of tumor burden was detected by magnetic resonance imaging **(7) Suppl. Fig. 7b**. RT2 mice and RT2.*Stat1*<sup>-/-</sup> mice were treated with AT, ICB, AT plus ICB or isotype control mAbs. A combination of anti-PD-L1 and anti-LAG-3 mAbs as

ICB treatment was used because the therapeutic effect of CD4<sup>+</sup> T with blockade of the PD-1/PD-L1 pathway alone failed to control tumor growth, whereas the combination of PD-L1 blockade with and anti-LAG-3 Abs showed therapeutic effect **(60)**. We analyzed RT2 mice in parallel with *Stat1*<sup>-/-</sup>-deficient RT2 mice to target in detail the IFN- $\gamma$  signaling pathway in the context of ICB therapy, as the IFN- $\gamma$  gene signature was defined as essential for a response to the applied therapy **(32, 71, 161)**. Immunotherapy with CD4<sup>+</sup> T<sub>H</sub>1 cells prolonged the life of RT2 mice, but could not inhibit the tumor outgrowth and stabilize the parameters of blood glucose level. Combination therapy with AT/ICB improved the survival of RT2 mice significantly compared to sham-treated RT2 mice or AT/ICB-treated RT2.*Stat1*<sup>-/-</sup> mice. Importantly, the therapy showed lower tumor burden in the pancreas section and stabilization of the blood glucose level in RT2 mice, but no difference between AT/ICB- and sham-treated RT2.*Stat1*<sup>-/-</sup> mice **(7) Figure 4 a-c**. The progression of the tumor can be determined by the decrease in blood glucose levels, as growing insulinomas secrete continuously insulin. These data showed a successful, *Stat1*-dependent intervention trails in a preclinical cancer immunotherapy with combination of CD4<sup>+</sup> T cells with anti-PD-L1 and LAG-3 mAbs.

To address if the difference in the clinical efficacy of immunotherapy is dependent on the IFN- $\gamma$  signaling and not due to reduced immune cell migration into *Stat1*<sup>-/-</sup>-deficient cancers, we stained the T cell marker CD3 by immunohistochemistry. CD3<sup>+</sup> T cells were present in the tumor microenvironment of RT2 or RT2.*Stat1*<sup>-/-</sup> mice after AT and AT/ICB treatment **(7) Figure 5a**. Next, we analyzed the expression of the SV40-Tag2 tumor antigen, which is recognized by the transferred T<sub>H</sub>1 cells, and found no difference in the Tag2 expression of RT2 or *Stat1*<sup>-/-</sup>-deficient tumors on RNA or protein level **(7) Figure 5b, c**. These data suggested that the transferred TAA-specific T<sub>H</sub>1 cells migrate to the  $\beta$ -cancer independent of the genotype of the mice.

To analyze putative differences between RT2 and RT2.*Stat1*<sup>-/-</sup> mice we further stained for the  $\beta$ -cancer cell markers insulin and synaptophysin and did not identify *Stat1*-dependent differences in the expression pattern of  $\beta$ -cancer cells **(7) Figure 5b**. In addition, we performed immunofluorescence staining of the treatment groups isotype control (Ctr), ICB/AT, ICB alone, or AT alone. We stained  $\beta$ -cancers with synaptophysin and found MHC class II expressing APCs and CD3 expressing T cells near the tumor cells in all treatment condition, but with a much greater extend after ICB/AT treatment in pancreas of RT2 and RT2.*Stat1*<sup>-/-</sup> mice **(7) Suppl. Fig. 8a**. Using labeled TAA-specific T<sub>H</sub>1,

we confirmed a rapid migration of the TAA-specific T<sub>H</sub>1 cells in the tumor environment of RT2 and RT2.*Stat1*<sup>-/-</sup> mice using 3-dimensional light sheet fluorescence microscopy and FACS measurement **(7) Suppl. Fig. 11**. Next, we stained PD-L1 and  $\beta$ 2-microglobulin ( $\beta$ 2M) a component of MHC class I molecules, as IFN- $\gamma$  signaling induces the expression of PD-L1 and  $\beta$ 2M **(56)**. PD-L1 and  $\beta$ 2M were detectible in the tumor section of RT2 and RT2.*Stat1*<sup>-/-</sup> mice **(7) Suppl. Fig. 8d**. The data showed that therapy with TAA-specific CD4<sup>+</sup> T<sub>H</sub>1, anti-PD-L1 mAbs, and anti-LAG-3 mAbs failed in *Stat1*-deficient mice not because of missing effector cells, antigen presentation or target receptor molecules. But rather because of the defect in the interferon signaling.

## 2.2 Immunotherapy with AT and AT/ICB Induce Senescence in Cancer Cells

The above described experiments showed that immunotherapy with AT and AT/ICB only partly destroyed the tumors. The mechanism is independent of CD8<sup>+</sup> T cells and apoptosis **(8)**, leaving residual tumors after immunotherapy. Senescence is a long-lasting growth arrest that frequently results from a stress response and could be one mechanism for the residual tumors in RT2 mice. To address the underlying mechanisms of T<sub>H</sub>1 cell therapy we examined multiple leading markers characterizing senescence *in vitro* and *in vivo*.

### 2.2.1 Characterization of Cancer Control after Immunotherapy *in vitro*

In order to analyze the role of senescence for the growth arrest in the residual tumors we isolated the tumors after a prevention trial with AT therapy of 12 week old mice, digested the tumor capsule and dissolved the cell clusters to obtain a primary  $\beta$ -cancer cell culture. We analyzed the growth capacity over several cell culture passages (p) *in vitro*. The culture of primary  $\beta$ -cancer cells starts with the cell number at p0 after isolation from sham- or AT-treated RT2 mice. A minority of the isolated cancer cells adhered to the cell culture plate, and the cell number of these  $\beta$ -cancer cells was analyzed in the following passages.  $\beta$ -cancer cells from sham-treated RT2 mice began to proliferate *in vitro*, whereas  $\beta$ -cancer cells from AT-treated RT2 mice remained growth arrested **(1) Figure 4a** and **Suppl. Fig. 15**. In sharp contrast,  $\beta$ -cancer cells from RT2.*Tnfr1*<sup>-/-</sup> mice **(1) Figure 4a** or RT2.*Stat1*<sup>-/-</sup> mice (unpublished data) started to grow exponentially *in vitro*, whether mice had received an immunotherapy or whether they were sham-treated. This

growth arrest was additionally performed after the intervention trails based on mice after therapy with ICB/AT with comparable results **(7) Figure 7a, b**. This data suggested that the therapeutic effect of T<sub>H</sub>1 cell immunotherapy stayed permanent in the  $\beta$ -cancer cells.

Next, we determined the percentage of the senescence marker SA- $\beta$ -gal after  $p \geq 5$ , and found an significant higher SA- $\beta$ -gal expression in  $\beta$ -cancer cells from RT2 mice after immunotherapy compared to sham-treated RT2 mice or AT/ICB-treated RT2.*Stat1*<sup>-/-</sup> mice **(7) Figure 7c**.

As the main characteristic of senescence is growth arrest we stained proliferation marker Ki67 and cell cycle inhibitor p16<sup>Ink4a</sup> in  $\beta$ -cancer cells after AT therapy and measured a significant reduction of the Ki67 and in parallel an induction of p16<sup>Ink4a</sup> **(1) Figure 3c**. Further, staining of the senescence markers pHP1 $\gamma$  and H3K9me3 showed significant induction in AT-treated RT2 mice compared to sham-treated mice. Whereas, analyzes of the apoptosis marker active caspase 3 was not induced by therapy **(1) Figure 3a, b**. This data indicated that the immunotherapy in RT2 mice leads to cancer cell senescence as tumor control mechanism.

### 2.2.2 Characterization of Cancer Control Mechanisms *in vivo*

To determine whether the tumor cells from AT-treated mice were long-term growth arrested,  $\beta$ -cancer cells were isolated after therapy and subcutaneously (s.c.) injected into immunodeficient NOD-*scid*IL2rg<sup>-/-</sup> (NSG) mice. NSG mice combining the severe combined immune deficiency (*scid*) and the complete loss of the IL-2 receptor common gamma chain (*IL2rg*<sup>-/-</sup>) allele on the NOD/ShiLtJ genetic background **(162)** and can therefore be used as *in vivo* model system to monitor the tumor growth capacity *in vivo* in the absence of a functional immune system.  $\beta$ -cancer cells isolated from mice after AT therapy remained growth arrested for 10 weeks, while tumors from sham-treated controls of *Tnfr1*-deficient mice **(1) Figure 4c**, and *Stat1*-deficient mice (unpublished data) grew exponentially. This data determined a permanent growth arrest of T<sub>H</sub>1 cell treated tumor cells, not only after *in vitro* seeding experiments (**chapter 2.2.1**), but also *in vivo*. To investigate senescence as an underlying mechanism, fresh cryosections were used to analyze established senescence markers. For this purpose, pancreas of RT2- and *Stat1*-deficient RT2 mice were examined after immunotherapy with AT and ICB/AT at the time point when the sham-treated mice reached the termination criteria. Immunofluorescence staining for p16<sup>Ink4a</sup> and Ki67 in the area of the  $\beta$ -cancer with

quantification of individual mice for each treatment group, showed clear and significant induction of p16<sup>Ink4a</sup> exclusively after ICB/AT treatment and reduction of Ki67 only in mice with functional IFN- $\gamma$  signaling **(7) Figure 4d, e**. p21<sup>Cip1</sup>, Ki67 double staining showed also a presence of p21<sup>Cip1</sup> exclusively after ICB/AT in RT2  $\beta$ -cancer with a loss of Ki67, and not in single-treated mice or in treated RT2.*Stat1*<sup>-/-</sup> mice **(7) Figure 6a**. To analyze heterochromatin formation as senescence marker we stained tumor sections of RT2 and RT2.*Stat1*<sup>-/-</sup> mice for pHP1 $\gamma$  and H3K9me3 **(7) Figure 6b, c**. pHP1 $\gamma$  expression was only detected in ICB/AT-treated RT2 mice. H3K9me3 nuclear staining was strongly detected after combined ICB/AT therapy while it revealed almost no signal in sham-treated tumor samples. ICB or AT monotherapy showed a slight nuclear signal of H3K9me3. SA- $\beta$ -gal activity is one of the main characteristic features of senescence, yet quantification of the SA- $\beta$ -gal activity in histological section was until now not established in the literature. To overcome this problem, we established histological staining at pH 5.5 on cryostat sections with subsequent objective color calculation of immunofluorescence signals within the tumor area. Using this technique **(7) Suppl. Fig. 2**, we evaluated strong expression of SA- $\beta$ -gal in the tumor cells of RT2 mice only after combined AT/ICB immunotherapy **(7) Figure 6d**. Together, detection of p16<sup>Ink4a</sup> and p21<sup>Cip1</sup> induction, loss of Ki67, heterochromatin formation by pHP1 $\gamma$  and H3K9me3, and SA- $\beta$ -gal analysis provided a reliable combination of senescence-associated markers to evaluate the senescence status *in vivo*. Moreover, electron microscopy analysis revealed accumulation of SA- $\beta$ -gal in the cytoplasm of senescent tumor cells **(7) Suppl. Fig. 10a-c**.

Immunotherapies with AT are regularly performed with CD8<sup>+</sup> T cells and lead to tumor infiltration by CTLs (see chapter 1.2.2 Adoptive T cell Transfer). However, in AT therapy with T<sub>H</sub>1 cells in combination with ICB therapy, hardly any infiltration of CD8<sup>+</sup> CTLs or CD49b<sup>+</sup> NK cells was detected **(7) Suppl. Fig. 8c**. Nevertheless, induction of apoptosis could be induced by combined AT/ICB therapy. Therefore, apoptosis induction via staining of DNA double-strand breaks (DSB) was investigated with the functional markers  $\gamma$ H2AX or DNA-dependent protein kinase (DNA-PK), which participate together in DSB repair **(163)**. However, no  $\gamma$ H2AX or DNA-PK positive cells were detected in the tumor sections of RT2 mice in tumor sections from AT/ICB-treated or in sham-treated mice **(7) Suppl. Fig. 9**. The data suggested that apoptosis was not a major mechanism leading to cancer containment in this system. Together, sham-treated tumors and *Stat1*-deficient tumors were strongly enriched in Ki67<sup>+</sup> cells that were negative for p16<sup>Ink4a</sup>,

p21<sup>Cip1</sup>, H3K9me3, pHP1 $\gamma$ , and SA- $\beta$ -gal. AT therapy alone, and ICB therapy alone showed intermediate results of these senescence markers. Only the combined AT/ICB treatment in advanced cancers showed tumor reduction and senescence induction.

As AT therapy with T<sub>H</sub>1 cells in early cancers **(1)** and the combined AT/ICB therapy in advanced cancers **(7)** was entirely inefficient in RT2.*Stat1*<sup>-/-</sup> mice the soluble factors IFN- $\gamma$  and TNF might be responsible for the immune control executed by TAA-specific T<sub>H</sub>1 cells. To proof this concept, the following assays were performed *in vitro* with the direct application of the cytokines to genetically modified  $\beta$ -cancer cell lines.

## 2.3 T<sub>H</sub>1 Cell Cytokine Induced Senescence in Cancer Cells

To address the role of IFN- $\gamma$  and TNF in T<sub>H</sub>1 cell-mediated immunotherapy, we used primary  $\beta$ -cancer cell lines, which were generated from 12 week old RT2 mice and treated them for 96 hours (h) with medium containing 100 ng ml<sup>-1</sup> IFN- $\gamma$  and 10 ng ml<sup>-1</sup> TNF. This treatment induced a cytokine-dependent G1 arrest **(1) Figure 1**, along with increased levels of p16<sup>Ink4a</sup> and hypophosphorylated Rb1 **(1) Figure 2d, e**. Cytokine treatment also increases SA- $\beta$ -gal expression **(7) Figure 3**. In summary, the data showed that this combined cytokine treatment induced a cellular status of senescence, CIS. Functional analyses were performed using genetic knockout cell lines.

### 2.3.1 *Stat1*/IFN- $\gamma$ -dependent Senescence Induction in Cancer Cells

Growth arrest assay with *Stat1*<sup>-/-</sup>  $\beta$ -cancer cells were performed to address the role of IFN signaling *in vitro*. No growth-inhibitory effect of the cytokines in the absence of *Stat1* were observed. Measurement of SA- $\beta$ -gal activity after 96 h treatment with the cytokine cocktail of IFN- $\gamma$  and TNF showed no change in the enzyme activity when compared with the medium-treated cells **(7) Figure 3a**. Treatment with only one cytokine failed to control  $\beta$ -cancer cell growth, which confirmed the need of IFN- $\gamma$  signaling for senescence induction **(1) Suppl. Fig. 6**.

### 2.3.2 *Tnfr1*/TNF-dependent Senescence Induction in Cancer Cells

*Tnfr1*<sup>-/-</sup> genetic knockout  $\beta$ -cancer cell lines did not achieve a status of senescence, which shows that the cofactor TNF is required for induction of senescence in a significant number of  $\beta$ -cancer cell lines from RT2 mice **(1) Figure 2c**.



### 2.3.3 Senescence Induction in Cytokine-dependent Cancer Immunotherapy

To test whether CIS can be detected in other tumor entities, we isolated primary cell lines from polyomavirus middle T antigen (PyV<sub>mT</sub>)-transgenic mice and treated cancer cells with IFN- $\gamma$  and TNF. Induction of the senescence markers SA- $\beta$ -gal and pHP1 $\gamma$  showed responsiveness of PyV<sub>mT</sub>-driven breast cancer cells to CIS **(1) Suppl. Fig. 10**. Further analysis were performed in human A-204 rhabdomyosarcoma cells and the induction of CIS was detected on the basis of proliferation and Rb1 phosphorylation **(1) Suppl. Fig. 11**. As A-204 cells are an established cell line with reliable CIS induction, the signal transduction was analyzed and gained insight in the Ago2 nuclear translocation and its potential importance for CIS **(5) Figures 2-6**.

In addition, various other cancer cell lines like melanoma (MALME-3M), lung cancer (HOP-62), colon cancer (COLO-205), ovarian cancer (OVCAR-5), and cancer cells from the central nervous system (SNB-75, SF-295) performed a permanent growth arrest after IFN- $\gamma$  and TNF treatment **(1) Suppl. Tab 2**, as well as in primary human cancer cells **(1) Suppl. Tab 3**, and **(7) Figure 10e**. The broad response of tumor cell lines to IFN- $\gamma$  and TNF suggests a fundamental relevance of CIS as a tumor control mechanism.

### 2.3.4 *Cdkn2a*-dependent Senescence Induction in Cancer Cells

Cell cycle control genes, especially p16<sup>Ink4a</sup>, are functionally relevant for senescence induction (see chapter 1.3.1, 1.3.2). Thus, models to delete the responsible gene locus for p16<sup>Ink4a</sup>, *Cdkn2a*, were generated in order to directly address the senescence mechanism in  $\beta$ -cancer cells. To test the validity of the hypothesis, three different approaches for the *Cdkn2a* depletion were chosen. First, a pool of seven different short hairpin RNAs (shRNA) targeting *Cdkn2a* was used **(1) Suppl. Fig. 9** to generate a p16<sup>Ink4a</sup>/p19<sup>Arf</sup>  $\beta$ -cancer cell line (*shp16-p19*). Growth arrest assay analysis revealed that CIS was *Cdkn2a*-dependent **(1) Figure 2f**. Second, a *Cdkn2a*-specific CRISPR/Cas9 transfected  $\beta$ -cancer cell line (RT2.CRISPR-*Cdkn2a*) was generated. Growth arrest and SA- $\beta$ -gal staining assay showed, that RT2.CRISPR-*Cdkn2a*  $\beta$ -cancer cells were resistant to senescence induction, whereas control-transfected  $\beta$ -cancer cells were susceptible to CIS. **(7) Figure 3c**. Third, spontaneous *Cdkn2a* loss mutants (RT2.*Cdkn2a*<sup>-/-</sup>) were analyzed **(7) Suppl. Fig. 5**. These RT2.*Cdkn2a*<sup>-/-</sup>  $\beta$ -cancer cells were resistant to CIS, but susceptible to apoptosis *in vitro* **(7) Figure 3b**. Together, depletion of *Cdkn2a*, resulted in loss of senescence induction in  $\beta$ -cancer cells, suggesting that IFN- $\gamma$ - and TNF-induced

senescence via regulation of the p16<sup>Ink4a</sup>/Rb1 cell cycle checkpoints is a crucial mechanism for immune therapy-mediated cancer control.

## 2.4 Tumor Intrinsic Conditions for Efficient Immunotherapy

We have shown that CIS requires IFN- $\gamma$ -, TNF- and p16<sup>Ink4a</sup>-signaling within the tumor cells *in vitro*. Solid tumors are known to evolve immunoediting strategies and create favorable conditions for their growth by recruitment of protumoral immune cells. Therefore, we asked whether CIS takes place in immunocompetent mice *in vivo*. We transplanted  $\beta$ -cancer cells with in wild type mice to analyze the role of the immune system during immunotherapy with anti-PD-L1 and anti-LAG-3 mAbs.

### 2.4.1 Efficient Responses in Mice with Ectopic Insulinomas using ICB Therapy

We used genetic knockout  $\beta$ -cancer cells to address the tumor intrinsic signaling pathways. We depleted the CD8<sup>+</sup> T cell with mAbs to focus on the CD4<sup>+</sup> T<sub>H</sub>1 cell response. Once tumor had reached the critical size of 3 mm in diameter, established tumors were treated with isotype control or ICB therapy **(7) Suppl. Fig. 1b**. We used RT2-, RT2.*Stat1*<sup>-/-</sup>-, RT2.*Cdkn2a*<sup>-/-</sup>-, and RT2.CRISPR-*Cdkn2a*-cancer cells, which were previously characterized by *in vitro* experiments. All tumors, irrespective of their genetic background, grew subcutaneously in mice. In the control groups the tumor volume increased exponentially **(7) Figure 1**. ICB therapy induced either a growth arrest or a continuous tumor regression in mice injected with the RT2  $\beta$ -cancer cells. Six of ten analyzed tumors were completely eradicated; in three mice small residual tumor load were found, and in one mouse the tumor size was retained at the initial level. In sharp contrast, RT2.*Stat1*<sup>-/-</sup> cancer cells were completely resistant to ICB therapy. Highlighted the role of IFN- $\gamma$  signaling for ICB therapy. Likewise, RT2.*Cdkn2a*<sup>-/-</sup>-, and RT2.CRISPR-*Cdkn2a*-cancer cells, did not respond to ICB therapy, showing that senescence induction via *Cdkn2a* induction is required for tumor control in ICB therapy **(7) Figure 1**. These experiments clearly demonstrate that efficient ICB did not only require *Stat1*-signaling, but *Stat1*-induced *Cdkn2a*. These proof of concept experiments showed that a functional senescence-signaling pathway is needed within the RT2  $\beta$ -cancer cells for an efficient ICB therapy.

To examine senescence markers, immunofluorescence staining of Ki67 in combination with p16<sup>Ink4a</sup> were performed using tumor sections of the isolated s.c. tumor

lesions **(7) Figure 1b, c**. For each experimental group, isotype antibody control and ICB were compared. Immunofluorescence staining showed that Ki67 was absent and p16<sup>Ink4a</sup> was exclusively expressed in the RT2-cancer receiving ICB therapy. Only these tumors also expressed other senescence marker like p21<sup>Cip1</sup>, pHP1 $\gamma$ , H3K9me3, and SA- $\beta$ -gal **(7) Figure 2**. Together these data revealed that ICB required *Stat1*- and *Cdkn2a*-signaling within the tumor cells for senescence induction and tumor control in immunocompetent mice.

## 2.5 CIS is Required for Efficient ICB Therapy of $\lambda$ -MYC Lymphomas

*Stat1*-deficient cancers expressed neither p16<sup>Ink4a</sup> nor p21<sup>Cip1</sup> in immunofluorescence staining of endogenous RT2-cancers **(7) Figure 4d, e** and **Figure 6a** and transplanted RT2-cancers **(7) Figure 1b, c** and **Figure 2a**. Thus, besides p16<sup>Ink4a</sup>, senescence induction can also function via p21<sup>Cip1</sup> activation. As Tag2 expression causes a defect in p53 activation **(164)**, the downstream protein p21<sup>Cip1</sup> cannot be appropriately investigated in this model. Therefore, different cancer types sensitive to T cell-mediated rejection were used to investigate the role of p21<sup>Cip1</sup> for cancer immunotherapy. In  $\lambda$ -*MYC* mice, the human *MYC* oncogene is expressed under the control of the immunoglobulin  $\lambda$  enhancer leading to the development of endogenous B-cell lymphomas **(160)**. In  $\lambda$ -*MYC* mice and double transgenic  $\lambda$ -*MYC.p21*<sup>-/-</sup> mice the combination of anti-PD-1 and anti-CTLA-4 mAbs were used in a treatment regime of two to four times every ten days, starting at day 55 after birth.

### 2.5.1 IFN- $\gamma$ -dependent Senescence Induction in $\lambda$ -*MYC* Lymphomas

To investigate the role of IFN- $\gamma$  signaling during ICB therapy in the  $\lambda$ -*MYC* mouse model, mice were treated with anti-IFN- $\gamma$  mAbs before ICB treatment and compared the overall survival of the mice with ICB-treated mice and untreated mice. ICB therapy significantly prolonged the life of  $\lambda$ -*MYC* mice. The cancer progression was delayed in 18 % of the mice for more than 250 days, whereas all untreated mice died within 150 days. Inhibiting the IFN- $\gamma$  signaling with blocking mAbs abolished the effect of the ICB therapy completely **(7) Figure 8a**. Immunotherapy effectively delayed the growth of these B-cell lymphomas and preserves normal lymph node structure **(7) Suppl. Fig. 12a**. Immunofluorescence staining of B cells in the lymph node showed an increase of p16<sup>Ink4a</sup>

and p21<sup>Cip1</sup> after ICB therapy, whereas the untreated and ICB/anti-IFN- $\gamma$  treatment group showed no expression of the cell cycle inhibitors **(7) Figure 8b**. Quantification of individual mice for each treatment group revealed a clear and significant induction of p16<sup>Ink4a</sup> exclusively after ICB treatment with simultaneous reduction of Ki67. These markers of senescence were absent in untreated and ICB/anti-IFN- $\gamma$  B cells **(7) Figure 8c**, suggesting that only mice with a functional IFN- $\gamma$  signaling can respond to ICB therapy.

### 2.5.2 p21<sup>Cip1</sup>-dependent Senescence Induction in $\lambda$ -MYC Lymphomas

To test whether ICB-mediated lymphoma prevention required the senescence-inducing p21<sup>Cip1</sup>, we generated syngeneic  $\lambda$ -MYC.p21<sup>Cip1</sup><sup>-/-</sup> mice. In  $\lambda$ -MYC.p21<sup>Cip1</sup><sup>-/-</sup> mice, ICB treatment failed to significantly improve the overall survival compared to untreated  $\lambda$ -MYC mice. B cells were Ki67 positive and negative for the CDK inhibitors p16<sup>Ink4a</sup>, p21<sup>Cip1</sup> **(7) Figure 8b, e**.

Immunotherapy failure could be part of an immune evasion mechanism of the cancer cells. Therefore, the expression of PD-L1 and  $\beta$ 2M was measured under all treatment conditions. As their expression was detected in the B-cell regions of the lymph node **(7) Suppl. Fig. 12b**, silencing of the IFN- $\gamma$  pathway did not prevent PD-1 binding ability or antigen presentation.

$\lambda$ -MYC mice did not respond to immunotherapy if the IFN- $\gamma$  or p21<sup>Cip1</sup> signaling was disturbed. To investigate whether this effect is due to senescence, we stained markers for senescence-associated epigenetic histone modifications pHP1 $\gamma$  and H3K9me3 expression were present in ICB-treated B cells of the lymph nodes and absent in the control group, in the ICB/anti-IFN- $\gamma$  treatment group, and in the ICB-treated  $\lambda$ -MYC.p21<sup>Cip1</sup><sup>-/-</sup> group. 90% of B cells in the lymph nodes of ICB-treated mice were SA- $\beta$ -gal positive, whereas ICB-treated- $\lambda$ -MYC.p21<sup>Cip1</sup><sup>-/-</sup> mice had only 14% SA- $\beta$ -gal positive B cells. In IFN-depleted ICB-treated mice and untreated mice, the average value was 8% SA- $\beta$ -gal staining. These data demonstrated that treatment of  $\lambda$ -MYC mice with ICB resulted in strong induction of the biomarker for cellular senescence **(7) Figure 8c**.

As ICB therapy can modulate T cell population frequencies and can activate CD8<sup>+</sup> T cells, and NK cells as effector cells, we stained cytotoxic T cells in fresh cryosections of the lymph nodes. Both, CD8<sup>+</sup> T cells and NK cells were present in small numbers in the pre-malignant B cell regions of ICB-treated mice and in the regions of B-cell lymphomas

of untreated, ICB/ $\lambda$ -MYC.p21<sup>Cip1</sup><sup>-/-</sup> and ICB/anti-IFN- $\gamma$ -treated mice, suggesting that T cell dependent lysis were not substantially involved in ICB therapy in  $\lambda$ -MYC mice **(7) Suppl. Fig. 12d**.

Cancer control mechanisms via immunotherapy can act via stress response on DNA level, hence we analyzed  $\gamma$ H2AX and DNA-PK. No signs of DNA double strand breaks after ICB therapy in  $\lambda$ -MYC mice were found **(7) Suppl. Fig. 12e**, suggesting that the delay of B-cell lymphoma development is a result of CIS.

The ICB treatment of  $\lambda$ -MYC mice revealed that p21<sup>Cip1</sup> activation was required to prevent the transition of pre-malignant B cells into B-cell lymphomas and that this mechanism was IFN- $\gamma$ -dependent and leads to an upregulation of senescence markers in B cells.

## 2.6 CIS is Required for Efficient ICB Therapy of Human Melanoma Metastases

ICB therapy can control tumor growth through by activating cell cycle arrest via cytokines. **Figure 4** shows molecules that are involved in CIS.

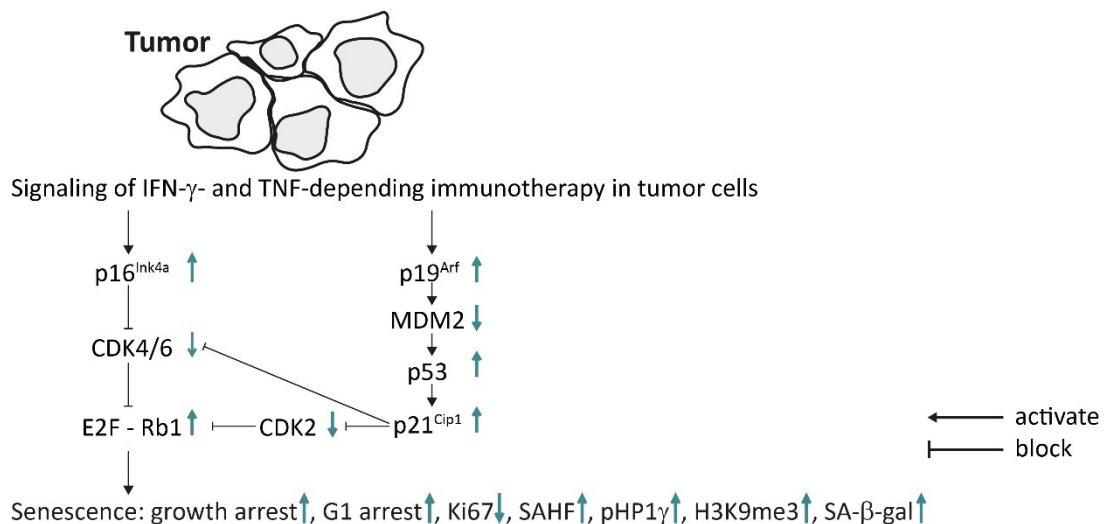


**Figure 4. Immunotherapy activates senescence mechanisms within the tumor cell.**

Immunotherapy with the T<sub>H</sub>1 cell cytokines IFN- $\gamma$  and TNF or ICB leads to increased expression of the tumor suppressor proteins p16<sup>Ink4a</sup>, p19<sup>Arf</sup> (p14<sup>Arf</sup> respectively in humans), and p21<sup>Cip1</sup>. This leads to suppression of the cyclin-dependent kinases CDK2, 4, 6. This suppresses the phosphorylation of the tumor suppressor protein Rb1 and thus the transcription of E2F-regulated promoters leading to induction of senescence of the tumor cells. Tumor control was measured via growth arrest, G1-arrest and loss of Ki67 expression. Senescence-associated epigenetic and metabolic modifications was detected by increased pHP1 $\gamma$ , H3K9me3 and SA- $\beta$ -gal.

To determine, whether ICB of melanoma metastases requires CIS, we genetically analyzed the frequencies of functionally inactivating mutations, losses or amplifications of these key signaling molecules in the senescence pathways. Therefore, we retrospectively analyzed melanoma metastases from patients with either regressing or with progressing metastases during ICB treatment. We sequenced melanoma biopsies after ICB therapy and compared the genetic alterations with the appropriate healthy tissue controls. In total, 42 patient samples collected during clinical routine were analyzed by targeted panel sequencing of 678 established cancer-associated genes. The panels were designed to detect somatic mutations (SNVs), small insertions and deletions (INDELs), copy number variations (CNVs,) and selected structural rearrangements. The sequencing reads were aligned to the human genome reference sequence. We focused exclusively on genes potentially relevant for IFN-dependent induction of senescence. Gene mutations from non-responder and responder patients were compared. Precisely named the gene sequences of the protein-tyrosine kinases *JAK1/2/3* that plays a key role in IFN signal transduction, the tumor suppressor genes *RB1* and *TP53*, the nuclear-localized E3 ubiquitin ligase MDM2/4 proto-oncogenes that can promote tumor formation by suppressing p53 (MDM2/4), the MYC proto-oncogene (*MYC*), the kinase inhibitors p21<sup>Cip1</sup>, p27<sup>Kip1</sup>, p16<sup>Ink4a</sup>/p14<sup>Arf</sup>, p15<sup>Ink4b</sup>, and p18<sup>Ink4c</sup> (*CDKN1A/B*, *CDKN2A/B/C*), the cyclin-dependent kinases 4/6 (*CDK4/6*), the cyclins D1/2/3 (*CCND1/2/3*), and cyclin E1 (*CCNE1*). Melanoma metastases of non-responder patients had significantly higher numbers of genes with severe fully inactivating mutations in CNVs of senescence-inducing cell cycle genes (*JAK1/2/3*, *RB1*, *TP53*, *CDKN1A/B*, *CDKN2A/B/C*) or more than threefold amplifications of genes promoting cell cycle progression (*MDM2/4*, *MYC*, *CDK4/6*, *CCND1/2/3*, *CCNE1*) than the melanoma metastases from responder patients **(7) Figure 10c, Suppl. Fig. 13 and 14**. These data confirmed that severe genetic aberrations of the CIS signaling pathways, which had previously identified as important for functional inactivation of CIS and ICB therapy in mice, were also significantly associated with a poor response to ICB therapy in humans.

To examine, whether melanoma metastases from patients not responding to cancer immunotherapy, are also resistance to CIS, we used isolated cells cultured from melanoma metastases to perform growth arrest assays. Indeed, primary melanoma cell lines generated from patients resistant to ICB therapy **(7) Figure 10d** also did not respond to CIS. In contrast, isolated primary melanoma cell lines from patients

responding to ICB therapy respond to CIS **(7) Figure 10e**. In conclusion, it seems reasonable to conclude that senescence pathways in melanoma metastases were necessary for responsiveness to ICB therapy. Mapping of senescence pathways will predict the efficacy of immunotherapy in patients with metastatic melanomas and possible also other cancers, but this prediction has yet to be confirmed by larger cohorts. As impaired senescence pathways in melanomas seem to be of high relevance for resistance to ICB, it is important to develop strategies to overcome these resistance mechanisms. It is likely that IFN- $\gamma$ -induced immune effects are not only required for ICB therapy-induced senescence but also other IFN- $\gamma$ -induced immune effects. Therefore, combining ICB therapy with CDK4/6 inhibitors may be a promising approach to overcome resistance in patients with melanoma that carry major defects in the senescence signaling pathways required for CIS.

# Figures

Figure 1. Cytokine therapy as soluble anticancer immunity.	24
Figure 2. Tumor responses to cancer immunotherapies.	28
Figure 3. AT/ICB therapy with CD4 <sup>+</sup> T <sub>H</sub> 1 cells, anti-PD-L1 mAbs, and anti-LAG-3 mAbs.	34
Figure 4. Immunotherapy activates senescence mechanisms within the tumor cell.	45



# Figures Appendix

## (1) T-helper-1-cell cytokines drive cancer into senescence

- Figure 1 Combined, the T<sub>H</sub>1 cytokines IFN- $\gamma$  and TNF induce stable growth arrest of Tag-driven  $\beta$ -cancer cells *in vitro*. A2
- Figure 2 *Stat1*- and *TNFR1*-dependent stabilization of the p16<sup>Ink4a</sup>-Rb senescence pathway in  $\beta$ -cancer cells by the combined action and TNF *in vitro*. A2
- Figure 3 *TNFR1*-dependent induction of growth arrest and senescence in  $\beta$ -cancer cells by T<sub>H</sub>1 immunity *in vivo*. A3
- Figure 4 T<sub>H</sub>1 immunity induces *TNFR1*-dependent, permanent growth arrest of  $\beta$ -cancer cells that remains stable for  $\geq 10$  weeks, even after transfer into immune-deficient NOD-*ScidII2rg*<sup>-/-</sup> mice. A4
- Suppl. Fig. 1 Treatment of RIP1-Tag2 mice with IFN- $\gamma$ - and TNF-secreting Tag- T<sub>H</sub>1 cells leads to *TNFR1*-dependent stabilization of blood glucose levels, and arrests islet cancer growth *in vivo*. A8
- Suppl. Fig. 2 CD3-positive T cells surrounding an endocrine  $\beta$ -cell tumor. A9
- Suppl. Fig. 3  $\beta$ -cancer cells fail to express MHC class II either *in vivo* or *in vitro* and are not lysed by Tag- T<sub>H</sub>1 cells *in vitro*. A10
- Suppl. Fig. 4 Treatment of RIP1-Tag2 mice with Tag- T<sub>H</sub>1 cells leads to inhibition of  $\beta$ -cancer cell proliferation *in vivo* and *ex vivo*. A11
- Suppl. Fig. 5 T<sub>H</sub>1 immunity and IFN- $\gamma$  do not suppress Tag expression. A12
- Suppl. Fig. 6 Combined IFN- $\gamma$  and TNF treatment but neither IFN- $\gamma$  alone nor TNF alone induce stable growth arrest in isolated  $\beta$ -cancer cells *in vitro*. A13
- Suppl. Fig. 7 Nuclear recruitment of pHP1 $\gamma$  into senescence-associated heterochromatin foci (SAHF) after IFN- $\gamma$ , TNF, or combined IFN- $\gamma$  and TNF treatment in isolated  $\beta$ -cancer cells *in vitro*. A14
- Suppl. Fig. 8 SA- $\beta$ -galactosidase activity in synaptophysin-positive  $\beta$ -cancer cells after treatment with IFN- $\gamma$  *in vitro*. A15
- Suppl. Fig. 9 Knock-down of p16<sup>Ink4a</sup> by the use of shRNA. A16
- Suppl. Fig. 10 Induction of SA- $\beta$ -galactosidase activity and nuclear recruitment of pHP1 $\gamma$  into SAHF after combined IFN- $\gamma$  and TNF treatment in isolated PyVmT-driven breast cancer cells *in vitro*. A17

Suppl. Fig. 11 Combined IFN- $\gamma$ and TNF treatment induces stable growth arrest and profound Rb hypophosphorylation in A-204 rhabdomyosarcoma cells.	A18
Suppl. Fig. 12 Expression of the proliferation marker MIB and the senescence marker p16 <sup>Ink4a</sup> in regressing melanoma.	A19
Suppl. Fig. 13 Induction of nuclear and cytoplasmic p16 <sup>Ink4a</sup> by T <sub>H</sub> 1 immunity <i>in vivo</i> (higher magnification from Fig. 3c).	A20
Suppl. Fig. 14 Failure of Tag- T <sub>H</sub> 1 cells to induce senescence markers in <i>TNFR1</i> <sup>-/-</sup> xRIP1-Tag2 mice <i>in vivo</i> .	A21
Suppl. Fig. 15 T <sub>H</sub> 1-immunity induces permanent growth arrest of $\beta$ -cancer cells which remains stable for 6 passages of <i>in vitro</i> culture.	A22
Suppl. Fig. 16 p16 <sup>Ink4a</sup> -independent induction of the chemokines CXCL9 and CXCL10 by combined IFN- $\gamma$ and TNF in RIP1-Tag2 $\beta$ -cancer cells.	A23

## **(2) Changing T-cell enigma**

Figure 1 Eradication vs. control of tumors.	A30
Figure 2 Suggested cytokine signaling leading to tumor cell senescence.	A31
Figure 3 Cytokine-mediated control of tumor cell growth by senescence induction.	A23

## **(3) Immunotherapy of melanoma: efficacy and mode of action**

Figure 1 Clinical appearance of a melanoma with areas marked both by regression and progression.	A38
Figure 2 Overall survival of melanoma patients with metastatic disease.	A40
Figure 3 Mechanisms of immunotherapies.	A40
Figure 4 Targets of modern cancer therapy.	A42

## **(4) Cytokine-induced senescence for cancer surveillance**

Figure 1 Cellular senescence in aging, embryogenesis, and tumorigenesis.	A47
Figure 2 Pathways of therapy-induced tumor cell senescence.	A49
Figure 3 Toxic and non-toxic pathways of immune system-mediated tumor suppression.	A50

## **(5) Nuclear Translocation of Argonaute 2 in Cytokine-Induced Senescence**

- Figure 1 Doxorubicin induces growth arrest, SA- $\beta$ -galactosidase activity, inhibition of BrdU incorporation and nuclear Ago2 translocation in MCF-7 cells. A60
- Figure 2 IFN- $\gamma$  and TNF induce senescence and nuclear Ago2 translocation in human cancer cells. A61
- Figure 3 Kinetics of cytokine-induced Ago2 translocation. A62
- Figure 4 Ago2 shuttling between the nucleus and cytosol. A63
- Figure 5 Repression of Ago2-regulated cell cycle control genes after cytokine treatment of cancer. A64
- Figure 6 Knockdown of Ago2 in A-204 cells by the use of siRNA. A65
- Figure 7 Influence of Ago2 knockdown on INF- $\gamma$ - and TNF-mediated growth behavior of A-204 cells. A66

## **(6) Immune checkpoint blockade therapy**

- Figure 1 Time course of immune responses with or without immune therapy. A72
- Figure 2 Molecular mechanisms of T-cell inhibition by immune checkpoints. A73
- Figure 3 Cytotoxic tumor reduction and consolidation phase during ICB. A74
- Figure 4 The dual role of IFN signaling during ICB: cytokine-induced regulation of PD-1 versus cytokine induced antitumor effects. A77

## **(7) Cancer immune control needs senescence induction by interferon-dependent cell cycle regulator pathways in tumours**

- Figure 1 *Stat1*- and *Cdkn2a*-dependent immune control of transplanted RT2-cancers and induction of Ki67-p16<sup>Ink4a+</sup> senescent cancer cells. A85
- Figure 2 *Stat1*- and *Cdkn2a*-dependent induction of the senescence markers pHP1 $\gamma$ , H3K9me3, and of SA- $\beta$ -gal in transplanted RT2-cancers. A87
- Figure 3 *Stat1*- and *Cdkn2a*-dependent induction of cytokine-induced senescence (CIS) in RT2-cancer cells, but independent induction of apoptosis. A89
- Figure 4 *Stat1*-dependent immune control of endogenous RT2-cancers and induction of Ki67-p16<sup>Ink4a+</sup> senescent cancer cells. A91

- Figure 5 Infiltration of either RT2 or RT2.*Stat1*<sup>-/-</sup> cancers by CD3<sup>+</sup> T cells, mRNA expression of tumour associated antigens (TAA) and protein expression of the SV40-Tag tumour antigen recognised by the transferred TAA-specific T<sub>H</sub>1 cells. A92
- Figure 6 *Stat1*-dependent induction of the nuclear senescence markers p21<sup>Cip1</sup>, pHP1 $\gamma$ , H3K9me3, and of SA- $\beta$ -gal in RT2-cancers by combined ICB/AT therapy. A93
- Figure 7 *Stat1*-dependent induction of senescence in RT2-cancers by combined ICB/AT therapy. A94
- Figure 8 IFN- $\gamma$  and p21<sup>Cip1</sup>-dependent immune control of  $\lambda$ -MYC-induced lymphomas by ICB therapy. A95
- Figure 9 IFN- $\gamma$  and p21<sup>Cip1</sup>-dependent senescence induction in B cells of  $\lambda$ -MYC mice during ICB. A96
- Figure 10 Loss of senescence-inducing and amplification of senescence-inhibiting cell cycle regulator genes in melanoma metastases of patients resistant to ICB. A97
- Suppl. Fig. 1 Treatment protocol depicting the immune therapy of transplanted RT2-cancers and the ability for CD8 T cell-mediated killing of RT2 and of RT2.*Stat1*<sup>-/-</sup>-cancer cells *in vitro*. A103
- Suppl. Fig. 2 Illustration of the digital image-processing, and of the calculation of the percentage of SA- $\beta$ -gal positive tumour cells within a tumour area. A104
- Suppl. Fig. 3 Absence of ICB-induced DNA double-strand break-associated  $\gamma$ H2AX or DNA-PK expression. A105
- Suppl. Fig. 4 PD-L1 or  $\beta$ 2-microglobulin protein expression. A106
- Suppl. Fig. 5 Genomic profiles of Cdkn2a-deficient variants of RT2-cancer cells and their parental RT2-cancer cells, expression of Cdkn2a mRNA and their engraftment *in vivo*. A108
- Suppl. Fig. 6 Infiltration of CD3<sup>+</sup>CD8<sup>-</sup> T cells and of F4/80<sup>+</sup> macrophages but absence of CD49b<sup>+</sup> NK cells in transplanted tumours after immune checkpoint blockade therapy. A110
- Suppl. Fig. 7 Treatment protocol depicting the immune therapy of either RT2 mice or RT2.*Stat1*<sup>-/-</sup> mice with advanced RT2-cancers. A111
- Suppl. Fig. 8 Immune infiltration and PD-L1 expression in cancers from RT2 mice or RT2.*Stat1*<sup>-/-</sup> mice. A112

- Suppl. Fig. 9 Absence of DNA double-strand break-associated  $\gamma$ H2AX or DNA-PK expression following immune therapy of RT2-cancers. A114
- Suppl. Fig. 10 Cytoplasmic localisation of SA- $\beta$ -gal in ultrathin sections. A115
- Suppl. Fig. 11 Presence of CD4<sup>+</sup> T cells, CD11c<sup>+</sup> and CD11b<sup>+</sup> leukocytes in the tumour microenvironment of RT2-cancers from either RT2 mice or RT2.*Stat1*<sup>-/-</sup> mice following the injection of Tag-specific T<sub>H</sub>1 cells (AT). A116
- Suppl. Fig. 12 Immune therapy with anti-CTLA-4 mAb and anti-PD-1 mAb of  $\lambda$ -MYC mice preserves the normal lymph node structure without inducing DNA-double strand breaks. A117
- Suppl. Fig. 13 Function-determining aberrations of IFN- $\gamma$ -dependent cell cycle regulator genes are increased in melanoma metastases not responding to ICB therapy. A118
- Suppl. Fig. 14 Schematic overview of the cell cycle control genes and their functional gains and losses in metastases of non-responder patients. A119

# Tables

Table 1. Immune checkpoints used in this study and their clinical description.

22

# Tables Appendix

## **(1) T-helper-1-cell cytokines drive cancer into senescence**

Suppl. T 1	Expression of cytokine receptors, and IFN- $\gamma$ - and TNF-induced anticancer effects in 6 murine cancer cell lines.	A24
Suppl. T 2	Expression of cytokine receptors, and IFN- $\gamma$ - and TNF-induced anticancer effects in 11 human cancer cell lines.	A25
Suppl. T 3	IFN- $\gamma$ - and TNF-induced anticancer effects in 6 primary human cancer cell preparations.	A26
Suppl. T 4	Clinical and pathological characterization of patients.	A27
Suppl. T 5	shRNA sequence for deletion of Cdkn2a in primary RT2-cell lines.	A28

## **(6) Immune checkpoint blockade therapy**

Suppl. T 1	Frequently applied treatment algorithm for patients with metastatic melanoma where surgery is no longer applicable.	A79
------------	---	-----

# References

1. Braumuller H, *et al.* T-helper-1-cell cytokines drive cancer into senescence. *Nature* **494**, 361-365 (2013).
2. Wieder T, Braumuller H, Brenner E, Zender L, Rocken M. Changing T-cell enigma: cancer killing or cancer control? *Cell Cycle* **12**, 3146-3153 (2013).
3. Wieder T, Brenner E, Braumuller H, Rocken M. Immunotherapy of melanoma: efficacy and mode of action. *J Dtsch Dermatol Ges* **14**, 28-36 (2016).
4. Wieder T, Brenner E, Braumuller H, Bischof O, Rocken M. Cytokine-induced senescence for cancer surveillance. *Cancer Metastasis Rev* **36**, 357-365 (2017).
5. Rentschler M, *et al.* Nuclear translocation of argonaute 2 in cytokine-induced senescence. *Cell Physiol Biochem* **51**, 1103-1118 (2018).
6. Wieder T, Eigentler T, Brenner E, Rocken M. Immune checkpoint blockade therapy. *J Allergy Clin Immunol* **142**, 1403-1414 (2018).
7. Brenner E, *et al.* Cancer immune control needs senescence induction by interferon-dependent cell cycle regulator pathways in tumours. *Nature communications* **11**, 1335 (2020).
8. Muller-Hermelink N, *et al.* TNFR1 signaling and IFN-gamma signaling determine whether T cells induce tumor dormancy or promote multistage carcinogenesis. *Cancer Cell* **13**, 507-518 (2008).
9. Hanahan D. Heritable formation of pancreatic [beta]-cell tumours in transgenic mice expressing recombinant insulin/simian virus 40 oncogenes. *Nature* **315**, 115-122 (1985).
10. Forster I, Hirose R, Arbeit JM, Clausen BE, Hanahan D. Limited capacity for tolerization of CD4+ T cells specific for a pancreatic beta cell neo-antigen. *Immunity* **2**, 573-585 (1995).
11. Racke MK, *et al.* Cytokine-induced immune deviation as a therapy for inflammatory autoimmune disease. *J Exp Med* **180**, 1961-1966 (1994).
12. Röcken M, Urban JF, Shevach EM. Infection breaks T-cell tolerance. *Nature* **359**, 79-82 (1992).
13. Biedermann T, *et al.* IL-4 instructs TH1 responses and resistance to *Leishmania major* in susceptible BALB/c mice. *Nat Immunol* **2**, 1054-1060 (2001).



14. Ziegler A, *et al.* EpCAM, a human tumor-associated antigen promotes Th2 development and tumor immune evasion. *Blood* **113**, 3494-3502 (2009).
15. Hanahan D, Weinberg RA. The hallmarks of cancer. *Cell* **100**, 57-70 (2000).
16. Hanahan D, Weinberg RA. Hallmarks of cancer: the next generation. *Cell* **144**, 646-674 (2011).
17. Radvanyi F, Christgau S, Baekkeskov S, Jolicoeur C, Hanahan D. Pancreatic beta cells cultured from individual preneoplastic foci in a multistage tumorigenesis pathway: a potentially general technique for isolating physiologically representative cell lines. *Mol Cell Biol* **13**, 4223-4232 (1993).
18. Schumacher TN, Schreiber RD. Neoantigens in cancer immunotherapy. *Science* **348**, 69-74 (2015).
19. Ishida Y, Agata Y, Shibahara K, Honjo T. Induced expression of PD-1, a novel member of the immunoglobulin gene superfamily, upon programmed cell death. *EMBO J* **11**, 3887-3895 (1992).
20. Harding FA, McArthur JG, Gross JA, Raulet DH, Allison JP. CD28-mediated signalling co-stimulates murine T cells and prevents induction of anergy in T-cell clones. *Nature* **356**, 607-609 (1992).
21. Alfarrar H, Weir J, Grieve S, Reiman T. Targeting NK cell inhibitory receptors for precision multiple myeloma immunotherapy. *Front Immunol* **11**, 575609 (2020).
22. Sharma P, Hu-Lieskovan S, Wargo JA, Ribas A. Primary, adaptive, and acquired resistance to cancer immunotherapy. *Cell* **168**, 707-723 (2017).
23. Bae SI, Cheriya V, Jacobs BS, Reu FJ, Borden EC. Reversal of methylation silencing of Apo2L/TRAIL receptor 1 (DR4) expression overcomes resistance of SK-MEL-3 and SK-MEL-28 melanoma cells to interferons (IFNs) or Apo2L/TRAIL. *Oncogene* **27**, 490-498 (2008).
24. Raisova M, *et al.* The Bax/Bcl-2 ratio determines the susceptibility of human melanoma cells to CD95/Fas-mediated apoptosis. *J Invest Dermatol* **117**, 333-340 (2001).
25. Gorgoulis V, *et al.* Cellular senescence: defining a path forward. *Cell* **179**, 813-827 (2019).
26. Tran E, Robbins PF, Rosenberg SA. 'Final common pathway' of human cancer immunotherapy: targeting random somatic mutations. *Nat Immunol* **18**, 255-262 (2017).

27. Kane LP, Andres PG, Howland KC, Abbas AK, Weiss A. Akt provides the CD28 costimulatory signal for up-regulation of IL-2 and IFN-gamma but not TH2 cytokines. *Nat Immunol* **2**, 37-44 (2001).
28. Dranoff G. Cytokines in cancer pathogenesis and cancer therapy. *Nat Rev Cancer* **4**, 11-22 (2004).
29. Nguyen LT, *et al.* Phase II clinical trial of adoptive cell therapy for patients with metastatic melanoma with autologous tumor-infiltrating lymphocytes and low-dose interleukin-2. *Cancer Immunol Immunother* **68**, 773-785 (2019).
30. Galon J, *et al.* Type, density, and location of immune cells within human colorectal tumors predict clinical outcome. *Science* **313**, 1960-1964 (2006).
31. Weide B, *et al.* Functional T cells targeting NY-ESO-1 or Melan-A are predictive for survival of patients with distant melanoma metastasis. *J Clin Oncol* **30**, 1835-1841 (2012).
32. Ayers M, *et al.* IFN- $\gamma$ -related mRNA profile predicts clinical response to PD-1 blockade. *J Clin Invest* **127**, 2930-2940 (2017).
33. Gajewski TF, Corrales L, Williams J, Horton B, Sivan A, Spranger S. Cancer immunotherapy targets based on understanding the T cell-inflamed versus non-T cell-inflamed tumor microenvironment. *Adv Exp Med Biol* **1036**, 19-31 (2017).
34. Yazdi AS, *et al.* Heterogeneity of T-cell clones infiltrating primary malignant melanomas. *J Invest Dermatol* **126**, 393-398 (2006).
35. Boon T, Coulie PG, Van den Eynde BJ, van der Bruggen P. Human T cell responses against melanoma. *Annu Rev Immunol* **24**, 175-208 (2006).
36. Kroemer G, Senovilla L, Galluzzi L, Andre F, Zitvogel L. Natural and therapy-induced immunosurveillance in breast cancer. *Nat Med* **21**, 1128-1138 (2015).
37. Blank CU, Haanen JB, Ribas A, Schumacher TN. Cancer immunology. The "cancer immunogram". *Science* **352**, 658-660 (2016).
38. Robert C, *et al.* Nivolumab in previously untreated melanoma without BRAF mutation. *N Engl J Med* **372**, 320-330 (2015).
39. Garon EB, *et al.* Pembrolizumab for the treatment of non-small-cell lung cancer. *N Engl J Med* **372**, 2018-2028 (2015).
40. Postow MA, *et al.* Nivolumab and ipilimumab versus ipilimumab in untreated melanoma. *N Engl J Med* **372**, 2006-2017 (2015).

41. Pulko V, *et al.* B7-h1 expressed by activated CD8 T cells is essential for their survival. *J Immunol* **187**, 5606-5614 (2011).
42. Juneja VR, *et al.* PD-L1 on tumor cells is sufficient for immune evasion in immunogenic tumors and inhibits CD8 T cell cytotoxicity. *J Exp Med* **214**, 895-904 (2017).
43. Couzin-Frankel J. Breakthrough of the year 2013. Cancer immunotherapy. *Science* **342**, 1432-1433 (2013).
44. Leach DR, Krummel MF, Allison JP. Enhancement of antitumor immunity by CTLA-4 blockade. *Science* **271**, 1734-1736 (1996).
45. Kelly PN. The cancer immunotherapy revolution. *Science* **359**, 1344-1345 (2018).
46. Hodi FS, *et al.* Improved survival with ipilimumab in patients with metastatic melanoma. *N Engl J Med* **363**, 711-723 (2010).
47. Robert C, *et al.* Ipilimumab plus dacarbazine for previously untreated metastatic melanoma. *N Engl J Med* **364**, 2517-2526 (2011).
48. Eggermont AM, *et al.* Prolonged survival in stage III melanoma with ipilimumab adjuvant therapy. *N Engl J Med* **375**, 1845-1855 (2016).
49. Hellmann MD, *et al.* Nivolumab plus ipilimumab in advanced non-small-cell lung cancer. *N Engl J Med* **381**, 2020-2031 (2019).
50. Hellmann MD, *et al.* Tumor mutational burden and efficacy of nivolumab monotherapy and in combination with ipilimumab in small-cell lung cancer. *Cancer Cell* **33**, 853-861.e854 (2018).
51. Formenti SC, *et al.* Radiotherapy induces responses of lung cancer to CTLA-4 blockade. *Nat Med* **24**, 1845-1851 (2018).
52. Alaia C, *et al.* Ipilimumab for the treatment of metastatic prostate cancer. *Expert Opin Biol Ther* **18**, 205-213 (2018).
53. Beer TM, *et al.* Randomized, double-blind, phase III trial of ipilimumab versus placebo in asymptomatic or minimally symptomatic patients with metastatic chemotherapy-naive castration-resistant prostate cancer. *J Clin Oncol* **35**, 40-47 (2017).
54. Wei SC, *et al.* Negative co-stimulation constrains T cell differentiation by imposing boundaries on possible cell states. *Immunity* **50**, 1084-1098.e1010 (2019).
55. Liakou CI, *et al.* CTLA-4 blockade increases IFN $\gamma$ -producing CD4+ICOS $^+$ hi cells to shift the ratio of effector to regulatory T cells in cancer patients. *Proc Natl Acad Sci U S A* **105**, 14987-14992 (2008).

56. Diskin B, *et al.* PD-L1 engagement on T cells promotes self-tolerance and suppression of neighboring macrophages and effector T cells in cancer. *Nat Immunol* **21**, 442-454 (2020).
57. Okazaki T, *et al.* PD-1 and LAG-3 inhibitory co-receptors act synergistically to prevent autoimmunity in mice. *J Exp Med* **208**, 395-407 (2011).
58. Baixeras E, *et al.* Characterization of the lymphocyte activation gene 3-encoded protein. A new ligand for human leukocyte antigen class II antigens. *J Exp Med* **176**, 327-337 (1992).
59. Huard B, Gaulard P, Faure F, Hercend T, Triebel F. Cellular expression and tissue distribution of the human LAG-3-encoded protein, an MHC class II ligand. *Immunogenetics* **39**, 213-217 (1994).
60. Goding SR, *et al.* Restoring immune function of tumor-specific CD4+ T cells during recurrence of melanoma. *J Immunol* **190**, 4899-4909 (2013).
61. Matsuzaki J, *et al.* Tumor-infiltrating NY-ESO-1-specific CD8+ T cells are negatively regulated by LAG-3 and PD-1 in human ovarian cancer. *Proc Natl Acad Sci U S A* **107**, 7875-7880 (2010).
62. Nguyen LT, Ohashi PS. Clinical blockade of PD1 and LAG3 - potential mechanisms of action. *Nat Rev Immunol* **15**, 45-56 (2015).
63. Baumeister SH, Freeman GJ, Dranoff G, Sharpe AH. Coinhibitory Pathways in Immunotherapy for Cancer. *Annu Rev Immunol* **34**, 539-573 (2016).
64. Soularue E, *et al.* Enterocolitis due to immune checkpoint inhibitors: a systematic review. *Gut* **67**, 2056-2067 (2018).
65. Morgan RA, *et al.* Cancer regression in patients after transfer of genetically engineered lymphocytes. *Science* **314**, 126-129 (2006).
66. Rosenberg SA, Restifo NP, Yang JC, Morgan RA, Dudley ME. Adoptive cell transfer: a clinical path to effective cancer immunotherapy. *Nat Rev Cancer* **8**, 299-308 (2008).
67. Restifo NP, Dudley ME, Rosenberg SA. Adoptive immunotherapy for cancer: harnessing the T cell response. *Nat Rev Immunol* **12**, 269-281 (2012).
68. Hinrichs CS, Rosenberg SA. Exploiting the curative potential of adoptive T-cell therapy for cancer. *Immunol Rev* **257**, 56-71 (2014).
69. Mellman I, Coukos G, Dranoff G. Cancer immunotherapy comes of age. *Nature* **480**, 480-489 (2011).

70. Robbins PF, *et al.* Mining exomic sequencing data to identify mutated antigens recognized by adoptively transferred tumor-reactive T cells. *Nat Med* **19**, 747-752 (2013).
71. Patel SJ, *et al.* Identification of essential genes for cancer immunotherapy. *Nature* **548**, 537-542 (2017).
72. Wieder T, Braumuller H, Kneilling M, Pichler B, Rocken M. T cell-mediated help against tumors. *Cell Cycle* **7**, 2974-2977 (2008).
73. Griessinger CM, *et al.* In vivo tracking of Th1 cells by PET reveals quantitative and temporal distribution and specific homing in lymphatic tissue. *J Nucl Med* **55**, 301-307 (2014).
74. Effern M, *et al.* Adoptive T cell therapy targeting different gene products reveals diverse and context-dependent immune evasion in melanoma. *Immunity* **53**, 564-580.e569 (2020).
75. Landsberg J, *et al.* Melanomas resist T-cell therapy through inflammation-induced reversible dedifferentiation. *Nature* **490**, 412-416 (2012).
76. Coussens LM, Werb Z. Inflammation and cancer. *Nature* **420**, 860-867 (2002).
77. Murata M. Inflammation and cancer. *Environ Health Prev Med* **23**, 50 (2018).
78. Rosenberg SA, *et al.* Observations on the systemic administration of autologous lymphokine-activated killer cells and recombinant interleukin-2 to patients with metastatic cancer. *N Engl J Med* **313**, 1485-1492 (1985).
79. Weide B, *et al.* High response rate after intratumoral treatment with interleukin-2: results from a phase 2 study in 51 patients with metastasized melanoma. *Cancer* **116**, 4139-4146 (2010).
80. Rosenberg SA. IL-2: the first effective immunotherapy for human cancer. *J Immunol* **192**, 5451-5458 (2014).
81. Rosenberg SA, *et al.* Durable complete responses in heavily pretreated patients with metastatic melanoma using T-cell transfer immunotherapy. *Clin Cancer Res* **17**, 4550-4557 (2011).
82. Schwartzentruber DJ, *et al.* gp100 peptide vaccine and interleukin-2 in patients with advanced melanoma. *N Engl J Med* **364**, 2119-2127 (2011).
83. Topalian SL, *et al.* Safety, activity, and immune correlates of anti-PD-1 antibody in cancer. *N Engl J Med* **366**, 2443-2454 (2012).

84. Larkin J, *et al.* Combined Nivolumab and Ipilimumab or Monotherapy in Untreated Melanoma. *N Engl J Med* **373**, 23-34 (2015).
85. Kirkwood JM, *et al.* High-dose interferon alfa-2b significantly prolongs relapse-free and overall survival compared with the GM2-KLH/QS-21 vaccine in patients with resected stage IIB-III melanoma: results of intergroup trial E1694/S9512/C509801. *J Clin Oncol* **19**, 2370-2380 (2001).
86. Eggermont AM, *et al.* Post-surgery adjuvant therapy with intermediate doses of interferon alfa 2b versus observation in patients with stage IIB/III melanoma (EORTC 18952): randomised controlled trial. *Lancet* **366**, 1189-1196 (2005).
87. Gogas H, *et al.* Prognostic significance of autoimmunity during treatment of melanoma with interferon. *N Engl J Med* **354**, 709-718 (2006).
88. Dunn GP, Koebel CM, Schreiber RD. Interferons, immunity and cancer immunoediting. *Nat Rev Immunol* **6**, 836-848 (2006).
89. Tarhini AA, Gogas H, Kirkwood JM. IFN- $\alpha$  in the treatment of melanoma. *J Immunol* **189**, 3789-3793 (2012).
90. Yang X, *et al.* Targeting the tumor microenvironment with interferon-beta bridges innate and adaptive immune responses. *Cancer Cell* **25**, 37-48 (2014).
91. Eggermont AM, *et al.* Long term follow up of the EORTC 18952 trial of adjuvant therapy in resected stage IIB-III cutaneous melanoma patients comparing intermediate doses of interferon-alpha-2b (IFN) with observation: Ulceration of primary is key determinant for IFN-sensitivity. *Eur J Cancer* **55**, 111-121 (2016).
92. Ribas A, *et al.* Oncolytic virotherapy promotes intratumoral T cell infiltration and improves anti-PD-1 immunotherapy. *Cell* **170**, 1109-1119.e1110 (2017).
93. Kammertoens T, *et al.* Tumour ischaemia by interferon-gamma resembles physiological blood vessel regression. *Nature* **545**, 98-102 (2017).
94. Benci JL, *et al.* Opposing functions of interferon coordinate adaptive and innate immune responses to cancer immune checkpoint blockade. *Cell* **178**, 933-948.e914 (2019).
95. Bach EA, Aguet M, Schreiber RD. The IFN gamma receptor: a paradigm for cytokine receptor signaling. *Annu Rev Immunol* **15**, 563-591 (1997).
96. Meraz MA, *et al.* Targeted disruption of the Stat1 gene in mice reveals unexpected physiologic specificity in the JAK-STAT signaling pathway. *Cell* **84**, 431-442 (1996).

97. Kaplan DH, *et al.* Demonstration of an interferon gamma-dependent tumor surveillance system in immunocompetent mice. *Proc Natl Acad Sci U S A* **95**, 7556-7561 (1998).
98. Sun Y, Yang S, Sun N, Chen J. Differential expression of STAT1 and p21 proteins predicts pancreatic cancer progression and prognosis. *Pancreas* **43**, 619-623 (2014).
99. Old LJ. Tumor necrosis factor. *Sci Am* **258**, 59-60, 69-75 (1988).
100. Wajant H, Pfizenmaier K, Scheurich P. Tumor necrosis factor signaling. *Cell Death Differ* **10**, 45-65 (2003).
101. Degterev A, Yuan J. Expansion and evolution of cell death programmes. *Nat Rev Mol Cell Biol* **9**, 378-390 (2008).
102. Brenner D, Blaser H, Mak TW. Regulation of tumour necrosis factor signalling: live or let die. *Nat Rev Immunol* **15**, 362-374 (2015).
103. Pfeffer K, *et al.* Mice deficient for the 55 kd tumor necrosis factor receptor are resistant to endotoxic shock, yet succumb to *L. monocytogenes* infection. *Cell* **73**, 457-467 (1993).
104. Williamson BD, Carswell EA, Rubin BY, Prendergast JS, Old LJ. Human tumor necrosis factor produced by human B-cell lines: synergistic cytotoxic interaction with human interferon. *Proc Natl Acad Sci U S A* **80**, 5397-5401 (1983).
105. Wu TH, *et al.* Long-term suppression of tumor growth by TNF requires a Stat1- and IFN regulatory factor 1-dependent IFN-gamma pathway but not IL-12 or IL-18. *J Immunol* **172**, 3243-3251 (2004).
106. Zhang B, Karrison T, Rowley DA, Schreiber H. IFN-gamma- and TNF-dependent bystander eradication of antigen-loss variants in established mouse cancers. *J Clin Invest* **118**, 1398-1404 (2008).
107. Ruegg C, Yilmaz A, Bieler G, Bamat J, Chaubert P, Lejeune FJ. Evidence for the involvement of endothelial cell integrin alphaVbeta3 in the disruption of the tumor vasculature induced by TNF and IFN-gamma. *Nat Med* **4**, 408-414 (1998).
108. Acquavella N, *et al.* Type I cytokines synergize with oncogene inhibition to induce tumor growth arrest. *Cancer Immunol Res* **3**, 37-47 (2015).
109. Schleich K, *et al.* H3K9me3-mediated epigenetic regulation of senescence in mice predicts outcome of lymphoma patients. *Nature communications* **11**, 3651 (2020).
110. Hayflick L, Moorhead PS. The serial cultivation of human diploid cell strains. *Exp Cell Res* **25**, 585-621 (1961).

111. Dimri GP, *et al.* A biomarker that identifies senescent human cells in culture and in aging skin in vivo. *Proc Natl Acad Sci U S A* **92**, 9363-9367 (1995).
112. Munoz-Espin D, *et al.* Programmed cell senescence during mammalian embryonic development. *Cell* **155**, 1104-1118 (2013).
113. Storer M, *et al.* Senescence is a developmental mechanism that contributes to embryonic growth and patterning. *Cell* **155**, 1119-1130 (2013).
114. Serrano M, Lin AW, McCurrach ME, Beach D, Lowe SW. Oncogenic ras provokes premature cell senescence associated with accumulation of p53 and p16INK4a. *Cell* **88**, 593-602 (1997).
115. Braig M, *et al.* Oncogene-induced senescence as an initial barrier in lymphoma development. *Nature* **436**, 660-665 (2005).
116. Dimri GP, Campisi J. Molecular and cell biology of replicative senescence. *Cold Spring Harb Symp Quant Biol* **59**, 67-73 (1994).
117. Beausejour CM, *et al.* Reversal of human cellular senescence: roles of the p53 and p16 pathways. *EMBO J* **22**, 4212-4222 (2003).
118. Chen Z, *et al.* Crucial role of p53-dependent cellular senescence in suppression of Pten-deficient tumorigenesis. *Nature* **436**, 725-730 (2005).
119. Schilbach K, *et al.* Cancer-targeted IL-12 controls human rhabdomyosarcoma by senescence induction and myogenic differentiation. *Oncoimmunology* **4**, e1014760 (2015).
120. Griessinger CM, *et al.* The administration route of tumor-antigen-specific T-helper cells differentially modulates the tumor microenvironment and senescence. *Carcinogenesis* **40**, 289-302 (2019).
121. Wang S, *et al.* Interferon-gamma induces senescence in normal human melanocytes. *PLoS One* **9**, e93232 (2014).
122. Hubackova S, *et al.* IFN $\gamma$  induces oxidative stress, DNA damage and tumor cell senescence via TGF $\beta$ /SMAD signaling-dependent induction of Nox4 and suppression of ANT2. *Oncogene* **35**, 1236-1249 (2016).
123. Rosembliit C, *et al.* Oncodriver inhibition and CD4(+) Th1 cytokines cooperate through Stat1 activation to induce tumor senescence and apoptosis in HER2+ and triple negative breast cancer: implications for combining immune and targeted therapies. *Oncotarget* **9**, 23058-23077 (2018).



124. Katlinskaya YV, *et al.* Suppression of type I interferon signaling overcomes oncogene-induced senescence and mediates melanoma development and progression. *Cell Rep* **15**, 171-180 (2016).
125. Acosta JC, Gil J. Senescence: a new weapon for cancer therapy. *Trends Cell Biol* **22**, 211-219 (2012).
126. O'Leary B, Finn RS, Turner NC. Treating cancer with selective CDK4/6 inhibitors. *Nat Rev Clin Oncol* **13**, 417-430 (2016).
127. Goel S, *et al.* CDK4/6 inhibition triggers anti-tumour immunity. *Nature* **548**, 471-475 (2017).
128. Klein ME, Kovatcheva M, Davis LE, Tap WD, Koff A. CDK4/6 inhibitors: the mechanism of action may not be as simple as once thought. *Cancer Cell* **34**, 9-20 (2018).
129. Shah M, Nunes MR, Stearns V. CDK4/6 inhibitors: game changers in the management of hormone receptor-positive advanced breast cancer? *Oncology (Williston Park)* **32**, 216-222 (2018).
130. Wagner V, Gil J. Senescence as a therapeutically relevant response to CDK4/6 inhibitors. *Oncogene* **39**, 5165-5176 (2020).
131. Ruscetti M, *et al.* Senescence-induced vascular remodeling creates therapeutic vulnerabilities in pancreas cancer. *Cell* **181**, 424-441.e421 (2020).
132. Michaloglou C, *et al.* BRAFE600-associated senescence-like cell cycle arrest of human naevi. *Nature* **436**, 720-724 (2005).
133. Mooi WJ, Peeper DS. Oncogene-induced cell senescence - halting on the road to cancer. *N Engl J Med* **355**, 1037-1046 (2006).
134. Dhomen N, *et al.* Oncogenic Braf induces melanocyte senescence and melanoma in mice. *Cancer Cell* **15**, 294-303 (2009).
135. Peeper DS. Oncogene-induced senescence and melanoma: where do we stand? *Pigment Cell Melanoma Res* **24**, 1107-1111 (2011).
136. Bartkova J, *et al.* Oncogene-induced senescence is part of the tumorigenesis barrier imposed by DNA damage checkpoints. *Nature* **444**, 633-637 (2006).
137. Di Micco R, *et al.* Interplay between oncogene-induced DNA damage response and heterochromatin in senescence and cancer. *Nat Cell Biol* **13**, 292-302 (2011).
138. Haferkamp S, *et al.* Vemurafenib induces senescence features in melanoma cells. *J Invest Dermatol* **133**, 1601-1609 (2013).

139. Sharpless NE, Sherr CJ. Forging a signature of in vivo senescence. *Nat Rev Cancer* **15**, 397-408 (2015).
140. Itahana K, Campisi J, Dimri GP. Methods to detect biomarkers of cellular senescence: the senescence-associated beta-galactosidase assay. *Methods Mol Biol* **371**, 21-31 (2007).
141. Schmitt CA, *et al.* A senescence program controlled by p53 and p16INK4a contributes to the outcome of cancer therapy. *Cell* **109**, 335-346 (2002).
142. Li J, Poi MJ, Tsai MD. Regulatory mechanisms of tumor suppressor P16(INK4A) and their relevance to cancer. *Biochemistry* **50**, 5566-5582 (2011).
143. Lee S, Schmitt CA. The dynamic nature of senescence in cancer. *Nat Cell Biol* **21**, 94-101 (2019).
144. Hernandez-Segura A, Nehme J, Demaria M. Hallmarks of cellular senescence. *Trends Cell Biol* **28**, 436-453 (2018).
145. Kosar M, Bartkova J, Hubackova S, Hodny Z, Lukas J, Bartek J. Senescence-associated heterochromatin foci are dispensable for cellular senescence, occur in a cell type- and insult-dependent manner and follow expression of p16(ink4a). *Cell Cycle* **10**, 457-468 (2011).
146. Narita M, *et al.* Rb-mediated heterochromatin formation and silencing of E2F target genes during cellular senescence. *Cell* **113**, 703-716 (2003).
147. Coppe JP, Desprez PY, Krtolica A, Campisi J. The senescence-associated secretory phenotype: the dark side of tumor suppression. *Annu Rev Pathol* **5**, 99-118 (2010).
148. Laberge RM, *et al.* mTOR regulates the pro-tumorigenic senescence-associated secretory phenotype by promoting IL1A translation. *Nat Cell Biol* **17**, 1049-1061 (2015).
149. Serrano M. The inflammTORy powers of senescence. *Trends Cell Biol* **25**, 634-636 (2015).
150. Demaria M, *et al.* Cellular senescence promotes adverse effects of chemotherapy and cancer relapse. *Cancer Discov* **7**, 165-176 (2017).
151. Schmitt CA. UnSASPing senescence: unmasking tumor suppression? *Cancer Cell* **34**, 6-8 (2018).
152. Faget DV, Ren Q, Stewart SA. Unmasking senescence: context-dependent effects of SASP in cancer. *Nat Rev Cancer* **19**, 439-453 (2019).

153. Brahmer JR, *et al.* Safety and activity of anti-PD-L1 antibody in patients with advanced cancer. *N Engl J Med* **366**, 2455-2465 (2012).
154. Hamid O, *et al.* Safety and tumor responses with lambrolizumab (anti-PD-1) in melanoma. *N Engl J Med* **369**, 134-144 (2013).
155. Robert C, *et al.* Pembrolizumab versus ipilimumab in advanced melanoma. *N Engl J Med* **372**, 2521-2532 (2015).
156. Wolchok JD, *et al.* Overall survival with combined nivolumab and ipilimumab in advanced melanoma. *N Engl J Med* **377**, 1345-1356 (2017).
157. Larkin J, *et al.* Five-year survival with combined nivolumab and ipilimumab in advanced melanoma. *N Engl J Med* **381**, 1535-1546 (2019).
158. Bergers G, Javaherian K, Lo KM, Folkman J, Hanahan D. Effects of angiogenesis inhibitors on multistage carcinogenesis in mice. *Science* **284**, 808-812 (1999).
159. Speiser DE, *et al.* Self antigens expressed by solid tumors do not efficiently stimulate naive or activated T cells: implications for immunotherapy. *J Exp Med* **186**, 645-653 (1997).
160. Kovalchuk AL, *et al.* Burkitt lymphoma in the mouse. *J Exp Med* **192**, 1183-1190 (2000).
161. Sucker A, *et al.* Acquired IFN $\gamma$  resistance impairs anti-tumor immunity and gives rise to T-cell-resistant melanoma lesions. *Nature communications* **8**, 15440 (2017).
162. Shultz LD, Ishikawa F, Greiner DL. Humanized mice in translational biomedical research. *Nat Rev Immunol* **7**, 118-130 (2007).
163. Blackford AN, Jackson SP. ATM, ATR, and DNA-PK: The trinity at the heart of the DNA damage response. *Mol Cell* **66**, 801-817 (2017).
164. Casanovas O, Hager JH, Chun MG, Hanahan D. Incomplete inhibition of the Rb tumor suppressor pathway in the context of inactivated p53 is sufficient for pancreatic islet tumorigenesis. *Oncogene* **24**, 6597-6604 (2005).

# Appendix

## 1. Publications

# T-helper-1-cell cytokines drive cancer into senescence

Heidi Braumüller<sup>1\*</sup>, Thomas Wieder<sup>1\*</sup>, Ellen Brenner<sup>1</sup>, Sonja Aßmann<sup>1</sup>, Matthias Hahn<sup>1</sup>, Mohammed Alkhaled<sup>2</sup>, Karin Schilbach<sup>2</sup>, Frank Essmann<sup>3</sup>, Manfred Kneilling<sup>1</sup>, Christoph Griessinger<sup>1,4</sup>, Felicia Ranta<sup>5</sup>, Susanne Ullrich<sup>5</sup>, Ralph Mocikat<sup>6</sup>, Kilian Braungart<sup>1</sup>, Tarun Mehra<sup>1</sup>, Birgit Fehrenbacher<sup>1</sup>, Julia Berdel<sup>1</sup>, Heike Niessner<sup>1</sup>, Friedegund Meier<sup>1</sup>, Maries van den Broek<sup>7</sup>, Hans-Ulrich Häring<sup>5</sup>, Rupert Handgretinger<sup>2,8</sup>, Leticia Quintanilla-Martinez<sup>9</sup>, Falko Fend<sup>8,9</sup>, Marina Pesic<sup>10</sup>, Jürgen Bauer<sup>1</sup>, Lars Zender<sup>10</sup>, Martin Schaller<sup>1</sup>, Klaus Schulze-Osthoff<sup>3,8</sup> & Martin Röcken<sup>1,8</sup>

**Cancer control by adaptive immunity involves a number of defined death<sup>1–8</sup> and clearance<sup>9–11</sup> mechanisms. However, efficient inhibition of exponential cancer growth by T cells and interferon- $\gamma$  (IFN- $\gamma$ ) requires additional undefined mechanisms that arrest cancer cell proliferation<sup>1–5,12,13</sup>. Here we show that the combined action of the T-helper-1-cell cytokines IFN- $\gamma$  and tumour necrosis factor (TNF) directly induces permanent growth arrest in cancers. To safely separate senescence induced by tumour immunity from oncogene-induced senescence<sup>9–11,14–17</sup>, we used a mouse model in which the Simian virus 40 large T antigen (Tag) expressed under the control of the rat insulin promoter creates tumours by attenuating p53- and Rb-mediated cell cycle control<sup>18,19</sup>. When combined, IFN- $\gamma$  and TNF drive Tag-expressing cancers into senescence by inducing permanent growth arrest in G1/G0, activation of p16INK4a (also known as CDKN2A), and downstream Rb hypophosphorylation at serine 795. This cytokine-induced senescence strictly requires STAT1 and TNFR1 (also known as TNFRSF1A) signalling in addition to p16INK4a. *In vivo*, Tag-specific T-helper 1 cells permanently arrest Tag-expressing cancers by inducing IFN- $\gamma$ - and TNFR1-dependent senescence. Conversely, *Tnfr1*<sup>-/-</sup> Tag-expressing cancers resist cytokine-induced senescence and grow aggressively, even in TNFR1-expressing hosts. Finally, as IFN- $\gamma$  and TNF induce senescence in numerous murine and human cancers, this may be a general mechanism for arresting cancer progression.**

Recent studies from targeted cancer immunotherapies show that adaptive immunity can efficiently control human cancer<sup>20–24</sup>. Many cancer immunotherapies do not cause cytotoxic cancer cell elimination, but instead arrest cancer growth or induce slow cancer regression<sup>21,22</sup>, despite the fact that immunotherapeutic strategies generally focus on CD8<sup>+</sup> cytotoxic T lymphocytes (CTL) or natural killer cells<sup>1–8,23,24</sup>. Moreover, where studied, growth arrest and cancer regression correlate with tumour-specific, IFN- $\gamma$ -producing CD4<sup>+</sup> T-helper 1 (T<sub>H</sub>1) cells rather than CTLs<sup>20–23</sup>. In addition, profiling of patients in clinical cancer trials shows a critical role for IFN- $\gamma$  and TNF in cancer control<sup>25,26</sup>.

Similarly, efficient immune control of murine cancers resulting from aberrant cell cycle control, oncogene expression and chemical or viral transformation strictly requires IFN- $\gamma$ <sup>3–7,12,27</sup>. In consequence, IFN- $\gamma$ - and TNF-producing T<sub>H</sub>1 cells specific for the tumour antigen Tag (Tag-T<sub>H</sub>1 cells) restrain Tag-induced islet cancers in mice expressing Tag

under the control of the rat insulin promoter (RIP-Tag2 mice; in which Tag2 indicates a mouse strain that carries five copies of the transgene) in all pancreatic islet cells<sup>12,18</sup>. T<sub>H</sub>1 immunity doubles the lifespan of mice through strictly IFN- $\gamma$ - and TNFR1-dependent mechanisms<sup>12</sup>, without causing detectable signs of cytotoxicity, tumour cell necrosis or apoptosis<sup>12</sup>. This was surprising, as Tag expression causes invasive  $\beta$ -cell cancers ( $\beta$ -cancers) in 2% of the islets by incomplete Rb suppression and p53 silencing<sup>18,19</sup>.

Only CD4<sup>+</sup> T<sub>H</sub>1 cells that produce IFN- $\gamma$  and TNF and are specific for Tag peptide induce IFN- $\gamma$ - and TNFR1-dependent arrest of RIP-Tag2 tumours (Supplementary Fig. 1a–c)<sup>12</sup>. This arrest occurs also in the absence of notable T-cell infiltration (Supplementary Figs 1c and 2)<sup>12</sup> and is independent of both CTLs<sup>12</sup> and enhanced apoptosis, as determined by TdT-mediated dUTP nick end labelling (TUNEL) assay<sup>12</sup> and caspase 3 staining, respectively. Moreover, IFN- $\gamma$ -exposed  $\beta$ -cancer cells failed to express major histocompatibility complex (MHC) class II *in vivo* as well as *in vitro*, a prerequisite for cancer killing by T<sub>H</sub>1 cells. In consequence, Tag-T<sub>H</sub>1 cells failed to kill IFN- $\gamma$ -stimulated  $\beta$ -cancer cells *in vitro* (Supplementary Fig. 3). In addition, as Tag-T<sub>H</sub>1 cells enhance, rather than attenuate, the growth of *Tnfr1*<sup>-/-</sup>  $\beta$ -cancers<sup>12</sup> (Supplementary Fig. 1), TNFR1-independent killing—for example, by perforin-granzyme B-mediated lysis—could not account for substantial control of  $\beta$ -cancers by Tag-T<sub>H</sub>1 cells. Instead, Tag-T<sub>H</sub>1 cells form follicle-like structures around the islets, where they interact with antigen-presenting cells<sup>12</sup>. Ki67 staining confirmed that Tag-T<sub>H</sub>1 cells arrested proliferation of  $\beta$ -cancers *in vivo* (Supplementary Fig. 4a). Freshly isolated  $\beta$ -cancer cells from Tag-T<sub>H</sub>1-cell-treated RIP-Tag2 mice failed to proliferate *in vitro*, whereas  $\beta$ -cancer cells from sham-treated mice strongly incorporated <sup>3</sup>H-thymidine (Supplementary Fig. 4b). This suggests that T<sub>H</sub>1 cytokines induce growth arrest *in vivo*, despite normal Tag expression (Supplementary Fig. 5).

To assess directly whether IFN- $\gamma$  and TNF induce senescence in  $\beta$ -cancers, we cultured freshly isolated  $\beta$ -cancer cells from sham-treated mice treated with either control medium, or with IFN- $\gamma$  and TNF. In cell cycle analysis, untreated  $\beta$ -cancer cells were  $\geq 25\%$  in S phase and 40% in G1/G0, explaining their rapid proliferation. When combined, IFN- $\gamma$  and TNF arrested most  $\beta$ -cancer cells in G1/G0 within 3 days (Fig. 1a). They reduced S-phase cells to 3% and increased the G1/S ratio 20-fold (Fig. 1b) without increasing the apoptotic sub-G1 fraction (Fig. 1a). As IFN- $\gamma$  and TNF arrested the  $\beta$ -cancer cells in G1/G0, a state characterizing cellular senescence, we wanted to know

<sup>1</sup>Department of Dermatology, Eberhard Karls University, Liebermeister Strasse 25, 72076 Tübingen, Germany. <sup>2</sup>Department of General Pediatrics, Oncology/Hematology, Eberhard Karls University, Hoppe-Seyler-Strasse 1, 72076 Tübingen, Germany. <sup>3</sup>Interfaculty Institute for Biochemistry, Eberhard Karls University, Hoppe-Seyler-Strasse 4, 72076 Tübingen, Germany. <sup>4</sup>Laboratory for Preclinical Imaging and Imaging Technology of the Werner Siemens-Foundation, Department for Preclinical Imaging and Radiopharmacy, Eberhard Karls University, Röntgenweg 13, 72076 Tübingen, Germany. <sup>5</sup>Department of Internal Medicine IV, Endocrinology, Diabetology and Clinical Chemistry, Eberhard Karls University, Otfried-Müller-Strasse 10, 72076 Tübingen, Germany. <sup>6</sup>Institut für Molekulare Immunologie, Helmholtz-Zentrum München, Deutsches Forschungszentrum für Gesundheit und Umwelt, Marchionini Strasse 25, 81377 München, Germany. <sup>7</sup>Clinic of Oncology, University Hospital Zurich, Raemistrasse 100, 8091 Zurich, Switzerland. <sup>8</sup>Comprehensive Cancer Center Tübingen, German Cancer Consortium (DKTK), Herrenberger Strasse 23, D-72070 Tübingen, Germany. <sup>9</sup>Department of Pathology, Eberhard Karls University, Liebermeister Strasse 8, 72076 Tübingen, Germany. <sup>10</sup>Division of Molecular Oncology of Solid Tumors, Department of Internal Medicine I, Eberhard Karls University, Otfried-Müller-Strasse 10, 72076 Tübingen, Germany.

\*These authors contributed equally to this work.

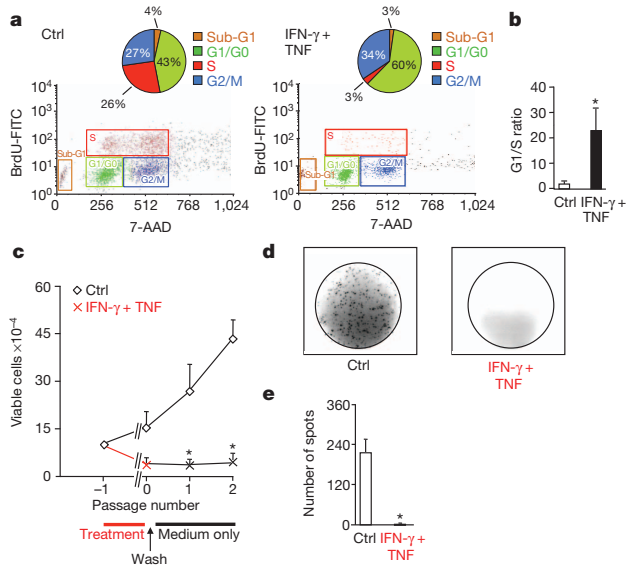


**Figure 1** | Combined, the T<sub>H</sub>1 cytokines IFN- $\gamma$  and TNF induce stable growth arrest of Tag-driven  $\beta$ -cancer cells *in vitro*. **a, b**, Cell cycle analysis (**a**) and mean G1/S-phase ratio (**b**) of  $\beta$ -cancer cells cultured either in the presence or absence of IFN- $\gamma$  and TNF. Ctrl, control; FITC, fluorescein isothiocyanate. 7-AAD, 7-Aminoactinomycin. **c–e**, Cell numbers (**c**), BrdU incorporation (**d**) and mean numbers of BrdU-positive spots (**e**) of  $\beta$ -cancer cells treated for 5 days with medium only, or with IFN- $\gamma$  and TNF. Thereafter, cells were washed and then cultured with medium in the absence of cytokines for another two passages. After the second passage 3,000 viable cells were seeded in 96-well plates and cell proliferation was analysed by BrdU staining. \* $P < 0.05$ . Error bars are mean  $\pm$  s.e.m.  $n = 3–6$  (**b, c, e**).

whether IFN- $\gamma$  and TNF caused senescence-defining permanent growth arrest.

Freshly isolated  $\beta$ -cancer cells proliferated rapidly in medium. When cultured in the presence of IFN- $\gamma$  and TNF,  $\beta$ -cancer cells were fully growth arrested (Fig. 1c). To determine whether the growth-arrested  $\beta$ -cancer cells were really senescent, we washed the cells on day 5 and cultured them for another 2 weeks with medium only. Although untreated  $\beta$ -cancer cells continued to expand,  $\beta$ -cancer cells that had been exposed for 5 days to the combined action of IFN- $\gamma$  and TNF were truly senescent, as they remained fully growth arrested (Fig. 1c). Even 2 weeks after withdrawal of IFN- $\gamma$  and TNF, the  $\beta$ -cancer cells failed to incorporate 5-bromo-2-deoxyuridine (BrdU), whereas untreated controls strongly incorporated BrdU (Fig. 1d, e and Supplementary Fig. 6).

IFN- $\gamma$  and TNF also induced characteristic senescence-associated epigenetic and lysosomal changes, such as nuclear recruitment of phosphorylated heterochromatin protein 1 $\gamma$  (pHP1 $\gamma$ ) into senescence-associated heterochromatin foci or senescence-associated  $\beta$ -galactosidase (SA- $\beta$ -gal) activity. Time-course studies revealed that within 3 days, IFN- $\gamma$  and TNF induced the early senescence marker pHP1 $\gamma$  in 75% (Supplementary Fig. 7a, b) and SA- $\beta$ -gal in 50% of the  $\beta$ -cancer cells (Fig. 2a, b). However, induction of stable growth arrest and the late senescence marker SA- $\beta$ -gal in 80% of the cells needed  $\geq 4$  days of incubation with both IFN- $\gamma$  and TNF (Fig. 2c). Double-staining with synaptophysin, an islet cell marker, confirmed SA- $\beta$ -gal expression by  $\beta$ -cancer cells (Supplementary Fig. 8). Combined IFN- $\gamma$  and TNF treatment established the senescence-defining permanent growth arrest in  $\beta$ -cancers cells, whereas neither IFN- $\gamma$  nor TNF alone was sufficient to induce full growth arrest (Supplementary Fig. 6), although early signs of senescence, such as pHP1 $\gamma$  recruitment to senescence-associated heterochromatin foci (Supplementary Fig. 7a, b) and SA- $\beta$ -gal positivity in 40% of the cells, were observed (Fig. 2c).

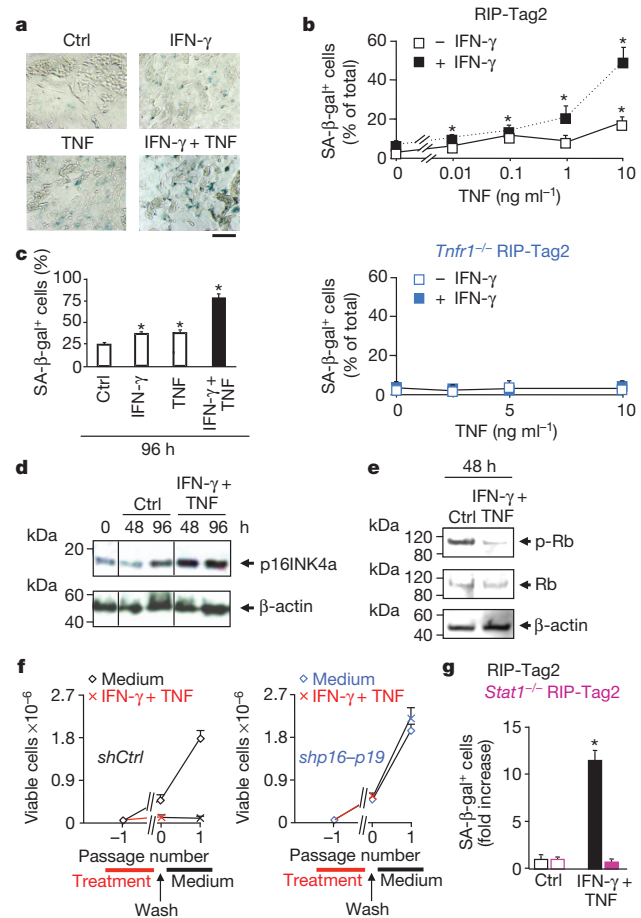


**Figure 2** | STAT1- and TNFR1-dependent stabilization of the p16INK4a-Rb senescence pathway in  $\beta$ -cancer cells by the combined action of IFN- $\gamma$  and TNF *in vitro*. **a**, SA- $\beta$ -gal activity of  $\beta$ -cancer cells after 72 h of treatment with medium, IFN- $\gamma$ , TNF, or IFN- $\gamma$  and TNF. Scale bar, 100  $\mu$ m. **b**, Concentration-dependent induction of SA- $\beta$ -gal<sup>+</sup> cells by TNF, either in the presence or absence of IFN- $\gamma$ , within 72 h in  $\beta$ -cancer cells from RIP-Tag2 or *Tnfr1*<sup>-/-</sup> RIP-Tag2 mice. **c**, Induction of SA- $\beta$ -gal activity by IFN- $\gamma$ , TNF, or IFN- $\gamma$  and TNF within 96 h. **d**, Detection of p16INK4a or  $\beta$ -actin by western blotting in  $\beta$ -cancer cells treated with medium or with IFN- $\gamma$  and TNF. **e**, Detection of phosphorylated Rb (p-Rb), total Rb or  $\beta$ -actin by western blotting in  $\beta$ -cancer cells treated with medium or IFN- $\gamma$  and TNF. **f**,  $\beta$ -cancer cells were transduced with *shCtrl* or *shp16-p19* murine stem cell virus (MSCV) vectors, and then treated for 5 days with medium only, or with IFN- $\gamma$  and TNF. Thereafter, cells were washed and cultured with medium in the absence of cytokines. Mean cell numbers of three cultures are shown. **g**, SA- $\beta$ -gal activity of  $\beta$ -cancer cells isolated from either RIP-Tag2 or *Stat1*<sup>-/-</sup> RIP-Tag2 mice after 72 h of treatment with medium or with IFN- $\gamma$  and TNF. \* $P < 0.05$ . Error bars are mean  $\pm$  s.e.m.  $n = 3–9$  (**b, c, f, g**).

As combined stimulation of islets or islet tumours with IFN- $\gamma$  and TNF strongly induces JUNB<sup>28</sup>, the combined IFN- $\gamma$  STAT1 and TNFR1 signalling may activate the JUNB downstream target p16INK4a and thus stabilize the p16INK4a-Rb senescence pathway in Tag-expressing  $\beta$ -cancers. Indeed, IFN- $\gamma$  and TNF strongly induced p16INK4a in subconfluent cultures within 48 h (Fig. 2d), whereas p16INK4a remained weak in medium-treated subconfluent  $\beta$ -cancer cells (Fig. 2d). This induction of p16INK4a also caused sustained and severe hypophosphorylation of Rb at Ser 795 (Fig. 2e). Corresponding to the conjoint IFN- $\gamma$ - and TNF-induced senescence through stabilization of the p16INK4a-Rb pathway in  $\beta$ -cancer cells, short hairpin RNA (shRNA)-mediated knockdown of *p16INK4a* and *p19* (hereafter termed *p16-p19*, in which *p19* refers to an alternate reading frame of

the *Ink4a/Arf* (*Cdkn2a*) locus) fully abrogated senescence induction by IFN- $\gamma$  and TNF (Fig. 2f and Supplementary Fig. 9). In line with this, STAT1- or TNFR1-deficient  $\beta$ -cancer cells fully resisted senescence induction by IFN- $\gamma$  and TNF, showing that hypophosphorylation of Rb strictly requires the combined action of the STAT1 and TNFR1 signalling pathways (Fig. 2b, g).

IFN- $\gamma$  and TNF induced senescence in breast cancers from polyomavirus middle T antigen (PyVMT)-transgenic mice (Supplementary Fig. 10), in 3 out of 6 mouse tumour lines (Supplementary Table 1), in human A204 rhabdomyosarcoma cells (Supplementary Fig. 11), in 6 out of 11 IFN-receptor- and TNF-receptor-expressing human cancers from the National Cancer Institute's NCI-60 panel (Supplementary Table 2), and in freshly isolated primary melanoma or sarcoma cells (Supplementary Table 3). Interestingly, primary melanomas frequently show areas of inflammation and regression. Such tumour areas harboured senescent melanoma cells strongly expressing p16INK4a but not the proliferation marker Ki67, whereas p16INK4a-deficient melanoma cells strongly expressed Ki67 even in the presence of an inflammatory infiltrate (Supplementary Fig. 12). Thus, cytokine-induced senescence was not restricted to Tag-expressing  $\beta$ -cancers, but seems to be of broad relevance for tumour immunotherapy and may cause tumour dormancy in sporadic human melanomas.

Combined IFN- $\gamma$  and TNFR1 signalling is also necessary to arrest  $\beta$ -cancers *in vivo*<sup>12</sup> (Supplementary Fig. 1) and a senescence-like phenotype was observed in spontaneously regressing melanomas. Thus, the *in vitro* and *in vivo* data suggest that T<sub>H</sub>1 immunity arrested cancer progression through IFN- $\gamma$ - and TNF-induced senescence *in vivo*. To test this hypothesis, we first quantified senescence-associated chromatin changes by counting cancer cells positive for pHP1 $\gamma$ , trimethylation of histone 3 lysine 9 (H3K9me3), or apoptosis-associated active caspase 3 by immunohistochemistry in either sham-treated mice or mice treated with Tag-T<sub>H</sub>1 cells. T<sub>H</sub>1 immunity significantly increased pHP1 $\gamma$ - and H3K9me3-positive nuclei in  $\beta$ -cancers, but not caspase-3-positive cells (Fig. 3a, b).

To address whether T<sub>H</sub>1 immunity also activated the p16INK4a-Rb pathway *in vivo*, we double-stained sections for p16INK4a and the proliferation marker Ki67. In sham-treated mice, the  $\beta$ -cancer cells were  $\geq 30\%$  Ki67 positive and only 5% p16INK4a positive. T<sub>H</sub>1 immunity diminished Ki67<sup>+</sup> cells to 3%, and increased the fraction of p16INK4a<sup>+</sup> cells (nuclear and cytoplasmic) to  $\geq 20\%$  (Fig. 3c, d and Supplementary Fig. 13).

Senescence induction by T<sub>H</sub>1 immunity *in vivo* also strictly required TNFR1 signalling. *Tnfr1*<sup>-/-</sup>  $\beta$ -cancers failed to increase pHP1 $\gamma$ , H3K9me3 or active caspase 3 when treated with Tag-T<sub>H</sub>1 cells (Supplementary Fig. 14a, b). In addition, whether isolated from sham- or Tag-T<sub>H</sub>1-treated mice, *Tnfr1*<sup>-/-</sup>  $\beta$ -cancer cells expressed Ki67 but not p16INK4a (Fig. 3c, d), even though Tag-T<sub>H</sub>1 cells migrate into pancreata of *Tnfr1*<sup>-/-</sup> RIP-Tag2 mice<sup>12</sup>. As T<sub>H</sub>1 immunity severely impaired  $\beta$ -cancer growth *in vivo*<sup>12</sup>, these data strongly suggest that the combined IFN- $\gamma$  and TNFR1 signalling also drove cancers into senescence *in vivo*.

The most stringent criterion defining senescence is stable and permanent growth arrest in the absence of T<sub>H</sub>1 immunity<sup>9,15,16</sup>. We therefore cultured freshly isolated  $\beta$ -cancer cells from 12-week-old mice with medium only. Cells from sham-treated RIP-Tag2 mice first suffered a critical loss and then re-initiated proliferation, yielding 10–20  $\times 10^5$   $\beta$ -cancer cells per pancreas after three passages (Fig. 4a). By contrast,  $\beta$ -cancer cells from RIP-Tag2 mice treated with Tag-T<sub>H</sub>1 cells were truly senescent, as they failed to proliferate over three passages and stably yielded only 0.5–2.0  $\times 10^5$  cells per pancreas (Fig. 4a). The T<sub>H</sub>1-induced growth arrest remained stable when cultures were extended for six passages (Supplementary Fig. 15). At 12 weeks,  $\beta$ -cancers from *Tnfr1*<sup>-/-</sup> RIP-Tag2 mice yielded similar cell counts as those from RIP-Tag2 mice (Fig. 4a). *In vitro*, *Tnfr1*<sup>-/-</sup>  $\beta$ -cancer cells grew exponentially, yielding 100  $\times 10^5$  cells within three passages even when derived from Tag-T<sub>H</sub>1-treated mice (Fig. 4a).

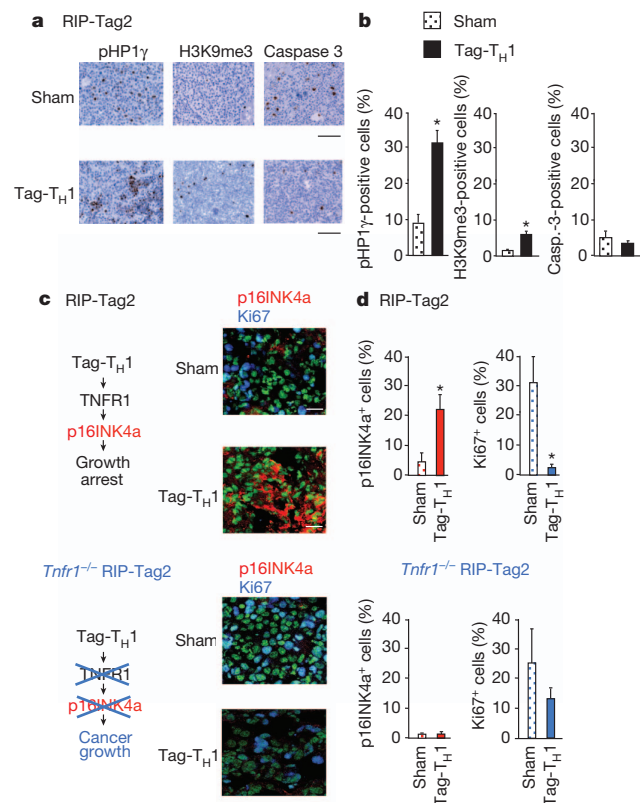


**Figure 3 | TNFR1-dependent induction of growth arrest and senescence in  $\beta$ -cancer cells by T<sub>H</sub>1 immunity *in vivo*.** a, b, Analysis of the senescence markers pHP1 $\gamma$  and H3K9me3, or the apoptosis marker active caspase 3, by immunohistochemistry (a), and percentage of pHP1 $\gamma$ -, H3K9me3- or active caspase-3-positive cells in  $\beta$ -cancers from RIP-Tag2 mice that were either sham- or Tag-T<sub>H</sub>1-cell-treated (b). Scale bars, 100  $\mu$ m. c, d, Double-staining for the senescence marker p16INK4a (red) and the proliferation marker Ki67 (blue) (c), and percentage of p16INK4a- and Ki67-positive cells in cancers from RIP-Tag2 or *Tnfr1*<sup>-/-</sup> RIP-Tag2 mice that were sham- or Tag-T<sub>H</sub>1-cell-treated (d). Nuclei are depicted in green. Scale bars, 25  $\mu$ m. \**P* < 0.05 from sham-treated control. Error bars are mean  $\pm$  s.e.m. *n* = 5–6 (b, d).

To determine whether senescence was also maintained *in vivo*, we re-implanted the four different  $\beta$ -cancer cell lines after the third passage under the skin of non-obese diabetic–severe combined immunodeficient (NOD-SCID) *Il2rg*<sup>-/-</sup> mice, as growth at ectopic sites characterizes cancers<sup>2</sup>. Within 7 weeks, as few as 1.2  $\times 10^5$   $\beta$ -cancer cells from sham-treated RIP-Tag2 mice significantly decreased blood glucose (Fig. 4b) and increased the serum insulin levels (Fig. 4c), demonstrating the metastatic potential of  $\beta$ -cancer cells from sham-treated mice. Senescent  $\beta$ -cancers from RIP-Tag2 mice treated with Tag-T<sub>H</sub>1 cells also remained growth arrested *in vivo*, as blood glucose remained stable in all transplanted mice throughout the 7 weeks (Fig. 4b). Minute adenomas in some NOD-SCID *Il2rg*<sup>-/-</sup> mice and marginally increased serum insulin (Fig. 4c) showed that the transplanted cells survived but remained growth arrested for  $\geq 10$  weeks of *in vitro* and *in vivo* culture. Again, senescence-resistant *Tnfr1*<sup>-/-</sup> RIP-Tag2  $\beta$ -cancer cells grew rapidly after transplantation and as little as 1.2  $\times 10^5$  *Tnfr1*<sup>-/-</sup> RIP-Tag2 cancer cells rapidly decreased blood glucose (Fig. 4b), irrespective of whether they were derived from sham-treated or Tag-T<sub>H</sub>1-treated mice. Transplanting 60% of total  $\beta$ -cancer cells from sham-treated RIP-Tag2 mice generated tumours within 7 weeks, whereas  $\beta$ -cancer cells from Tag-T<sub>H</sub>1-cell-treated mice failed to grow (Fig. 4d). Only 10% of  $\beta$ -cancer cells from sham- or Tag-T<sub>H</sub>1-treated *Tnfr1*<sup>-/-</sup> RIP-Tag2 mice generated large tumours within the same timeframe (Fig. 4d).

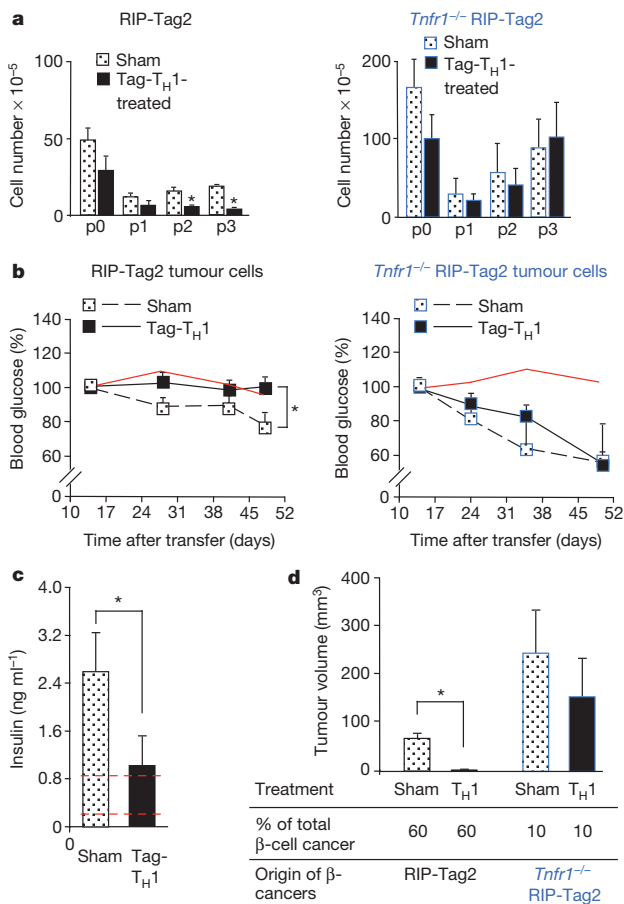


**Figure 4** | T<sub>H</sub>1 immunity induces TNFR1-dependent, permanent growth arrest of β-cancer cells that remains stable for ≥10 weeks, even after transfer into immune-deficient NOD-SCID *Il2rg*<sup>-/-</sup> mice. **a**, Cell numbers of β-cancer cells isolated from 12-week-old RIP-Tag2 or *Tnfr1*<sup>-/-</sup> RIP-Tag2 mice that were sham- or Tag-T<sub>H</sub>1-cell-treated. The number of cell passages (p) is indicated, and the data are presented as number of living β-cancer cells per mouse. **b**, Blood glucose levels in NOD-SCID *Il2rg*<sup>-/-</sup> mice after transfer of  $1.2 \times 10^5$  β-cancer cells isolated from sham- or Tag-T<sub>H</sub>1-cell-treated RIP-Tag2 or *Tnfr1*<sup>-/-</sup> RIP-Tag2 mice. Red lines indicate blood glucose of untreated NOD-SCID *Il2rg*<sup>-/-</sup> mice. **c**, Insulin levels in NOD-SCID *Il2rg*<sup>-/-</sup> mice after transfer of  $1.2 \times 10^5$  β-cancer cells isolated from sham- or Tag-T<sub>H</sub>1-cell-treated RIP-Tag2 mice. Dashed red lines indicate normal range of insulin in healthy mice. **d**, Top, tumour volumes in NOD-SCID *Il2rg*<sup>-/-</sup> mice after transfer of β-cancer cells isolated from sham- or Tag-T<sub>H</sub>1-cell-treated mice. Bottom, origin and percentage of total β-cancer cells per mouse injected. \**P* < 0.05 from sham-treated control. Error bars are mean ± s.e.m. *n* = 3–6 (**a–d**).

Oncogenes, DNA damage and chemotherapeutics induce senescence that, in human cells, is reinforced by the senescence-associated secretome<sup>14–17,29,30</sup>. Uncovering that adaptive T<sub>H</sub>1 immunity directly restrains cancer proliferation through IFN-γ- and TNF-induced cancer cell senescence provides a long-sought-for direct mechanism explaining the anti-proliferative effects of T<sub>H</sub>1 immunity on cancers<sup>2,3</sup>. T<sub>H</sub>1 immunity can induce antiangiogenic chemokines<sup>12</sup>, even in cancer cells (Supplementary Fig. 16a, b), and permanent growth arrest leading to cancer cell senescence. Although both effects protect against cancer<sup>12,18</sup>, *p16-p19* knockdown experiments revealed that the arrest of cancer growth strictly needed T<sub>H</sub>1-induced senescence. shRNA-mediated knockdown of *p16-p19* affected neither the IFN-γ- and TNF-induced mRNA expression nor protein production of antiangiogenic chemokines, but it fully abrogated senescence. Following the *p16-p19* knockdown, β-cancer cells grew exponentially in the

presence of IFN-γ, TNF and the antiangiogenic chemokines CXCL9 and CXCL10 (Fig. 2f and Supplementary Fig. 16c, d). Importantly, this is also valid *in vivo*. Despite the absence of antiangiogenic signals, senescent cancers remained growth arrested when transferred into NOD-SCID *Il2rg*<sup>-/-</sup> mice (Fig. 4b, c). As the T<sub>H</sub>1-induced cancer cell senescence thus explains the therapeutic efficiency of tumour-specific T<sub>H</sub>1 immunity in early cervical cancer<sup>21</sup> and disseminated melanoma<sup>20</sup>, T<sub>H</sub>1-cytokine-induced senescence may be of broad relevance for cancer control, also in humans under therapeutic conditions.

## METHODS SUMMARY

RIP-Tag2 and *Tnfr1*<sup>-/-</sup> RIP-Tag2 mice were either sham-treated or treated with Tag2-specific T<sub>H</sub>1 cells starting at week 6. Cancer cells were isolated by consecutive collagenase–trypsin digestion from tumour tissues of RIP-Tag2, *Stat1*<sup>-/-</sup> RIP-Tag2, *Tnfr1*<sup>-/-</sup> RIP-Tag2, or PyVmT-transgenic mice. Isolated β-cancer cells were identified by immunofluorescence using anti synaptophysin (early β-cell marker) antibodies. Proliferation *in vivo* and *in vitro* of tumour cells was measured by BrdU incorporation, Ki67 staining, <sup>3</sup>H-thymidine incorporation or cell cycle analysis. Senescence was assessed by SA-β-gal staining, immunofluorescence, immunohistochemistry or western blotting using anti-pHP1γ, anti-p16INK4a, anti-Rb, anti-phospho-Rb, or anti-H3K9me3 antibodies, or by *in vitro* and *in vivo* growth assays. Apoptosis was determined by cell cycle analysis, or immunohistochemistry with an anti-active-caspase-3 antibody. *p16INK4a* was knocked down in β-cancer cells by the use of *shp16-p19* MSCV vectors. For transfer experiments, β-cancer cells from sham- or T<sub>H</sub>1-cell-treated mice (either RIP-Tag2 or *Tnfr1*<sup>-/-</sup> RIP-Tag2) were injected subcutaneously into NOD-SCID *Il2rg*<sup>-/-</sup> mice, and tumour growth was monitored with a caliper and by measuring blood glucose and insulin levels.

**Full Methods** and any associated references are available in the online version of the paper.

Received 11 April; accepted 6 December 2012.

Published online 3 February 2013.

- Finn, O. J. Cancer immunology. *N. Engl. J. Med.* **358**, 2704–2715 (2008).
- Hanahan, D. & Weinberg, R. A. Hallmarks of cancer: the next generation. *Cell* **144**, 646–674 (2011).
- Schreiber, R. D., Old, L. J. & Smyth, M. J. Cancer immunoeediting: integrating immunity's roles in cancer suppression and promotion. *Science* **331**, 1565–1570 (2011).
- Koebel, C. M. *et al.* Adaptive immunity maintains occult cancer in an equilibrium state. *Nature* **450**, 903–907 (2007).
- van den Broek, M. E. *et al.* Decreased tumor surveillance in perforin-deficient mice. *J. Exp. Med.* **184**, 1781–1790 (1996).
- Willmsky, G. & Blankenstein, T. Sporadic immunogenic tumours avoid destruction by inducing T-cell tolerance. *Nature* **437**, 141–146 (2005).
- Mocikat, R. *et al.* Natural killer cells activated by MHC class I<sup>low</sup> targets prime dendritic cells to induce protective CD8 T cell responses. *Immunity* **19**, 561–569 (2003).
- Hung, K. *et al.* The central role of CD4<sup>+</sup> T cells in the antitumor immune response. *J. Exp. Med.* **188**, 2357–2368 (1998).
- Xue, W. *et al.* Senescence and tumour clearance is triggered by p53 restoration in murine liver carcinomas. *Nature* **445**, 656–660 (2007).
- Rakhra, K. *et al.* CD4<sup>+</sup> T cells contribute to the remodeling of the microenvironment required for sustained tumor regression upon oncogene inactivation. *Cancer Cell* **18**, 485–498 (2010).
- Kang, T. W. *et al.* Senescence surveillance of pre-malignant hepatocytes limits liver cancer development. *Nature* **479**, 547–551 (2011).
- Müller-Hermelink, N. *et al.* TNFR1 signaling and IFN-γ signaling determine whether T cells induce tumor dormancy or promote multistage carcinogenesis. *Cancer Cell* **13**, 507–518 (2008).
- Röcken, M. Early tumor dissemination, but late metastasis: insights into tumor dormancy. *J. Clin. Invest.* **120**, 1800–1803 (2010).
- Braig, M. *et al.* Oncogene-induced senescence as an initial barrier in lymphoma development. *Nature* **436**, 660–665 (2005).
- Campisi, J. & d'Adda di Fagagna, F. Cellular senescence: when bad things happen to good cells. *Nature Rev. Mol. Cell Biol.* **8**, 729–740 (2007).
- Collado, M. & Serrano, M. Senescence in tumours: evidence from mice and humans. *Nature Rev. Cancer* **10**, 51–57 (2010).
- Nardella, C., Clohessy, J. G., Alimonti, A. & Pandolfi, P. P. Pro-senescence therapy for cancer treatment. *Nature Rev. Cancer* **11**, 503–511 (2011).
- Bergers, G., Javaherian, K., Lo, K. M., Folkman, J. & Hanahan, D. Effects of angiogenesis inhibitors on multistage carcinogenesis in mice. *Science* **284**, 808–812 (1999).
- Casanovas, O., Hager, J. H., Chun, M. G. & Hanahan, D. Incomplete inhibition of the Rb tumor suppressor pathway in the context of inactivated p53 is sufficient for pancreatic islet tumorigenesis. *Oncogene* **24**, 6597–6604 (2005).



20. Hunder, N. N. *et al.* Treatment of metastatic melanoma with autologous CD4+ T cells against NY-ESO-1. *N. Engl. J. Med.* **358**, 2698–2703 (2008).
21. Kenter, G. G. *et al.* Vaccination against HPV-16 oncoproteins for vulvar intraepithelial neoplasia. *N. Engl. J. Med.* **361**, 1838–1847 (2009).
22. Hodi, F. S. *et al.* Improved survival with ipilimumab in patients with metastatic melanoma. *N. Engl. J. Med.* **363**, 711–723 (2010).
23. Schwartzentruber, D. J. *et al.* gp100 peptide vaccine and interleukin-2 in patients with advanced melanoma. *N. Engl. J. Med.* **364**, 2119–2127 (2011).
24. Morgan, R. A. *et al.* Cancer regression in patients after transfer of genetically engineered lymphocytes. *Science* **314**, 126–129 (2006).
25. Canova, C. *et al.* Genetic associations of 115 polymorphisms with cancers of the upper aerodigestive tract across 10 European countries: the ARCAGE project. *Cancer Res.* **69**, 2956–2965 (2009).
26. Critchley-Thorne, R. J. *et al.* Impaired interferon signaling is a common immune defect in human cancer. *Proc. Natl Acad. Sci. USA* **106**, 9010–9015 (2009).
27. Zhang, B., Karrison, T., Rowley, D. A. & Schreiber, H. IFN- $\gamma$ - and TNF-dependent bystander eradication of antigen-loss variants in established mouse cancers. *J. Clin. Invest.* **118**, 1398–1404 (2008).
28. Gurzov, E. N. *et al.* Pancreatic  $\beta$ -cells activate a JunB/ATF3-dependent survival pathway during inflammation. *Oncogene* **31**, 1723–1732 (2012).
29. Kuilman, T. *et al.* Oncogene-induced senescence relayed by an interleukin-dependent inflammatory network. *Cell* **133**, 1019–1031 (2008).
30. Acosta, J. C. *et al.* Chemokine signaling via the CXCR2 receptor reinforces senescence. *Cell* **133**, 1006–1018 (2008).

**Supplementary Information** is available in the online version of the paper.

**Acknowledgements** The authors thank A. Knuth, H. G. Rammensee, K. Ghoreschi, J. Brück, G. Riethmüller, G. Stingl, T. Biedermann and A. Yazdi for discussions,

T. Haug for technical support in the chromium release assay, R. Dummer for melanoma samples, W. Kempf for technical support in the cell cycle analysis and S. Lowe for the *p16-p19* shRNA concept. The technical assistance of S. Weidemann and M. Dierstein is gratefully acknowledged. This work is part of the doctoral thesis of E.B., S.A., M.H., K.B., J.Berdel and C.G., and was supported by the Sander Stiftung (2005.043.2 and 2005.043.3), the Deutsche Krebshilfe (No. 109037), the IZKF-Promotionskolleg 'Molekulare Medizin' 2010 (1886-0-0), 2011 (PK 2011-3) and 2012 (PK 2012-1), the Deutsche Forschungsgemeinschaft (SFB 685, SFB 773 and Wi 1279/3-1) and in part by the German Federal Ministry of Education and Research (BMBF) to the German Center for Diabetes Research (DzD e.V.).

**Author Contributions** M.R. originally developed the concept, further elaborated on it, and designed the experiments together with H.B., T.W., R.M. and K.S.-O. H.B., T.W., S.A., M.K., C.G., F.E., M.H., K.B., T.M. and E.B. performed experiments and analysed the data. B.F. and M.S. established and carried out fluorescence microscopy. L.Q.-M. and F.F. performed light microscopy and advised on cell biology. M.A., K.S. and R.H. supervised and performed the  $\beta$ -cancer-cell-transfer experiments. L.Z. and M.P. generated *shp16-p19* MSCV vectors and supervised the knockdown experiments. H.N. and F.M. isolated primary melanoma cells, J.Berdel and J.Bauer collected human melanoma specimen and performed immunohistochemical analysis. F.R., S.U. and H.-U.H. isolated  $\beta$ -cancer cells and advised on  $\beta$ -cell physiology. H.B., T.W., M.v.d.B., K.S.-O. and M.R. interpreted the data and wrote the paper.

**Author Information** Reprints and permissions information is available at [www.nature.com/reprints](http://www.nature.com/reprints). The authors declare no competing financial interests. Readers are welcome to comment on the online version of the paper. Correspondence and requests for materials should be addressed to M.R. ([mrocken@med.uni-tuebingen.de](mailto:mrocken@med.uni-tuebingen.de)).

## METHODS

**Animals.** C3HeB/FeJ (C3H) mice from The Jackson Laboratory, transgenic RIP-Tag2 mice<sup>31</sup>, double-transgenic *Tnfr1*<sup>-/-</sup> RIP-Tag2<sup>2,32</sup> and *Stat1*<sup>-/-</sup> RIP-Tag2 mice (backcross of *Stat1*<sup>-/-</sup> mice from Taconic over 12 generations to C3H), TCR2 mice<sup>33</sup> all on a C3H background, and PyVmT-transgenic mice on a C57BL/6 background<sup>34</sup>, were bred under specific pathogen-free conditions. NOD-SCID *Il2rg*<sup>-/-</sup> mice (NOD.Cg-Prkdc<sup>scid</sup> *Il2rg*<sup>tm1Wjl/SzJ</sup>)<sup>35</sup> were from The Jackson Laboratory. Animal experiments were approved by the local authorities (Regierungspräsidium Tübingen, Germany; reference numbers HT 2/03, HT2/07 and K1/07).

**Isolation of primary human cancer cells.** Two human rhabdomyosarcoma and four human melanoma cancer cell preparations were isolated from patients. The isolation of cancer cells from patient-derived material and histology of cancers were approved by the local ethics committees (Ethik-Kommission an der Medizinischen Fakultät der Eberhard-Karls-Universität und am Universitätsklinikum Tübingen, Germany, reference numbers 072/2011BO2, 105/2008BO1 and 017/2012BO2; and Ethik-Kommission (KEK), Gesundheitsdirektion Kanton Zürich, Switzerland, reference number Nr. 647). Informed consent was obtained from all patients.

**Cell culture and single-cell analysis.** Tag-specific T<sub>H</sub>1 cells were isolated and generated from female TCR2 mice and characterized by flow cytometry<sup>12</sup>.

Tumours were isolated from sham- or Tag-T<sub>H</sub>1-cell-treated female RIP-Tag2 mice, sham- or Tag-T<sub>H</sub>1-cell-treated female *Tnfr1*<sup>-/-</sup> RIP-Tag2 mice, female *Stat1*<sup>-/-</sup> RIP-Tag2 mice, or mammary-tumour-bearing PyVmT-transgenic mice by collagenase digestion (1 mg ml<sup>-1</sup>, Serva) for 10 min at 37 °C, and then separated under a dissection microscope (Leica Microsystems). Tumour cells were obtained by incubation in 0.05% trypsin/EDTA solution (Invitrogen) at 37 °C for 10 min, and seeded on tissue culture plates. Adherent cells were cultured for 2–7 weeks in RPMI 1640 supplemented with 10% fetal calf serum, non-essential amino acids, antibiotics and 50 µM 2-mercaptoethanol at 37 °C and 5% CO<sub>2</sub>. The murine cancer cell lines B16, LLC and CT26 EpCam<sup>36</sup> in addition to 11 human cancer cell lines from the NCI-60 panel<sup>37</sup>, six primary human cancer cell preparations and human rhabdomyosarcoma cells (A204 cells) were grown in complete RPMI 1640 medium. If not otherwise stated, subconfluent cells were treated with 100 ng ml<sup>-1</sup> mouse or human IFN-γ (R&D Systems), or 10 ng ml<sup>-1</sup> mouse or human TNF (R&D Systems), or with a combination of mouse or human IFN-γ (50–100 ng ml<sup>-1</sup>) and mouse or human TNF (0.1–10 ng ml<sup>-1</sup>) for 2–6 days. β-cancer cells were identified by immunofluorescence using an anti-synaptophysin antibody (undiluted; Lifespan Biosciences).

**Knockdown of p16INK4a.** 5 × 10<sup>4</sup> β-cancer cells were seeded in 6-well culture plates. After 72 h, cells were transfected with 2 ml cell culture supernatant containing *shCtrl* or *shp16-p19* MSCV vectors<sup>38,39</sup> in the presence of 1 µg ml<sup>-1</sup> polybrene (Sigma) for a total transduction time of 12 h. After 5 days, transduced cells were selected by treatment with 1 µg ml<sup>-1</sup> puromycin (Sigma) for 72 h. The transduction rate was determined by counting green fluorescent protein-positive cells under a Zeiss Axiovert 200 microscope (Zeiss).

**In vitro proliferation assays.** After treatment, cancer cell proliferation was measured either by the [<sup>3</sup>H]-thymidine-incorporation assay<sup>40</sup>, or by the BrdU-based Cell Proliferation ELISA and XTT-based Cell Proliferation Kit II according to the manufacturer's protocols (Roche Diagnostics). [<sup>3</sup>H]-thymidine incorporation was quantified using a MicroBeta TriLux counter (PerkinElmer) and colorimetric analyses were performed on a Multiskan EX microplate reader (Thermo Electron).

**In vitro growth-arrest assays.** The different cancer cells were seeded at a density of 1 × 10<sup>4</sup> cells cm<sup>-2</sup>. Next, the cells were treated with control medium or cytokines as described above for 4–5 days. After treatment, the cells were trypsinized and viable cells (trypan blue exclusion) were counted under a Zeiss Axiovert 25 microscope (Zeiss) using a Neubauer counting-chamber (Karl Hecht GmbH). The cells were seeded at 2 × 10<sup>4</sup> cells cm<sup>-2</sup> and grown in complete RPMI 1640 medium until the control cultures reached confluence. Then, the cells were trypsinized, counted and seeded again. After passage 1–2, 1,000–3,000 viable cells were seeded on Multiscreen<sup>TM</sup> HTS 96 well Filtration Plates (Millipore), and proliferation was measured by the BrdU-based Cell Proliferation ELISA (Roche Diagnostics) in combination with the VectorSG Substrate Kit for Peroxidase from Vector Laboratories to visualize BrdU-incorporating cell clusters. BrdU-positive spots were counted with an ELISPOT reader (Bioreader-3000; Bio-Sys). In addition, some cultures were stained with 4',6-diamidino-2-phenylindole (DAPI; Invitrogen) to visualize the nuclei of adherent cells.

**Analysis of CXCL9 or CXCL10 in the supernatant of β-cancer cells.** β-cancer cells were either treated with medium alone or with IFN-γ and TNF. After 24 h incubation, CXCL9 or CXCL10 levels were determined in the cell culture supernatants using the mouse CXCL9 or mouse CXCL10 ELISA kit from R&D Systems.

**Treatment of mice with Tag-T<sub>H</sub>1 cells.** Before the first Tag-T<sub>H</sub>1-cell-based therapy, all mice received 2-Gy total-body irradiation. Then, 1 × 10<sup>7</sup> Tag-T<sub>H</sub>1 cells in

0.9% NaCl solution (Tag-T<sub>H</sub>1) or NaCl solution alone (sham) was injected intraperitoneally once per week starting at week 6 (ref. 12). After 6 weeks of Tag-T<sub>H</sub>1 treatment, all mice received a second 2-Gy total-body irradiation<sup>12</sup>. Blood glucose was measured using an Accu-Check sensor (Roche Diagnostics). If not otherwise stated, mice were euthanized at week 12.

**Transfer of β-cancer cells into immune-deficient mice.** β-cancer cells isolated from the various groups of mice were cultured for three passages. Then, 10–60% of the β-cancer cells were injected subcutaneously into immune-deficient NOD-SCID *Il2rg*<sup>-/-</sup> mice. Tumour growth was monitored with a caliper, and blood glucose was measured using an Accu-Check sensor for up to 7 weeks. Serum insulin levels were determined using the rat/mouse insulin ELISA kit from Millipore.

**Immunofluorescence and immunohistochemistry.** The different cancer cells were grown on chamber slides (BD Biosciences). After treatment, the cells were fixed with acetone/methanol 1:1. The slides were washed with PBS buffer and 0.05% Tween 20 at room temperature (21–23 °C), blocked with serum-free DAKO-Block (DAKO), washed again, and then incubated with the following antibodies: anti-Ki67 (dilution 1:100; Abcam), anti-PCNA (dilution 1:100; Cell Signaling Technology), anti-pHP1γ (dilution 1:100; Abcam), anti-H3K9me3 (dilution 1:500; Millipore), anti-p16INK4a (dilution 1:100; Santa Cruz Biotechnology), anti-SV40 Tag (dilution 1:100; BD Biosciences), anti-MHCII (dilution 1:50; eBioscience) or anti-synaptophysin (undiluted; Lifespan Biosciences). After washing, the slides were incubated with anti-rabbit Alexa488 (Invitrogen), anti-rabbit-Cy3 (Dianova), anti-mouse Alexa555, or anti-mouse Alexa488 (both from Cell Signaling Technology), washed again and incubated with DAPI (Invitrogen). Finally, the slides were washed, mounted with fluorescence mounting medium (DAKO) and analysed using a Zeiss Axiovert 200 microscope (Zeiss) with the VisiView software (VisiTron Systems).

Fresh-frozen cryostat sections of whole pancreata were stained as described<sup>40</sup>. In brief, the sections were fixed with periodate–lysine–paraformaldehyde, blocked with donkey serum (dilution 1:20), and then incubated with rabbit anti-pHP1γ (dilution 1:80), mouse anti-PCNA (dilution 1:50), mouse anti-p16INK4a (dilution 1:50), or rabbit anti-Ki67, rat-anti-MHCII (dilution 1:50), or rabbit anti-synaptophysin (undiluted) antibodies. After washing, the sections were incubated with Cy3-conjugated donkey anti-rabbit, donkey anti-mouse, or Cy5-conjugated donkey anti-rabbit, donkey anti-mouse, or donkey anti-rat-dylight 549 and donkey anti-rabbit-dylight 649 IgG (all from Dianova). Before mounting the slides with Mowiol (Hoechst), nuclei were stained with Yopro (1:2,000; Invitrogen). The sections were analysed using a Leica TCS-Sp/Leica DM RB confocal laser scanning microscope (Leica Microsystems). Images were processed with the Leica Confocal Software LCS (Version 2.61).

Formalin-fixed pancreata were embedded in paraffin. Sections (3–5-µm thick) were cut and stained with haematoxylin and eosin. Immunohistochemistry was performed on an automated immunostainer (Ventana Medical System) according to the manufacturer's protocol, with minor modifications<sup>41</sup>. The antibody panel used included activated caspase 3 (Cell Signaling Technology), Ki67 (DCS Innovative Diagnostik-Systeme), pHP1γ (Abcam) and H3K9me3 (Cell Signaling Technology). Formalin-fixed and paraffin-embedded melanoma were stained using monoclonal mouse-anti human Ki67 (clone MIB-1; DAKO) or the CINtec p16INK4a Cytology Kit (Roche mtm laboratories AG).

**SA-β-gal activity assay.** Cancer cells were fixed for 15 min at room temperature, and then stained for 16 h at 37 °C using the β-Galactosidase Staining Kit (United States Biological). SA-β-gal-positive and -negative cells were then counted using a Zeiss Axiovert 200 microscope (Zeiss). In some experiments, the cells were counterstained for synaptophysin by immunofluorescence, and synaptophysin-SA-β-gal double-positive cells were counted.

**Cell cycle analysis.** After treatment of β-cancer cells, cell cycle analysis was performed using the BD Pharmingen FITC-BrdU Flow Kit according to the manufacturer's protocol (BD Biosciences). The samples were analysed by flow cytometry on a LSR II from Becton Dickinson, and the following cell cycle phases were determined as a percentage of the total population: sub-G1 (apoptotic cells), G1/G0 (2n, BrdU-negative), S (2n to 4n, BrdU-positive) and G2/M phase (4n, BrdU-negative).

**Western blotting.** After treatment, cancer cells were lysed in lysis buffer (50 mM Tris-HCl, pH 7.5, 150 mM NaCl, 1% Triton X-100, 0.5% SDS, 1 mM NaF, 1 mM Na<sub>3</sub>VO<sub>4</sub> and 0.4% β-mercaptoethanol) containing a protease inhibitor cocktail and a phosphatase inhibitor cocktail (PhosSTOP, Roche Diagnostics). Alternatively, cytoplasmic protein extracts were obtained from the cell cultures using the NE-PER extraction kit (Thermo Fisher Scientific) according to the manufacturer's protocol. Before use, protease inhibitors and PhosSTOP were added to the lysis buffers CER I and NER. After determination of protein content by the bicinchoninic acid assay (Thermo Fisher Scientific), proteins were resolved by 12% SDS-PAGE or by Mini-PROTEAN TGX Precast Gels (4–15%; BioRad), transferred

onto a polyvinylidene difluoride (PVDF) membrane and blocked with 3% non-fat milk in TBS/0.1% Tween 20 (TBST) as described<sup>42</sup>. The membrane was incubated with anti-p16INK4a (1:1,000; Santa Cruz), anti-Rb (Ab-780) (1:1,000), anti-Rb(phospho-Ser-795) (1:1,000; both from SAB Signalway Antibody), anti-CXCL9 (1:2,000), anti-CXCL10 (1:2,000; both from R&D Systems), or anti- $\beta$ -actin antibody (1:1,000; BioVision). After washing with TBST and subsequent blocking, the blots were incubated with goat anti-mouse horseradish peroxidase (HRP)-conjugated antibody or with goat anti-rabbit HRP-conjugated antibody (1:3,000; Cell Signaling Technology), washed again, and antibody binding was detected with the ECL detection reagent (Amersham). Immunoreactive bands were quantified using the ImageJ software (National Institutes of Health), and the phospho-Rb/Rb ratio of the samples was calculated.

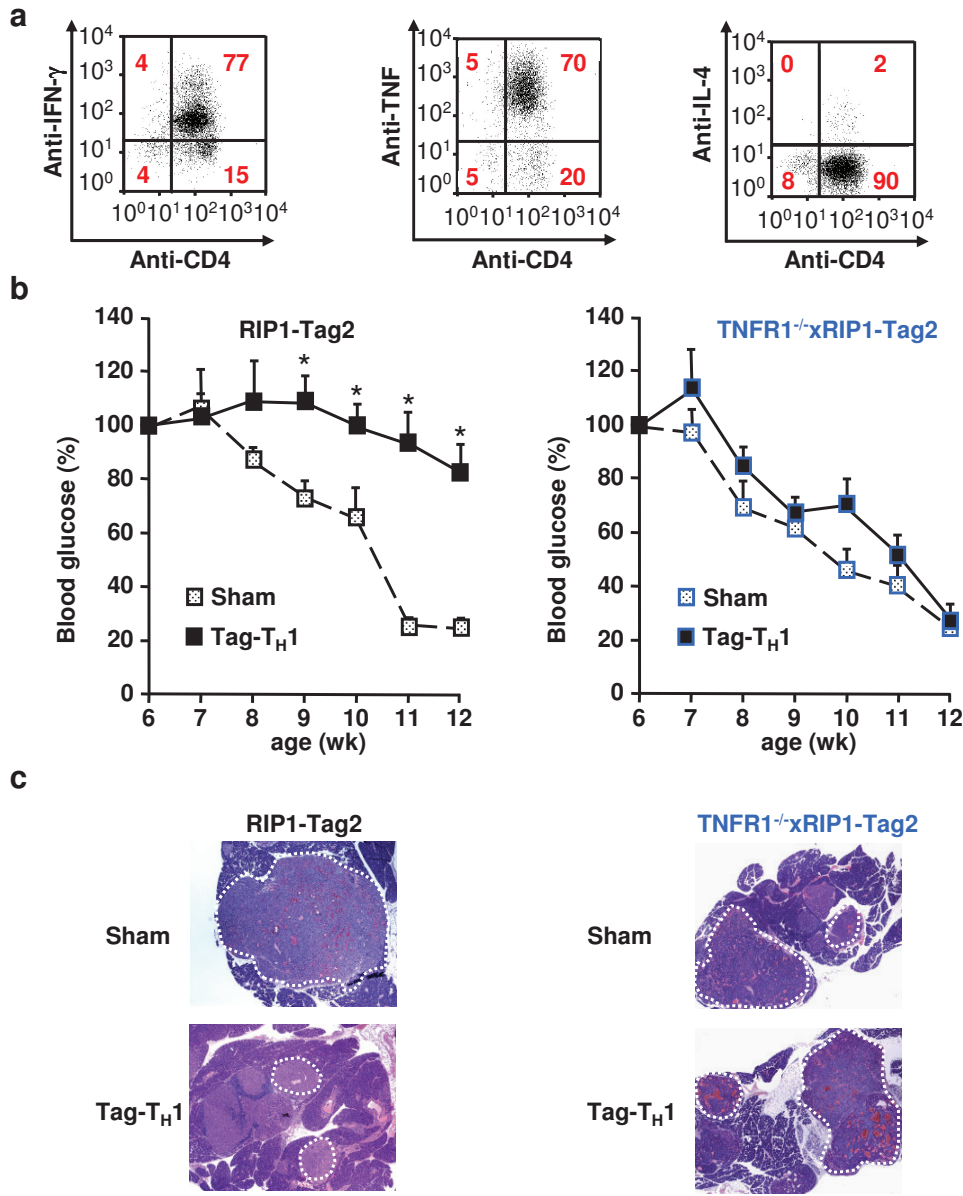
**Chromium release assay.**  $2.5 \times 10^6$  target cells were labelled with 250  $\mu$ Ci (9.25 MBq) <sup>51</sup>NaCr (Hartmann Analytic) at 37 °C for 1.5 h. After incubation, cells were washed and plated into microtitre round bottom plates at  $1 \times 10^4$  cells per well. Effector cells were added at different effector to target ratios and incubated at 37 °C for 4 h. Spontaneous release in the absence of effector cells was always less than 30% of the maximal release induced by Triton X-100 (1%). After incubation, 50  $\mu$ l supernatant per well was mixed with 200  $\mu$ l scintillation cocktail (Ultima Gold, PerkinElmer) and measured in a liquid scintillation counter (MicroBeta, PerkinElmer).

**Gene-expression analysis.** The gene expression of  $\beta$ -cancer cells and different mouse and human cancer cell lines was analysed after RNA purification and reverse transcription by PCR essentially as described<sup>43</sup>. The following primers were used: mouse *Cdkn2a* (*p16INK4a*) (146 base pairs (bp)): sense TTGCCC ATCATCATCACCT and antisense GGGTTTCTTGGTGAAGTTCG; mouse *Ifngr1* (474 bp): sense AGGAGGAAGAAGGAAGAACAG and antisense TACCACAGAGAGCAAGGAC; mouse *Ifngr2* (533 bp): sense TCATACACTTC TCCCCTCCC and antisense CACATCATCTCGTCCCTTTTC; mouse *Tnfrsf1a* (531 bp): sense TCCCCCTCCTACCTTCTCTCT C and antisense TGCCCTTTT CACTCCCTG; mouse *Hprt* (90 bp): sense TCCTCCTCAGACCGCTTTT and antisense CCTGGTTCATATCGTAATC; mouse *Eef1a1* (119 bp): sense ACACGTAGATTCCGGCAAGT and antisense AGGAGCCCTTCCCATCTC; mouse *Cxcl9* (80 bp): sense TTTTCTCTTGGGCATCATCTT and antisense AGCATCGTGCATTCTTATCACT; mouse *Cxcl10* (111 bp): sense GCTGCCG TCATTTTCTGC and antisense TCTCACTGGCCCGTCATC; human *IFNGR1* (417 bp): sense TCTCCTCTTTCTCCTACCCC and antisense ATTTGCTTCTCC

TCCTTTCTG; human *IFNGR2* (558 bp): sense GTACACAGATCACAGC AACAG and antisense TCAGGACCAGGAAGAAACAG; human *TNFRSF1A* (580 bp): sense GGACAGGGAGAAGAGAGATAG and antisense GAGGAGGG ATAAAAGGCAAAG.

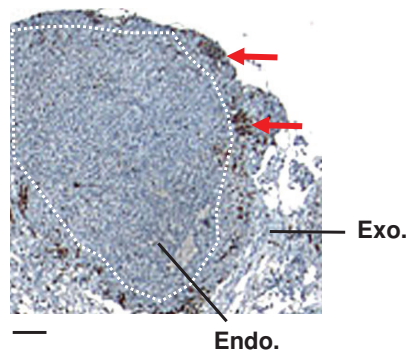
**Statistics.** If not otherwise stated, data were expressed as arithmetic means  $\pm$  s.e.m., and statistical analyses were made by unpaired *t*-test, or analysis of variance using Dunnett's or Tukey's test as a post hoc test, where appropriate.  $P < 0.05$  was considered statistically significant.

31. Hanahan, D. Heritable formation of pancreatic  $\beta$ -cell tumours in transgenic mice expressing recombinant insulin/simian virus 40 oncogenes. *Nature* **315**, 115–122 (1985).
32. Pfeffer, K. *et al.* Mice deficient for the 55 kd tumor necrosis factor receptor are resistant to endotoxic shock, yet succumb to *L. monocytogenes* infection. *Cell* **73**, 457–467 (1993).
33. Förster, I., Hirose, R., Arbeit, J. M., Clausen, B. E. & Hanahan, D. Limited capacity for tolerization of CD4<sup>+</sup> T cells specific for a pancreatic  $\beta$  cell neo-antigen. *Immunity* **2**, 573–585 (1995).
34. Maglione, J. E. *et al.* Transgenic polyoma middle-T mice model premalignant mammary disease. *Cancer Res.* **61**, 8298–8305 (2001).
35. Shultz, L. D., Ishikawa, F. & Greiner, D. L. Humanized mice in translational biomedical research. *Nature Rev. Immunol.* **7**, 118–130 (2007).
36. Ziegler, A. *et al.* EpCAM, a human tumor-associated antigen promotes Th2 development and tumour immune evasion. *Blood* **113**, 3494–3502 (2009).
37. Monks, A. *et al.* Feasibility of a high-flux anticancer drug screen using a diverse panel of cultured human tumor cell lines. *J. Natl. Cancer Inst.* **83**, 757–766 (1991).
38. Keyes, W. M. *et al.* p63 deficiency activates a program of cellular senescence and leads to accelerated aging. *Genes Dev.* **19**, 1986–1999 (2005).
39. Dickins, R. A. *et al.* Probing tumor phenotypes using stable and regulated synthetic microRNA precursors. *Nature Genet.* **37**, 1289–1295 (2005).
40. Kneilling, M. *et al.* Direct crosstalk between mast cell-TNF and TNFR1-expressing endothelia mediates local tissue inflammation. *Blood* **114**, 1696–1706 (2009).
41. Kunder, S. *et al.* A comprehensive antibody panel for immunohistochemical analysis of formalin-fixed, paraffin-embedded hematopoietic neoplasms of mice: analysis of mouse specific and human antibodies cross-reactive with murine tissue. *Toxicol. Pathol.* **35**, 366–375 (2007).
42. Hennige, A. M. *et al.* Overexpression of kinase-negative protein kinase C $\delta$  in pancreatic  $\beta$ -cells protects mice from diet-induced glucose intolerance and  $\beta$ -cell dysfunction. *Diabetes* **59**, 119–127 (2010).
43. Biedermann, T. *et al.* Mast cells control neutrophil recruitment during T cell-mediated delayed-type hypersensitivity reactions through tumor necrosis factor and macrophage inflammatory protein 2. *J. Exp. Med.* **192**, 1441–1452 (2000).



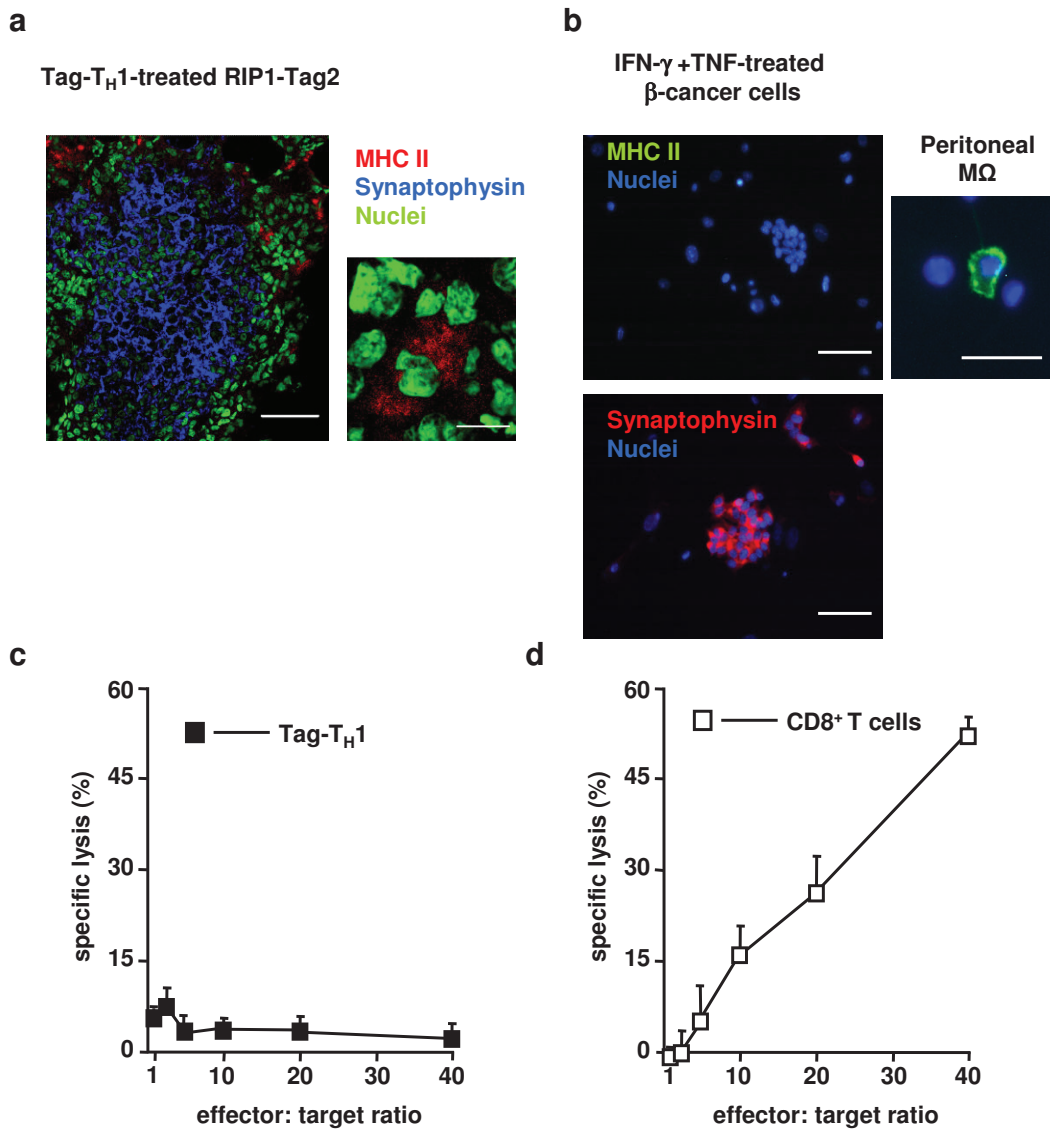
**Suppl. Fig. 1 | Treatment of RIP1-Tag2 mice with IFN- $\gamma$  and TNF-secreting Tag-T<sub>H</sub>1 cells leads to TNFR1-dependent stabilization of blood glucose levels, and arrests islet cancer growth *in vivo*.**

**a**, Intracellular staining of IFN- $\gamma$  (left), TNF (middle) and IL-4 (right) in Tag-T<sub>H</sub>1 cells stimulated with PMA/ionomycin. **b**, Blood glucose levels in RIP1-Tag2 or TNFR1<sup>-/-</sup>x RIP1-Tag2 mice that were treated with either NaCl (Sham) or with  $1 \times 10^7$  Tag-T<sub>H</sub>1 cells. **c**, H&E staining of pancreata of RIP1-Tag2 mice or TNFR1<sup>-/-</sup>xRIP1-Tag2 mice that were either sham-treated or treated with Tag-T<sub>H</sub>1 cells. The dashed lines indicate the size of the tumors. Bar, 400  $\mu$ m. \*P < 0.05 from sham-treated control. n=3-4 (b).



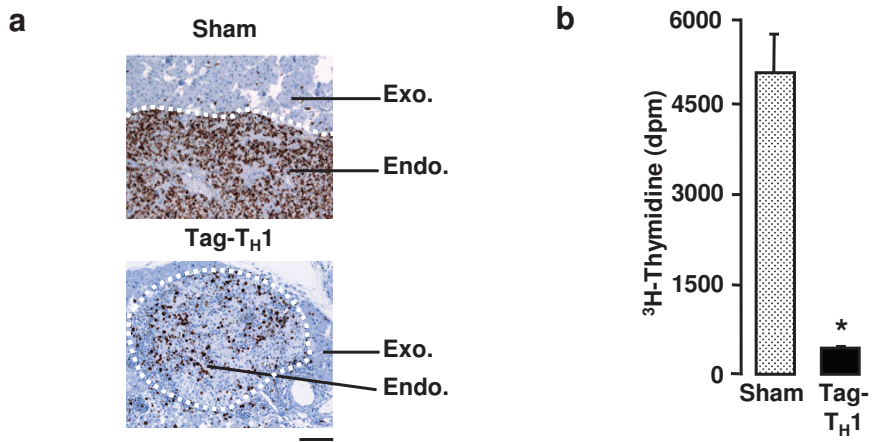
**Suppl. Fig. 2 | CD3-positive T cells surrounding an endocrine  $\beta$ -cell tumor**

Immunohistochemistry of CD3<sup>+</sup> lymphocytes in the peritumoral microenvironment of Tag-T<sub>H</sub>1 cell-treated RIP1-Tag2 mice. Exo., exocrine tissue; Endo., endocrine tissue. Bar, 50  $\mu$ m. Arrows point to clusters of CD3<sup>+</sup> lymphocytes.



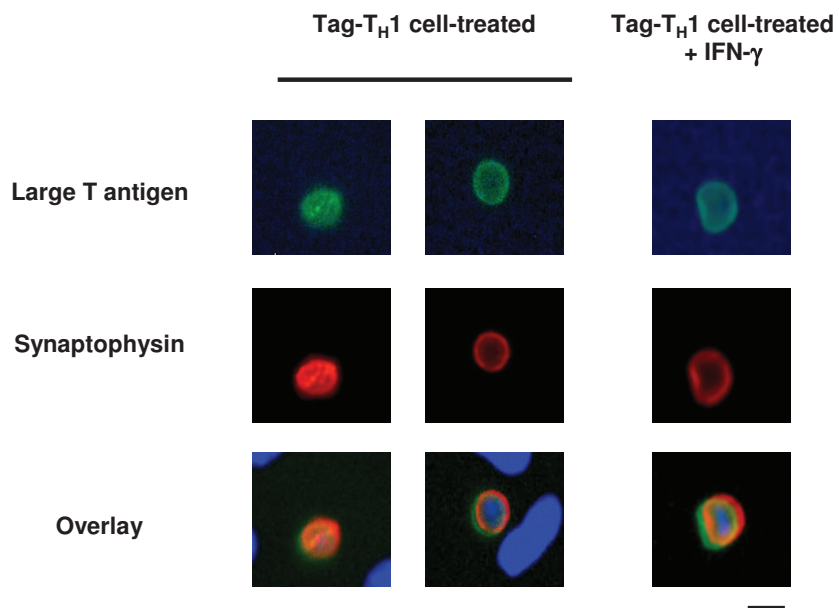
**Suppl. Fig. 3 |  $\beta$ -cancer cells fail to express MHC class II either *in vivo* or *in vitro* and are not lysed by Tag- $T_H1$  cells *in vitro***

**a**, Double-staining for MHC II (red) and the islet cell marker synaptophysin (blue) in cancers from RIP1-Tag2 mice that were Tag- $T_H1$  cell-treated. Nuclei are green. Bar, 50  $\mu$ m. Note that the synaptophysin<sup>+</sup> tumor areas are devoid of MHC II. A higher magnification of an antigen-presenting cell is shown on the right. Bar, 10  $\mu$ m. **b**, Staining for MHC II (green, upper panel) or the islet cell marker synaptophysin (red, lower panel) of isolated  $\beta$ -cancer cells treated with IFN- $\gamma$  and TNF. Nuclei are blue. Peritoneal macrophages ( $M\Omega$ ) are shown on the right and were used as a positive control. Bars, 50  $\mu$ m. **c**, Antigen-specific cytotoxicity of Tag- $T_H1$  cells against  $\beta$ -cancer cells *in vitro*. Lysis of  $\beta$ -cancer cells was measured by chromium-51 release and is given in % (mean  $\pm$  s.e.m., n=8). **d**, Cytotoxicity of CD8<sup>+</sup> T cells against C57Bl/6 spleen cells *in vitro*. Mean lysis of C57Bl/6 spleen cells as assayed in triplicate is given in %  $\pm$  s.e.m. and was used as a positive control.



**Suppl. Fig. 4 | Treatment of RIP1-Tag2 mice with Tag- $T_H1$  cells leads to inhibition of  $\beta$ -cancer cell proliferation *in vivo* and *ex vivo*.**

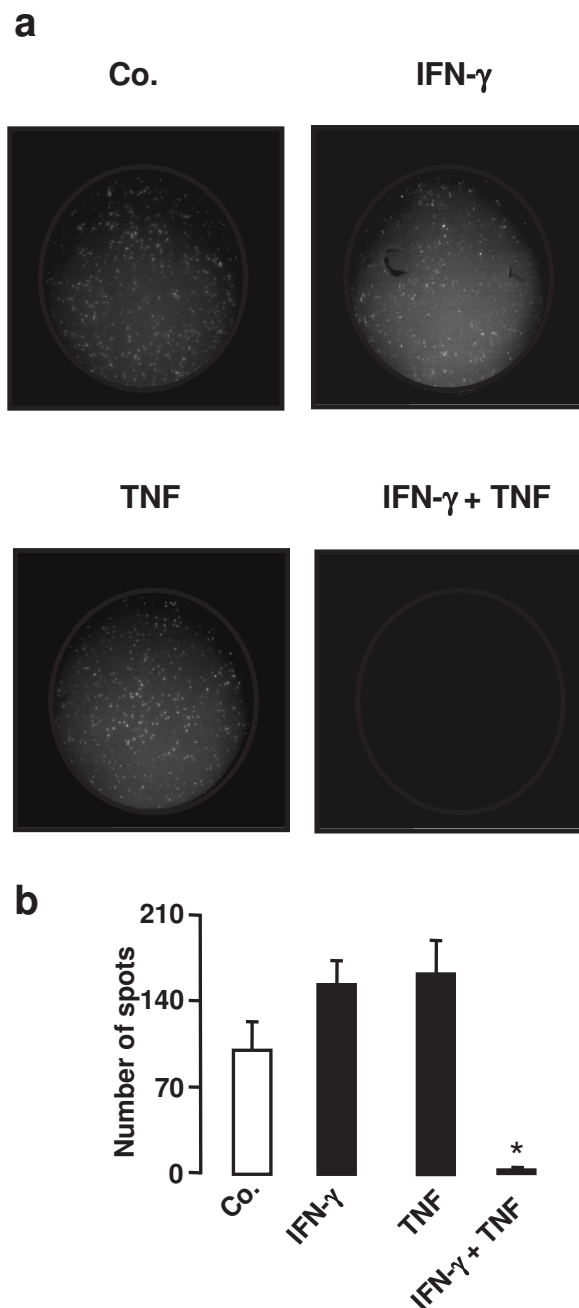
**a**, Ki67 staining of pancreata from sham- or Tag- $T_H1$  cell-treated RIP1-Tag2 mice. Exo., exocrine tissue; Endo., endocrine tissue. Bar, 50  $\mu$ m. **b**, *Ex vivo*  $^3H$ -thymidine incorporation of  $\beta$ -cancer cells isolated from sham- or Tag- $T_H1$  cell-treated RIP1-Tag2 mice.



**Suppl. Fig. 5 |  $T_H1$  immunity and IFN- $\gamma$  do not suppress Tag expression.**

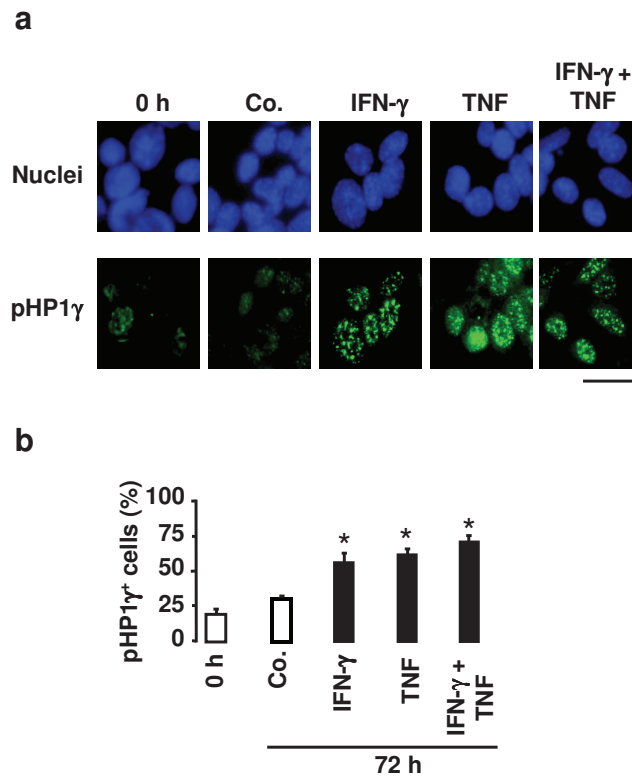
Triple-staining for Tag (green), the  $\beta$ -cell marker protein synaptophysin (red) and nuclei (blue) of  $\beta$ -cancer cells isolated from RIP1-Tag2 mice that had been treated with Tag- $T_H1$  cells. Some cell cultures were in addition treated with IFN- $\gamma$ . Bar, 10  $\mu$ m.





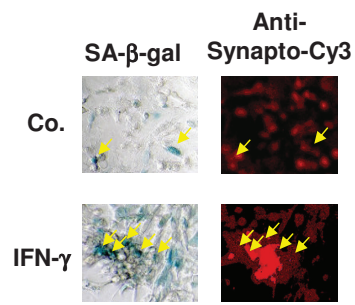
**Suppl. Fig. 6 | Combined IFN- $\gamma$  and TNF treatment but neither IFN- $\gamma$  alone nor TNF alone induce stable growth arrest in isolated  $\beta$ -cancer cells *in vitro*.**

**a**,  $\beta$ -cancer cells isolated from RIP1-Tag2 mice were treated for 4-5 days with medium (Co.), IFN- $\gamma$ , TNF, or IFN- $\gamma$  and TNF. After incubation, the cells were washed and trypsinized and then grown in the absence of the cytokines for another two passages. After passage two, 3,000 viable cells were seeded in 96 well plates and cell proliferation was analyzed by BrdU staining. **b**, Mean numbers of BrdU-positive spots of  $\beta$ -cancer cells after treatment with medium (Co.), IFN- $\gamma$ , TNF, or IFN- $\gamma$  and TNF, and subsequent removal of the cytokines as described in **a**. \* $P$ <0.05 from control.  $n$ =8-20 (**b**).



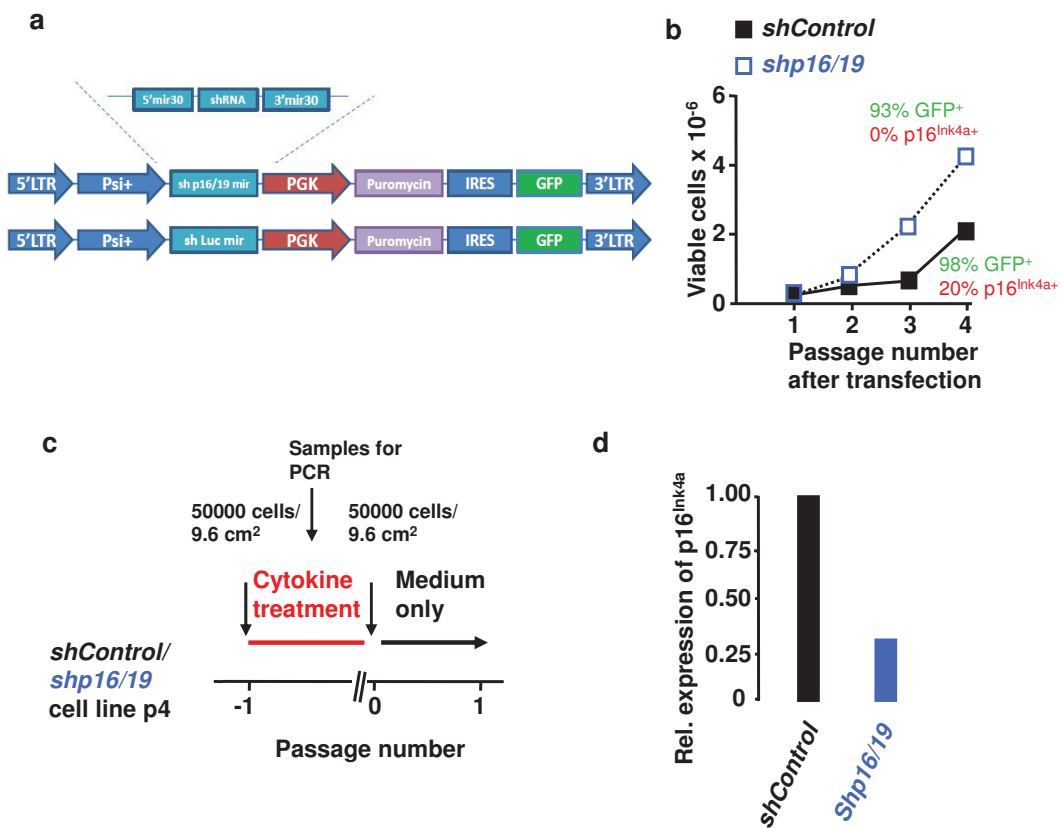
**Suppl. Fig. 7 | Nuclear recruitment of pHP1 $\gamma$  into senescence-associated heterochromatin foci (SAHF) after IFN- $\gamma$ , TNF, or combined IFN- $\gamma$  and TNF treatment in isolated  $\beta$ -cancer cells *in vitro*.**

**a**,  $\beta$ -cancer cells isolated from RIP1-Tag2 mice were treated for 72 h with medium (Co.), IFN- $\gamma$ , TNF, or IFN- $\gamma$  and TNF. After incubation, the cells were analyzed by pHP1 $\gamma$ -staining. Nuclei are blue. Bar, 25  $\mu$ m. **b**, Mean percentage of pHP1 $\gamma$ -positive  $\beta$ -cancer cells (i.e., cells with more than 5 nuclear dots) after treatment with medium (Co.), IFN- $\gamma$ , TNF, or IFN- $\gamma$  and TNF. \* $P$ <0.05 from control. n=6-10.



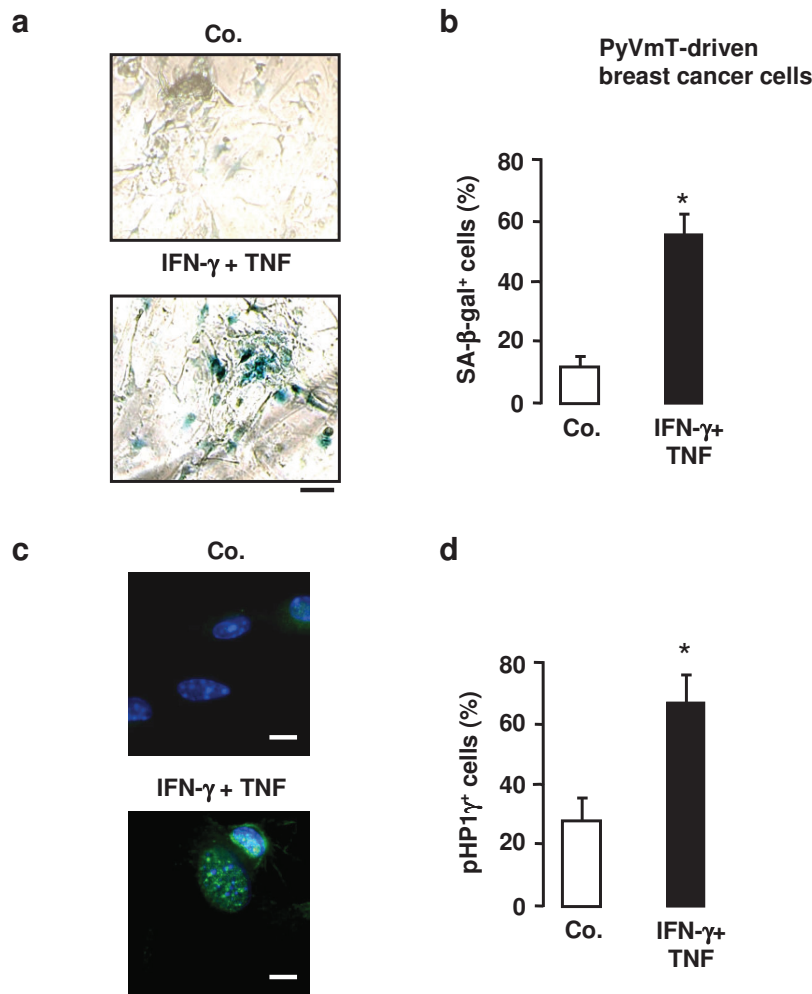
**Suppl. Fig. 8 | SA-β-gal activity in synaptophysin-positive β-cancer cells after treatment with IFN-γ *in vitro***

Double-staining for SA-β-gal activity (blue) and the β-cell marker protein synaptophysin (red) of β-cancer cells after incubation for 72 h with medium (Co.) or IFN-γ. The yellow arrows point to SA-β-gal<sup>+</sup>/synapto-physin<sup>+</sup> cells. Bar, 100 μm.



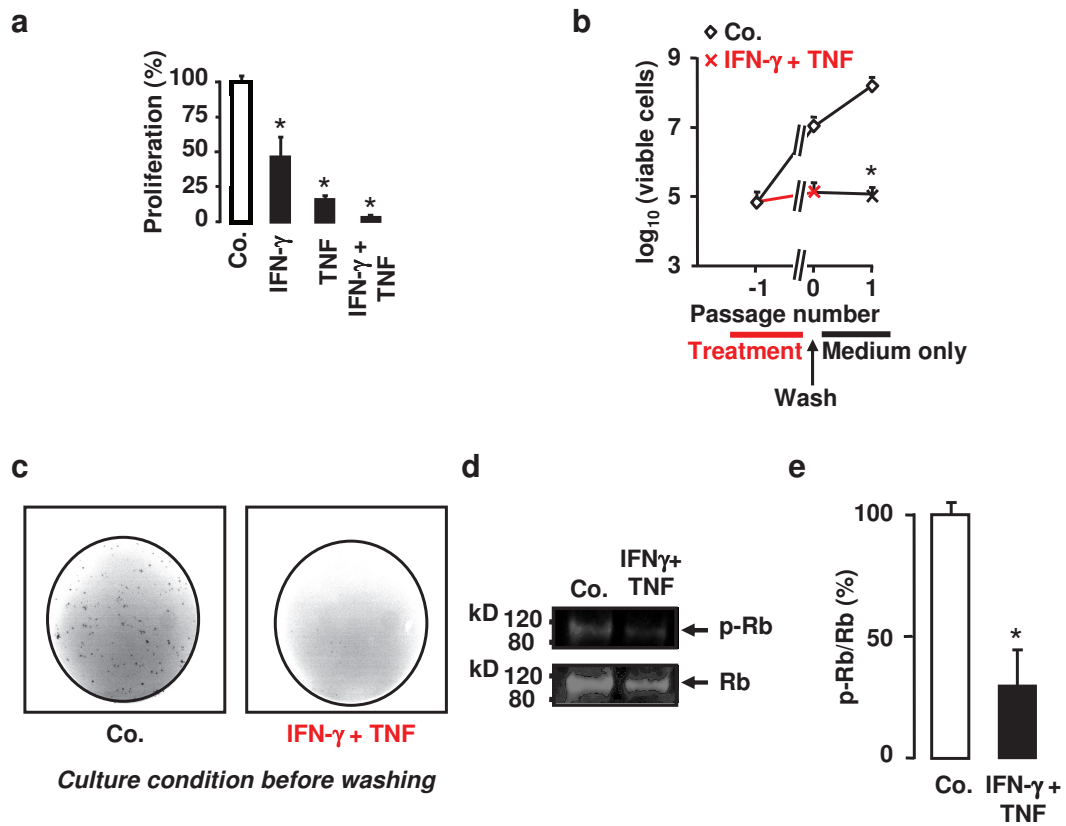
**Suppl. Fig. 9 | Knock-down of p16<sup>Ink4a</sup> by the use of shRNA.**

**a**, Mscv vectors (shControl = sh Luc mir) used for the p16<sup>Ink4a</sup> knock-down experiments. **b**, Growth curves of RIP1-Tag2 β-cancer cells transfected with shControl or shp16/19 particles. At passage 4, the transfection rates (green numbers, GFP<sup>+</sup> cells) and the p16<sup>Ink4a</sup> expression levels (red numbers, p16<sup>Ink4a+</sup> cells) of the two cell lines were determined by (immuno-) fluorescence microscopy. **c**, Experimental set up for the growth arrest assay of the shRNA-transfected cell lines. **d**, Knock-down of p16<sup>Ink4a</sup> expression by shp16/19 as measured by quantitative RT-PCR. Data represent the mean of two determinations (**b**, **d**). The experiment was repeated with similar results using β-cancer cells from a second RIP1-Tag2 mouse.



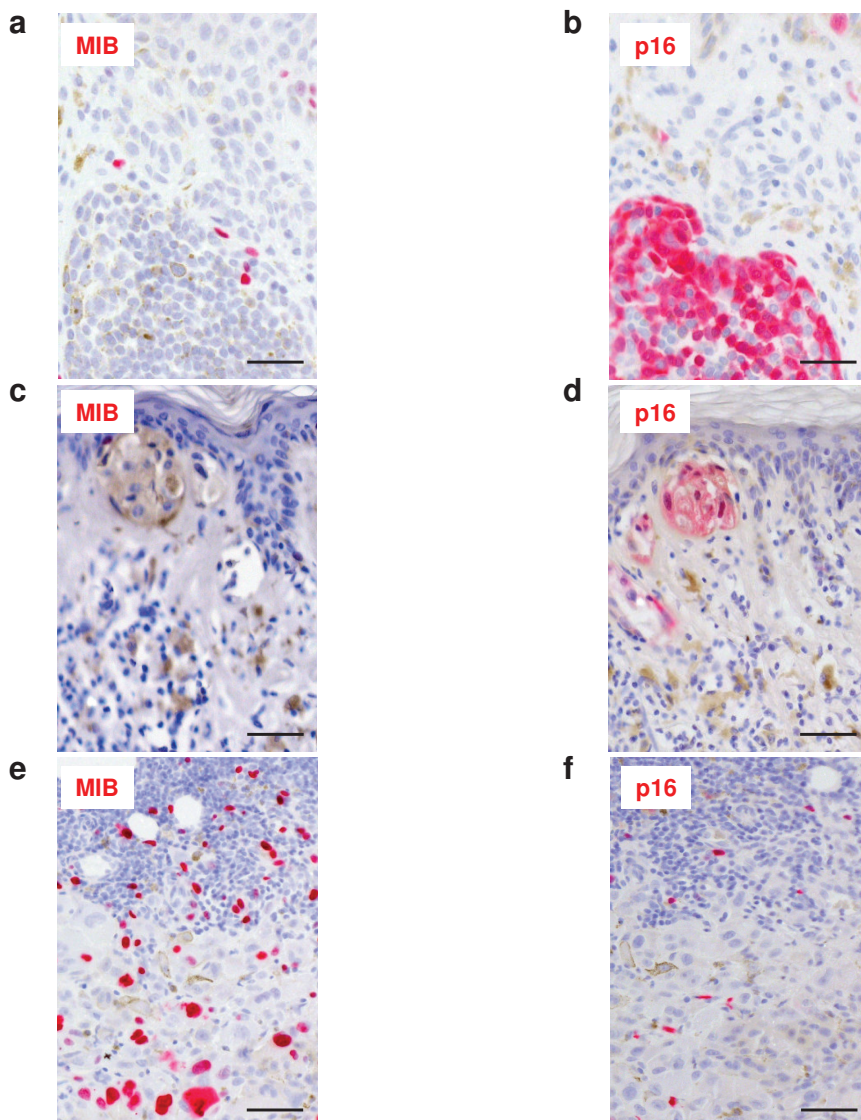
**Suppl. Fig. 10** | Induction of SA- $\beta$ -gal activity and nuclear recruitment of pHP1 $\gamma$  into SAHF after combined IFN- $\gamma$  and TNF treatment in isolated PyVmT-driven breast cancer cells *in vitro*.

**a, b**, SA- $\beta$ -gal activity (**a**) and mean percentage of SA- $\beta$ -gal<sup>+</sup> cells (**b**) in breast cancer cells isolated from PyVmT-transgenic mice after treatment for 72 h with medium (Co.) or IFN- $\gamma$  and TNF. Bar, 50  $\mu$ m. \* $P$ <0.05 from control.  $n$ =9-10. **c, d**, Immunofluorescence images of pHP1 $\gamma$  (**c**) and percentage (**d**) of pHP1 $\gamma$ -positive cells (i.e. cells with more than 5 nuclear dots) in breast cancer cells isolated from PyVmT-transgenic mice after treatment for 96 h with medium (Co.) or IFN- $\gamma$  and TNF. Nuclei are shown in blue and pHP1 $\gamma$  stainings in green. Bar, 5  $\mu$ m. \* $P$ <0.05 from control.  $n$ =8-9.



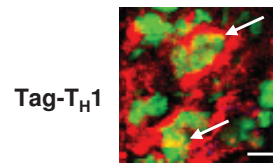
**Suppl. Fig. 11 | Combined IFN- $\gamma$  and TNF treatment induces stable growth arrest and profound Rb hypophosphorylation in A204 rhabdomyosarcoma cells.**

**a**, Mean proliferation of A204 cells as measured by BrdU incorporation in % after treatment for 72 h with medium (Co.), IFN- $\gamma$ , TNF, or IFN- $\gamma$  and TNF. \* $P$ <0.05 from control.  $n$ =6. **b, c**, A204 cells were seeded at low density and then treated for 4-5 days with medium (Co.) or IFN- $\gamma$  and TNF. After incubation, the cells were washed and trypsinized, and then grown in the absence of the cytokines for one passage with medium only, and counted. Finally, 1,000 viable cells were seeded in 96 well plates and analyzed by BrdU staining. Mean cell numbers (**b**) and BrdU staining (**c**) of A204 cells after treatment with medium (Co.) or IFN- $\gamma$  and TNF, and subsequent removal of the cytokines for one week are shown. \* $P$ <0.05 from control.  $n$ =4-6 (**b**). **d, e**, Detection of phosphorylated Rb (pRb) and total Rb (Rb) by Western blot in A204 cells treated for 48 h with medium (Co.) or IFN- $\gamma$  and TNF (**d**), and quantification of the p-Rb/Rb ratio by videodensitometry (**e**). \* $P$ <0.05 from control.  $n$ =4 (**e**).



**Suppl. Fig. 12 | Expression of the proliferation marker MIB and the senescence marker p16<sup>Ink4a</sup> in regressing melanoma**

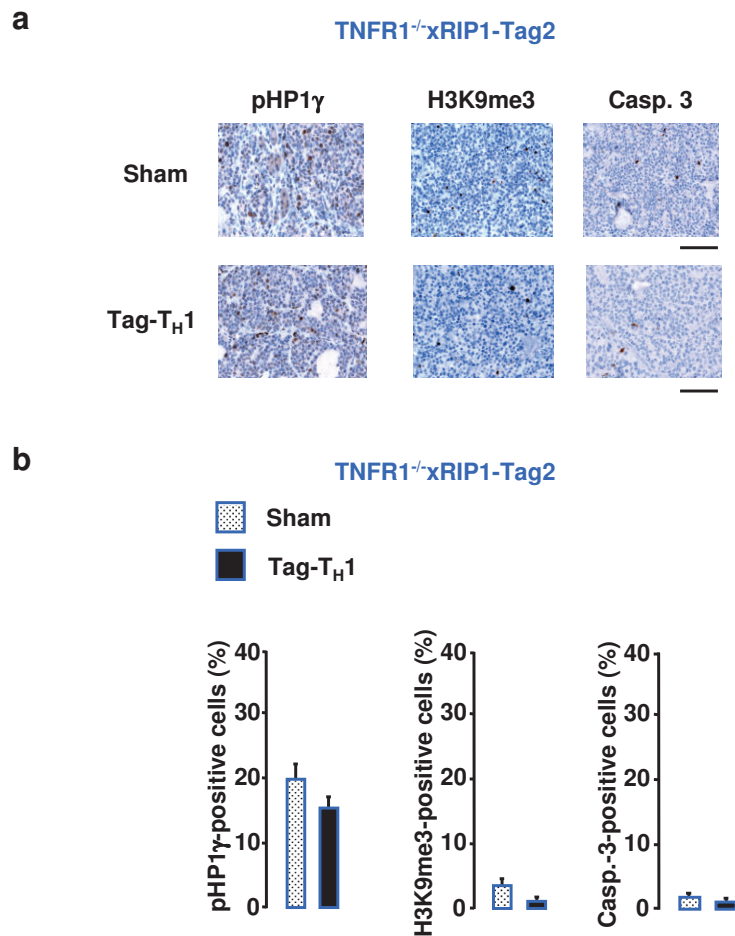
**a, c, e,** Staining for MIB (red) of a regressing halo nevus (**a**), a superficial spreading melanoma with inflammation-associated regression (**c**) and proliferating melanoma metastasis again in association with mononuclear cells (**e**). **b, d, f,** Staining for p16<sup>Ink4a</sup> (red) of a regressing halo nevus (**b**), a superficial spreading melanoma with inflammation-associated regression (**d**) and proliferating melanoma metastasis again in association with mononuclear cells (**f**). Bars, 50  $\mu$ m. Melanin-containing cells appear brown. The regressing halo nevus shown in (**a**) and (**b**) was used as a positive control for non-proliferating, p16<sup>Ink4a+</sup> cells (Michaloglou, C. *et al.* BRAF<sup>E600</sup>-associated senescence-like cell cycle arrest of human naevi. *Nature* **436**, 720-724 (2005)). The melanoma metastasis shown in (**e**) and (**f**) was used as a highly proliferating, p16<sup>Ink4a-</sup> control (Monahan, KB. *et al.* Somatic p16<sup>Ink4a</sup> loss accelerates melanomagenesis. *Oncogene* **29**, 5809-5817 (2010)).



**Suppl. Fig. 13| Induction of nuclear and cytoplasmic p16<sup>Ink4a</sup> by T<sub>H</sub>1 immunity *in vivo* (higher magnification from Fig. 3c).**

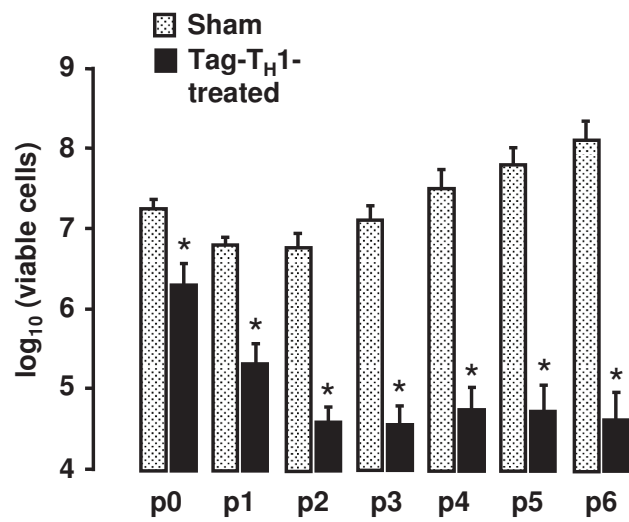
Triple-staining for either p16<sup>Ink4a</sup> (red), Ki67 (blue) and nuclei (green) in cancers from RIP1-Tag2 mice that had been treated with Tag-T<sub>H</sub>1 cells. Overlay of red (p16<sup>Ink4a</sup> staining) and green (nuclear staining) appears yellow. Arrows point to p16<sup>Ink4a</sup>-positive nuclei of cancer cells from mice treated with Tag-T<sub>H</sub>1 cells. Bar, 10 μm.





**Suppl. Fig. 14 | Failure of Tag-T<sub>H</sub>1 cells to induce senescence markers in TNFR1<sup>-/-</sup>xRIP1-Tag2 mice *in vivo***

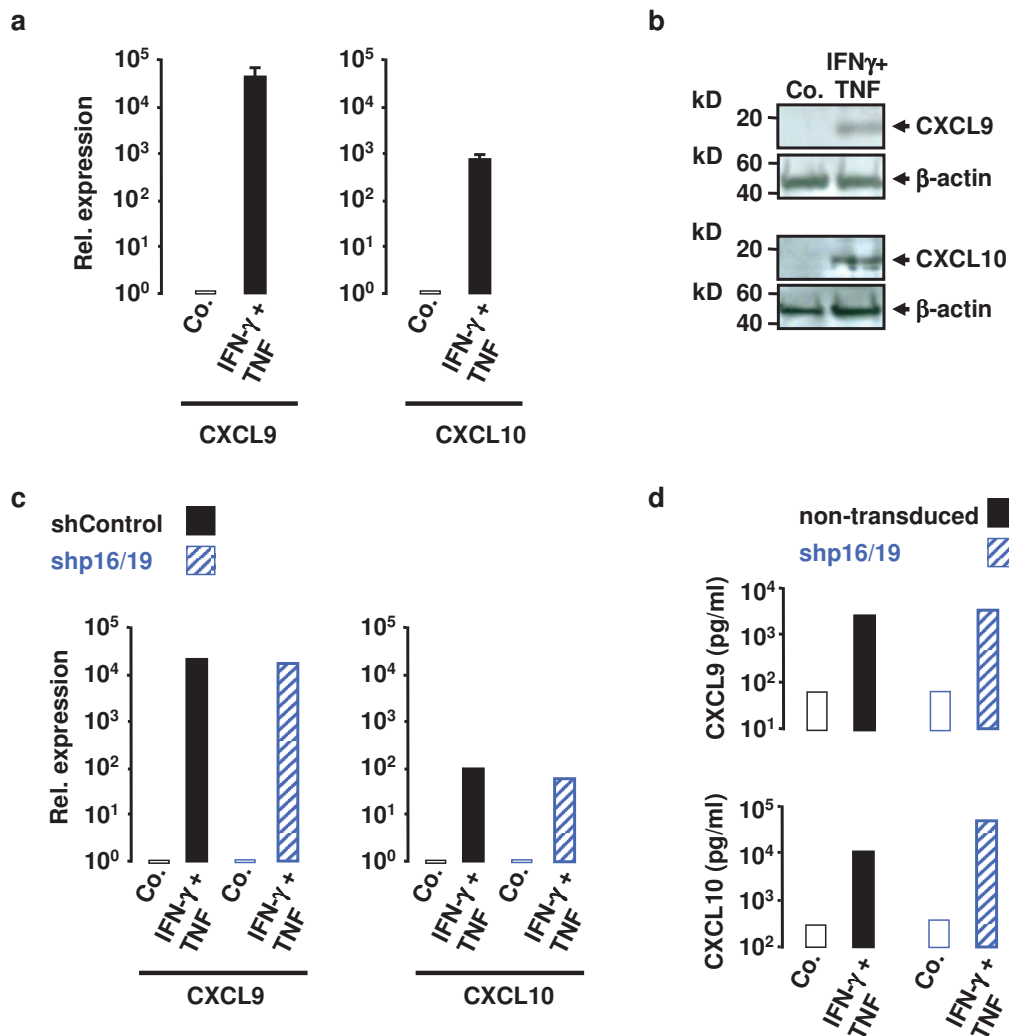
**a**, Immunohistochemical detection of pHP1 $\gamma$ <sup>\*</sup>, tri-methylated H3K9 (H3K9me3), and active caspase-3 in tissue sections from TNFR1<sup>-/-</sup>xRIP1-Tag2 mice that were treated with NaCl (Sham) or Tag-T<sub>H</sub>1 cells. **b**, Mean percentage of pHP1 $\gamma$ <sup>\*</sup>, H3K9me3<sup>-</sup>, and active caspase-3-positive cells in five high-power fields in tumors derived from Tag-T<sub>H</sub>1- or sham-treated TNFR1<sup>-/-</sup>xRIP1-Tag2 mice. Note that Tag-T<sub>H</sub>1 cell treatment did not increase the expression of the senescence markers pHP1 $\gamma$  and MeH3, or of the apoptosis marker active caspase-3. For RIP1-Tag2 controls see **Fig. 3a, b** which was done in parallel. Bar, 100  $\mu$ m. \*pHP1 $\gamma$  binds to spread chromosomes during mitosis (Minc, E. *et al.* Localization and phosphorylation of HP1 proteins during the cell cycle in mammalian cells. *Chromosoma* **108**, 220-234 (1999)).



**Suppl. Fig. 15 |  $T_H1$ -immunity induces permanent growth arrest of  $\beta$ -cancer cells which remains stable for 6 passages of *in vitro* culture.**

Mean cell numbers of  $\beta$ -cancer cells isolated from RIP1-Tag2 mice that were sham- or Tag- $T_H1$  cell-treated. The number of cell passages (p) is indicated, and the data are presented as  $\log_{10}$  of the number of living  $\beta$ -cancer cells per mouse  $\pm$  s.e.m.

\* $P < 0.05$  from sham-treated control. n=3-4.



**Suppl. Fig. 16** | p16<sup>Ink4a</sup>-independent induction of the chemokines CXCL9 and CXCL10 by combined IFN- $\gamma$  and TNF in RIP1-Tag2  $\beta$ -cancer cells.

**a**, Mean relative expression of CXCL9 or CXCL10 after treatment of  $\beta$ -cancer cells with medium (Co.) or IFN- $\gamma$  and TNF as measured by quantitative RT-PCR (n=3-6). Expression of medium-treated  $\beta$ -cancer cells was set as 1. **b**, Detection of CXCL9, CXCL10 or  $\beta$ -actin as loading control by Western blot in  $\beta$ -cancer cells treated with medium (Co.) or IFN- $\gamma$  and TNF. **c**,  $\beta$ -cancer cells were transduced with shControl or shp16/19 Mscv vectors. Then, the relative expression of CXCL9 or CXCL10 after treatment of the cells with medium (Co.) or IFN- $\gamma$  and TNF was measured by quantitative RT-PCR. Expression of medium-treated  $\beta$ -cancer cells was set as 1. **d**, Amount of CXCL9 or CXCL10 released into the supernatant of non- or shp16/19-transduced  $\beta$ -cancer cells after treatment with medium (Co.) or IFN- $\gamma$  and TNF as measured by ELISA.

The data show one representative example of transduced  $\beta$ -cancer cell lines assayed in duplicate out of three shp16/19-, two shControl- and two non-transduced RIP1-Tag2 preparations (**c**, **d**).

**Suppl. Table 1 | Expression of cytokine receptors, and IFN- $\gamma$  and TNF-induced anticancer effects in 6 murine cancer cell lines.**

Cell line	IFNGR1	IFNGR2	TNFRSF1	Inhibition of proliferation (%)	Growth arrest (%)
PyVmT breast	+	+	+	75 $\pm$ 19	100 $\pm$ 29
STAT1 <sup>-/-</sup> xRIP1-Tag2 pancreas	+	+	+	26 $\pm$ 9	13 $\pm$ 4
RIP1-Tag2 pancreas	+	+	+	100 $\pm$ 32	100 $\pm$ 30
B16 melanoma	+	+	+	36 $\pm$ 11	25 $\pm$ 3
LLC lung carcinoma	+	+	+	72 $\pm$ 24	100 $\pm$ 38
CT26 EpCam colon	+	+	+	92 $\pm$ 37	83 $\pm$ 37

The expression of IFN- $\gamma$  receptors IFNGR1 and IFNGR2, and TNF receptor TNFRSF1 was detected in untreated cancer cell lines by RT-PCR. The antiproliferative effect was measured by counting living cells at p0 after 4-5 days of IFN- $\gamma$  and TNF treatment. Permanent growth arrest was determined by counting living cells at p1 after 3-4 days of IFN- $\gamma$  and TNF removal (see also Suppl. Fig. 9b). Data represent the mean  $\pm$  s.e.m. of three independent cultures. yellow = responder; white = non-responder.

**Suppl. Table 2 | Expression of cytokine receptors, and IFN- $\gamma$  and TNF-induced anticancer effects in 11 human cancer cell lines.**

Cell line	IFNGR1	IFNGR2	TNFRSF1	Inhibition of proliferation (%)	Growth arrest (%)
HOP-62 small cell lung	+	+	+	92 $\pm$ 24	100 $\pm$ 33
COLO-205 colon	+	+	+	96 $\pm$ 25	100 $\pm$ 35
MDA-MB-231 breast	+	+	+	89 $\pm$ 18	94 $\pm$ 16
OVCAR-5 ovar	+	+	+	98 $\pm$ 35	100 $\pm$ 33
K562 leukemia	+	+	+	17 $\pm$ 6	16 $\pm$ 3
SR leukemia	+	+	+	-7 $\pm$ 1	11 $\pm$ 6
CAKI-1 kidney	+	+	+	66 $\pm$ 20	20 $\pm$ 5
786-O kidney	+	+	+	35 $\pm$ 7	84 $\pm$ 17
MALME-3M melanoma	+	+	+	100 $\pm$ 29	100 $\pm$ 22
SNB-75 brain	+	+	+	97 $\pm$ 41	100 $\pm$ 20
SF-295 brain	+	+	+	95 $\pm$ 36	100 $\pm$ 44

The expression of IFN- $\gamma$  receptors IFNGR1 and IFNGR2, and TNF receptor TNFRSF1 was detected in untreated cancer cell lines by RT-PCR. The antiproliferative effect was measured by counting living cells at p0 after 4 days of IFN- $\gamma$  and TNF treatment. Permanent growth arrest was determined by counting living cells at p1 after 3-4 days of IFN- $\gamma$  and TNF removal (see also Suppl. Fig. 9b). Data represent the mean  $\pm$  s.e.m. of three independent cultures. yellow = responder; white = non-responder.

**Suppl. Table 3 | IFN- $\gamma$  and TNF-induced anticancer effects in 6 primary human cancer cell preparations.**

Internal code	Cancer type and origin	Passage number	Inhibition of proliferation (%)	Growth arrest (%)
SRH	embryonic rhabdomyosarcoma	6	35	100
ZCRH	alveolar rhabdomyosarcoma	5	100	>100 <sup>a</sup>
TüMel75	melanoma lung	2	94 ± 13	100 ± 34
TüMel74H	melanoma brain	1	100 ± 40	>100 <sup>a</sup>
ZüMel1H	melanoma brain	50	85 ± 17	88 ± 16
ZüMel1	melanoma lymph node	50	89 ± 13	100 ± 12

The antiproliferative effect on primary human cancer cells was measured by counting living cells at p0 after 4 (melanoma cells) or 12 days (rhabdomyosarcoma cells) of IFN- $\gamma$  and TNF treatment. SRH, TüMel75, TüMel74H, ZüMel1H, or ZüMel1 were treated with standard cytokine concentrations of 100 ng/ml IFN- $\gamma$  and 10 ng/ml TNF. ZCRH were treated with 10 ng/ml IFN- $\gamma$  and 1 ng/ml TNF. Permanent growth arrest was determined by counting living cells at p1 after 4 (melanoma cells) or 10 days (rhabdomyosarcoma cells) of IFN- $\gamma$  and TNF removal (see also Suppl. Fig. 9b). The data show one representative out of 3 independent experiments (SRH and ZCRH) or the mean  $\pm$  s.e.m. of three independent cultures (TüMel75, TüMel74H, ZüMel1H, and ZüMel1). yellow = responder; white = non-responder. <sup>a</sup>here stable growth arrest was combined with cytotoxic effects, as determined by cell loss.

**Clinical and pathological characterization of patients**

Internal code/ Histology number	Cancer type and site of excision	Passage number	Prior systemic therapy	Metastases	Mutational status	Staging	Gender and age
SRH	embryonic rhabdomyosarcoma  muscle	6	vincristine, actinomycinD, ifosfamide, doxorubicin, carboplatin, etoposide	progressive: multifocal brain, lung, bone	p53 mutated	pT <sub>2b</sub> pN <sub>x</sub> pM <sub>x</sub> , L0, V0 tumor size: 23x11x12 cm degree of regression according to Salzer- Kuntschik: 5	Female, 24
ZCRH	alveolar rhabdomyosarcoma  muscle	5	None	progressive: subpleural, intrapulmonal, mesenteric, thoracal, peritoneal, intramuscular, lung, bone marrow, skin	translocation at 13q14 breakpoint	pT <sub>3b</sub> pN <sub>1</sub> pM <sub>1</sub>	Female, 8
TüMel75	melanoma lymph node	2	None	progressive	BRAF V600E NRAS WT	pT <sub>1a</sub> N <sub>1b</sub> M <sub>1a</sub>	Male, 45
TüMel74H	melanoma brain	1	fotemustine	progressive	BRAF WT NRAS WT	pT <sub>2b</sub> N <sub>3</sub> M <sub>1c</sub>	Female, 52
ZüMel1H M000301	melanoma brain	50	None	progressive	BRAF WT NRAS Q61R	pT <sub>2</sub> N <sub>2b</sub> M <sub>1c</sub>	Male, 54
ZüMel1 M981201	melanoma lymph node	50	None	progressive	BRAF WT NRAS Q61R	pT <sub>2</sub> N <sub>2b</sub> M <sub>1c</sub>	Male, 54
15386-07	Halo nevus, compound type, skin	n.a.	Excision, no recurrence	primary	Not done	n.a.	Female, 16
6606-07	Melanoma primary tumor, skin	n.a.	Excision, no recurrence	primary	Not done	pT <sub>1a</sub> , N0, M0	Male, 72
14298-06	Melanoma metastasis, skin	n.a.	Excision and intralesional IL-2, 5 years recurrent metastases, then 5 years NED	progressive	Not done	pTX, N2c, M0	Female, 75

n.a., not applicable  
NED, no evidence of disease

ID	Hairpin ID	Sequence 97bp (used for knockdown experiments)
1	Cdkn2a.23	TGCTGTTGACAGTGAGCGAAACGTTACAGTAGCAGCTCTTTAGTGAAGCCACAGATGTAAGAGCTGCTACGTGAACGTTGTGCCTACTGCCTCGGA
2	Cdkn2a.34	TGCTGTTGACAGTGAGCGCAGCAGCTCTTCTGCTCAACTATAGTGAAGCCACAGATGTATAGTTGAGCAGAAGAGCTGCTATGCCTACTGCCTCGGA
3	Cdkn2a.318	TGCTGTTGACAGTGAGCGAACGGGCATAGCTTCAGCTCAATAGTGAAGCCACAGATGTATTGAGCTGAAGCTATGCCCGTCTGCCTACTGCCTCGGA
4	Cdkn2a.410	TGCTGTTGACAGTGAGCGCTTCTTCTTAGCTTCACTTCTATAGTGAAGCCACAGATGTATAGAAGTGAAGCTAAGAAGAAATGCCTACTGCCTCGGA
5	Cdkn2a.428	TGCTGTTGACAGTGAGCGCTAGCGATGCTAGCGTGTCTATAGTGAAGCCACAGATGTATAGACACGCTAGCATCGCTAGATGCCTACTGCCTCGGA
6	Cdkn2a.562	TGCTGTTGACAGTGAGCGCTGGCATGAGAACTGAGCGAATAGTGAAGCCACAGATGTATTGCTCAGTTTCTCATGCCATTGCCTACTGCCTCGGA
0	sh p16/p19	tgctgttgacagtgagcgcccctgggtgctctttgtgttagtgaagccacagatgtaaacacaagagcaccagcggatgcctactgcctcgga
sh Control	sh Luc	tgctgttgacagtgagcgcccctgaagtctctgattaatagtgaagccacagatgattaatcagagacttcaggcgggtgcctactgcctcgga



## Changing T-cell enigma Cancer killing or cancer control?

Thomas Wieder<sup>1,†</sup>, Heidi Braumüller<sup>1,†</sup>, Ellen Brenner<sup>1</sup>, Lars Zender<sup>2</sup>, and Martin Röcken<sup>1,\*</sup>

<sup>1</sup>Department of Dermatology; Eberhard Karls University; Tübingen, Germany; <sup>2</sup>Division of Molecular Oncology of Solid Tumors; Department of Internal Medicine I; Eberhard Karls University; Tübingen, Germany

<sup>†</sup>These authors contributed equally to this work.

**D**ata from different laboratories and theoretical considerations challenge our current view on anticancer immunity. Immune cells are capable of destroying cancer cells under *in vitro* and *in vivo* conditions. Therefore, cellular immunity is considered to control cancers through mechanisms that kill cancers. Yet, therapeutic anticancer immune responses rarely delete cancers. If efficient, they rather establish a life with stable disease. This raises the question of whether killing is the sole mechanism by which immune therapy attacks cancers. Here, we show that, besides cancer eradication by cytotoxic lymphocytes, other modes of action are operative and strictly required for cancer control. We show that T helper-1 cells arrest cancer growth by driving cancers into a state of stable or permanent growth arrest, called senescence. Such immune cells establish cytokine-producing walls around developing cancers. When producing interferon- $\gamma$  and tumor necrosis factor, this cytokine-induced tumor immune-surveillance keeps the cancer cells in a permanently non-proliferating state. Simultaneously, antiangiogenic chemokines cut their connections to the surrounding tissues. This strategy significantly reduces tumor burden and prolongs life of cancer-bearing animals. As human cancers also undergo senescence, the current data suggest tumor-immune surveillance through cytokine-induced senescence, instead of tumor eradication, as the more realistic and primary goal of cancer control.

### Old Ideas, New Insights

The best and probably only real eradication of solid cancers is complete surgical excision. This is important, as most cancer patients die from cancer metastases and disseminated disease and not from the primary cancer. Only very few cancers, like basal cell carcinomas (BCC), can definitely be eradicated by surgery. Analysis of single disseminated tumor cells and experimental data from mice strongly suggest that most cancers are already disseminated at the time of excision.<sup>1,2</sup> Thus, tumor dissemination seems to occur very early during tumor development. Nonetheless, a large proportion, and sometimes even the majority of patients are “clinically” cured. Most cancers seem to survive definitely at a state of “dormancy” in various organs, mainly the bone marrow.<sup>3,4</sup> As the risk of dying from cancer seems to depend on the tumor burden caused by the metastases and is related to the extend of micrometastasis observed, surgery is frequently followed by complementary treatments. The main goal of such complementary strategies is the reduction of cancer load.

The “magic bullets” concept was originally introduced by Paul Ehrlich more than 100 years ago. Today this concept, based on the eradication of the remaining tumor mass, was extended to concepts that include cellular destruction using chemotherapy, different physico-chemical regimen such as radiation therapy, or immune therapy using cytotoxic T cells (CTL) or natural killer (NK) cells

**Keywords:** immune therapy, tumor dormancy, cancer therapy, growth arrest, cell cycle control, senescence, T helper-1 cells, interferon- $\gamma$ , tumor necrosis factor, p16<sup>Ink4a</sup>

**Abbreviations:** For list of abbreviations, see page 6.

Submitted: 07/16/2013

Accepted: 08/05/2013

<http://dx.doi.org/10.4161/cc.26060>

\*Correspondence to: Martin Röcken;  
Email: mrocken@med.uni-tuebingen.de

(Fig. 1A). The clinical realization of this concept was reflected on one side by the extensive cancer surgery that included large excision of cancers, the cancer surrounding tissues, and all related lymph node areas, as exemplified by the Halsted procedure in case of breast cancer,<sup>5,6</sup> a method which was most popular between 1960 and 1980.<sup>7</sup> On the other side, the discovery of methotrexate and its therapeutic effects by Sidney Farber and the subsequent beneficial effects of the multi-drug chemotherapy as treatment of childhood leukemia helped to declare the “war on cancer” that was developed to ultimately delete the cancer disease (for a review, see refs. 8 and 9). Subsequently multiple strategies were developed, all

with the common principle based on the induction of cell death through different mechanisms. They include apoptosis,<sup>10</sup> various modes of necrosis,<sup>11</sup> autophagy,<sup>12</sup> or lysis of cancer cells by T cells or NK cells.<sup>13,14</sup> Recent strategies combine chemotherapy and immune responses.<sup>15</sup>

In the last 2 decades, great intellectual and financial efforts were made to further develop the “magic bullets” concept. New drugs, including biologic response modifiers such as monoclonal antibodies (mAb), antibody fusion constructs such as bispecific antibodies,<sup>16</sup> monoclonal antibodies drug conjugates like Trastuzumab emtansine,<sup>17</sup> or recombinant proteins like interferon- $\alpha$ <sup>18</sup> have been successfully introduced as cancer treatment. Yet, most

of these therapies help only a minority of patients, and the mean prolongation of life is only in the range of months, even for the most aggressive therapies. The recurrence of drug- or radiation-resistant cancer cells and metastases remains the most important problem of those strategies. In addition, this problem is complicated by the unavoidable side effects of many cytotoxic treatments on normally proliferating tissues, like hair follicle, bone marrow, or mucosa and, in some cases, hormone-producing cells. The collateral damages such as those resulting from the impairment of normal hormone-producing cells still represent important problems of those strategies.

Given that tumors share a quite diverse spectrum of mechanisms to secure their growth and to escape from treatment-mediated or the body’s “counter-attack,”<sup>18</sup> alternatives to “war-based” fighting strategies should be sought to cope with this devastating disease.

The “defensive wall” concept is an alternative approach that relies on a less militant approach of cancer control<sup>9</sup> (Fig. 1B). Such a strategy tries to create conditions of normal life in the presence of tumor dormancy, rather than focusing on maximal killing of disseminated cancer cells. This approach has not been thoroughly tested. Yet, the benefit of different treatment strategies may be subsumed under such a “tumor dormancy strategy.”

One well-established cancer treatment that may work by building a “defensive wall” against cancer is hormone withdrawal for prostate<sup>19</sup> or breast cancer.<sup>20</sup> Neither testosterone nor estrogen withdrawal has chemotherapeutic properties; nonetheless, both treatments are among the most efficient anticancer therapies currently available. For example, testosterone withdrawal for prostate cancer prolongs the progression-free survival of patients by 8 mo.<sup>19</sup> On the other hand, estrogen withdrawal by combination therapy for breast cancer prolongs the life of patients by 6 mo, with a median overall survival of 47.7 mo.<sup>20</sup> In comparison, the median overall-advantage of Trastuzumab emtansine for HER2-positive breast cancer is 5 mo, with a median overall survival of 30.9 mo.<sup>17</sup> One has to be extremely careful in comparing different patient populations with different

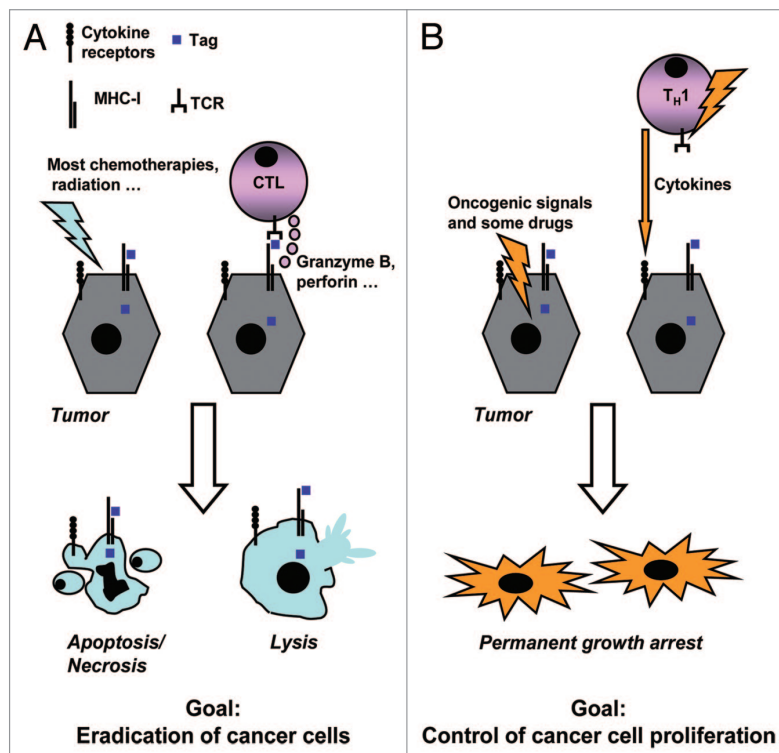


**Figure 1.** Eradication vs. control of tumors. (A) Treatment of tumor cells with chemotherapeutic drugs or radiation, or targeting TAA-, e.g., Tag-expressing tumor cells with cytotoxic T cells either induce apoptosis or necrosis (left) or lysis (right). Both mechanisms should finally lead to complete eradication of the cancer cells. Note that only CD8<sup>+</sup> CTL can specifically bind to MHC-I<sup>+</sup>, TAA-presenting cancer cells. (B) Intrinsic, oncogenic signals (left) or immune surveillance by cytokines, i.e., IFN- $\gamma$ - and TNF, produced by T helper-1 cells (right) that specifically bind to TAA-presenting MHC-II<sup>+</sup>, antigen-presenting cells in the vicinity of the tumor, induce permanent growth arrest, or senescence, of tumor cells without destruction of the cells. Both mechanisms in (B) lead to cancer control. Note that CD4<sup>+</sup> T<sub>H</sub>1 cells cannot directly bind to MHC-I<sup>+</sup>, TAA-presenting cancer cells. For details, see text. Abbreviations: CTL, cytotoxic T cells; IFN- $\gamma$ , interferon- $\gamma$ ; MHC, major histocompatibility complex; TAA, tumor-associated antigen; Tag, T antigen; TCR, T-cell receptor; T<sub>H</sub>1, T helper-1 cells; TNF, tumor necrosis factor.

types of cancer; nonetheless the data above urge the question, why may non-cytotoxic cancer therapies be so effective?

Following multiple therapies, patients may arrive at a stage where they suffer from drug- and radiation-resistant metastatic cancer. A phase I/II trial recently suggested that in the case of metastatic melanoma, up to 30–40% of these desperate patients improve clinically and show objective responses when treated with antibodies that simultaneously suppress the negative, T cell-inhibitory CTLA-4 and the PD-1/PD-L1 signaling cascade.<sup>21</sup> This treatment success can be interpreted as enhanced cancer cell killing by cytotoxic T cells. Yet, is it possible that a tumor burden consisting of several billions of cancer cells is controlled over months and years by rapidly proliferating killer cells?

Similarly in mice, interferon- $\gamma$  (IFN- $\gamma$ )- and tumor necrosis factor (TNF)-producing CD4<sup>+</sup> T helper cells can arrest either endogenously, growing insulin-producing  $\beta$ -cell cancers that develop as a result of transgenic suppression of the cell cycle regulators p53 and Rb, or adoptively transferred cancer cells.<sup>22,23</sup> Similar results have been reported by others.<sup>24–27</sup> Until now, the underlying mechanisms had been interpreted either as a consequence of cancer killing by CD4<sup>+</sup> T cells,<sup>24,26</sup> induction of CD8<sup>+</sup> killer cells,<sup>14</sup> or activation of cytotoxic macrophages. While in some models dependence on CTL or NK cells could be demonstrated,<sup>14</sup> cancer cell killing was rather associative in other studies. Together the current state suggests that cancer cell destruction is a real phenomenon, yet it remains questionable to what extent cancer control relies on killing mechanisms, and to what extent on other mechanisms that are fundamentally different from killing.

Treatment of mice with IFN- $\gamma$ - and TNF-producing T helper (T<sub>H</sub>1) cells specific for a tumor-associated antigen (TAA) more than doubles the entire lifespan of a cancer-prone mouse. Interestingly, this cancer control occurs in the absence of detectable tumor/ $\beta$ -cell destruction. In consequence, the treatment does not cause autoimmune diabetes,<sup>22</sup> and the tumor-specific T helper cells poorly infiltrate the endocrine  $\beta$ -cell tumors. They rather

surround the diseased tissue,<sup>28</sup> resembling a defensive wall. Further elaboration of this treatment regimen revealed that the TAA-specific T<sub>H</sub>1 cells induce a cytokine-dependent permanent growth arrest of the  $\beta$ -cell cancers<sup>4</sup> that will be discussed in detail below.

## Cancer Eradication

Destruction of cancers by chemotherapy, immune therapy, or radiation therapy is still considered a cornerstone of cancer treatment. The relevance of the 3 main death pathways, i.e., lysis, apoptosis, and

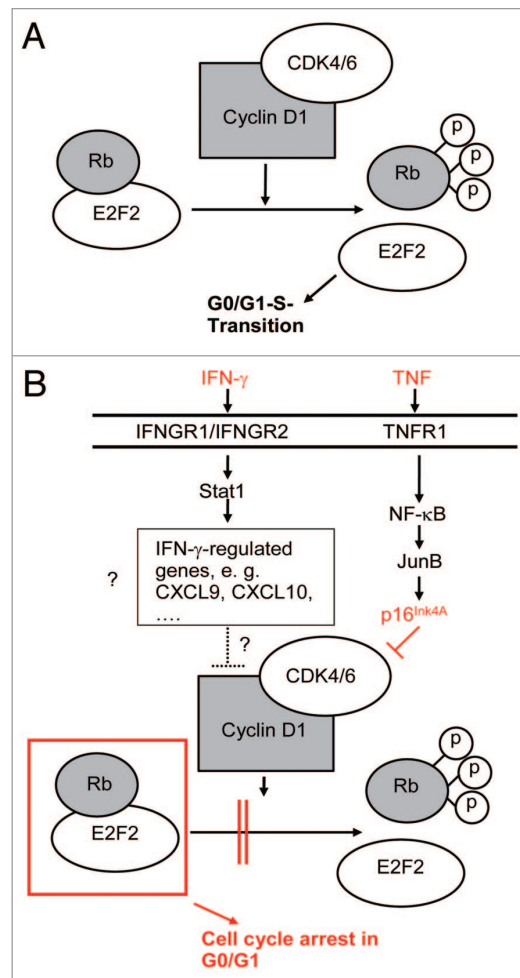


**Figure 2.** Suggested cytokine signaling leading to tumor cell senescence. **(A)** In proliferating cells, phosphorylation of Rb by the cyclin D1-CDK4/6 kinase complex leads to release of the transcription factor E2F2, which, in turn, helps to overcome the G<sub>0</sub>/G<sub>1</sub> restriction point and induces G<sub>0</sub>/G<sub>1</sub>-S transition of the cells. **(B)** After binding to its receptor on the surface of the tumor cells, IFN- $\gamma$  leads to phosphorylation and activation of Stat1, which, in turn, translocates to the nucleus and induces the expression of IFN- $\gamma$ -regulated genes, e.g., CXCL9 or CXCL10. These IFN- $\gamma$ -induced gene products and other unknown IFN- $\gamma$ -induced factors may then directly inhibit the CDK4/6 by modulating cyclin D1 activity. On the other hand, TNF leads to NF- $\kappa$ B-mediated JunB upregulation, which, in turn, induces the CDK4/6 inhibitor p16<sup>Ink4a</sup>. Together, both signaling pathways lead to severe hypophosphorylation of Rb, which retains the transcription factor E2F2 and keeps the cell in the G<sub>0</sub>/G<sub>1</sub> phase of the cell cycle. Abbreviations: CDK4/6, cyclin-dependent kinase 4/6; CXCL9, also known as monokine induced by IFN- $\gamma$  (MIG); CXCL10, also known as interferon-inducible protein 10 (IP-10); E2F2, transcription factor E2F2; IFN- $\gamma$ , interferon- $\gamma$ ; IFNGR1, interferon- $\gamma$  receptor 1; IFNGR2, interferon- $\gamma$  receptor 2; JunB, transcription factor JunB; NF- $\kappa$ B, nuclear factor  $\kappa$ B; p16<sup>Ink4a</sup>, also known as CDKN2A or Cyclin-dependent kinase inhibitor 2A; Rb, retinoblastoma protein; TNF, tumor necrosis factor; TNFR1, tumor necrosis factor receptor 1.

necrosis, for cancer chemotherapy has long been anticipated.<sup>29,30</sup> Further elaboration of the signaling pathways revealed that drug-induced apoptosis might either be death receptor-dependent<sup>10</sup> or death receptor-independent and mediated by the mitochondrial apoptosis pathway.<sup>31</sup> In both cases, apoptosis depends on the activation of caspases, the main effector pathways of programmed cell death. Necrosis signaling by drug treatment clearly differs from apoptosis induction, as drug-induced regulated necrosis causes a caspase-independent cell death.<sup>11,30</sup> In the case of TNF treatment under specified conditions (e.g., high leukotriene A4 hydrolase levels), programmed necrosis (necroptosis) may be mediated through RIP1 and RIP3, cyclophilin D, and acid sphingomyelinase.<sup>32</sup>

Cancer immune therapy also mainly focuses on cancer eradication. These strategies generally rely on CD8<sup>+</sup> cytotoxic T lymphocytes (CTL) or natural killer cells.<sup>14,33</sup> Especially during the elimination phase of cancer, cytotoxic lymphocytes seem to be capable of destroying highly immunogenic transformed tumor cells.<sup>34</sup> Alternatively, macrophages may clear cancer cells that underwent oncogene-induced senescence.<sup>35</sup> Therefore, immune surveillance is discussed as being critically involved in cancer control.<sup>18</sup> One prevailing concept suggests that dendritic cells orchestrate CD4<sup>+</sup> T helper cells and CD8<sup>+</sup> cytotoxic T cells to contribute to the bodies anticancer machinery.<sup>36</sup> Eventually, poorly immunogenic or death-resistant tumor cells may escape immune surveillance and reestablish tumor growth.<sup>34</sup> Thus, the critical question which lymphocyte is most effective for the treatment of cancer disease may differ with the cancer developmental stage and the specific phase of immune surveillance.

### Tumor Dormancy

Besides cancer cell killing, various studies show that cancers often acquire a kind of non-proliferative state, and the term tumor dormancy has been coined in the early seventies of the last century. This state was originally described *in vivo* and induced by prevention of neovascularization of the tumor tissue.<sup>37</sup> Further

elaboration of the model in 3-dimensional *in vitro* cell culture experiments led to the description of tumor dormancy as an equilibrium of cell death (necrosis) in the center and proliferation in the periphery of spherical tumors.<sup>38</sup> Later, tumor dormancy was discussed either as an equilibrium between cancer cell killing and cancer cell proliferation,<sup>39</sup> or as an active suppression of cancer growth and tumor-angiogenesis.<sup>22</sup> Since then, this concept was extended by two important aspects: the induction of permanent tumor growth arrest and the role of the tumor environment.

### Permanent Growth Arrest or Senescence, and the Intrinsic Signals

Permanent growth arrest (senescence) of eukaryotic cells was first observed in freshly isolated and cultured fibroblasts<sup>40</sup> and thought to define the final lifespan of a normal cell, when it has lost the capacity to divide. It was shown that normal cells harbor an intrinsic aging program that determines their lifespan, and 3 different Hayflick factors regulating the lifespan of an organism, namely telomere shortening, p16<sup>Ink4a</sup> derepression, and DNA damage, were defined (for review, see ref. 41). Senescence is different from any type of killing, as growth-arrested cells can live for long periods of time. More importantly, senescence was found to be the major difference that distinguishes a “normal” from a “cancer” cell. The concept of senescence changed fundamentally, when oncogene activation,<sup>42</sup> DNA damage,<sup>43</sup> and cellular stress<sup>44</sup> were described as fundamental endogenous triggers for transcriptional gene silencing.<sup>45</sup> These data showed that premature senescence provides a natural barrier against cancer development and thus represents a genuine protective physiological barrier against cancer. The concept was further supported by data showing that impairing this barrier promotes the progression of benign tumors into malignant cancers.<sup>46,47</sup> Although these data from independent research groups clearly reveal that senescence is a physiological defense mechanism against cancer, the questions remain whether oncogene-induced senescence relies only on an intrinsic signaling

cascade originating from the tumor cells themselves, or whether extrinsic signals may prevent cancer by driving potential cancer cells into a state of permanent dormancy. In order to ultimately solve the problem of these dormant, yet still hazardous cells, the organism should also provide a mechanism to clear senescent cells in the long run. Indeed, immune cells can clear senescent cells as a final act of cancer clearance. This step seems to play a critical role in cancer prevention and was termed “senescence surveillance”.<sup>35</sup>

### Induction of Permanent Growth Arrest and Senescence through Extrinsic Signals

Recently, Braumüller et al. found for the first time that not only intrinsic but also extrinsic factors can drive cancer cells into the senescence program.<sup>4</sup> This first description showing that extrinsic factors can induce senescence has multiple implications. An important one is that it fundamentally changes the current concept on the interaction of the immune system with cancers. Until then, it was believed that the immune system can only be considered in terms of killing. The authors, however, showed that IFN- $\gamma$ - and TNF-producing TAA-specific T<sub>H</sub>1 cells are capable to drive cancer cells into senescence-defining permanent growth arrest, a process occurring even in the absence of oncogene-stress or substantial DNA damage.<sup>4</sup> Detailed *in vitro* and *in vivo* analysis revealed that the combined action of IFN- $\gamma$  and TNF is needed to stabilize the p16<sup>Ink4a</sup>-Rb pathway by keeping Rb in a hypophosphorylated state, to arrest the cells in the G<sub>0</sub>/G<sub>1</sub> phase of the cell cycle, and to induce a permanent cell cycle arrest (Fig. 2A and B). Importantly, this growth arrest was permanent, i.e., cancer cells did not restart to proliferate after cytokine removal. Others had reported that signaling for a cell cycle arrest can only be converted into senescence when the cell cycle arrest is associated with a second signal, e.g., inappropriate growth-promotion through mTOR activation.<sup>48</sup> In line with this, the cytokine-induced permanent growth arrest also needs at least 2 simultaneously acting input signals: IFN- $\gamma$  and TNF receptor 1-dependent signaling

(Fig. 2B). This recent experimental evidence showing that extrinsic signals can induce senescence<sup>4</sup> will encourage researchers and clinicians to investigate other extrinsic senescence inducers and address senescence induction as a special form of cancer immune therapy. In addition to the immunotherapeutic approaches using tumor-specific lymphocytes and/or immune-modulating cytokines, p53-enhancing approaches, modulation of the cell cycle machinery by kinase inhibitors, or targeting replicative senescence by telomerase inhibitors may serve as promising strategies for the therapeutic activation of the senescence program, and may be especially suitable for the development of novel types of cancer immune therapies.<sup>49</sup> In this context, it is interesting that newly developed cancer therapies targeting other cellular signal transduction pathways, e.g., the mutant BRAF<sup>V600E</sup>, may also cause permanent growth arrest.<sup>50</sup> Taken together, senescence is not only an intrinsic process that protects the organism from harmful proliferation of transformed cells; senescence can also be triggered either by small molecules interfering with intrinsic signaling cascades, like the Ras-Raf phosphorylation cascade, and, most importantly, also by extrinsic signals, such as cytokines when delivering coordinated senescence signals.<sup>4</sup> In this respect, active senescence induction resembles the apoptosis program which can also be activated by either intrinsic or extrinsic signals, and is therefore an established target of multiple anticancer strategies, e.g., chemotherapy or radiation therapy.

### Tumor Environment

Tumor dormancy occurs not only cell autonomously, but also strictly depends on the tumor environment (for review, see ref. 51). An intact immune system is required for the remodeling of the tumor microenvironment and the induction of sustained tumor regression in mice suffering from lymphoma or leukemia. Interestingly, this cancer-protective effect of the immune system is at least in part mediated through chemokines, such as thrombospondins.<sup>52</sup> Using another transgenic mouse lymphoma model, it was demonstrated that apoptotic lymphoma

cells activate macrophages of the tumor stroma. Stimulated macrophages then secrete transforming growth factor  $\beta$  that acts as a critical non-cell-autonomous inducer of cellular senescence. The tumor stroma may therefore serve as a reservoir for signals mediating the feedback senescence induction loop necessary to limit tumor development.<sup>53</sup> Yet, this control

mechanism strictly depends on an appropriate microenvironment. Thus, loss of p53 in cancer-surrounding macrophages leads to an inflammatory microenvironment that promotes lymph node metastasis of colorectal tumors.<sup>54</sup> This tumor microenvironment is affected by multiple genetic and acquired factors; it is definitely not only affected by the tumor itself, and

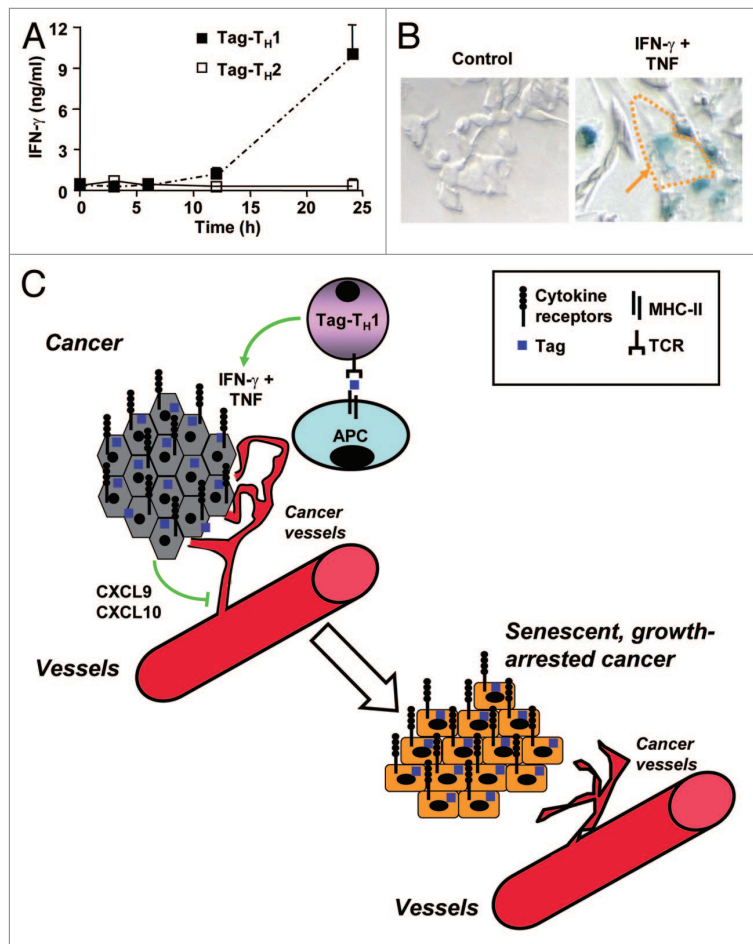


**Figure 3.** Cytokine-mediated control of tumor cell growth by senescence induction. (A) Characterization of TAA-, e.g., Tag-specific  $T_H1$  cells<sup>22</sup> that were restimulated in vitro using antigen-presenting cells in the presence of Tag peptide 362–384. After different incubation times, IFN- $\gamma$  in the cell culture supernatant was measured by ELISA. Tag- $T_H2$  cells were used as controls. (B)  $\beta$ -cancer cells from RIP-Tag2 mice were either treated with medium alone (control) or medium containing IFN- $\gamma$  and TNF. After treatment, senescence-associated  $\beta$ -galactosidase (SA- $\beta$ -gal) activity was determined. Senescent, SA- $\beta$ -gal<sup>+</sup> cells show blue staining around the nucleus and a flattened morphology (right, see arrow). (C)  $CD4^+$   $T_H1$  cells home around the tumors in the pancreas, where they bind to TAA-presenting MHC-II<sup>+</sup> cells and subsequently secrete IFN- $\gamma$  and TNF (upper left). The 2 proinflammatory cytokines together induce senescence in cytokine receptor-expressing tumor cells and, in parallel, the release of the antiangiogenic chemokines CXCL9 and CXCL10. This finally leads to senescent tumors with degenerated vascular supply (lower right). For details, see references<sup>4,22</sup>, and the text. Abbreviations: APC, antigen-presenting cell; CXCL9, also known as monokine induced by IFN- $\gamma$  (MIG); CXCL10, also known as interferon-inducible protein 10 (IP-10); IFN- $\gamma$ , interferon- $\gamma$ ; MHC, major histocompatibility complex; RIP, rat insulin promoter; TAA, tumor-associated antigen; Tag, T antigen; TCR, T-cell receptor;  $T_H1$ , T helper-1 cells; TNF, tumor necrosis factor.

$T_H1$  immunity, for example, can heavily change the cancer surrounding milieu.<sup>4,22</sup> The key importance of such a microenvironment for cancer control and prognosis in humans was best demonstrated for gastrointestinal cancers. Here, the description of the cellular microenvironment surrounding and infiltrating the cancers provides by far the best prognostic insight, with functional  $T_H1$  cytokines-producing clusters and IFN- and TNF-associated cytokines or chemokines indicating the best prognosis.<sup>55</sup> Thus, the concept of an immunoscore to predict the clinical outcome in cancer and to classify human cancers has recently been proposed.<sup>56</sup>

### Clinical Impact

Classical cytotoxic chemotherapy often shows dramatic adverse effects. Besides this, drug resistance is one of the most important drawbacks of chemotherapy. After initial regression of the tumors, some malignant cells survive and eventually restart growing. Interestingly, the authors of a recent publication introduced a discontinuous dosing strategy for Vemurafenib, a drug that specifically targets *BRAF* mutations in melanoma patients.<sup>57</sup> In addition, the combination of 2 drugs by using an antibody–drug conjugate, i.e., Trastuzumab emtansine, improved the clinical outcome in patients with HER2-positive advanced breast cancer.<sup>17</sup> Very recent clinical results showed that a combination of T cell-activating anti-PD-1 and anti-CTLA-4 antibodies provided clinical activity that differed from monotherapy, with objective response rates in up to 40% of the patients.<sup>21</sup> Thus, future clinical research will not only concentrate on the introduction of new drugs, but also on optimized drug combination and/or dosing.

### Conclusion

In the present perspective, we summarized recent work dealing with the antitumoral effects of  $T_H1$  cells and their cytokines IFN- $\gamma$  and TNF in the context of new anticancer strategies, which do not rely on cancer cell destruction. Based on our data, we propose the following mechanism (Fig. 3): small amounts of intracellular tumor-associated antigens (TAAs),

including antigenic peptides of tumor drivers, like the tumor driver T antigen (Tag), are generally released by damaged tumor cells. TAAs are then taken up and presented by dendritic cells in the draining lymph node<sup>22</sup> or in the cancer surrounding lymphoid tissues, where they stimulate adoptively transferred TAA-specific  $T_H1$  cells when presented by MHC class II-positive antigen-presenting cells.<sup>4,22</sup> These  $T_H1$  cells subsequently migrate to the hyperproliferative islets,<sup>4,22</sup> where they secrete high amounts of IFN- $\gamma$  and TNF after restimulation with antigen through antigen-presenting cells, like macrophages<sup>4,22-24</sup> (Fig. 3A). The cytokines together then drive the tumor cells into senescence<sup>4</sup> (Fig. 3B). Ultimately, such senescent cancer cells may be cleared.<sup>35</sup> Importantly, this mechanism is different from the well-known toxic antitumor effect of proinflammatory cytokines,<sup>58</sup> and even independent of the antiangiogenic effect mediated by CXCL9 and CXCL10<sup>4</sup> (see also Fig. 3C). These insights may pave the way for a combination of a targeted chemotherapy regimen, such as BRAF inhibition for reduction of cancer burden, with an immune therapy based on TAA-specific  $T_H1$  cells that ultimately induce cancer cell senescence.<sup>4,22-24</sup>

### Outlook

The description that immunity cannot only destroy cancers, but can also drive cancers into senescence raises many questions. Thus, where does the immune system present intracellular tumor antigens to MHC class II-dependent CD4<sup>+</sup> T cells? How can T-cell cytokines from T helper cells best affect the MHC class II-negative cancer cells? What is the relation between tumor dormancy, senescence, and cancer stem cells? How stable is senescence in vivo? What is the role of the Warburg effect and the metabolic transition of tumor cells, and how can clinicians target this hallmark of cancer cells. Independent of these questions, the insight that extrinsic signals like T-cell cytokines can drive cancers into senescence liberates clinicians and scientists from the military “war on cancer” that searches for ever more efficient killer mechanisms and earlier targets. Showing a path that will allow

peaceful life with a domesticated cancer opens a long-sought door to basic and clinical research to develop more efficient and, most importantly, long-lasting and significantly less toxic treatments for this life-threatening group of diseases.<sup>4</sup>

### Disclosure of Potential Conflicts of Interest

No potential conflicts of interest were disclosed.

### Acknowledgments

The work of the authors is supported by the Deutsche Forschungsgemeinschaft (SFB 685), the Wilhelm Sander-Stiftung (2012.056.1), and the Deutsche Krebshilfe (109037). The authors want to thank S Weidemann and V Galinat for excellent technical assistance.

### Abbreviations

APC, antigen-presenting cell; BCC, basal cell carcinoma; BRAF, proto-oncogene protein B-raf; CD, cluster of differentiation; CTLA-4, cytotoxic T-lymphocyte antigen 4; CTL, cytotoxic T cells; CXCL9, chemokine (C-X-C motif) ligand 9; CXCL10, chemokine (C-X-C motif) ligand 10; DNA, Deoxyribonucleic acid; G0, G zero phase of the cell cycle; E2F2, transcription factor E2F2; ELISA, enzyme-linked immunosorbent assay; HER2, human epidermal growth factor receptor 2; IFN- $\gamma$ , interferon- $\gamma$ ; IFNGR1, interferon- $\gamma$  receptor 1; IFNGR2, interferon- $\gamma$  receptor 2; JunB, proto-oncogene protein JunB; MHC, major histocompatibility complex; mTOR, mammalian target of rapamycin; NK, natural killer cells; PD-1, programmed cell death 1; PD-L1, programmed cell death 1 ligand 1; p16<sup>Ink4a</sup> also known as CDKN2a, cyclin-dependent kinase inhibitor 2a; p53, protein 53; ras, small GTP-binding protein; Rb, retinoblastoma protein; RIP, rat insulin promoter; RIP1 also known as RIPK1, receptor-interacting serine/threonine-protein kinase 1; RIP3 also known as RIPK3, receptor-interacting serine/threonine-protein kinase 3; SA- $\beta$ -gal, senescence-associated  $\beta$ -galactosidase; TAA, tumor-associated antigen; Tag, T antigen;  $T_H1$ , T helper-1 cells; TCR, T-cell receptor; TNF, tumor necrosis factor; TNFR1, tumor necrosis factor receptor 1

## References

- Pantel K, Alix-Panabières C, Riethdorf S. Cancer micrometastases. *Nat Rev Clin Oncol* 2009; 6:339-51; PMID:19399023; <http://dx.doi.org/10.1038/nrclinonc.2009.44>
- Eyles J, Puaux AL, Wang X, Toh B, Prakash C, Hong M, Tan TG, Zheng L, Ong LC, Jin Y, et al. Tumor cells disseminate early, but immunosurveillance limits metastatic outgrowth, in a mouse model of melanoma. *J Clin Invest* 2010; 120:2030-9; PMID:20501944; <http://dx.doi.org/10.1172/JCI42002>
- Röcken M. Early tumor dissemination, but late metastasis: insights into tumor dormancy. *J Clin Invest* 2010; 120:1800-3; PMID:20501952; <http://dx.doi.org/10.1172/JCI43424>
- Braumüller H, Wieder T, Brenner E, Aßmann S, Hahn M, Alkhaled M, Schilbach K, Essmann F, Kneilling M, Griessinger C, et al. T-helper-1-cell cytokines drive cancer into senescence. *Nature* 2013; 494:361-5; PMID:23376950; <http://dx.doi.org/10.1038/nature11824>
- Halsted WS. I. The Results of Radical Operations for the Cure of Carcinoma of the Breast. *Ann Surg* 1907; 46:1-19; PMID:17861990; <http://dx.doi.org/10.1097/0000658-190707000-00001>
- Orr TG Jr. An incision and method of wound closure for radical mastectomy. *Ann Surg* 1951; 133:565-6; PMID:14819996
- Péloquin A, Poljicak M, Falardeau M, Gravel D, Moïseu R, Péloquin L. Cancer of the breast: a study of 1520 consecutive patients operated on between 1960 and 1980. *Can J Surg* 1991; 34:151-6; PMID:1888359
- Sporn MB. The war on cancer. *Lancet* 1996; 347:1377-81; PMID:8637346; [http://dx.doi.org/10.1016/S0140-6736\(96\)91015-6](http://dx.doi.org/10.1016/S0140-6736(96)91015-6)
- Gatenby RA. A change of strategy in the war on cancer. *Nature* 2009; 459:508-9; PMID:19478766; <http://dx.doi.org/10.1038/459508a>
- Friesen C, Herr I, Krammer PH, Debatin KM. Involvement of the CD95 (APO-1/FAS) receptor/ligand system in drug-induced apoptosis in leukemia cells. *Nat Med* 1996; 2:574-7; PMID:8616718; <http://dx.doi.org/10.1038/nm0596-574>
- Scholz C, Wieder T, Stärck L, Essmann F, Schulze-Osthoff K, Dörken B, Daniel PT. Arsenic trioxide triggers a regulated form of caspase-independent necrotic cell death via the mitochondrial death pathway. *Oncogene* 2005; 24:1904-13; PMID:15674346; <http://dx.doi.org/10.1038/sj.onc.1208233>
- Baldwin AS. Regulation of cell death and autophagy by IKK and NF- $\kappa$ B: critical mechanisms in immune function and cancer. *Immunol Rev* 2012; 246:327-45; PMID:22435564; <http://dx.doi.org/10.1111/j.1600-065X.2012.01095.x>
- Baum V, Bühler P, Gierschner D, Herchenbach D, Fiala GJ, Schamel WW, Wolf P, Elsässer-Beile U. Antitumor activities of PSMA $\times$ CD3 diabodies by redirected T-cell lysis of prostate cancer cells. *Immunotherapy* 2013; 5:27-38; PMID:23256796; <http://dx.doi.org/10.2217/imt.12.136>
- Mocikat R, Braumüller H, Gummy A, Egeter O, Ziegler H, Reusch U, Bubeck A, Louis J, Mailhammer R, Riethmüller G, et al. Natural killer cells activated by MHC class I(low) targets prime dendritic cells to induce protective CD8 T-cell responses. *Immunity* 2003; 19:561-9; PMID:14563320; [http://dx.doi.org/10.1016/S1074-7613\(03\)00264-4](http://dx.doi.org/10.1016/S1074-7613(03)00264-4)
- Michaud M, Martins I, Sukkurwala AQ, Adjemian S, Ma Y, Pellegatti P, Shen S, Kepp O, Scoazec M, Mignot G, et al. Autophagy-dependent anticancer immune responses induced by chemotherapeutic agents in mice. *Science* 2011; 334:1573-7; PMID:22174255; <http://dx.doi.org/10.1126/science.1208347>
- Dreier T, Lorenczewski G, Brandl C, Hoffmann P, Syring U, Hanakam F, Kufer P, Riethmüller G, Bargou R, Baeuerle PA. Extremely potent, rapid and costimulation-independent cytotoxic T-cell response against lymphoma cells catalyzed by a single-chain bispecific antibody. *Int J Cancer* 2002; 100:690-7; PMID:12209608; <http://dx.doi.org/10.1002/ijc.10557>
- Verma S, Miles D, Gianni L, Krop IE, Welslau M, Baselga J, Pegram M, Oh DY, Diéras V, Guardino E, et al. EMILIA Study Group. Trastuzumab emtansine for HER2-positive advanced breast cancer. *N Engl J Med* 2012; 367:1783-91; PMID:23020162; <http://dx.doi.org/10.1056/NEJMoa1209124>
- Hanahan D, Weinberg RA. Hallmarks of cancer: the next generation. *Cell* 2011; 144:646-74; PMID:21376230; <http://dx.doi.org/10.1016/j.cell.2011.02.013>
- Ryan CJ, Smith MR, de Bono JS, Molina A, Logothetis CJ, de Souza P, Fizazi K, Mainwaring P, Piulats JM, Ng S, et al.; COU-AA-302 Investigators. Abiraterone in metastatic prostate cancer without previous chemotherapy. *N Engl J Med* 2013; 368:138-48; PMID:23228172; <http://dx.doi.org/10.1056/NEJMoa1209096>
- Mehta RS, Barlow WE, Albain KS, Vandenberg TA, Dakhil SR, Tirumali NR, Lew DL, Hayes DF, Gralow JR, Livingston RB, et al. Combination anastrozole and fulvestrant in metastatic breast cancer. *N Engl J Med* 2012; 367:435-44; PMID:22853014; <http://dx.doi.org/10.1056/NEJMoa1201622>
- Wolchok JD, Kluger H, Callahan MK, Postow MA, Rizvi NA, Lesokhin AM, Segal NH, Ariyan CE, Gordon RA, Reed K, et al. Nivolumab plus ipilimumab in advanced melanoma. *N Engl J Med* 2013; 369:122-33; PMID:23724867; <http://dx.doi.org/10.1056/NEJMoa1302369>
- Müller-Hermelink N, Braumüller H, Pichler B, Wieder T, Mailhammer R, Schaak K, Ghoreschi K, Yazdi A, Haubner R, Sander CA, et al. TNFR1 signaling and IFN- $\gamma$  signaling determine whether T cells induce tumor dormancy or promote multistage carcinogenesis. *Cancer Cell* 2008; 13:507-18; PMID:18538734; <http://dx.doi.org/10.1016/j.ccr.2008.04.001>
- Ziegler A, Heidenreich R, Braumüller H, Wolburg H, Weidemann S, Mocikat R, Röcken M. EpCAM, a human tumor-associated antigen promotes Th2 development and tumor immune evasion. *Blood* 2009; 113:3494-502; PMID:19188665; <http://dx.doi.org/10.1182/blood-2008-08-175109>
- Egeter O, Mocikat R, Ghoreschi K, Dieckmann A, Röcken M. Eradication of disseminated lymphomas with CpG-DNA activated T helper type 1 cells from nontransgenic mice. *Cancer Res* 2000; 60:1515-20; PMID:10749115
- Xie Y, Akpınarlı A, Maris C, Hipkiss EL, Lane M, Kwon EK, Muranski P, Restifo NP, Antony PA. Naive tumor-specific CD4(+) T cells differentiated in vivo eradicate established melanoma. *J Exp Med* 2010; 207:651-67; PMID:20156973; <http://dx.doi.org/10.1084/jem.20091921>
- Quezada SA, Simpson TR, Peggs KS, Merghoub T, Vider J, Fan X, Blasberg R, Yagita H, Muranski P, Antony PA, et al. Tumor-reactive CD4(+) T cells develop cytotoxic activity and eradicate large established melanoma after transfer into lymphopenic hosts. *J Exp Med* 2010; 207:637-50; PMID:20156971; <http://dx.doi.org/10.1084/jem.20091918>
- Goding SR, Wilson KA, Xie Y, Harris KM, Baxi A, Akpınarlı A, Fulton A, Tamada K, Strome SE, Antony PA. Restoring immune function of tumor-specific CD4+ T cells during recurrence of melanoma. *J Immunol* 2013; 190:4899-909; PMID:23536636; <http://dx.doi.org/10.4049/jimmunol.1300271>
- Wieder T, Braumüller H, Kneilling M, Pichler B, Röcken M. T cell-mediated help against tumors. *Cell Cycle* 2008; 7:2974-7; PMID:18838866; <http://dx.doi.org/10.4161/cc.7.19.6798>
- Sen S, D'Incalci M. Apoptosis. Biochemical events and relevance to cancer chemotherapy. *FEBS Lett* 1992; 307:122-7; PMID:1639187; [http://dx.doi.org/10.1016/0014-5793\(92\)80914-3](http://dx.doi.org/10.1016/0014-5793(92)80914-3)
- Boujrad H, Gubkina O, Robert N, Krantic S, Susin SA. AIF-mediated programmed necrosis: a highly regulated way to die. *Cell Cycle* 2007; 6:2612-9; PMID:17912035; <http://dx.doi.org/10.4161/cc.6.21.4842>
- Wieder T, Essmann F, Prokop A, Schmelz K, Schulze-Osthoff K, Beyaert R, Dörken B, Daniel PT. Activation of caspase-8 in drug-induced apoptosis of B-lymphoid cells is independent of CD95/Fas receptor-ligand interaction and occurs downstream of caspase-3. *Blood* 2001; 97:1378-87; PMID:11222383; <http://dx.doi.org/10.1182/blood.V97.5.1378>
- Roca FJ, Ramakrishnan L. TNF dually mediates resistance and susceptibility to mycobacteria via mitochondrial reactive oxygen species. *Cell* 2013; 153:521-34; PMID:23582643; <http://dx.doi.org/10.1016/j.cell.2013.03.022>
- Morgan RA, Dudley ME, Wunderlich JR, Hughes MS, Yang JC, Sherry RM, Royal RE, Topalian SL, Kammula US, Restifo NP, et al. Cancer regression in patients after transfer of genetically engineered lymphocytes. *Science* 2006; 314:126-9; PMID:16946036; <http://dx.doi.org/10.1126/science.1129003>
- Schreiber RD, Old LJ, Smyth MJ. Cancer immunoeediting: integrating immunity's roles in cancer suppression and promotion. *Science* 2011; 331:1565-70; PMID:21436444; <http://dx.doi.org/10.1126/science.1203486>
- Kang TW, Yevsa T, Woller N, Hoenicke L, Wuestefeld T, Dauch D, Hohmeyer A, Gereke M, Rudalska R, Potapova A, et al. Senescence surveillance of pre-malignant hepatocytes limits liver cancer development. *Nature* 2011; 479:547-51; PMID:22080947; <http://dx.doi.org/10.1038/nature10599>
- Finn OJ. Cancer immunology. *N Engl J Med* 2008; 358:2704-15; PMID:18565863; <http://dx.doi.org/10.1056/NEJMra072739>
- Gimbrone MA Jr., Leachman SB, Cotran RS, Folkman J. Tumor dormancy in vivo by prevention of neovascularization. *J Exp Med* 1972; 136:261-76; PMID:5043412; <http://dx.doi.org/10.1084/jem.136.2.261>
- Folkman J, Hochberg M. Self-regulation of growth in three dimensions. *J Exp Med* 1973; 138:745-53; PMID:4744009; <http://dx.doi.org/10.1084/jem.138.4.745>
- Koebel CM, Vermi W, Swann JB, Zerava N, Rodig SJ, Old LJ, Smyth MJ, Schreiber RD. Adaptive immunity maintains occult cancer in an equilibrium state. *Nature* 2007; 450:903-7; PMID:18026089; <http://dx.doi.org/10.1038/nature06309>
- Hayflick L, Moorhead PS. The serial cultivation of human diploid cell strains. *Exp Cell Res* 1961; 25:585-621; PMID:13905658; [http://dx.doi.org/10.1016/0014-4827\(61\)90192-6](http://dx.doi.org/10.1016/0014-4827(61)90192-6)
- Collado M, Blasco MA, Serrano M. Cellular senescence in cancer and aging. *Cell* 2007; 130:223-33; PMID:17662938; <http://dx.doi.org/10.1016/j.cell.2007.07.003>
- Wajapeyee N, Serra RW, Zhu X, Mahalingam M, Green MR. Oncogenic BRAF induces senescence and apoptosis through pathways mediated by the secreted protein IGFBP7. *Cell* 2008; 132:363-74; PMID:18267069; <http://dx.doi.org/10.1016/j.cell.2007.12.032>

43. Santra MK, Wajapeyee N, Green MR. F-box protein FBXO31 mediates cyclin D1 degradation to induce G1 arrest after DNA damage. *Nature* 2009; 459:722-5; PMID:19412162; <http://dx.doi.org/10.1038/nature08011>
44. Kodama R, Kato M, Furuta S, Ueno S, Zhang Y, Matsuno K, Yabe-Nishimura C, Tanaka E, Kamata T. ROS-generating oxidases Nox1 and Nox4 contribute to oncogenic Ras-induced premature senescence. *Genes Cells* 2013; 18:32-41; PMID:23216904; <http://dx.doi.org/10.1111/gtc.12015>
45. Benhamed M, Herbig U, Ye T, Dejean A, Bischof O. Senescence is an endogenous trigger for microRNA-directed transcriptional gene silencing in human cells. *Nat Cell Biol* 2012; 14:266-75; PMID:22366686; <http://dx.doi.org/10.1038/ncb2443>
46. Michaloglou C, Vredeveld LC, Soengas MS, Denoyelle C, Kuilman T, van der Horst CM, Majoor DM, Shay JW, Mooi WJ, Peeper DS. BRAF<sup>V600E</sup>-associated senescence-like cell cycle arrest of human naevi. *Nature* 2005; 436:720-4; PMID:16079850; <http://dx.doi.org/10.1038/nature03890>
47. Collado M, Gil J, Efeyan A, Guerra C, Schuhmacher AJ, Barradas M, Bengurfa A, Zaballos A, Flores JM, Barbacid M, et al. Tumour biology: senescence in premalignant tumours. *Nature* 2005; 436:642; PMID:16079833; <http://dx.doi.org/10.1038/436642a>
48. Blagosklonny MV. Cell cycle arrest is not yet senescence, which is not just cell cycle arrest: terminology for TOR-driven aging. *Aging (Albany NY)* 2012; 4:159-65; PMID:22394614
49. Nardella C, Clohessy JG, Alimonti A, Pandolfi PP. Pro-senescence therapy for cancer treatment. *Nat Rev Cancer* 2011; 11:503-11; PMID:21701512; <http://dx.doi.org/10.1038/nrc3057>
50. Haferkamp S, Borst A, Adam C, Becker TM, Motschenbacher S, Windhövel S, Hufnagel AL, Houben R, Meierjohann S. Vemurafenib induces senescence features in melanoma cells. *J Invest Dermatol* 2013; 133:1601-9; PMID:23321925; <http://dx.doi.org/10.1038/jid.2013.6>
51. Bissell MJ, Hines WC. Why don't we get more cancer? A proposed role of the microenvironment in restraining cancer progression. *Nat Med* 2011; 17:320-9; PMID:21383745; <http://dx.doi.org/10.1038/nm.2328>
52. Rakhra K, Bachireddy P, Zabuawala T, Zeiser R, Xu L, Kopelman A, Fan AC, Yang Q, Braunstein L, Crosby E, et al. CD4(+) T cells contribute to the remodeling of the microenvironment required for sustained tumor regression upon oncogene inactivation. *Cancer Cell* 2010; 18:485-98; PMID:21035406; <http://dx.doi.org/10.1016/j.ccr.2010.10.002>
53. Reimann M, Lee S, Lodenkemper C, Dörr JR, Tabor V, Aichele P, Stein H, Dörken B, Jenuwein T, Schmitt CA. Tumor stroma-derived TGF-beta limits myc-driven lymphomagenesis via Suv39h1-dependent senescence. *Cancer Cell* 2010; 17:262-72; PMID:20227040; <http://dx.doi.org/10.1016/j.ccr.2009.12.043>
54. Schwitalla S, Ziegler PK, Horst D, Becker V, Kerle I, Begus-Nahrman Y, Lechel A, Rudolph KL, Langer R, Slotta-Huspenina J, et al. Loss of p53 in enterocytes generates an inflammatory microenvironment enabling invasion and lymph node metastasis of carcinogen-induced colorectal tumors. *Cancer Cell* 2013; 23:93-106; PMID:23273920; <http://dx.doi.org/10.1016/j.ccr.2012.11.014>
55. Tosolini M, Kirilovsky A, Mlecnik B, Fredriksen T, Mauger S, Bindea G, Berger A, Bruneval P, Fridman WH, Pagès F, et al. Clinical impact of different classes of infiltrating T cytotoxic and helper cells (Th1, th2, treg, th17) in patients with colorectal cancer. *Cancer Res* 2011; 71:1263-71; PMID:21303976; <http://dx.doi.org/10.1158/0008-5472.CAN-10-2907>
56. Galon J, Pagès F, Marincola FM, Angell HK, Thurin M, Lugli A, Zlobec I, Berger A, Bifulco C, Botti G, et al. Cancer classification using the Immunoscore: a worldwide task force. *J Transl Med* 2012; 10:205; PMID:23034130; <http://dx.doi.org/10.1186/1479-5876-10-205>
57. Das Thakur M, Salangang F, Landman AS, Sellers WR, Pryer NK, Levesque MP, Dummer R, McMahon M, Stuart DD. Modelling vemurafenib resistance in melanoma reveals a strategy to forestall drug resistance. *Nature* 2013; 494:251-5; PMID:23302800; <http://dx.doi.org/10.1038/nature11814>
58. Aggarwal BB, Eessalu TE, Hass PE. Characterization of receptors for human tumour necrosis factor and their regulation by gamma-interferon. *Nature* 1985; 318:665-7; PMID:3001529; <http://dx.doi.org/10.1038/318665a0>
59. Stein WD, Wilkerson J, Kim ST, Huang X, Motzer RJ, Fojo AT, Bates SE. Analyzing the pivotal trial that compared sunitinib and IFN-α in renal cell carcinoma, using a method that assesses tumor regression and growth. *Clin Cancer Res* 2012; 18:2374-81; PMID:22344231; <http://dx.doi.org/10.1158/1078-0432.CCR-11-2275>





Review Article

Submitted: 30.12.2014

Accepted: 14.8.2015

Conflict of interest

MR is co-responsible for all oncological studies at the Department of Dermatology and owns shares in pharmaceutical companies (Bristol-Myers Squibb, Merck & Co) that market oncologic drugs.

DOI: 10.1111/ddg.12819

# Immunotherapy of melanoma: efficacy and mode of action

**Thomas Wieder\*, Ellen Brenner\*, Heidi Braumüller, Martin Röcken**

Department of Dermatology, Eberhard Karls University, Tübingen, Germany

\*The first two named authors were equally responsible for writing the article.

## Summary

Forty years of research have brought about the development of antibodies that induce effective antitumor immune responses through sustained activation of the immune system. These “immune checkpoint inhibitors” are directed against immune inhibitory molecules, such as cytotoxic T lymphocyte antigen 4 (CTLA-4), programmed death 1 (PD-1) or programmed death ligand 1 (PD-L1). Disruption of the PD-1/PD-L1 interaction improves the intermediate-term prognosis even in patients with advanced stage IV melanoma. One and a half years after treatment initiation, 30–60 % of these patients are still alive. While cancer immunotherapies usually do not eradicate metastases completely, they do cause a regression by 20–80 %. It is well established that the immune system is able to kill tumor cells, and this has also been demonstrated for immunotherapies. Preclinical data, however, has shown that anti-cancer immunity is not limited to killing cancer cells. Thus, through interferon gamma and tumor necrosis factor, the immune system is able to induce stable tumor growth arrest, referred to as senescence. Ensuring patient survival by long-term stabilization of metastatic growth will therefore become a central goal of antitumor immunotherapies. This therapeutic approach is effective in melanoma and non-small-cell lung cancer. Once immunotherapies also have an indication for common cancer types, drug prices will have to drop considerably in order to be able to keep them available to those dependent on such therapies.

## Fundamentals and historic review of melanoma therapy

Melanoma ranks among those tumors that are able to metastasize even when they are still very thin. Applying to all patients with stage I to III disease, the most important prognostic factors in melanoma include tumor thickness, the presence of absence of ulceration, the number of mitoses in thin melanomas, and micrometastases in the sentinel lymph node [1]. In addition to surgical melanoma removal, immunotherapy with 3 million units of alpha-interferon three times a week for 18 months may improve recurrence-free survival,

especially in patients with melanomas thicker than 2.0 mm, ulcerated melanomas, or micrometastases [2]. In case of macroscopic lymph node metastases or those diagnosed by ultrasound, the 5-year survival rate drops to roughly 30 % [3]. Until 2008, the 3-year survival rate of stage IV melanoma with disseminated metastases was only 6–12 % [4]. At that time, the only standardized therapeutic option was dacarbazine (DTIC) [5], an alkylating cytostatic agent given every four weeks, either at a higher (single) dose or daily for five days at a dose of 250 mg/kg. However, chemotherapeutic agents have been unable to improve overall survival in advanced melanoma patients. A prospective study published in 2011 showed an overall survival after three years of 10–15 %

in patients with metastatic melanoma after four cycles of dacarbazine [6]. While the introduction of “targeted therapies” and immunotherapies [7] has markedly increased the likelihood of longer survival in stage IV melanoma patients, the spectrum of possible side effects has also broadened [8].

## Developmental stages of immunotherapy in metastatic melanoma

Although various therapeutic approaches – chemotherapy, polychemotherapy, or chemoimmunotherapy – in metastatic melanoma yielded better response rates and even long-term remission in individual cases, none of these therapies led to a statistically significant improvement in overall survival [5].

Melanoma was one of the first tumors in which the possibility of immunotherapy was investigated [9–11]. Many basic science-oriented but relatively few randomized clinical studies provide evidence for the theoretical possibilities of successful immunotherapy. Important clinically translated immunotherapies include intracutaneous treatment with interleukin-2 [12], systemic interleukin-2 therapy with simultaneous peptide vaccination [13], systemic interferon alpha therapy [14], vaccination with peptide-pulsed dendritic cells [15], or adoptive T-cell therapies [16], to name but a few. Two important observations have shaped melanoma immunotherapy: (i) On principle, melanomas may regress with and rarely also without immunotherapy, and may sometimes even completely resolve (Figure 1a, b). This regression is usually associated with an oligoclonal T-cell infiltrate [17]. On immunotherapy, melanomas and melanoma metastases constantly regress, either partially or completely. However, these therapeutic studies rarely led to statistically significant and sustained tumor regression. Peptide vaccination combined with interleukin-2 achieved a statistically significant prolongation of progression-free survival of about one month compared to treatment with interleukin-2 alone [13]. Adoptive T-cell transfer, too, may result in metastatic regression and sustained clinical improvement in individual patients [16, 18]. (ii) Conversely, however, tumor immunotherapy may also accelerate tumor growth and metastasis if it induces the “wrong” immune response [19–22]. With respect to everyday clinical practice, these data show that, outside of clinical studies, tumor patients should receive neither a tumor vaccine nor immunostimulants that are not supported by studies. Moreover, while illustrating the risks and difficulties in developing adequate tumor-protective immunotherapies, they also demonstrate that immune responses are able to influence tumor growth.

Collected over the course of more than 40 years, these data raised serious doubts regarding the rationale behind the development of immunotherapies [23]. Until the treatment of

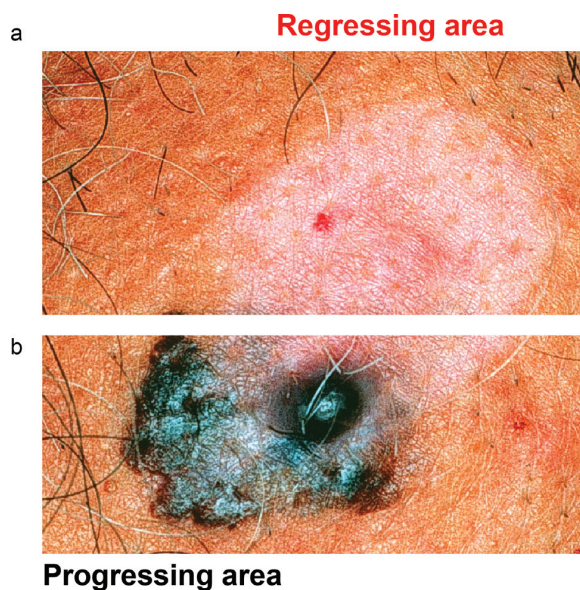


**Figure 1** Clinical appearance of a melanoma with areas marked both by regression and progression. View from above of a melanoma lesion with a regressing part (a) and a highly pigmented, progressing part (b).

metastatic melanoma directed against cytotoxic T lymphocyte antigen 4 (CTLA-4) was described [6, 24], the subject of tumor immunotherapy had been regarded very critically in clinical practice, research, and the pharmaceutical industry.

## Immunotherapy in the treatment of melanoma

Every immune response – whether directed against infectious agents, autoantigens, or tumors – is characterized by a prime and boost phase as well as a ‘stop phase’ in which the response is once again subdued. The vast majority of tumor immunotherapies has focused on initiating the strongest possible immune responses, however, these therapies have not yet found their way into clinical practice. This situation changed when the opposite approach was adopted in studies that investigated whether releasing the immune brake could be used therapeutically. This had been repeatedly attempted since the discovery of “immunosuppression”. The breakthrough came when studies began to examine the inhibitory signaling pathways of CTLA-4 or programmed death 1 (PD-1) and its ligand, programmed death ligand 1 (PD-L1), in patients with stage IV melanoma.

In 2011, a prospective study showed that tumor immunotherapy in stage IV melanoma patients was able to

achieve a small but statistically significant improvement in 3-year survival. The overall survival of patients who received the anti-CTLA-4 antibody ipilimumab in combination with dacarbazine was 20 % and thus about 5 % greater than in individuals treated with dacarbazine and placebo [6]. In this study, patients received four one-day doses of dacarbazine at four-week intervals. At the same time, one group was given placebo, while the other received a monoclonal antibody (mAb) directed against CTLA-4. The latter was given at a dose of 10 mg/kg instead of 3 mg/kg, which today is the usual therapeutic dose. Induction therapy included four doses of anti-CTLA-4 antibody at four-week intervals. This was followed by maintenance therapy with 10 mg/kg every three months for three years; the control group received placebo. The study yielded the following important results: (i) At the end of the study, after 45 months, the number of survivors in the anti-CTLA-4-treated group was roughly 5 % greater than in the placebo group; the difference was significant. This observation marked a breakthrough, as this was the first placebo-controlled study that showed that, compared to placebo, tumor immunotherapy indeed improves survival in stage IV melanoma patients. (ii) Although this therapy resulted in a statistically significant survival advantage, even continued anti-CTLA-4 antibody therapy, using a five- to seven-fold higher anti-CTLA-4 dose than currently licensed, led only to a slight improvement in survival. Patients showing a treatment-induced immune response, in which T lymphocytes that produce interferon gamma (IFN- $\gamma$ ) and tumor necrosis factor (TNF) prevail, appear to particularly benefit from “immune checkpoint inhibitor” therapy [25].

The currently licensed therapy with ipilimumab (four doses of 3 mg/kg at four-week intervals) differs markedly from the aforementioned regimen. It would therefore be necessary to compare the currently approved treatment regimen with placebo and dacarbazine in order to ascertain whether this form of immunotherapy (as monotherapy) is able to achieve a significant therapeutic advantage over dacarbazine. A randomized, placebo-controlled trial that investigated the effect of adjuvant anti-CTLA-4 therapy in patients with stage III disease showed significantly improved recurrence-free survival at three years [26]. However, a conclusion regarding overall survival using adjuvant anti-CTLA-4 therapy cannot be drawn at this time.

## Immunotherapy with antibodies against PD-1 or PD-L1

Following reports of the efficacy of anti-CTLA-4 antibodies, five publications showed that non-depleting monoclonal antibodies (mAbs) with a similar mode of action – blocking the interaction between PD-1 and its ligand PD-L1 – resulted in

stabilization or regression of metastases in a strikingly large number of patients with metastatic melanoma and a range of other tumors [27–31]. Moreover, even this initial data obtained from phase I and II studies suggested that mAbs directed against the PD-1/PD-L1 interaction were able to prolong overall survival not only in patients with stage III or IV melanoma but also with other tumors such as lung cancer. While all previous immunotherapies had only been successful in individual cases, these studies provided evidence of a broader efficacy, also impacting overall survival. Four recently published clinical metastatic melanoma trials yielded the following important results: (i) 18 months after treatment initiation, 70 % of patients treated with anti-PD-1 antibodies were still alive, marking a clear improvement in overall survival by roughly 50 % compared to the dacarbazine control group [32]. (ii) Direct comparison between anti-CTLA-4 and anti-PD-1 antibody therapy showed a significant advantage for patients treated with anti-PD-1 antibodies with respect to overall survival after 18 months and also progression-free survival after ten months [33]. (iii) The combination of anti-CTLA-4 and anti-PD-1 antibodies resulted in progression-free survival at twelve months in 55 % of patients without a BRAF-V600E mutation, which, compared to anti-CTLA-4 monotherapy, was a significant improvement by 32 % [34]. (iv) Another study was able to confirm the greater therapeutic benefit of combined anti-CTLA-4 and anti-PD-1 antibody therapy compared to the respective monotherapies. Moreover, that particular study also showed that only patients with PD-L1-negative tumors benefited from additional anti-CTLA-4 antibody treatment [35].

In patients with non-small cell lung cancer, too, the overall survival rate at one year may roughly be tripled by anti-PD-1 mAbs compared to classic therapy [36]. Thus, using immunotherapy, two to three times as many patients with tumors that up to now have been considered treatment-refractory at the metastatic stage will in the future be rendered stable for at least two years. The introduction of immune checkpoint inhibitors has therefore markedly improved the prognosis of patients with metastatic melanoma and numerous other tumors (Figure 2). Further prognostic improvement may be achieved by combining anti-CTLA-4 and anti-PD-1 treatment. Despite the frequently severe side effects associated with this form of therapy [26], successfully treated patients will be symptom-free after the conclusion of treatment.

Not only will these new anti-tumor therapies improve the prognosis of patients with stage IV disease, they will also change our understanding of tumor immunotherapy. While therapeutic strategies have so far focused on attempts aimed at complete tumor eradication, new therapies show us that this is obviously neither possible nor necessary. Although tumors regress partially, residual tumors or residual metastases

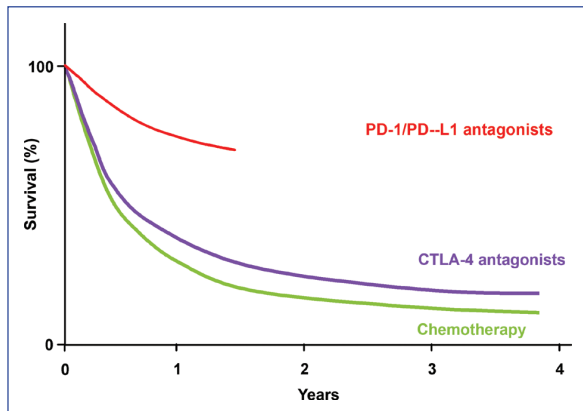


**Figure 2** Overall survival of melanoma patients with metastatic disease. The figure depicts the estimated overall survival in % of melanoma patients with metastatic disease receiving standard chemotherapy (green curve, [6]), antibody-based immunotherapy with anti-CTLA-4 (violet curve, [6]) or with anti-PD-1/anti-PD-L1 antibodies (red curve, [32]). Note: actual percentages of the survival curves have to be validated in future clinical trials. Thus, only the 100 % value and the 0 % value are marked on the y-axis.

persist in a long-term resting state [6, 11, 27–30, 32, 34, 35], also known as tumor dormancy.

### Mechanisms of tumor immune control

Up to now, the therapeutic goal has been to eradicate tumors as completely as possible, using chemotherapeutic agents or genetically targeted therapies [23], such as BRAF or MEK inhibitors in the case of melanoma [37]. Within a short time, these therapies can lead to marked, clinically almost complete metastatic regression [37]. However, this regression is nearly always followed by a V-shaped recurrence of metastases. Thus, the effect of these targeted treatment approaches – BRAF inhibitors and chemotherapies – on overall survival has been insignificant [37, 38]. Even in case of a good initial response, the overall survival of patients with stage IV melanoma at nine to ten months usually corresponds to that of patients on dacarbazine.

With the conviction that tumors have to be removed completely, immunological approaches have been aimed at inducing as many efficient killer cells as possible. Here, the focus has been on cytotoxic T lymphocytes (CTLs) characterized by the CD8 molecule and natural killer cells (NK cells). A central therapeutic function of these two immune cells is the destruction of target tumors. There are two basic mechanisms for killing target cells: (i) Following activation,

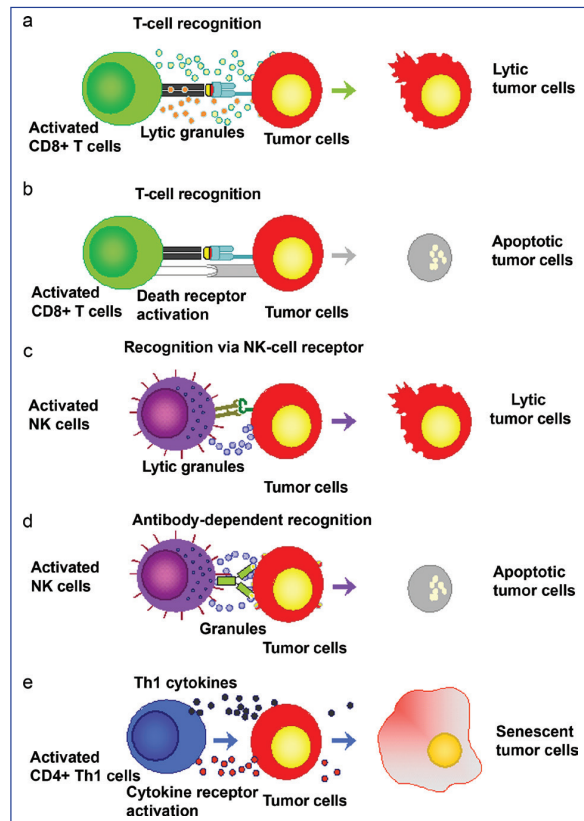


**Figure 3** Mechanisms of immunotherapies. The figure depicts established immunotherapy mechanisms: cytotoxicity by CD8-positive killer cells (a), receptor-mediated induction of programmed cell death or apoptosis (b), MHC-independent NK cell-mediated cytotoxicity (c), NK cell-mediated antibody-dependent cellular cytotoxicity (ADCC) (d), and the newly described mechanism of Th1 cytokine-induced permanent growth arrest or cellular senescence (e).

the killer cells produce lytic granules that contain perforin and granzyme B. These substances induce holes in the cell membrane of the target cells, thereby initiating lytic cell death (Figure 3a). For tumors to be recognized specifically by CTLs, it is necessary that they express antigens that may only be found on them, designated as tumor-associated antigens (TAA). This was first demonstrated for melanoma-associated molecules known as cancer/testis antigens. The most important tumor antigens expressed by melanomas include MAGE-1, MAGE-3 [39], and the NY-ESO antigen [40]. (ii) Apart from lysis, the most important way of killing cells is by induction of apoptosis. Here, the tumor cell receives a signal, leading to active self-destruction by nuclear fragmentation (Figure 3b). This signal cascade is initiated through

specific death receptors such as the Fas molecule [41]. The T lymphocytes involved in transmitting the death signal to tumor cells have to express the corresponding Fas ligand (FasL).

Just like CTLs, NK cells, too, are able to kill tumor cells through the two aforementioned mechanisms [42, 43] (Figure 3c). However, the recognition mechanism is fundamentally different. Cytotoxic T lymphocytes can only recognize tumor cells if they present the correct major histocompatibility complex (MHC) molecule together with the TAA. In order to evade this immune response, tumors have developed various evasive strategies that prevent presentation of their TAA. One of the most important strategies involves the suppression of the MHC molecule to such an extent that CTLs are no longer able to recognize the tumor cells. In this case, NK cells intervene [42] recognizing all those cells that have suppressed the MHC molecule and thus can no longer activate inhibitory receptor molecules on the surface of NK cells. In addition to inhibitory receptor molecules, NK cells also express activating receptors such as the Fc $\gamma$  receptor IIIa, also known as CD16, which in turn is able to bind the nonspecific Fc segment of antibodies. The Fc $\gamma$  receptor IIIa is then able to trigger antibody-dependent cellular cytotoxicity (ADCC) in tumor cells marked by specific antibodies (Figure 3d).

Although these cell-killing mechanisms have been meticulously studied in detail for 30 years, it has so far only rarely been possible to successfully and effectively use CTL and NK cells in the treatment of tumors [9, 10, 44]. Possible causes for the frequently inadequate tumor control by cytotoxic therapies include killing-resistant tumor stem cells [45] and highly immunosuppressant myeloid-derived suppressor cells (MDSC) [46].

## Tumor control by induction of tumor cell senescence

While therapeutic studies have primarily focused on effectively killing tumor cells, it has been shown that in some tumors a favorable prognosis for long-term survival or successful therapy is associated with the expression of the two cytokines IFN- $\gamma$  and TNF [47, 48]. By contrast, tumor-specific immune responses predominantly marked by interleukin-17, interleukin-4, or TGF- $\beta$ 1 are associated with a poor prognosis or unsatisfactory therapeutic response [22, 49–51]. Together, this data suggests that there is another tumor control mechanism besides the induction of tumor cell death through cytolysis or apoptosis. Given that patients frequently live in a stable disease state for many years, IFN- and TNF-dominated immune responses apparently result in long-term tumor growth arrest.

A few years ago, it was first shown that IFN- $\gamma$ - and TNF-producing T lymphocytes that do not themselves have

the capacity to kill tumor cells induce permanent growth arrest in various tumors [22, 52–54]. Common to all these studies was that control of tumor growth was strictly dependent on the T helper 1 (Th1) cell cytokines IFN- $\gamma$  and TNF [22], thus precisely those cytokines associated with overall survival in clinical trials.

The underlying mechanism has therefore long been sought. Recent studies have shown that the joint action of IFN- $\gamma$  and TNF in many tumor cells, especially in primary human tumor cells such as melanoma, induces permanent growth arrest [11] (Figure 3e). This means that the tumor cells remain alive but – for a period of weeks and months – lose their ability to divide. Biologically speaking, these tumors become too old to grow. Such growth arrest is referred to as cellular senescence. There are basically two forms of senescence. The first form is associated with growing old, and prevents cells from proliferating like young cells. The second form of senescence involves a permanent proliferation stop of tumor cells – otherwise growing unchecked – through senescence mechanisms [11, 55]. It has hitherto been assumed that cell cycle arrest in tumors is solely mediated by endogenous signals. This cell cycle arrest is coupled, for instance, with aging or with oncogenes such as the mutated BRAF gene, or is triggered by certain chemotherapeutic agents [56]. By demonstrating cytokine-induced senescence in tumors, it has been shown that senescence mechanisms are not only activated by endogenous signals but also by signals delivered to the cell from the outside. This has been confirmed under immunotherapy conditions [11].

Only in the correct concentration and composition do IFN- $\gamma$  and TNF induce senescence in tumor cells (Figure 3e). Adverse cytokine combinations, such as the presence of TNF in the absence of interferons or the presence of interferons in the absence of TNF receptor 1 signals may even promote tumor growth or tumor recurrence after successful therapy [22, 57]. Conversely, not only the observation that Th1 cytokines IFN- $\gamma$  and TNF are able to inhibit tumor growth by senescence induction but also insights into cytokine-induced growth arrest have been confirmed and expanded. For instance, IL-12-coding gene constructs that elicit IFN- $\gamma$  production induce senescence in human tumors *in vivo* [58], and liposomes containing interleukin-12 inhibit the growth of breast cancer cells through the induction of an IFN- $\gamma$ /TNF signature [59]. Moreover, the soluble messenger thrombospondin-1 may induce senescence in lung tumor cells [60].

## Clinical relevance of cytokine-induced senescence for tumor immunotherapy

The observation that kinase inhibitors specifically block disease-relevant molecules such as the BRAF-V600E molecule,

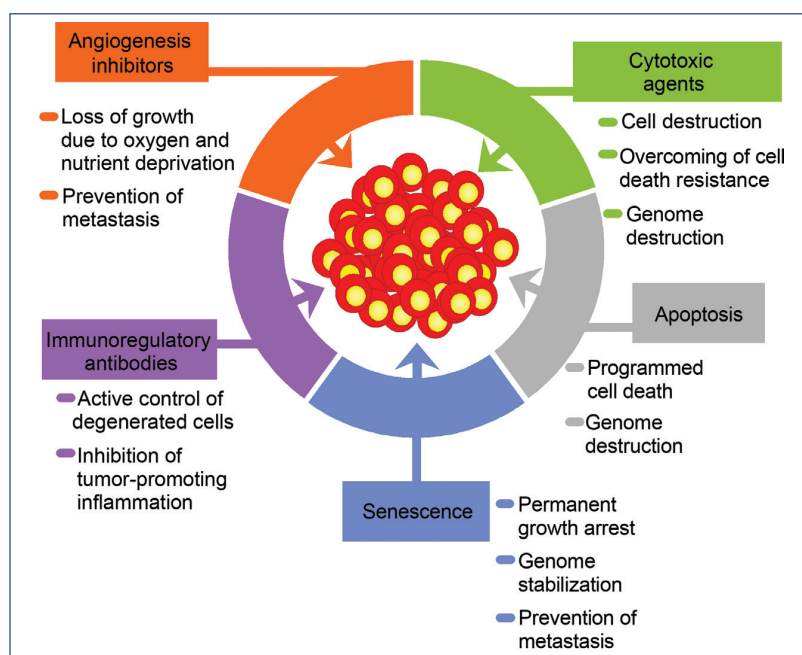


**Figure 4** Targets of modern cancer therapy. Therapeutic approaches of cancer therapy (without surgery) are depicted. With the exception of angiogenesis inhibitors [74], which inhibit the formation of tumor-supplying blood vessels, all other cytotoxic, apoptosis- or senescence-inducing agents, including the immune checkpoint inhibitors, are described in detail in the text.

thereby leading to clinical regression of melanoma metastases, ushered in a new era of melanoma therapy [61]. However, given the rapid recurrence of metastases, these therapies were only able to prolong average survival in patients with metastatic melanoma by a mere few months, if at all [37]. Results of phase I to III studies with mAbs, known as immune checkpoint inhibitors and directed against the molecules CTLA-4, PD-1, or PD-L1 [6, 25, 27–30, 32–35], have so far shown effects and disease courses previously unknown in tumor therapies. Three aspects ought to be highlighted: (i) Following treatment initiation, tumors appear to initially grow radiographically. This must not be misinterpreted as melanoma growth, as metastases tend to swell due to the accompanying inflammation. Only after partial destruction and regression of inflammation (after three to six months) do they also regress radiographically. (ii) While patients with advanced metastases frequently display disease symptoms, patients clinically recover with tumor regression. For years, patients thus exhibit no clinical symptoms, while still affected by a demonstrable tumor burden. (iii) Following the regression phase, “residual metastases” remain stable [27–30, 32–35]. They may remain dormant for 24 to 30 months without significantly changing in size.

The new therapies show that the original goal of complete tumor eradication by killing all tumor cells is no longer required in every case. In this respect, the primary treatment objective is changing from an all-out “war on cancer” – necessitating tumor eradication – to the concept

of living nearly symptom-free with few and smaller tumors that are kept in check by the immune system. According to the classic concept [9, 10], it is postulated that the stability of metastases following treatment with CTLA-4, PD-1, or PD-L1 antibodies is solely based on the equilibrium between tumor cell growth, on the one hand, and continuous killing of tumor cells on the other [27–32]. Given that immune cells are able to arrest tumor growth through proinflammatory cytokines, one might argue whether successful tumor immunotherapies induce such growth arrest in melanoma metastases at least partially through Th1 cytokines IFN- $\gamma$  and TNF. Tumor-infiltrating T cells [47] with a high interferon/interleukin-4 ratio [48, 51] are surrogate markers for a good prognosis in various malignant diseases. Thus, besides killing tumor cells, there have to be other mechanisms in play that inhibit tumor growth either directly or through the tumor-surrounding tissue. These mechanisms have also been summarized as cell death-independent “tumor immune surveillance model” [62–64]. Non-toxic tumor control mechanisms play a key role in modern targeted cancer therapy (Figure 4).

This type of tumor immune surveillance displays great similarities with mechanisms leading to organ-specific autoimmune disorders. Thus, side effects of effective tumor immunotherapies, such as mAbs against CTLA-4 or PD-1 and IFN alpha therapy, may include the triggering of organ-specific autoimmune diseases [65–67]. Conversely, experiments have shown that effective inhibition of TNF- or IL-12-induced

IFN- $\gamma$  in autoimmune disorders may increase the risk for developing malignant tumors [68, 69].

## Outlook and comments on clinical implementation

Monoclonal antibody-mediated blockade of the immune brakes CTLA-4, PD-1, and PD-L1 is therapeutically useful in the treatment of melanoma and other tumors such as non-small cell lung cancer [31, 36]. The clinical use of immune checkpoint inhibitors has ushered in a new era of cancer therapy. In particular, patients with treatment-refractory cancers might now be helped long-term, and immunotherapy could, in the near future, become a real option for many patients with advanced or metastatic tumors. However, as exemplified by chronic myeloid leukemia in an analysis by 119 hematologists, a certain therapy can only be implemented if its costs remain acceptable for society. In their article, the authors discuss that even rich nations cannot afford annual treatment costs of € 50,000 to € 100,000 per patient in the long term [70]. With the successful introduction of mAb-based therapeutic agents, the costs of modern cancer therapy have risen yet again. In the ongoing discussion, clinically active cancer researchers have proposed the need for a cost-benefit assessment, including the demand for lower prices [71]. Based on current pricing, the new “immune checkpoint inhibitors” will lead to two-year drug costs of up to 250,000 € per patient. These costs have to be considered problematic insofar as they are even higher than those of the kinase inhibitors, which the hematologists already deemed problematic. Moreover, these costs will not only be incurred in the context of rare tumors but in common cancers as well. What is more, the financial or scientific justification for the current pricing of innovative cancer drugs is not immediately understandable, either [72, 73], especially considering the fact that the majority of research findings that have ultimately led to the development of new drugs come from state-sponsored and tax-funded research projects [72, 73]. It is therefore time for physicians, politicians, health system institutions, and society to negotiate with the pharmaceutical industry over the prices of these modern cancer drugs. This is the only way to ensure the long-term financing of medically promising drugs.

## Acknowledgments

The authors' research is supported by the Wilhelm Sander Foundation (2012.056.1 and 2012.056.2), German Cancer Aid (application numbers 109037 and 110664), and the German Research Association (SFB 685 and DFG WI 1279/4-1).

## Correspondence to

Prof. Dr. med. Martin Röcken  
 Universitätsklinik  
 Eberhard-Karls-Universität Tübingen  
 Liebermeisterstraße 25

72076 Tübingen  
 Germany

E-mail: mrocken@med.uni-tuebingen.de

## References

- 1 Ulmer A, Dietz K, Hodak I et al. Quantitative measurement of melanoma spread in sentinel lymph nodes and survival. *PLoS Med* 2014; 11: e1001604.
- 2 Hauschild A, Weichenthal M, Rasmussen K et al. Efficacy of low-dose interferon  $\alpha$ 2a 18 versus 60 months of treatment in patients with primary melanoma of  $\geq 1.5$  mm tumor thickness: results of a randomized phase III DeCOG trial. *J Clin Oncol* 2010; 28: 841–6.
- 3 Leiter U, Buettner PG, Eigentler TK et al. Hazard rates for recurrent and secondary cutaneous melanoma: an analysis of 33 384 patients in the German Central Malignant Melanoma Registry. *J Am Acad Dermatol* 2012; 66: 37–45.
- 4 Korn EL, Liu PY, Lee SJ et al. Meta-analysis of phase II cooperative group trials in metastatic stage IV melanoma to determine progression-free and overall survival benchmarks for future phase II trials. *J Clin Oncol* 2008; 26: 527–34.
- 5 Garbe C, Eigentler TK. Diagnosis and treatment of cutaneous melanoma: state of the art 2006. *Melanoma Res* 2007; 17: 117–27.
- 6 Robert C, Thomas L, Bondarenko I et al. Ipilimumab plus dacarbazine for previously untreated metastatic melanoma. *N Engl J Med* 2011; 364: 2517–26.
- 7 Pflugfelder A, Kochs C, Blum A et al. Malignant melanoma S3-guideline “diagnosis, therapy and follow-up of melanoma”. *J Dtsch Dermatol Ges* 2013; 11 (Suppl 6): 1–116, 1–26.
- 8 Zimmer L, Vaubel J, Livingstone E, Schadendorf D. Side effects of systemic oncological therapies in dermatology. *J Dtsch Dermatol Ges* 2012; 10: 475–86.
- 9 Finn OJ. Cancer immunology. *N Engl J Med* 2008; 358: 2704–15.
- 10 Schreiber RD, Old LJ, Smyth MJ. Cancer immunoediting: integrating immunity's roles in cancer suppression and promotion. *Science* 2011; 331: 1565–70.
- 11 Braumüller H, Wieder T, Brenner E et al. T-helper-1-cell cytokines drive cancer into senescence. *Nature* 2013; 494: 361–5.
- 12 Weide B, Derhovanessian E, Pflugfelder A et al. High response rate after intratumoral treatment with interleukin-2: results from a phase 2 study in 51 patients with metastasized melanoma. *Cancer* 2010; 116: 4139–46.
- 13 Schwartzentruber DJ, Lawson DH, Richards JM et al. gp100 peptide vaccine and interleukin-2 in patients with advanced melanoma. *N Engl J Med* 2011; 364: 2119–27.
- 14 Flaherty LE, Othus M, Atkins MB et al. Southwest Oncology Group S0008: a phase III trial of high-dose interferon  $\alpha$ -2b versus cisplatin, vinblastine, and dacarbazine, plus interleukin-2

- and interferon in patients with high-risk melanoma – an intergroup study of cancer and leukemia Group B, Children’s Oncology Group, Eastern Cooperative Oncology Group, and Southwest Oncology Group. *J Clin Oncol* 2014; 32: 3771–8.
- 15 Thurner B, Haendle I, Roder C et al. Vaccination with mage-3A1 peptide-pulsed mature, monocyte-derived dendritic cells expands specific cytotoxic T cells and induces regression of some metastases in advanced stage IV melanoma. *J Exp Med* 1999; 190: 1669–78.
- 16 Rosenberg SA, Restifo NP, Yang JC et al. Adoptive cell transfer: a clinical path to effective cancer immunotherapy. *Nat Rev Cancer* 2008; 8: 299–308.
- 17 Yazdi AS, Morstedt K, Puchta U et al. Heterogeneity of T-cell clones infiltrating primary malignant melanomas. *J Invest Dermatol* 2006; 126: 393–8.
- 18 Tran E, Turcotte S, Gros A et al. Cancer immunotherapy based on mutation-specific CD4+ T cells in a patient with epithelial cancer. *Science* 2014; 344: 641–5.
- 19 Eggermont AM, Spatz A, Robert C. Cutaneous melanoma. *Lancet* 2014; 383: 816–27.
- 20 Kirkwood JM, Ibrahim JG, Sosman JA et al. High-dose interferon  $\alpha$ -2b significantly prolongs relapse-free and overall survival compared with the GM2-KLH/QS-21 vaccine in patients with resected stage IIB-III melanoma: results of intergroup trial E1694/S9512/C509801. *J Clin Oncol* 2001; 19: 2370–80.
- 21 Schadendorf D, Ugurel S, Schuler-Thurner B et al. Dacarbazine (DTIC) versus vaccination with autologous peptide-pulsed dendritic cells (DC) in first-line treatment of patients with metastatic melanoma: a randomized phase III trial of the DC study group of the DeCOG. *Ann Oncol* 2006; 17: 563–70.
- 22 Muller-Hermelink N, Braumuller H, Pichler B et al. TNFR1 signaling and IFN-gamma signaling determine whether T cells induce tumor dormancy or promote multistage carcinogenesis. *Cancer Cell* 2008; 13: 507–18.
- 23 Hanahan D. Rethinking the war on cancer. *Lancet* 2014; 383: 558–63.
- 24 Hodi FS, O’Day SJ, McDermott DF et al. Improved survival with ipilimumab in patients with metastatic melanoma. *N Engl J Med* 2010; 363: 711–23.
- 25 Herbst RS, Soria JC, Kowanetz M et al. Predictive correlates of response to the anti-PD-L1 antibody MPDL3280A in cancer patients. *Nature* 2014; 515: 563–7.
- 26 Eggermont AM, Chiarion-Sileni V, Grob JJ et al. Adjuvant ipilimumab versus placebo after complete resection of high-risk stage III melanoma (EORTC 18071): a randomised, double-blind, phase 3 trial. *Lancet Oncol* 2015; 16(6): e262.
- 27 Topalian SL, Hodi FS, Brahmer JR et al. Safety, activity, and immune correlates of anti-PD-1 antibody in cancer. *N Engl J Med* 2012; 366: 2443–54.
- 28 Brahmer JR, Tykodi SS, Chow LQ et al. Safety and activity of anti-PD-L1 antibody in patients with advanced cancer. *N Engl J Med* 2012; 366: 2455–65.
- 29 Hamid O, Robert C, Daud A et al. Safety and tumor responses with lambrolizumab (anti-PD-1) in melanoma. *N Engl J Med* 2013; 369: 134–44.
- 30 Wolchok JD, Kluger H, Callahan MK et al. Nivolumab plus ipilimumab in advanced melanoma. *N Engl J Med* 2013; 369: 122–33.
- 31 Tumeq PC, Harview CL, Yearley JH et al. PD-1 blockade induces responses by inhibiting adaptive immune resistance. *Nature* 2014; 515: 568–71.
- 32 Robert C, Long GV, Brady B et al. Nivolumab in previously untreated melanoma without BRAF mutation. *N Engl J Med* 2015; 372: 320–30.
- 33 Robert C, Schachter J, Long GV et al. Pembrolizumab versus ipilimumab in advanced melanoma. *N Engl J Med* 2015; 372(26): 2521–32.
- 34 Postow MA, Chesney J, Pavlick AC et al. Nivolumab and ipilimumab versus ipilimumab in untreated melanoma. *N Engl J Med* 2015; 372: 2006–17.
- 35 Larkin J, Chiarion-Sileni V, Gonzalez R et al. Combined Nivolumab and Ipilimumab or Monotherapy in Untreated Melanoma. *N Engl J Med* 2015; 373(1): 23–34.
- 36 Garon EB, Rizvi NA, Hui R et al. Pembrolizumab for the treatment of non-small-cell lung cancer. *N Engl J Med* 2015; 372: 2018–28.
- 37 McArthur GA, Chapman PB, Robert C et al. Safety and efficacy of vemurafenib in BRAF(V600E) and BRAF(V600K) mutation-positive melanoma (BRIM-3): extended follow-up of a phase 3, randomised, open-label study. *Lancet Oncol* 2014; 15: 323–32.
- 38 Hauschild A, Agarwala SS, Trefzer U et al. Results of a phase III, randomized, placebo-controlled study of sorafenib in combination with carboplatin and paclitaxel as second-line treatment in patients with unresectable stage III or stage IV melanoma. *J Clin Oncol* 2009; 27: 2823–30.
- 39 Van den Eynde B, Peeters O, De Backer O et al. A new family of genes coding for an antigen recognized by autologous cytolytic T lymphocytes on a human melanoma. *J Exp Med* 1995; 182: 689–98.
- 40 Chen YT, Gure AO, Tsang S et al. Identification of multiple cancer/testis antigens by allogeneic antibody screening of a melanoma cell line library. *Proc Natl Acad Sci U S A* 1998; 95: 6919–23.
- 41 Daniel PT, Wieder T, Sturm I, Schulze-Osthoff K. The kiss of death: promises and failures of death receptors and ligands in cancer therapy. *Leukemia* 2001; 15: 1022–32.
- 42 Mocikat R, Braumuller H, Gumy A et al. Natural killer cells activated by MHC class I(low) targets prime dendritic cells to induce protective CD8 T cell responses. *Immunity* 2003; 19: 561–9.
- 43 Holsken O, Miller M, Cerwenka A. Exploiting natural killer cells for therapy of melanoma. *J Dtsch Dermatol Ges* 2015; 13: 23–9.
- 44 Mackensen A, Meidenbauer N, Vogl S et al. Phase I study of adoptive T-cell therapy using antigen-specific CD8+ T cells for the treatment of patients with metastatic melanoma. *J Clin Oncol* 2006; 24: 5060–9.
- 45 Roesch A. Melanoma stem cells. *J Dtsch Dermatol Ges* 2015; 13: 118–24.
- 46 Skabytska Y, Wolbing F, Gunther C et al. Cutaneous innate immune sensing of Toll-like receptor 2–6 ligands suppresses T cell immunity by inducing myeloid-derived suppressor cells. *Immunity* 2014; 41: 762–75.
- 47 Weide B, Zelba H, Derhovanessian E et al. Functional T cells targeting NY-ESO-1 or Melan-A are predictive for survival of patients with distant melanoma metastasis. *J Clin Oncol* 2012; 30: 1835–41.



- 48 Pages F, Berger A, Camus M et al. Effector memory T cells, early metastasis, and survival in colorectal cancer. *N Engl J Med* 2005; 353: 2654–66.
- 49 Egeter O, Mocikat R, Ghoeschi K et al. Eradication of disseminated lymphomas with CpG-DNA activated T helper type 1 cells from nontransgenic mice. *Cancer Res* 2000; 60: 1515–20.
- 50 Mendez R, Ruiz-Cabello F, Rodriguez T et al. Identification of different tumor escape mechanisms in several metastases from a melanoma patient undergoing immunotherapy. *Cancer Immunol Immunother* 2007; 56: 88–94.
- 51 Zelba H, Weide B, Martens A et al. Circulating CD4+ T cells that produce IL4 or IL17 when stimulated by melan-A but not by NY-ESO-1 have negative impacts on survival of patients with stage IV melanoma. *Clin Cancer Res* 2014; 20: 4390–9.
- 52 Wieder T, Braumüller H, Kneilling M et al. T cell-mediated help against tumors. *Cell Cycle* 2014; 7: 2974–77.
- 53 Ziegler A, Heidenreich R, Braumüller H et al. EpCAM, a human tumor-associated antigen promotes Th2 development and tumor immune evasion. *Blood* 2009; 113: 3494–502.
- 54 Koebel CM, Vermi W, Swann JB et al. Adaptive immunity maintains occult cancer in an equilibrium state. *Nature* 2007; 450: 903–7.
- 55 Perez-Mancera PA, Young AR, Narita M. Inside and out: the activities of senescence in cancer. *Nat Rev Cancer* 2014; 14: 547–58.
- 56 Schmitt CA, Fridman JS, Yang M et al. A senescence program controlled by p53 and p16INK4a contributes to the outcome of cancer therapy. *Cell* 2002; 109: 335–46.
- 57 Landsberg J, Kohlmeyer J, Renn M et al. Melanomas resist T-cell therapy through inflammation-induced reversible dedifferentiation. *Nature* 2012; 490: 412–6.
- 58 Schilbach K, Alkhaled M, Welker C et al. Cancer-targeted IL-12 controls human rhabdomyosarcoma by senescence induction and myogenic differentiation. *Oncol Immunology*. 2015; 4: e1014760.
- 59 Meraz IM, Savage DJ, Segura-Ibarra V et al. Adjuvant cationic liposomes presenting MPL and IL-12 induce cell death, suppress tumor growth, and alter the cellular phenotype of tumors in a murine model of breast cancer. *Mol Pharm* 2014; 11: 3484–91.
- 60 Baek KH, Bhang D, Zaslavsky A et al. Thrombospondin-1 mediates oncogenic Ras-induced senescence in premalignant lung tumors. *J Clin Invest* 2013; 123: 4375–89.
- 61 Chapman PB, Hauschild A, Robert C et al. Improved survival with vemurafenib in melanoma with BRAF V600E mutation. *N Engl J Med* 2011; 364: 2507–16.
- 62 Gatenby RA. A change of strategy in the war on cancer. *Nature* 2009; 459: 508–9.
- 63 Rocken M. Early tumor dissemination, but late metastasis: insights into tumor dormancy. *J Clin Invest* 2010; 120: 1800–3.
- 64 Wieder T, Braumüller H, Brenner E et al. Changing T-cell enigma: cancer killing or cancer control? *Cell Cycle* 2013; 12: 3146–53.
- 65 Voskens CJ, Goldinger SM, Loquai C et al. The price of tumor control: an analysis of rare side effects of anti-CTLA-4 therapy in metastatic melanoma from the ipilimumab network. *PLoS One* 2013; 8: e53745.
- 66 Raker V, Steinbrink K. Research in practice: the impact of interferon-alpha therapy on immune tolerance. *J Dtsch Dermatol Ges* 2014; 12: 315–9.
- 67 Racke MK, Bonomo A, Scott DE et al. Cytokine-induced immune deviation as a therapy for inflammatory autoimmune disease. *J Exp Med* 1994; 180: 1961–6.
- 68 Lopez-Olivo MA, Tayar JH, Martinez-Lopez JA et al. Risk of malignancies in patients with rheumatoid arthritis treated with biologic therapy: a meta-analysis. *JAMA* 2012; 308: 898–908.
- 69 Gordon KB, Langley RG, Gottlieb AB et al. A phase III, randomized, controlled trial of the fully human IL-12/23 mAb briakinumab in moderate-to-severe psoriasis. *J Invest Dermatol* 2012; 132: 304–14.
- 70 Experts in Chronic Myeloid Leukemia. The price of drugs for chronic myeloid leukemia (CML) is a reflection of the unsustainable prices of cancer drugs: from the perspective of a large group of CML experts. *Blood* 2013; 121: 4439–42.
- 71 Saltz LB. Can money really be no object when cancer care is the subject? *J Clin Oncol* 2015; 33: 1093–4.
- 72 Stevens AJ, Jensen JJ, Wyller K et al. The role of public-sector research in the discovery of drugs and vaccines. *N Engl J Med* 2011; 364: 535–41.
- 73 Avorn J. The \$ 2.6 billion pill – methodologic and policy considerations. *N Engl J Med* 2015; 372: 1877–9.
- 74 Gligorov J, Doval D, Bines J et al. Maintenance capecitabine and bevacizumab versus bevacizumab alone after initial first-line bevacizumab and docetaxel for patients with HER2-negative metastatic breast cancer (IMELDA): a randomised, open-label, phase 3 trial. *Lancet Oncol* 2014; 15: 1351–60.

# Cytokine-induced senescence for cancer surveillance

Thomas Wieder<sup>1</sup> · Ellen Brenner<sup>1</sup> · Heidi Braumüller<sup>1</sup> · Oliver Bischof<sup>2,3</sup> · Martin Röcken<sup>1</sup>

Published online: 8 April 2017  
© Springer Science+Business Media New York 2017

**Abstract** The immune response is a first-line systemic defense to curb tumorigenesis and metastasis. Much effort has been invested to design antitumor interventions that would boost the immune system in its fight to defeat or contain cancerous growth. Tumor vaccination protocols, transfer of tumor-associated-antigen-specific T cells, T cell activity-regulating antibodies, and recombinant cytokines are counted among a toolbox filled with immunotherapeutic options. Although the mechanistic underpinnings of tumor immune control remain to be deciphered, these are studied with the goal of cancer cell destruction. In contrast, tumor dormancy is considered as a dangerous equilibrium between cell proliferation and cell death. There is, however, emerging evidence that tumor immune control can be achieved in the absence of overt cancer cell death. Here, we propose cytokine-induced senescence (CIS) by transfer of T helper-1 cells (T<sub>H</sub>1) or by recombinant cytokines as a novel therapeutic intervention for cancer treatment. Immunity-induced senescence triggers a stable cell cycle arrest of cancer cells. It engages the immune system to construct defensive, isolating barriers around tumors, and prevents tumor growth through the delivery or induction of T<sub>H</sub>1-cytokines in the tumor microenvironment. Keeping cancer cells in a non-proliferating state is a strategy, which directly copes with the lost homeostasis of aggressive tumors. As most studies

show that even after efficient cancer therapies minimal residual disease persists, we suggest that therapies should include immune-mediated senescence for cancer surveillance. CIS has the goal to control the residual tumor and to transform a deadly disease into a state of silent tumor persistence.

**Keywords** Receptor-mediated growth arrest · Tumor dormancy · Inflammation · Cytokine-induced senescence

## 1 Cellular senescence

### 1.1 The concept of cellular senescence

Cellular senescence has been linked to a number of physiological and patho-physiological conditions such as aging, age-related diseases, tissue homeostasis, and embryogenesis (for review see [1]). In the context of aging of multicellular organisms, cellular senescence has been described as one of the nine hallmarks of aging. Besides, senescence is considered to be part of the compensatory or antagonistic damage responses [2]. Some senescence-associated biomarkers, foremost the cell cycle inhibitor cyclin-dependent kinase inhibitor 2A (p16<sup>Ink4a</sup>) and telomere-damage induced foci (TIFs), accumulate in cells of various tissues of aged individuals, indicating that senescence and aging are closely linked [3, 4]. Importantly, elimination of senescent cells from aged tissues improves overall tissue fitness [5], whereas the tissue-degenerative effects of senescence are likely to be transmitted by the senescence-associated secretory phenotype (SASP), at least in part [6] (Fig. 1a). Developmental senescence (Fig. 1b) is a physiologically programmed senescence pathway that has recently been described to actively contribute to embryonic patterning [7, 8]. This process is also accompanied by a SASP that attracts macrophages which in turn seem to be necessary to remove senescent cells in a coordinate manner in order to foster the physical

Thomas Wieder and Ellen Brenner contributed equally.

✉ Thomas Wieder  
thomas.wieder@med.uni-tuebingen.de

<sup>1</sup> Department of Dermatology, Eberhard Karls University, Liebermeisterstr. 25, 72076 Tübingen, Germany

<sup>2</sup> Nuclear Organization and Oncogenesis Unit, Department of Cell Biology and Infection, Institut Pasteur, 28, Rue du Dr. Roux, 75724 Paris, France

<sup>3</sup> Inserm, U993, Paris, France

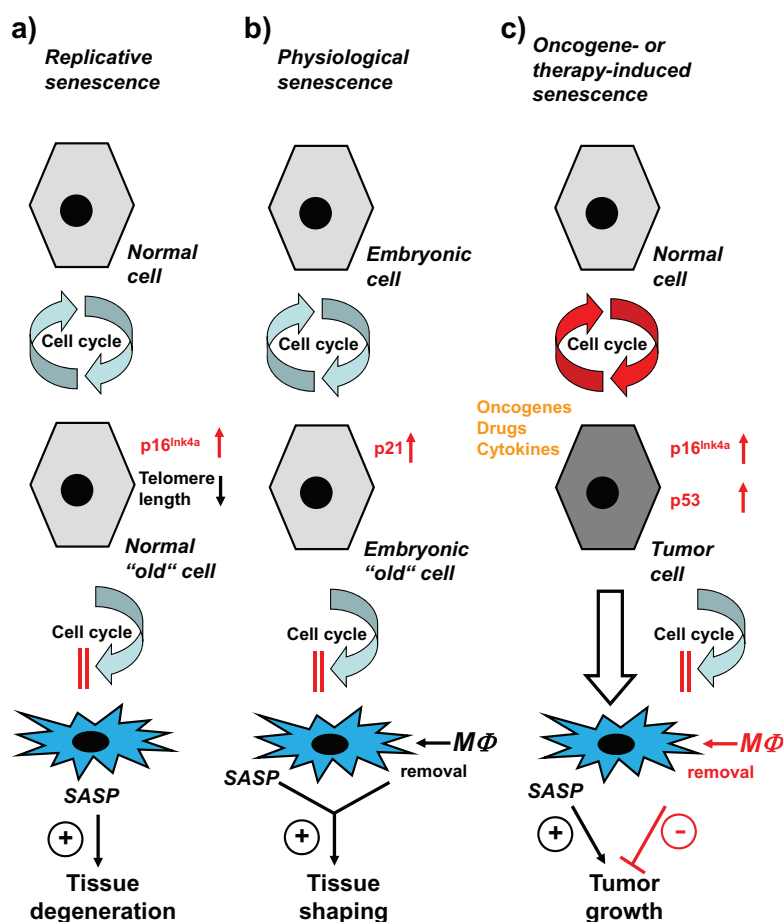


**Fig. 1** Cellular senescence in aging, embryogenesis, and tumorigenesis. **a** During aging of the organism, normal cells may enter the cell cycle. After several cell divisions, the chromosomal telomere length decreases and the expression of the cell cycle inhibitor  $p16^{\text{Ink4a}}$  increases. This leads to permanent arrest of the cell cycle and in the case of “old” cells to replicative senescence. Senescent cells produce secretory factors, and the SASP may contribute to enhanced tissue degeneration in older individuals. **b** During embryogenesis, some embryonic cells may run through the cell cycle leading to p53-independent p21 accumulation and permanent cell cycle arrest. On the one hand, these “old” embryonic cells produce secretory factors (SASP), and on the other hand, the senescent cells are cleared by macrophages. Both mechanisms then contribute to the tissue shaping during embryogenesis. **c** During

tumorigenesis, normal cells may enter an accelerated cell cycle (for example by activation of oncogenes). These rapidly cycling tumor cells upregulate p53 and the cell cycle inhibitor  $p16^{\text{Ink4a}}$  leading to permanent cell cycle arrest or oncogene-induced senescence. The tumor cells can also be driven into senescence by other cellular stressors, e.g., by drugs or cytokines. Interestingly, tumor cell senescence can both exert a pro- or antitumoral effect. Whereas the components of the SASP have been shown to enhance tumor growth, the macrophage-mediated clearance of senescent tumor cells inhibits tumor growth.  $M\Phi$  macrophages,  $p16^{\text{Ink4a}}$  cyclin-dependent kinase inhibitor 2A,  $p21$  cyclin-dependent kinase inhibitor 1,  $p53$  cellular tumor antigen p53, SASP senescence-associated secretory phenotype

development of the embryo (Fig. 1b). In contrast, oncogene- or therapy-induced premature senescence is a mere stress response mechanism (Fig. 1c). It is a cell intrinsic anticancer mechanism that is triggered by various genetic or epigenetic perturbations including hyperactive oncogenes [9, 10], cytotoxic drugs [11, 12], or by cytokines [13–15] leading to an essentially irreversible cell cycle arrest. Oncogene-induced senescence is eventually accompanied by macrophage-mediated removal of the affected cancer cells, and this clearance mechanism of senescent cancers substantially improves the anti-cancer defense machinery of the immune system [16]. On the other hand, it is still unclear whether the

SASP, which is an integral part of oncogene- as well as cytokine-induced senescence, and leads to the secretion of various chemokines and growth factors, may play a tumor-promoting role, and should therefore be considered as harmful [17]. Thus, it is currently believed that it is necessary to clear senescent cells from the organism.

## 1.2 Cytokine-induced senescence

Cytotoxic cancer therapy is currently the gold standard of clinical practice. A bevy of cytotoxic regimens has been

developed over six decades to destroy or remove cancerous tissue. The complete surgical excision of cancer tissue including all adjacent or distant metastases is the most effective curative treatment option. It may be accompanied or followed by other mainly cytotoxic therapies, i.e., radiation therapy [18], chemotherapy [19], or cytotoxic immunotherapy [20, 21]. These therapies rely on (i) the induction of programmed cell death [19, 22]; (ii) caspase-independent programmed necrotic cell death [23, 24] or necroptosis, that is dependent on the ripoptosome [25]; (iii) autophagic cell death [26]; (iv) target cell lysis [21]; and (v) respiratory burst mediated by neutrophils [27].

The common goal of all cytotoxic therapies is the ultimate destruction of the cancer cells [28]. In clear contrast, pro-senescence therapy is not aimed at destroying cancer cells but to contain their expansion and thus can be considered as a non-destructive alternative tumor control mechanism [14, 15, 29–31]. In principle, cancer cell senescence can be triggered by intrinsic or extrinsic pathways (Fig. 2). The intrinsic pathways are triggered by reactivation/stabilization of the tumor suppressor protein p53 [32], by inactivation of the oncogene Myc [33], or by tumor suppressor phosphatase and tensin homolog deleted on chromosome 10 (Pten) inhibition by VO-OHPic [34]. Pten inhibition-induced senescence (PICS) in prostate cancer is especially intriguing, as loss of Pten is usually associated with oncogenesis, e.g., in aggressive breast cancer [35] or in follicular thyroid carcinomas [36]. Thus, the fate of a given precancerous cell after Pten loss may strongly depend on its ancestry and/or its molecular background. Nevertheless, the three intrinsic senescence pathways mentioned above lead to cell cycle arrest (Fig. 2a). The activation of these pathways results either in tumor growth inhibition or in tumor regression. Therapy-induced cancer cell senescence can be induced by genotoxic stress, i.e., by drugs targeting genomic DNA (Fig. 2b). Thus, doxorubicin [37] or cyclophosphamide treatment [12] induces a senescence-like phenotype in tumor cells. However, chemotherapeutics rather induce a mixed response including both apoptosis and senescence. In most cases, the senescent phenotype is only observed when the apoptosis machinery has been inhibited [12]. Thus, targeted therapies, like the B-Raf inhibitor vemurafenib, trigger senescence primarily in apoptosis-resistant melanoma cells [38]. First hints that not only membrane-penetrating drugs with a low molecular weight can induce intrinsic senescence pathways came from the observation that cytokines, such as the T helper-1 ( $T_H1$ )-cytokines interferon- $\gamma$  (IFN- $\gamma$ ) and tumor necrosis factor (TNF) [14] or transforming growth factor- $\beta$  (TGF- $\beta$ ) [13], can drive cancer cells into permanent growth arrest (Fig. 2c). This is astonishing as senescence was mainly considered to be an intrinsic antitumor mechanism. Cytokine-induced senescence (CIS) is the first example of an extrinsic senescence pathway leading to a permanent stop of the cell cycle. For the

proinflammatory  $T_H1$  cytokines, the senescence signaling pathways have been partially deciphered: permanent growth arrest needs the simultaneous activation of TNF receptor 1, IFN- $\gamma$ -signaling, and downstream stabilization of the pro-senescence p16<sup>Ink4a</sup>/Rb pathway [14, 15]. CIS also occurs in vivo after adoptive transfer of tumor-associated antigen (TAA)-specific  $T_H1$  cells in transgenic rat-insulin promoter T antigen (RIP-Tag) mice (Fig. 2d) [14], or after vaccination of sarcoma-bearing mice with an IL-12 transcribing gene construct that induces IFN- $\gamma$ - and TNF-mediated immune responses [15]. This demonstrates for the first time that (i) exogenous signals can override endogenous proliferative signals in cancer cells and (ii) that the immune system is able to restrict cancer growth by senescence induction without eradication of the cancer cells.

## 2 The immune system strikes back

### 2.1 Immune destruction and immune surveillance of cancer

Apart from the destruction of tumor cells by chemotherapy, radiation therapy or cytotoxic immune therapy, novel treatment options appear that control cancers without complete eradication. Some of these treatment options take advantage of the immune system: (i) adoptive transfer of tumor-specific, non-cytotoxic T helper cells may lead to durable clinical remission in melanoma patients [39] or to tumor dormancy in TAA-driven islet-cell cancer [40] and (ii) enhancement of T cell-mediated antitumor immune response in patients with stage IV melanoma or non-small-cell lung cancer. Here, blocking antibodies directed against immune checkpoints, e.g., primary monoclonal antibodies (mAbs) against the programmed death 1 (PD-1) receptor or its ligand PD-L1. The therapeutic efficiency may be enhanced by combining these mAbs with a mAb against cytotoxic T-lymphocyte-associated antigen 4 (CTLA-4) [41–44]. The mechanisms underlying the observed immunotherapeutic effects are still to be defined in detail. These antibodies can destroy cancers at least in part [45]. However, under most conditions, tumors of patients are not completely eradicated and the responding patients continue to live with stable disease. Thus, at the beginning of immune checkpoint inhibitor therapies, the tumor load tends to decline, most probably due to infiltration of cytotoxic immune cells [42, 43, 46–49]. After this first cytotoxic phase, the remaining tumor or metastases tend to stay at a constant level but will not disappear [50, 51]. This indicates that immunotherapy may follow the *defensive wall* concept, which relies on non-toxic control of the tumor burden [52–54] and which is based on the induction of tumor dormancy. Tumor dormancy is considered as an equilibrium between cancer cell proliferation and killing of cancer cells [55, 56] with apoptosis or

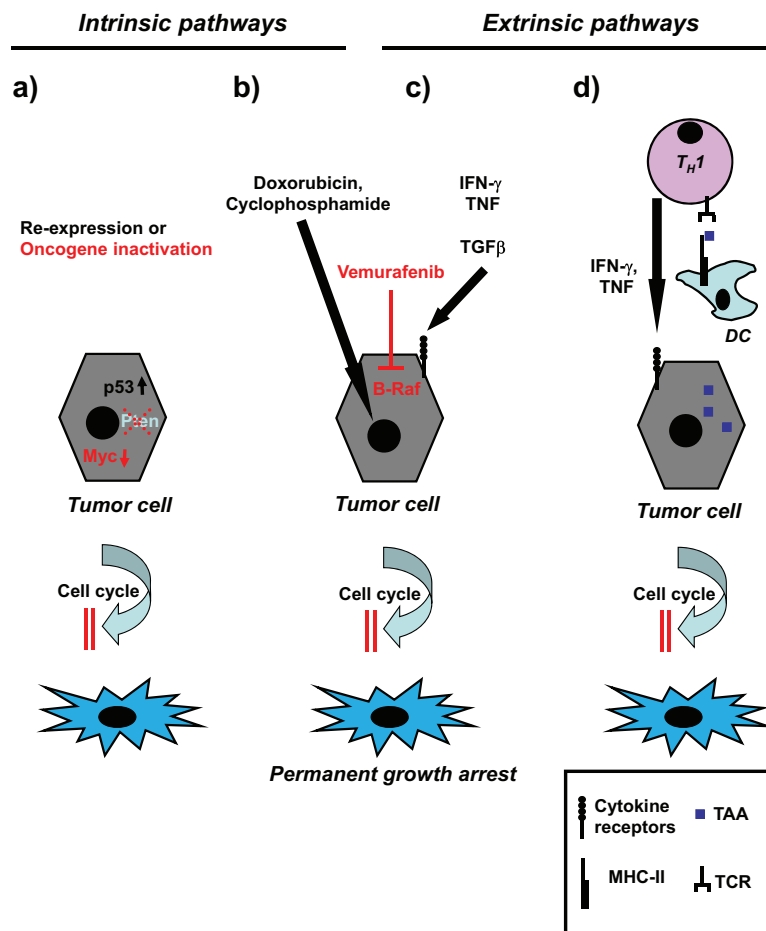


**Fig. 2** Pathways of therapy-induced tumor cell senescence. Tumor cell senescence during therapy is induced either by intrinsic (**a, b**) or extrinsic pathways (**c, d**). **a** Molecular induction of cellular senescence can be realized by reexpression of pro-senescence factors (e.g., p53), complete loss of Pten, or oncogene inactivation (e.g., Myc). These molecular manipulations eventually lead to permanent growth arrest of tumor cells. **b** Different drugs, such as doxorubicin or cyclophosphamide, target the DNA of the cycling tumor cells leading to DNA stress which in turn induces a permanent cell cycle arrest. More specific drugs, e.g., the B-Raf kinase inhibitor vemurafenib, target intracellular signaling pathways and also lead to permanent cell cycle arrest. **c** Different cytokines, such as IFN- $\gamma$ , TNF or TGF- $\beta$ , bind to their specific receptors on the surface of the tumor cells. Activation of the cytokine

receptors then triggers intracellular signaling pathways leading to permanent cell cycle arrest. **d** Immune cells are also able to induce extrinsic senescence in tumor cells. Here, tumor-specific T<sub>H</sub>1 cells are activated by MHC-II-positive DCs. After activation, the T<sub>H</sub>1 cells secrete the soluble factors IFN- $\gamma$  and TNF in the vicinity of the tumors. The secreted cytokines then bind to their specific receptors on the surface of the tumor cells thereby activating intracellular senescence pathways. *BRAF* proto-oncogene B-Raf or v-Raf murine sarcoma viral oncogene homolog B1, *DC* dendritic cells, *IFN- $\gamma$*  interferon- $\gamma$ , *MHC-II* major histocompatibility complex class II, *p53* cellular tumor antigen p53, *Pten* phosphatase and tensin homolog deleted on chromosome 10, *TAA* tumor-associated antigen, *TCR* T cell receptor, *TGF- $\beta$*  transforming growth factor- $\beta$ , *T<sub>H</sub>1* T helper-1 cells, *TNF* tumor necrosis factor

immune cell-mediated lysis of cancer cells being the main killing mechanisms. This interpretation of the state of *silent tumors* has now been complemented by four non-toxic mechanisms, namely (i) active cell cycle control through regulation of cyclin-dependent kinases [57]; (ii) induction of cellular senescence [9, 14, 15, 58]; (iii) control of differentiation by regulating inhibitor of DNA binding (ID) proteins [59]; and (iv) inhibition of angiogenesis [60].

Evasion from immune-mediated control of tumors has been added to the six original hallmarks of cancer [61]. As shown in Fig. 3, control of tumors by the immune system can

be divided into a cytotoxic branch leading to tumor eradication and a non-cytotoxic branch leading either to stable disease or tumor regression. Immune destruction of tumors relies on cellular immunity: (i) cytotoxic T cells (CTLs) (Fig. 3a) or natural killer cells (NK) (Fig. 3b) specifically attack tumors by releasing pore-forming perforin together with proteases such as granzyme B or soluble toxic factors such as TNF [55, 56, 62–64]; (ii) specific CTLs may directly target the cancer cells by inducing death receptor-dependent apoptosis *via* the cluster of differentiation 95 ligand/cluster of differentiation 95 (CD95L/CD95) death-inducing signaling complex (for

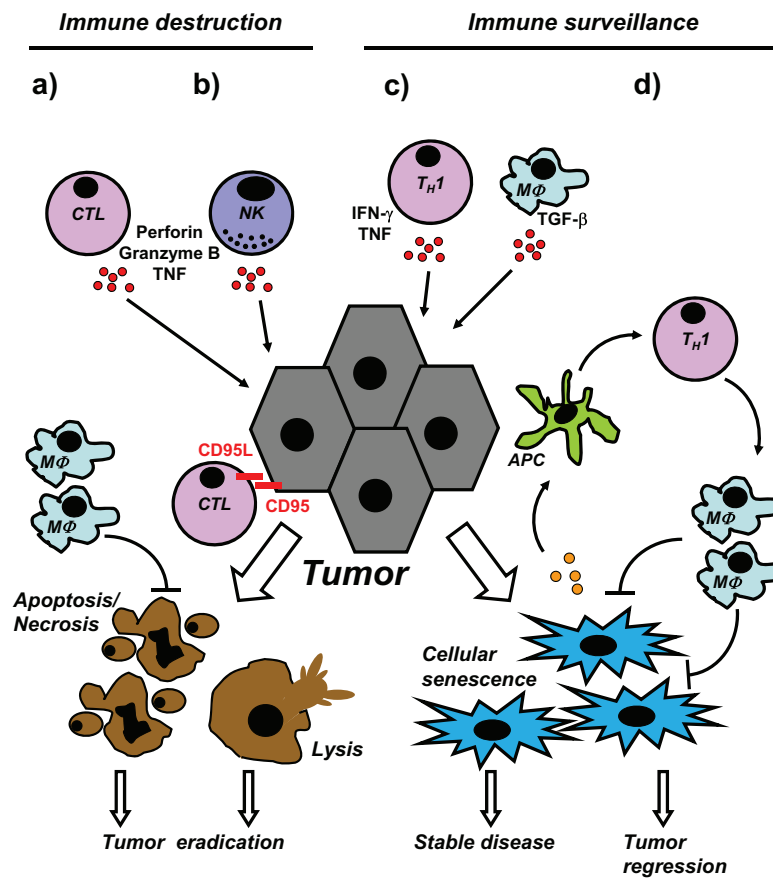


**Fig. 3** Toxic and non-toxic pathways of immune system-mediated tumor suppression. The control of tumors by the immune system is achieved by immune destruction (**a, b**) or immune surveillance (**c, d**). **a** CTL either indirectly or directly attack tumor cells by secretion of toxic factors, such as perforin, granzyme B, or TNF, or by planting a kiss of death *via* CD95L-CD95 interaction and induction of the apoptosis cascade. This leads to tumor cell death by apoptosis, clearance of apoptotic bodies by macrophages, necrosis, or to tumor cell lysis. Finally, the immune system completely eradicates the tumor. **b** NK cells, like CTL, indirectly attack tumor cells by secretion of toxic substances, such as perforin, granzyme B, or TNF. This leads to tumor cell death and complete eradication of the tumor. **c**  $T_H1$  cells or macrophages silence tumor cells by secretion of  $IFN-\gamma$  and TNF or  $TGF-\beta$ , respectively. After binding to their specific

receptors on the surface of the tumor cells, the cytokines activate intracellular senescence pathways leading to permanent cell cycle arrest and stable disease. **d** Senescent tumor cells may also be cleared. Molecular factors released by senescent tumor cells lead to activation of APC. The APCs then stimulate a  $T_H1$  cell response followed by activation of macrophages which in turn mediate the clearance of senescent cancer cells. If senescence induction and subsequent clearance of senescent tumor cells is effective, immune surveillance may also induce tumor regression. APC antigen-presenting cells, CD95 cluster of differentiation 95, CD95L cluster of differentiation 95 ligand, CTL cytotoxic T cells,  $IFN-\gamma$  interferon- $\gamma$ ,  $M\Phi$  macrophages cells, NK natural killer cells,  $TGF-\beta$  transforming growth factor- $\beta$ ,  $T_H1$  T helper-1, TNF tumor necrosis factor

review see [62]). If tumor immune destruction is successful, the apoptotic cells will be cleared by macrophages and the tumors will be eradicated. In addition, it has been shown that the immune system can also control tumors by senescence surveillance, a mechanism mainly based on cytokine-induced cellular senescence (Fig. 3c) and an immune-cell-mediated clearance pathway (Fig. 3d). Senescence has been shown to be induced *in vivo* in murine islet cell tumors by a combination of  $IFN-\gamma$  and TNF released from tumor-specific  $T_H1$  cells in the vicinity of the tumors [14]. Similarly, human sarcoma cell lines can be driven into senescence by IL-12-mediated induction of a  $T_H1$ -phenotype in human T cells [15]. In this line, it has been demonstrated that the loss of

$IFN-\gamma$  pathway genes in cancer cells serves as a mechanism of resistance during immune checkpoint inhibitor therapies [65] and that the disruption of cyclin-dependent kinase 5 (Cdk5) strengthens antitumor immunity [66]. Likewise,  $TGF-\beta$  originating from macrophages was shown to induce cellular senescence in lymphoma cells [13]. Thus, senescence induction alone leads to permanent growth arrest and stable disease with a remarkable prolongation of the survival of death-prone RIP-Tag mice [40]. In the long run, however, it may be necessary that senescent cancer cells become cleared: the SASP of N-ras-expressing senescent hepatocytes leads to activation of professional antigen-presenting cells (APCs) which in turn drive a  $T_H1$  cell response followed by activation

of macrophages. One concept then suggests the subsequent clearance of senescent cancer cells by activated macrophages [16]. Yet, it remains unclear whether elimination of senescent cells always supports cancer cure or whether it may on the contrary promote cancer progression [67]. Senescence-inducing treatment of cancer patients is apparently based on re-enhancement or restoration of dormant intrinsic pathways. As survival with silenced tumors or with disseminated, silenced tumor cells is possible [41, 52], cancer patients will benefit from successful restoration of intrinsic senescence surveillance. In addition, it is likely that the resulting side effects of non-cytotoxic, pro-senescence therapies should be less severe as compared with cytotoxic regimens [68]. However, similar to cytotoxic tumor treatment, the benefits of pro-senescence therapy described above are only effective if the vast majority of the tumor cells is driven into senescence. Furthermore, the resting state of the silenced cancer cells has to be maintained, either by a permanent growth arrest or by exogenous (immune)-signals that keep the cancer cells silent. The main problems of senescence surveillance of tumors which have to be solved in the near future are therefore: (i) fast growing tumor cells, e.g., acute leukemias, may escape senescence surveillance [14, 15]; (ii) resting tumor cells may eventually awake and start regrowing if CIS turns out to be reversible, at least in some very aggressive cancers; (iii) the fate of non-proliferating tumor stem cells is unclear; (iv) the regeneration of normal tissues may be impaired; and (v) chronic inflammation [61] and some molecular components of the SASP [1, 17, 69] may even promote tumorigenesis in neighboring premalignant cells.

## 2.2 Evolutionary aspects of immune destruction and immune surveillance of cancer

Eradication of tumors is mainly based on cytotoxic principles, and the biological targets of different chemotherapeutics are genomic DNA (genetic code) as in the case of epirubicin [22], the plasma membrane (outward demarcation of the cell) as in the case of miltefosin [70], or the cytoskeleton as in the case of taxol [22]. This holds also true for the destruction of tumors by the immune system. It is generally accepted that apoptosis induction by death receptors (e. g., CD95/CD95L, TNF/TNFR1, etc.) finally leads to caspase-dependent DNA fragmentation [19, 22, 62] whereas the perforin/granzyme B system leads to target cell lysis, cell membrane rupture, and activation of specialized serine proteases [63, 64]. However, if DNA fragmentation is incomplete, mutated tumor cell clones might emerge and a Darwinian selection process is triggered [71]. This is to say that the vast majority of mutated tumor cells carrying large genomic aberrations (such as loss or gain of whole chromosome arms) will die, but those mutated cells that survive will restart proliferation and lose important endogenous or exogenous control mechanisms. Uncontrolled

proliferation then leads to accumulation of additional DNA damage and chromosomal chaos. Together, the genetic instability of cancers and the highly selective local microenvironmental forces, e.g., hypoxia, acidosis, and reactive oxygen species, are able to further promote somatic evolution. In addition, cytotoxic regimens impose strong selection pressures on the surviving cancer cells; the treatment should therefore rather enhance the evolutionary rate and promote selection of mutated cancer clones [71].

In clear contrast to conventional chemotherapy, immune surveillance of tumors is not exclusively dependent on tumor cell destruction, and the biological target structures are mainly signal transduction pathways and the respective signaling molecules, e.g., receptors, adaptor proteins, kinases, or kinase inhibitors. For example, CIS by T<sub>H</sub>1 cell cytokines (IFN- $\gamma$ , TNF *etc.*) leads to stabilization of the p16<sup>Ink4a</sup>/Rb pathway thereby permanently arresting the tumor cells in the G0/G1 phase of the cell cycle [14]. Furthermore, tumor-specific T<sub>H</sub>1 cells that can now be generated for the use in humans [72] induce the production of antiangiogenic chemokines, e.g., chemokine (C-X-C motif) ligand 9 (CXCL9) and chemokine (C-X-C motif) ligand 10 (CXCL10) [14, 40] thereby leading to isolation of the tumor cells [40, 54]. Inhibitory antibodies, on the other hand, target *cellular exhaustion pathways* by interfering with ligand-receptor interactions thereby maintaining the antitumoral activity of specific immune cells [41]. Last but not least, small molecules targeting signal transduction pathways, such as proto-oncogene B-Raf (BRAF) inhibitors or oncogenic BCR-ABL gene fusion product (BCR-ABL) inhibitors, specifically inhibit kinases thereby driving the cancer cells into cell cycle arrest [38]. The common feature of those strategies is that they directly or indirectly impair cancer cell proliferation. The selection pressure on the arrested cancer cells is therefore strongly reduced and the treatment should not promote somatic evolution.

## 2.3 Metabolic aspects of immune destruction and immune surveillance of cancer cells

Cancer cells are distinct from normal cells as they switch from aerobic to anaerobic metabolism, even in the presence of sufficient oxygen support. Thus, they use anaerobic glycolysis for adenosin triphosphate (ATP) production rather than oxidative phosphorylation, the so called *Warburg effect* [1, 61]. As a result, the oxygen consumption by the mitochondria is reduced. The cells produce lactic acid which is released into the blood and transported to the liver where it is used for gluconeogenesis.

Chemotherapy- or radiation therapy-induced apoptosis should enhance the switch of tumors towards anaerobic metabolism. In this line, it has been shown that drug-induced apoptosis signaling leads to dissipation of the mitochondrial membrane potential, release of cytochrome c, and

downstream activation of caspase-3 [22, 73]. Thus, oxidative phosphorylation *via* the mitochondrial respiratory chain is further inhibited during drug-induced apoptosis.

On the other hand, cancer cells undergoing oncogene-induced senescence (OIS) switch back to mitochondrial oxidative phosphorylation. By regulating the mitochondrial gate keeper pyruvate dehydrogenase, senescent cells make enhanced use of pyruvate in the tricarboxylic acid cycle [74]. This causes increased respiration and oxidative stress thereby counteracting metabolic reprogramming in the cancer cells. Interestingly, premature senescence is often accompanied by activation of the target of rapamycin (TOR) pathway which is considered to be a central regulator of mammalian metabolism and physiology. Activation of TOR in the context of cell cycle arrest then leads to *real* senescence with irreversible loss of the regenerative potential [75]. Metabolic reprogramming as seen by the Warburg effect provides tumor cells with ATP and with the substrates required for biomass generation. Recently, it was demonstrated that the mitochondrial nicotinamide adenine dinucleotide (NAD)-dependent deacetylase SIRT3 is a crucial regulator of the Warburg effect by destabilizing hypoxia-inducible factor-1 $\alpha$  (HIF-1 $\alpha$ ). HIF-1 $\alpha$  downregulation then leads to repression of glycolysis and inhibition of proliferation of breast cancer cells thereby pointing to a new tumor suppressor mechanism [76]. Activation of the immune system is also connected with cellular metabolism. It has been shown that succinate, an important metabolite of the tricarboxylic acid cycle, serves as an inflammatory signal that induces interleukin-1 $\beta$  (IL-1 $\beta$ ) through HIF-1 $\alpha$  [77]. Thus, there are several experimental hints that tight connections between the regulation pathways of the cell cycle and the main metabolic pathways of eukaryotic cells, i.e., glycolysis, tricarboxylic acid cycle, and oxidative phosphorylation, really exist. Future work will decipher the signaling networks underlying inflammation, oncogenesis, cancer cell senescence, and metabolic reprogramming.

### 3 Outlook: combining cytotoxic and pro-senescence therapy

Due to the still unsatisfactory clinical success of cancer treatments, additional efforts including new concepts are urgently needed. As therapy resistance is the most important drawback of the main cytotoxic cancer regimens, it is reasonable to target different cellular structures or hallmarks of cancer. Nevertheless, a combination approach may even be successful if similar cellular signaling pathways are inhibited or induced at the same time. For example, the combination of T cell-activating anti-PD-1 and anti-CTLA-4 antibodies showed improved clinical activity that clearly exceeded monotherapy [41]. The finding that it is possible to induce extrinsic premature senescence by treatment of cancer cells with a cytokine

combination of IFN- $\gamma$  and TNF [14] opens the way to non-toxic treatment options. Both cytokines are endogenous signaling molecules which are already available as drugs. Their toxicity profiles are known and less toxic alternatives, such as IFN- $\alpha$ , are at hand. More importantly, stopping the fulminant growth of malignant cancers by CIS will thus perfectly complement the cytotoxic effect of most anti-cancer drugs. The combination of cytotoxic drugs in the acute phase of the disease with CIS as therapy during the consolidation phase is one of the most promising approaches which may be introduced into clinical practice in the near future. In conclusion, besides the development and introduction of new drugs for cancer cell destruction or senescence induction, clinical research should also focus on optimized strategies that combine already approved medication with CIS.

**Acknowledgments** The work of the authors is supported by the Sander Stiftung (2012.056.1, 2012.056.2 and 2012.056.3), the Deutsche Krebshilfe (No. 109037 and 110664), the Deutsche Forschungsgemeinschaft (DFG WI 1279/4-1 and Sonderforschungsbereich SFB 685) and Fondation ARC pour la recherche sur le Cancer, Agence Nationale Recherche ANR, Fondation Pasteur-Weizmann, and Association LNCC La Ligue National Contre le Cancer. O. Bischof is CNRS-DR2.

#### Compliance with ethical standards

**Conflict of interest** The authors declare that they have no conflict of interest.

#### References

1. Perez-Mancera, P. A., Young, A. R., & Narita, M. (2014). Inside and out: the activities of senescence in cancer. *Nature Reviews: Cancer*, 14(8), 547–558.
2. Lopez-Otin, C., Blasco, M. A., Partridge, L., Serrano, M., & Kroemer, G. (2013). The hallmarks of aging. *Cell*, 153(6), 1194–1217.
3. Fumagalli, M., Rossiello, F., Clerici, M., Barozzi, S., Cittaro, D., Kaplunov, J. M., et al. (2012). Telomeric DNA damage is irreparable and causes persistent DNA-damage-response activation. *Nature Cell Biology*, 14(4), 355–365.
4. Burd, C. E., Sorrentino, J. A., Clark, K. S., Darr, D. B., Krishnamurthy, J., Deal, A. M., et al. (2013). Monitoring tumorigenesis and senescence *in vivo* with a p16(INK4a)-luciferase model. *Cell*, 152(1–2), 340–351.
5. Baker, D. J., Wijshake, T., Tchkonja, T., LeBrasseur, N. K., Childs, B. G., van de Sluis, B., et al. (2011). Clearance of p16Ink4a-positive senescent cells delays ageing-associated disorders. *Nature*, 479(7372), 232–236.
6. Campisi, J., Andersen, J. K., Kapahi, P., & Melov, S. (2011). Cellular senescence: a link between cancer and age-related degenerative disease? *Seminars in Cancer Biology*, 21(6), 354–359.
7. Munoz-Espin, D., Canamero, M., Maraver, A., Gomez-Lopez, G., Contreras, J., Murillo-Cuesta, S., et al. (2013). Programmed cell senescence during mammalian embryonic development. *Cell*, 155(5), 1104–1118.
8. Storer, M., Mas, A., Robert-Moreno, A., Pecoraro, M., Ortells, M. C., Di Giacomo, V., et al. (2013). Senescence is a developmental



- mechanism that contributes to embryonic growth and patterning. *Cell*, 155(5), 1119–1130.
9. Michaloglou, C., Vredeveld, L. C., Soengas, M. S., Denoyelle, C., Kuilman, T., van der Horst, C. M., et al. (2005). BRAFE600-associated senescence-like cell cycle arrest of human naevi. *Nature*, 436(7051), 720–724.
  10. Lee, S., Schmitt, C. A., & Reimann, M. (2011). The Myc/macrophage tango: oncogene-induced senescence, Myc style. *Seminars in Cancer Biology*, 21(6), 377–384.
  11. Chang, B. D., Broude, E. V., Dokmanovic, M., Zhu, H., Ruth, A., Xuan, Y., et al. (1999). A senescence-like phenotype distinguishes tumor cells that undergo terminal proliferation arrest after exposure to anticancer agents. *Cancer Research*, 59(15), 3761–3767.
  12. Schmitt, C. A., Fridman, J. S., Yang, M., Lee, S., Baranov, E., Hoffman, R. M., et al. (2002). A senescence program controlled by p53 and p16INK4a contributes to the outcome of cancer therapy. *Cell*, 109(3), 335–346.
  13. Reimann, M., Lee, S., Loddenkemper, C., Dorr, J. R., Tabor, V., Aichele, P., et al. (2010). Tumor stroma-derived TGF-beta limits myc-driven lymphomagenesis via Suv39h1-dependent senescence. *Cancer Cell*, 17(3), 262–272.
  14. Braumüller, H., Wieder, T., Brenner, E., Assmann, S., Hahn, M., Alkhaled, M., et al. (2013). T-helper-1-cell cytokines drive cancer into senescence. *Nature*, 494(7437), 361–365.
  15. Schilbach, K., Alkhaled, M., Welker, C., Eckert, F., Blank, G., Ziegler, H., et al. (2015). Cancer-targeted IL-12 controls human rhabdomyosarcoma by senescence induction and myogenic differentiation. *OncoImmunology*, 4(7), e1014760.
  16. Kang, T.-W., Yevsa, T., Woller, N., Hoenicke, L., Wuestefeld, T., Dauch, D., et al. (2011). Senescence surveillance of pre-malignant hepatocytes limits liver cancer development. *Nature*, 479(7374), 547–551. doi:10.1038/nature10599.
  17. Campisi, J. (2013). Aging, cellular senescence, and cancer. *Annual Review of Physiology*, 75, 685–705.
  18. Durante, M., & Loeffler, J. S. (2010). Charged particles in radiation oncology. *Nature Reviews: Clinical Oncology*, 7(1), 37–43.
  19. Friesen, C., Herr, I., Krammer, P. H., & Debatin, K. M. (1996). Involvement of the CD95 (APO-1/FAS) receptor/ligand system in drug-induced apoptosis in leukemia cells. *Nature Medicine*, 2(5), 574–577.
  20. Mocikat, R., Braumüller, H., Gumy, A., Egeter, O., Ziegler, H., Reusch, U., et al. (2003). Natural killer cells activated by MHC class I (low) targets prime dendritic cells to induce protective CD8 T cell responses. *Immunity*, 19(4), 561–569.
  21. Baum, V., Buhler, P., Gierschner, D., Herchenbach, D., Fiala, G. J., Schamel, W. W., et al. (2013). Antitumor activities of PSMAXCD3 diabodies by redirected T-cell lysis of prostate cancer cells. *Immunotherapy*, 5(1), 27–38.
  22. Wieder, T., Essmann, F., Prokop, A., Schmelz, K., Schulze-Osthoff, K., Beyaert, R., et al. (2001). Activation of caspase-8 in drug-induced apoptosis of B-lymphoid cells is independent of CD95/Fas receptor-ligand interaction and occurs downstream of caspase-3. *Blood*, 97(5), 1378–1387.
  23. Scholz, C., Wieder, T., Starck, L., Essmann, F., Schulze-Osthoff, K., Dörken, B., et al. (2005). Arsenic trioxide triggers a regulated form of caspase-independent necrotic cell death via the mitochondrial death pathway. *Oncogene*, 24(11), 1904–1913.
  24. Boujrad, H., Gubkina, O., Robert, N., Krantic, S., & Susin, S. A. (2007). AIF-mediated programmed necrosis: a highly regulated way to die. *Cell Cycle*, 6(21), 2612–2619.
  25. Feoktistova, M., Geserick, P., Panayotova-Dimitrova, D., & Leverkus, M. (2012). Pick your poison: the Ripoptosome, a cell death platform regulating apoptosis and necroptosis. *Cell Cycle*, 11(3), 460–467.
  26. Wang, Y., Zhan, Y., Xu, R., Shao, R., Jiang, J., & Wang, Z. (2015). Src mediates extracellular signal-regulated kinase 1/2 activation and autophagic cell death induced by cardiac glycosides in human non-small cell lung cancer cell lines. *Molecular Carcinogenesis*, 54(Suppl 1), E26–E34.
  27. van Spruiel, A. B., Leusen, J. H., van Egmond, M., Dijkman, H. B., Assmann, K. J., Mayadas, T. N., et al. (2001). Mac-1 (CD11b/CD18) is essential for Fc receptor-mediated neutrophil cytotoxicity and immunologic synapse formation. *Blood*, 97(8), 2478–2486.
  28. Sporn, M. B. (1996). The war on cancer. *Lancet*, 347(9012), 1377–1381.
  29. Ewald, J. A., Desotelle, J. A., Wilding, G., & Jarrard, D. F. (2010). Therapy-induced senescence in cancer. *Journal of the National Cancer Institute*, 102(20), 1536–1546.
  30. Nardella, C., Clohessy, J. G., Alimonti, A., & Pandolfi, P. P. (2011). Pro-senescence therapy for cancer treatment. *Nature Reviews: Cancer*, 11(7), 503–511.
  31. Acosta, J. C., & Gil, J. (2012). Senescence: a new weapon for cancer therapy. *Trends in Cell Biology*, 22(4), 211–219.
  32. Xue, W., Zender, L., Miething, C., Dickins, R. A., Hernando, E., Krizhanovskiy, V., et al. (2007). Senescence and tumour clearance is triggered by p53 restoration in murine liver carcinomas. *Nature*, 445(7128), 656–660. doi:10.1038/nature05529.
  33. Rakhra, K., Bachireddy, P., Zabuawala, T., Zeiser, R., Xu, L., Kopelman, A., et al. (2010). CD4(+) T cells contribute to the remodeling of the microenvironment required for sustained tumor regression upon oncogene inactivation. *Cancer Cell*, 18(5), 485–498.
  34. Alimonti, A., Nardella, C., Chen, Z., Clohessy, J. G., Carracedo, A., Trotman, L. C., et al. (2010). A novel type of cellular senescence that can be enhanced in mouse models and human tumor xenografts to suppress prostate tumorigenesis. *Journal of Clinical Investigation*, 120(3), 681–693.
  35. Boelens, M. C., Nethe, M., Klarenbeek, S., de Ruiter, J. R., Schut, E., Bonzanni, N., et al. (2016). PTEN loss in E-cadherin-deficient mouse mammary epithelial cells rescues apoptosis and results in development of classical invasive lobular carcinoma. *Cell Reports*, 16(8), 2087–2101.
  36. Jolly, L. A., Massoll, N., & Franco, A. T. (2016). Immune suppression mediated by myeloid and lymphoid derived immune cells in the tumor microenvironment facilitates progression of thyroid cancers driven by HrasG12V and Pten loss. *Journal of Clinical & Cellular Immunology*, 7(5), 451.
  37. Benhamed, M., Herbig, U., Ye, T., Dejean, A., & Bischof, O. (2012). Senescence is an endogenous trigger for microRNA-directed transcriptional gene silencing in human cells. *Nature Cell Biology*, 14(3), 266–275.
  38. Haferkamp, S., Borst, A., Adam, C., Becker, T. M., Motschenbacher, S., Windhovel, S., et al. (2013). Vemurafenib induces senescence features in melanoma cells. *Journal of Investigative Dermatology*, 133(6), 1601–1609.
  39. Hunder, N. N., Wallen, H., Cao, J., Hendricks, D. W., Reilly, J. Z., Rodmyre, R., et al. (2008). Treatment of metastatic melanoma with autologous CD4+ T cells against NY-ESO-1. *New England Journal of Medicine*, 358(25), 2698–2703.
  40. Müller-Hermelink, N., Braumüller, H., Pichler, B., Wieder, T., Mailhammer, R., Schaak, K., et al. (2008). TNFR1 signaling and IFN-gamma signaling determine whether T cells induce tumor dormancy or promote multistage carcinogenesis. *Cancer Cell*, 13(6), 507–518.
  41. Wolchok, J. D., Kluger, H., Callahan, M. K., Postow, M. A., Rizvi, N. A., Lesokhin, A. M., et al. (2013). Nivolumab plus ipilimumab in advanced melanoma. *New England Journal of Medicine*, 369(2), 122–133.
  42. Robert, C., Long, G. V., Brady, B., Dutriaux, C., Maio, M., Mortier, L., et al. (2015). Nivolumab in previously untreated melanoma without BRAF mutation. *New England Journal of Medicine*, 372(4), 320–330.

43. Borghaei, H., Paz-Ares, L., Horn, L., Spigel, D. R., Steins, M., Ready, N. E., et al. (2015). Nivolumab versus docetaxel in advanced nonsquamous non-small-cell lung cancer. *New England Journal of Medicine*, 373(17), 1627–1639.
44. Herbst, R. S., Soria, J. C., Kowanetz, M., Fine, G. D., Hamid, O., Gordon, M. S., et al. (2014). Predictive correlates of response to the anti-PD-L1 antibody MPDL3280A in cancer patients. *Nature*, 515(7528), 563–567.
45. Tumeh, P. C., Harview, C. L., Yearley, J. H., Shintaku, I. P., Taylor, E. J., Robert, L., et al. (2014). PD-1 blockade induces responses by inhibiting adaptive immune resistance. *Nature*, 515(7528), 568–571.
46. Larkin, J., Chiarion-Sileni, V., Gonzalez, R., Grob, J. J., Cowey, C. L., & Lao, C. D., et al. (2015). Combined nivolumab and ipilimumab or monotherapy in untreated melanoma. *New England Journal of Medicine*.
47. Le, D. T., Uram, J. N., Wang, H., Bartlett, B. R., Kemberling, H., Eyring, A. D., et al. (2015). PD-1 blockade in tumors with mismatch-repair deficiency. *New England Journal of Medicine*, 372(26), 2509–2520.
48. Rosenberg, J. E., Hoffman-Censits, J., Powles, T., van der Heijden, M. S., Balar, A. V., Necchi, A., et al. (2016). Atezolizumab in patients with locally advanced and metastatic urothelial carcinoma who have progressed following treatment with platinum-based chemotherapy: a single-arm, multicentre, phase 2 trial. *Lancet*, 387(10031), 1909–1920.
49. Mlecnik, B., Bindea, G., Angell, H. K., Maby, P., Angelova, M., Tougeron, D., et al. (2016). Integrative analyses of colorectal cancer show immunoscore is a stronger predictor of patient survival than microsatellite instability. *Immunity*, 44(3), 698–711.
50. Topalian, S. L., Hodi, F. S., Brahmer, J. R., Gettinger, S. N., Smith, D. C., McDermott, D. F., et al. (2012). Safety, activity, and immune correlates of anti-PD-1 antibody in cancer. *New England Journal of Medicine*, 366(26), 2443–2454.
51. Brahmer, J. R., Tykodi, S. S., Chow, L. Q., Hwu, W. J., Topalian, S. L., Hwu, P., et al. (2012). Safety and activity of anti-PD-L1 antibody in patients with advanced cancer. *New England Journal of Medicine*, 366(26), 2455–2465.
52. Gatenby, R. A. (2009). A change of strategy in the war on cancer. *Nature*, 459(7246), 508–509.
53. Wieder, T., Braumüller, H., Kneilling, M., Pichler, B., & Röcken, M. (2008). T cell-mediated help against tumors. *Cell Cycle*, 7(19), 2974–2977.
54. Wieder, T., Braumüller, H., Brenner, E., Zender, L., & Röcken, M. (2013). Changing T-cell enigma: cancer killing or cancer control? *Cell Cycle*, 12(19), 3146–3153.
55. Finn, O. J. (2008). Cancer immunology. *New England Journal of Medicine*, 358(25), 2704–2715.
56. Schreiber, R. D., Old, L. J., & Smyth, M. J. (2011). Cancer immunoediting: integrating immunity's roles in cancer suppression and promotion. *Science*, 331(6024), 1565–1570.
57. Bruyere, C., & Meijer, L. (2013). Targeting cyclin-dependent kinases in anti-neoplastic therapy. *Current Opinion in Cell Biology*, 25(6), 772–779.
58. Collado, M., Gil, J., Efeyan, A., Guerra, C., Schuhmacher, A. J., Barradas, M., et al. (2005). Tumour biology: senescence in premalignant tumours. *Nature*, 436(7051), 642.
59. Lasorella, A., Benezra, R., & Iavarone, A. (2014). The ID proteins: master regulators of cancer stem cells and tumour aggressiveness. *Nature Reviews: Cancer*, 14(2), 77–91.
60. Folkman, J., & Ingber, D. (1992). Inhibition of angiogenesis. *Seminars in Cancer Biology*, 3(2), 89–96.
61. Hanahan, D., & Weinberg, R. A. (2011). Hallmarks of cancer: the next generation. *Cell*, 144(5), 646–674.
62. Daniel, P. T., Wieder, T., Sturm, I., & Schulze-Osthoff, K. (2001). The kiss of death: promises and failures of death receptors and ligands in cancer therapy. *Leukemia*, 15(7), 1022–1032.
63. Trapani, J. A., & Smyth, M. J. (2002). Functional significance of the perforin/granzyme cell death pathway. *Nature Reviews: Immunology*, 2(10), 735–747.
64. Thiery, J., & Lieberman, J. (2014). Perforin: a key pore-forming protein for immune control of viruses and cancer. *Sub-Cellular Biochemistry*, 80, 197–220.
65. Gao, J., Shi, L. Z., Zhao, H., Chen, J., Xiong, L., He, Q., et al. (2016). Loss of IFN-gamma pathway genes in tumor cells as a mechanism of resistance to anti-CTLA-4 therapy. *Cell*, 167(2), 397–404.e399.
66. Dorand, R. D., Nthale, J., Myers, J. T., Barkauskas, D. S., Avril, S., Chirieleison, S. M., et al. (2016). Cdk5 disruption attenuates tumor PD-L1 expression and promotes antitumor immunity. *Science*, 353(6297), 399–403.
67. Pencik, J., Schleder, M., Gruber, W., Unger, C., Walker, S. M., Chalaris, A., et al. (2015). STAT3 regulated ARF expression suppresses prostate cancer metastasis. *Nature Communications*, 6, 7736.
68. Hortobagyi, G. N., Stemmer, S. M., Burris, H. A., Yap, Y. S., Sonke, G. S., Paluch-Shimon, S., et al. (2016). Ribociclib as first-line therapy for HR-positive, advanced breast cancer. *New England Journal of Medicine*, 375(18), 1738–1748.
69. Parrinello, S., Coppe, J. P., Krtolica, A., & Campisi, J. (2005). Stromal-epithelial interactions in aging and cancer: senescent fibroblasts alter epithelial cell differentiation. *Journal of Cell Science*, 118(Pt 3), 485–496.
70. Wieder, T., Orfanos, C. E., & Geilen, C. C. (1998). Induction of ceramide-mediated apoptosis by the anticancer phospholipid analog, hexadecylphosphocholine. *Journal of Biological Chemistry*, 273(18), 11025–11031.
71. Gillies, R. J., Verduzco, D., & Gatenby, R. A. (2012). Evolutionary dynamics of carcinogenesis and why targeted therapy does not work. *Nature Reviews: Cancer*, 12(7), 487–493.
72. Kayser, S., Bobeta, C., Feucht, J., Witte, K. E., Scheu, A., Bulow, H. J., et al. (2015). Rapid generation of NY-ESO-1-specific CD4 T1 cells for adoptive T-cell therapy. *Oncoimmunology*, 4(5), e1002723.
73. Prokop, A., Wrasidlo, W., Lode, H., Herold, R., Lang, F., Henze, G., et al. (2003). Induction of apoptosis by enediyne antibiotic calicheamicin thetaII proceeds through a caspase-mediated mitochondrial amplification loop in an entirely Bax-dependent manner. *Oncogene*, 22(57), 9107–9120.
74. Kaplon, J., Zheng, L., Meissl, K., Chaneton, B., Selivanov, V. A., Mackay, G., et al. (2013). A key role for mitochondrial gatekeeper pyruvate dehydrogenase in oncogene-induced senescence. *Nature*, 498(7452), 109–112.
75. Blagosklonny, M. V. (2012). Cell cycle arrest is not yet senescence, which is not just cell cycle arrest: terminology for TOR-driven aging. *Aging (Albany NY)*, 4(3), 159–165.
76. Finley, L. W., Carracedo, A., Lee, J., Souza, A., Egia, A., Zhang, J., et al. (2011). SIRT3 opposes reprogramming of cancer cell metabolism through HIF1alpha destabilization. *Cancer Cell*, 19(3), 416–428.
77. Tannahill, G. M., Curtis, A. M., Adamik, J., Palsson-McDermott, E. M., McGettrick, A. F., Goel, G., et al. (2013). Succinate is an inflammatory signal that induces IL-1beta through HIF-1alpha. *Nature*, 496(7444), 238–242.

Original Paper

## Nuclear Translocation of Argonaute 2 in Cytokine-Induced Senescence

Maximilian Rentschler<sup>a</sup> Yan Chen<sup>a</sup> Jana Pahl<sup>a</sup> Laura Soria-Martinez<sup>a</sup>  
Heidi Braumüller<sup>a</sup> Ellen Brenner<sup>a</sup> Oliver Bischof<sup>b,c,d</sup> Martin Röcken<sup>a</sup>  
Thomas Wieder<sup>a</sup>

<sup>a</sup>Department of Dermatology, University Medical Center Tübingen, Eberhard Karls University, Tübingen, Germany, <sup>b</sup>Institut Pasteur, Nuclear Organisation and Oncogenesis Unit, Department of Cell Biology and Infection, Paris, <sup>c</sup>INSERM, U993, Paris, <sup>d</sup>Equipe Labellisée Fondation ARC pour la recherche sur le cancer, Paris, France

### Key Words

Cellular Senescence • Interferons • Stable Growth Arrest • Tumor Necrosis Factor • Tumor Surveillance

### Abstract

**Background/Aims:** Cellular senescence, or permanent growth arrest, is known as an effective tumor suppressor mechanism that can be induced by different stressors, such as oncogenes, chemotherapeutics or cytokine cocktails. Previous studies demonstrated that the growth-repressing state of oncogene-induced senescent cells depends on argonaute protein 2 (Ago2)-mediated transcriptional gene silencing and Ago2/Rb corepression of E2F-dependent cell cycle genes. Cytokine-induced senescence (CIS) likewise depends on activation of the p16<sup>INK4a</sup>/Rb pathway, and consecutive inactivation of the E2F family of transcription factors. In the present study, we therefore analyzed the role of Ago2 in CIS. **Methods:** Human cancer cell lines were treated with interferon-gamma (IFN- $\gamma$ ) and tumor necrosis factor (TNF) to induce senescence. Senescence was determined by growth assays and measurement of senescence-associated  $\beta$ -galactosidase (SA- $\beta$ -gal) activity, Ago2 translocation by Ago2/Ki67 immunofluorescence staining and western blot analysis, and gene transcription by quantitative polymerase chain reaction (qPCR). **Results:** IFN- $\gamma$  and TNF permanently stopped cell proliferation and time-dependently increased SA- $\beta$ -gal activity. After 24 – 48 h of cytokine treatment, Ago2 translocated from the cytoplasm into the nucleus of Ki67-negative cells, an effect which was shown to be reversible. Importantly, the proinflammatory cytokine cocktail suppressed Ago2-regulated cell cycle control genes, and siRNA-mediated depletion of Ago2 interfered with cytokine-induced growth inhibition. **Conclusion:** IFN- $\gamma$  and TNF induce a stable cell cycle arrest of cancer cells that is accompanied by a fast nuclear Ago2 translocation

Prof. Dr. Thomas Wieder

Department of Dermatology, University Medical Center Tübingen  
Liebermeisterstr. 25, 72076 Tübingen (Germany)  
Tel. +4970712986871, Fax +497071294405, E-Mail [thomas.wieder@med.uni-tuebingen.de](mailto:thomas.wieder@med.uni-tuebingen.de)

and repression of Ago2-regulated cell cycle control genes. As Ago2 downregulation impairs cytokine-induced growth regulation, Ago2 may contribute to tissue homeostasis in human cancers.

© 2018 The Author(s)  
Published by S. Karger AG, Basel

## Introduction

Argonaute (Ago) proteins comprise a family of evolutionary conserved proteins that have emerged as key molecules in the control of transcriptional and post-transcriptional processes by association with small RNAs [1]. In humans, the family member Ago2 is a central part of the RNA interference (RNAi) platform with enzymatic endoribonuclease activity [2]. Ago proteins are often recognized by their cytoplasmic function in which they regulate gene transcripts via post-transcriptional gene silencing (PTGS) mechanisms. However, nuclear functions have also been well characterized in fission yeast and plants in which they assist in mechanisms of transcriptional gene silencing (TGS). In fission yeast, Ago binds to antisense transcripts to form the RITS (RNA-induced transcriptional silencing) complex at centromeric regions to induce heterochromatin formation [3]. Thus, Ago proteins normally reside in the cytoplasm, e.g. as part of the RNA-induced silencing complex (RISC), but may eventually translocate into the nucleus and play a functional role in TGS in animal cells, too [4].

Cellular senescence is an efficient intrinsic anticancer mechanism (for reviews see [5, 6]) that stops the growth of premalignant lesions, as in the case of benign human naevi [7] or lung adenomas [8]. Cellular senescence can be triggered by overexpression or activation of oncogenes [9], and the loss of oncogene-induced senescence effectors may lead to the development of malignant tumors [7, 8]. Intrinsic senescence can also be induced by therapeutic intervention, and it has been demonstrated that different antitumor drugs, such as cyclophosphamide [10] or the BRAF inhibitor vemurafenib [11], drive cancer cells into permanent growth arrest. Recently, we and others described cytokine-induced senescence (CIS) as an extrinsic form of senescence. In these studies, adoptive transfer of T helper 1 (T<sub>H</sub>1) cells [12] or the application of T<sub>H</sub>1 cell cytokines IFN- $\gamma$  and TNF [12-14] permanently growth-arrested different cancer cells and induced various senescence markers *in vitro* and *in vivo*. Thus, CIS can be considered to be a part of the bodies' immune surveillance machinery [15] playing an important role in the equilibrium phase [16] of cancer development. CIS mainly depends on activation of the p16<sup>Ink4a</sup>/Rb pathway [12] and consecutive inactivation of the E2F family of transcription factors. However, the exact molecular mechanisms remained enigmatic. As it has been shown that Ago2 plays an active role during intrinsic senescence by corepressing E2F target genes [17], we therefore analyzed its role in CIS. For this, we treated human cancer cell lines with IFN- $\gamma$  + TNF and measured senescence-associated markers, i.e. permanent growth arrest [12] and senescence-associated  $\beta$ -galactosidase (SA- $\beta$ -gal) activity [18]. We then analyzed the expression and nuclear translocation of Ago2 protein after cytokine challenge using Ago2/Ki67 immunofluorescence staining. Finally, we tested its functional role in extrinsic, cytokine-induced growth arrest by analyzing the regulation of Ago2-dependent cell cycle control genes and by siRNA-mediated downregulation of Ago2.

## Materials and Methods

### Reagents

Recombinant human IFN- $\gamma$  and recombinant human TNF were purchased from R & D Systems (Bio-Techne GmbH; Wiesbaden, Germany). IFN- $\gamma$  and TNF were dissolved in complete RPMI 1640 medium, containing stable L-glutamine, 10% fetal calf serum, HEPES buffer (100 mM), non-essential amino acids, sodium pyruvate (1 mM) and penicillin/streptomycin (100 U/ml; all from Biochrom AG, Berlin, Germany) to give final concentrations of 100 ng/ml for IFN- $\gamma$  or 200 pg/ml – 10 ng/ml for TNF. Doxorubicin hydrochloride was dissolved in dimethyl sulfoxide (DMSO; both from Sigma-Aldrich Chemie GmbH, Taufkirchen, Germany) and used at a concentration of 1  $\mu$ M.

### Cell lines

MCF-7 control vector-transfected breast cancer cells [19] and A204 rhabdomyosarcoma cells [12] were a generous gift by F. Essmann (University of Tübingen, Germany) and K. Schilbach (University of Tübingen, Germany), respectively. Prior to treatment, cells were seeded at a density of  $1 \times 10^4$  cells/cm<sup>2</sup> and cultured overnight in complete medium to allow adherence and logarithmic growth. Subsequently, medium was removed and cells were either incubated in complete medium alone or in medium containing doxorubicin, IFN- $\gamma$  + TNF, various siRNAs, or IFN- $\gamma$  + TNF in combination with siRNAs at the indicated concentrations and for the indicated time periods.

### Viability assay

Cell viability was determined using the colorimetric XTT (2, 3-bis-(2-methoxy-4-nitro-5-sulphophenyl)-2H-tetrazolium-5-carboxanilide) salt-based assay kit from Roche Diagnostics Deutschland GmbH (Mannheim, Germany) according to the manufacturer's instructions.

### In vitro growth assay

The growth assay was performed as described earlier [12]. Briefly, cancer cells were seeded at a density of  $1 \times 10^4$  cells/cm<sup>2</sup>. Then, the cells were treated with control medium, doxorubicin or cytokines as described above for 24 h or 4 d, respectively. After treatment, medium, doxorubicin or cytokines were removed, the cells were trypsinized, and viable cells (trypan blue exclusion) were counted under a Zeiss Axiovert 25 microscope (Carl Zeiss AG, Oberkochen, Germany) using a Neubauer chamber (Karl Hecht GmbH, Sondheim, Germany). The cells were reseeded at  $2 \times 10^4$  cells/cm<sup>2</sup>, and grown in the absence of doxorubicin or cytokines in complete RPMI 1640 medium for 1 – 2 passages (p (1) – p (2)).

In Ago2 knockdown experiments, A204 cells were grown to a confluence level of 50 – 60% and then treated either with siRNAs, IFN- $\gamma$  + TNF or a combination of siRNAs plus IFN- $\gamma$  + TNF for 48 h. For the growth assay, the number of viable cells was counted after the treatment phase at passage 0 (p (0)), and after the subsequent passage (p (1)).

To exclude interference of the combined siRNA/cytokine treatment with the trypan blue exclusion assay, we also counted dead cells directly after the treatment phase at p (0) and after further growth at p (1). In the absence of cytokines, siRNA-treated cell populations showed  $12.2 \pm 3.5\%$  (n=4) dead cells at p (0) and  $6.2 \pm 1.2\%$  (n=4) dead cells at p (1), whereas the combination of siRNAs plus cytokines induced  $20.2 \pm 3.2\%$  (n=4) dead cells at p (0) and  $14.1 \pm 5.3\%$  (n=4) dead cells at p (1).

### Proliferation assay

For measurement of proliferation, A204 cancer cells were seeded at a density of  $5 \times 10^3$  cells/well onto 96-well flat-bottomed plates. After 24 h, the cells were either treated with the cytokine cocktail alone, siRNAs alone or a combination of both for the indicated time. In other experiments, the cells were pretreated for 48 h with siRNAs alone or in combination with the cytokine cocktail. Then, the cells were reseeded to measure the cellular proliferation after removal of the treatment. [<sup>3</sup>H]-thymidine (0.25  $\mu$ Ci/well) was added 24 h before the respective plates were harvested and finally measured using a FilterMate harvester and a MicroBeta TriLux counter (all reagents and equipment from PerkinElmer, Boston, MA, USA) as previously described [12].

### Immunofluorescence

Cancer cells were grown on chamber slides (BD Biosciences GmbH, Heidelberg, Germany), and immunofluorescence analyses were performed essentially as described [12]. After treatment, the cells were fixed with acetone/methanol (1:1). The slides were washed with PBS/0.05% Tween 20 at room temperature (RT), blocked with serum-free DAKO-Block (DAKO Deutschland GmbH, Hamburg, Germany), washed again, and incubated with anti-Ki67 (dilution 1:100; Abcam, Cambridge, UK) and anti-Ago2, clone 9E8.2 (dilution 1:200; EMD Millipore, Billerica, MA, USA). After washing, the slides were incubated with anti-rabbit Alexa488 (Invitrogen; distributed via Thermo Fisher Scientific, Waltham, MA, USA) and anti-mouse Alexa555 (Cell Signaling Technology, Boston, MA, USA), washed again and incubated with 4',6-diamidino-2-phenylindole (DAPI; Invitrogen). Finally, the slides were washed, mounted with fluorescence mounting medium (DAKO) and analyzed using a Zeiss Axiovert 200 microscope (Zeiss) with the VisiView software

(Visitron Systems, Puchheim, Germany). To exclude unspecific, doxorubicin-mediated fluorescence signals, negative controls (in the absence of anti-Ago2 and anti-Ki67 antibodies) of medium- or doxorubicin-treated cells were performed. At the appropriate device settings, all negative controls were virtually free of red or green fluorescence signals (data not shown).

#### Subcellular fractionation

Cell lysis was performed using the NE-PER™ Nuclear and Cytoplasmic Extraction kit (Thermo Fisher) as described in the manufacturer's protocol.

#### Immunoblotting

Western blot analysis was performed essentially as described [20]. After doxorubicin or cytokine treatment, cancer cells were lysed in lysis buffer (50 mM Tris-HCl, pH 7.5, 150 mM NaCl, 1% Triton X-100, 0.5% SDS, 1 mM NaF, 1 mM Na<sub>3</sub>VO<sub>4</sub>, and 0.4% β-mercaptoethanol) containing a protease inhibitor cocktail (cOmplete™ from Roche). After determination of protein content using the bicinchoninic acid assay (BCA) from Thermo Fisher Scientific or the RotiQuant™ assay (Carl Roth GmbH + Co. KG, Karlsruhe, Germany), proteins were resolved by SDS-PAGE and transferred onto a polyvinylidene difluoride (PVDF) membrane. Then, specific bands were visualized by the use of anti-Ago2, clone 9E8.2 (1:2000; EMD Millipore), anti-lamin A/C, clone 131C3 (1:1000; EMD Millipore) or anti-β-actin monoclonal antibody MAB1501R (1:5000; EMD Millipore) in combination with an anti-mouse horseradish peroxidase (HRP)-conjugated antibody (1:3000; Cell Signaling Technology). Cell lysates from HeLa cells overexpressing Ago2 were used as positive controls (data not shown).

#### Measurement of SA-β-galactosidase activity

SA-β-gal activity was measured as previously described [12, 18]. After incubation with doxorubicin, IFN-γ + TNF, different siRNAs in combination with IFN-γ + TNF, or medium, cancer cells were fixed for 15 min at RT, and then stained for 16 h at 37 °C using the β-Galactosidase Staining kit (United States Biological; Swampscott, MA, USA). The staining solution was removed, the cells were washed with PBS and subsequently stained with DAPI to allow determination of the total cell number. SA-β-gal-positive (blue) and -negative (white) cells were counted using a Zeiss Axiovert 200 microscope (Zeiss), and the percentage of SA-β-gal-positive cells was calculated.

#### RNA isolation and quantitative PCR

Isolation of total RNA from cancer cells was performed using the NucleoSpin® RNA Plus kit from Macherey-Nagel (Macherey-Nagel GmbH & Co. KG, Düren, Germany) according to the manufacturer's protocol. Subsequently, the iScript™ cDNA synthesis kit (Bio-Rad Laboratories GmbH, Munich, Germany) was used for reverse transcription. Gene expression analysis by quantitative real-time PCR (qPCR) was then conducted essentially as described [12] with a LightCycler® 480 II system (Roche) using the following primer pairs in combination with a KAPA SYBR® FAST LC480 qPCR master mix (Sigma-Aldrich):

(i) human *PCNA*: sense AAGAGAGTGGAGTGGCTTTTG and antisense TGTCGATAAAGAGGAGGAAGC; (ii) human *CCNA2*: sense CACTCACTGGCTTTTCATCTTC and antisense CAGAAAACCATTTGGTCCCTC; (iii) human *CCNE2*: sense TCTTCACTGCAAGCACCATC and antisense ACCTCATTTATTCATTGCTCCAA; (iv) human *CDCA8*: sense CTTCGCCCTTGGAGGAAACAA and antisense GGTGTCTGAATAGCTTCTGCTG; (v) human *CDC2*: sense CATGGCTACCACTTGACCTGT and antisense AAGCCGGATCTACCATAAC; (vi) human *AGO2*: sense ACTGACAAGAACGAGCG and antisense AGAAACGATTGTCGTCCC; (vii) human *ACTB*: sense AGCCTCGCTTTGCCGA and antisense CTGGTGCCTGGGGCG; (viii) human *ALDOA*: sense GTGTTGTGGGCATCAAGGTAGA and antisense CGAAGTCAGTCCGTCCTTCT; (ix) human *HPRT1*: sense TGATAGATCCATTCTATGACTGTAGA and antisense AAGACATTTCTCCAGTTAAAGTTGAG. β-actin, aldolase A and hypoxanthine-guanine phosphoribosyltransferase (HPRT) served as housekeeping genes. For normalization the medium condition or control setting was set as 1.

#### Transfection and knockdown of Ago2 by siRNA

For Ago2 knockdown experiments, A204 cells were transfected with 25 nM ON-TARGETplus siRNAs using the DharmaFECT® 1 transfection reagent (Dharmacon Inc., Lafayette, CO, USA) according to the supplier's instructions. Specific siRNA duplexes tested included 4 different single Ago2-targeting siRNAs

as well as an Ago2 SMARTpool siRNA. A non-targeting pool was used as control. Functionality of all listed siRNAs was either analyzed in combination with the cytokine cocktail or in culture medium for up to 48 h. After incubation, cancer cells were either used for RNA isolation and immunoblotting to check for knockdown efficiency, or for further *in vitro* viability, proliferation or senescence assays.

siRNA 1 target sequence: GCACGACUGUGGACACGAA; siRNA 2 target sequence: CCAAGGCGGUCCAGGUUCA; siRNA 3 target sequence: GGUCUAAAGGUGGAGAUAA; siRNA 4 target sequence: CAAGCAGGCCUUCGCACUA; SMARTpool target sequences: GCACGACUGUGGACACGAA, CCAAGGCGGUCCAGGUUCA, GGUCUAAAGGUGGAGAUAA, CAAGCAGGCCUUCGCACUA; Non-targeting pool sequences: UGGUUACAUGUCGACUAA, UGGUUACAUGUUGUGUGA, UGGUUACAUGUUUCUGA, UGGUUACAUGUUUCCUA.

#### Statistics

Data are expressed as arithmetic means  $\pm$  s.e.m. (technical replicates), and statistical analyses were made by unpaired t-test, or ANOVA using Dunnett's or Tukey's test as post hoc test, where appropriate.  $P < 0.05$  was considered statistically different. Experiments were performed in two human cancer cell lines (MCF-7 and A204; biological replicates).

## Results

### *Nuclear translocation of Ago2 during doxorubicin-induced senescence*

First, we established the methods to analyze the role of Ago2 in cellular senescence. MCF-7 breast cancer cells were treated with 1  $\mu$ M doxorubicin for 24 h followed by removal of the drug for 96 h essentially as described previously [17]. As expected, doxorubicin treatment of the apoptosis-refractory MCF-7 cell line [19] inhibited the proliferation of the cancer cells. Most importantly, doxorubicin also stopped MCF-7 cell growth for 2 passages after removal of the drug (Fig. 1A). In addition, doxorubicin induced a flat, senescence-like cell morphology (Fig. 1B), increased senescence-associated  $\beta$ -galactosidase (SA- $\beta$ -gal)-positive cells to approximately 80% (Fig. 1C), and blunted BrdU incorporation into the DNA of proliferating cells by  $>95\%$  (Fig. 1D). Next, we analyzed Ago2 translocation into the nucleus during drug-induced senescence. Immunofluorescence analysis indeed showed translocation of Ago2 into the nucleus of non-proliferating, Ki67-negative MCF-7 cells after doxorubicin treatment (Fig. 1E, F). Importantly, Ago2 translocation could also be demonstrated by western blot analysis of nuclear extracts of doxorubicin-treated MCF-7 cells. As compared with medium-treated control cells, the ratio of nuclear to cytoplasmic Ago2 was clearly increased after doxorubicin treatment (Fig. 1G). Thus, the methods described above are well suited to analyze Ago2 translocation during cytokine-induced senescence (CIS).

### *Nuclear translocation of Ago2 during cytokine-induced senescence*

The combined action of interferon- $\gamma$  (IFN- $\gamma$ ) and tumor necrosis factor (TNF) drives various cancer cells into senescence [12-14]. We therefore treated MCF-7 cells with the established cytokine cocktail for 96 h, and then analyzed different senescence-associated markers. Indeed, IFN- $\gamma$  + TNF permanently stopped the proliferation of MCF-7 cells, also after cytokine removal (Fig. 2A), and induced the typical egg-shaped, senescence-like morphology and SA- $\beta$ -gal activity (Fig. 2B). As in the case of drug-induced senescence, Ago2 translocated into the nucleus of IFN- $\gamma$  + TNF-treated MCF-7 cells (Fig. 2C) thereby increasing Ago2<sup>+</sup>/Ki67<sup>-</sup> cells from 10% to 77% (Fig. 2D). Cytokine-induced translocation of Ago2 into the nucleus of MCF-7 cells was verified by western blot analysis of nuclear extracts (Fig. 2E). Further experiments using the cytokine-sensitive rhabdomyosarcoma cell line A204 [12, 13] demonstrated that IFN- $\gamma$  + TNF also induced the flat senescence-associated morphology (Fig. 2F), increased SA- $\beta$ -gal activity (Fig. 2F), and enhanced nuclear translocation of Ago2 in those cells (Fig. 2G, H). These data clearly demonstrate that nuclear Ago2 translocation occurs during CIS in two different cancer cell lines.

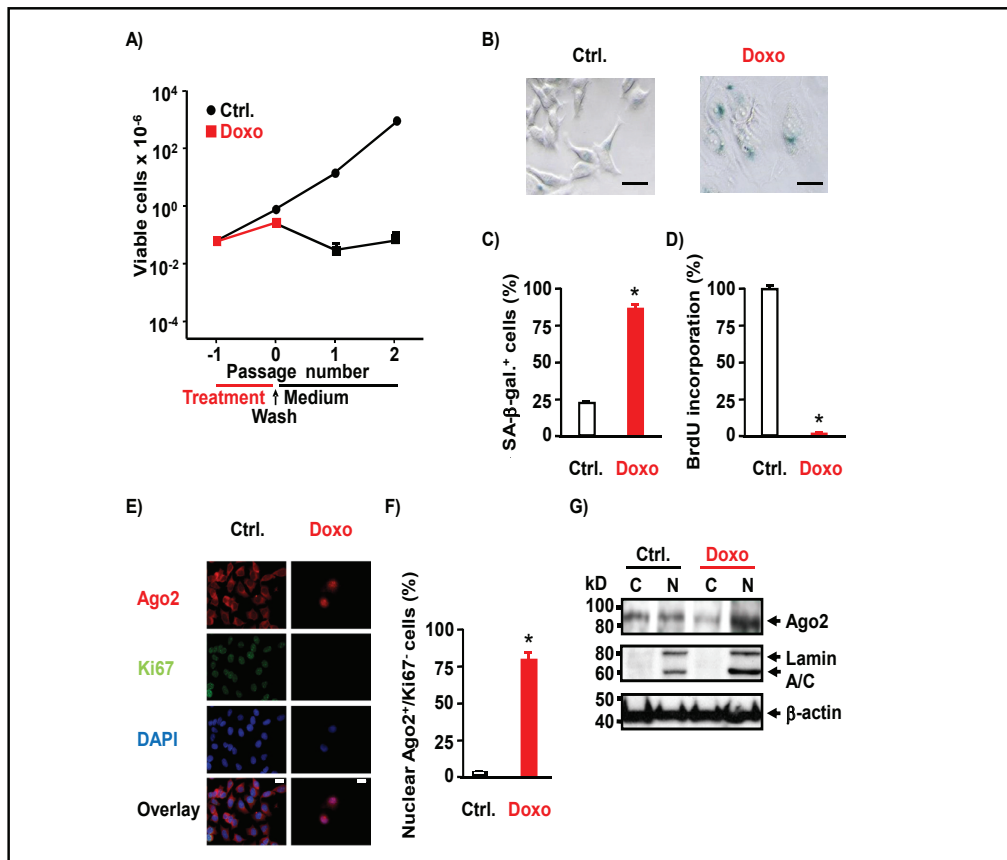


**Fig. 1.** Doxorubicin induces growth arrest, SA-β-galactosidase activity, inhibition of BrdU incorporation and nuclear Ago2 translocation in MCF-7 cells. A) MCF-7 breast cancer cells were treated for 24 h with medium (Ctrl.) or with medium containing 1 μM doxorubicin (Doxo). The cytostatic drug was removed, cells were trypsinized, counted, and seeded at  $2 \times 10^4$  cells/well. The cells were grown for 96 h in medium alone, trypsinized and reseeded for two further passages (p (1) – p (2)). Cell counts are represented as mean ± s.e.m. (n=4). B-D) Alternatively, SA-β-gal staining (B, C) or a BrdU incorporation assay (D) was performed 96 h after drug removal, and the percentage of SA-β-gal<sup>+</sup> cells (C; mean ± s.e.m., n=5) or BrdU incorporation (D; mean ± s.e.m., n=12) is given. E, F) In addition, nuclear Ago2 translocation after 24 h drug treatment and 96 h drug removal is shown by immunofluorescence staining for Ago2 (red) and Ki67 (green), nuclei appear in blue (E), and the percentage of nuclear Ago2<sup>+</sup>/Ki67<sup>-</sup> cells is given (F; mean ± s.e.m., n=12 for Ctrl., n=20 for Doxo). (G) Ago2, lamin A/C, or β-actin in cytosolic (C) or nuclear (N) extracts as detected by western blotting in MCF-7 cells treated with medium (Ctrl.) or doxorubicin (Doxo) are shown 96 h after removal of the drug. Bar = 25 μm (B) or 10 μm (E). \*P<0.05 from medium-treated control (C, D, F).

#### *Kinetics of Ago2 translocation after cytokine treatment*

IFN-γ + TNF-induced senescence is an extrinsic senescence pathway that has been shown to be TNF receptor 1 (TNFR1)- and signal transducer and activator of transcription 1 (STAT1)-dependent [12]. After simultaneous stimulation of the cytokine receptors, senescence signaling via two converging signaling pathways takes place [21]. In this setting, complete senescence induction takes about 4 to 5 days [12]. To disclose the kinetics of senescence induction and Ago2 translocation in more detail, we treated A204 or MCF-7 cells with IFN-γ + TNF for 24 – 72 h, and measured SA-β-gal activity and Ago2 translocation in parallel (Fig. 3A-D). In A204 cells (Fig. 3A) as well as in MCF-7 cells (Fig. 3C), the percentage of SA-β-gal<sup>+</sup> cells steadily increased as compared with medium-treated controls during the whole incubation



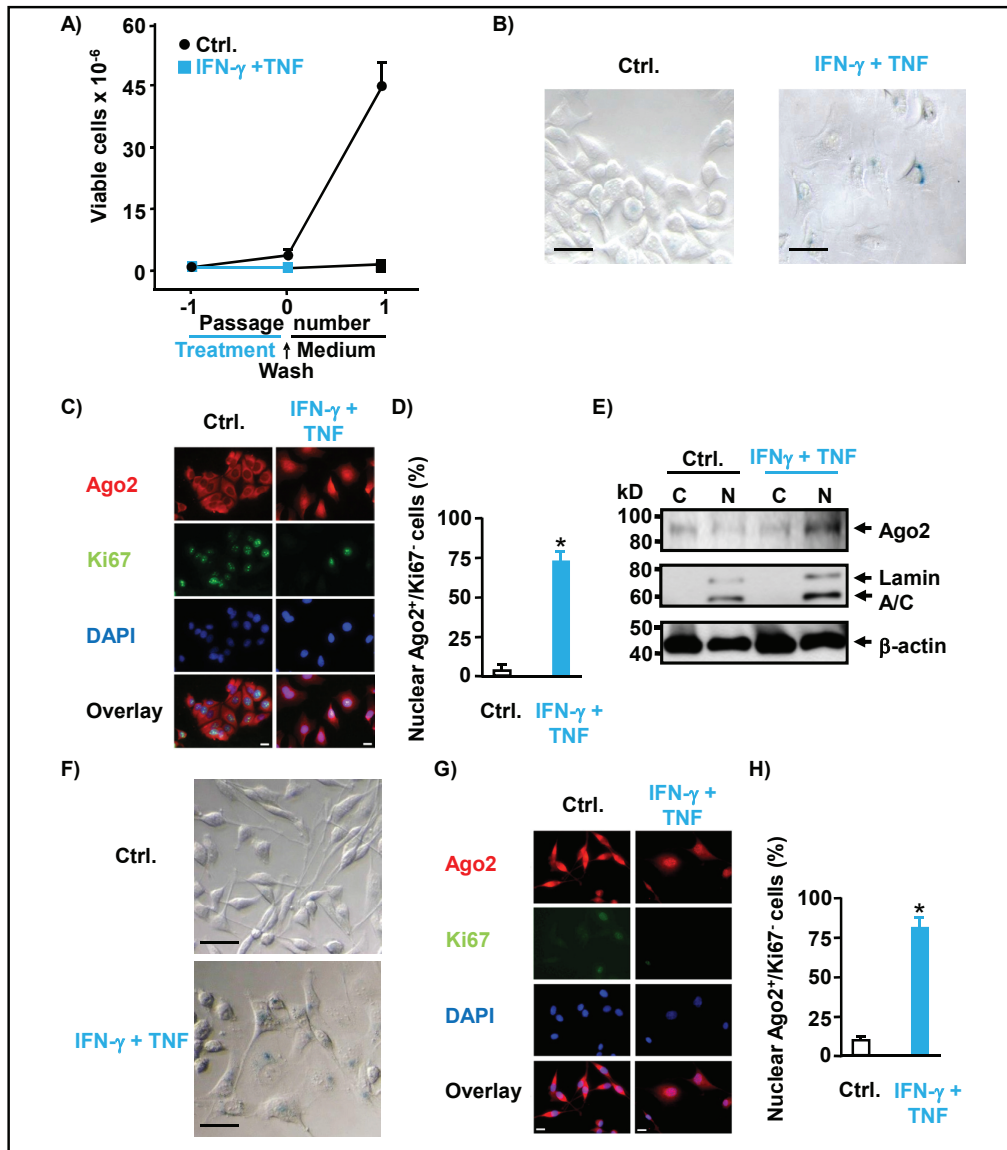


**Fig. 2.** IFN- $\gamma$  and TNF induce senescence and nuclear Ago2 translocation in human cancer cells. A) MCF-7 breast cancer cells were treated for 96 h with medium (Ctrl.) or with medium containing 100 ng/ml IFN- $\gamma$  and 10 ng/ml TNF (IFN- $\gamma$  + TNF). The cytokines were removed, cells were trypsinized, reseeded at  $1.5 \times 10^4$  cells/well and grown for one additional passage (p (1)) in medium alone. After 96 h of cytokine removal, cells were trypsinized and counted. Cell counts are represented as mean  $\pm$  s.e.m. (n=4). B) SA- $\beta$ -gal staining of MCF-7 cells after 72 h of IFN- $\gamma$  + TNF treatment. Note the flat senescence-associated morphology of cytokine-treated cells. C, D) Immunofluorescence staining for Ago2 (red), Ki67 (green) or DAPI (blue) (C) and percentage of nuclear Ago2<sup>+</sup>/Ki67<sup>-</sup> cells (D; mean  $\pm$  s.e.m., n=7) after 48 h of IFN- $\gamma$  + TNF treatment. E) Ago2, lamin A/C, or  $\beta$ -actin in cytosolic (C) or nuclear (N) extracts as detected by western blotting in MCF-7 cells treated with medium (Ctrl.) or IFN- $\gamma$  + TNF are shown after 72 h of treatment. F) SA- $\beta$ -gal activity staining of A204 rhabdomyosarcoma cells after 72 h of treatment with 100 ng/ml IFN- $\gamma$  + 400 pg/ml TNF. Note the flat senescence-associated morphology of cytokine-treated cells. G, H) Immunofluorescence staining for Ago2 (red), Ki67 (green) or DAPI (blue) (G) and percentage of nuclear Ago2<sup>+</sup>/Ki67<sup>-</sup> cells (H; mean  $\pm$  s.e.m., n=6 for Ctrl. or n=8 for IFN- $\gamma$  + TNF) after 72 h of IFN- $\gamma$  + TNF treatment. Bar = 25  $\mu$ m (B, F), or 10  $\mu$ m (C, G). \*P<0.05 from medium-treated control (D, H).

time of 72 h thereby indicating that senescence induction continuously proceeds after start of the cytokine treatment. On the other hand, 20% or 50% of the total cell population already showed nuclear Ago2 translocation after 24 h of treatment in A204 or MCF-7 cells, respectively (Fig. 3B, D). In these experiments, Ago2 translocation reached a peak of 65% (A204) or 74% (MCF-7) after 48 h of treatment with the cytokine cocktail (Fig. 3B, D). Thus, Ago2 translocation into the nucleus appears as an early event in the signaling pathway of CIS and does not simply represent another senescence marker of permanently arrested cancer cells.

*Ago2 translocation after cytokine challenge is reversible*

Higher magnification of the immunofluorescence pictures revealed that Ago2 is present in three cellular compartments. Besides its cytoplasmic and nuclear localization, we also detected Ago2 in the perinuclear region of cytokine-treated A204 cells (Fig. 4A). We therefore reasoned that Ago2 might shuttle between the cytosol and the nucleus of the cells. To study this in more detail, we treated cells for 72 h with IFN- $\gamma$  + TNF, then removed the cytokines, and incubated the cells for another 48 h or 120 h in the absence of the stressors. Again, Ago2 accumulated in the nucleus of Ki67-negative A204 cells after 72 h of cytokine treatment (Fig. 4B). 48 h after cytokine removal, the percentage of Ago2<sup>+</sup>/Ki67<sup>-</sup> cells already declined, and nearly reached control levels another 72 h later (Fig. 4B). Taken together, Ago2 rapidly translocates into the nucleus after stimulation of the cytokine receptors, and the protein reenters the cytosol when cytokine signaling is terminated.

*Suppression of Ago2-regulated cell cycle control genes during cytokine-induced senescence*

Ago2 has been described as a corepressor of several cell cycle genes thereby interfering with enhanced cell proliferation [17]. We thus measured the time-dependent influence of IFN- $\gamma$  + TNF on the expression of known Ago2-regulated cell cycle control genes in A204 cells. 24 h of cytokine treatment, a time point where Ago2 is already present in the nucleus, reduced the expression of proliferating cell nuclear antigen (PCNA), cyclin A2 (CCNA2), cyclin E2 (CCNE2), cell division cycle associated 8 (CDC48), and cell division control protein 2 (CDC2; also known as cyclin-dependent kinase 1 (CDK1)) by 25 – 50% (Fig. 5A). With the exception of PCNA, suppression of the cell cycle control genes was continuing for the whole period of 96 h of sustained cytokine treatment and did not resume the starting levels at time point 0 (Fig. 5A). Further experiments with A204 rhabdomyosarcoma (blue dots) or MCF-7

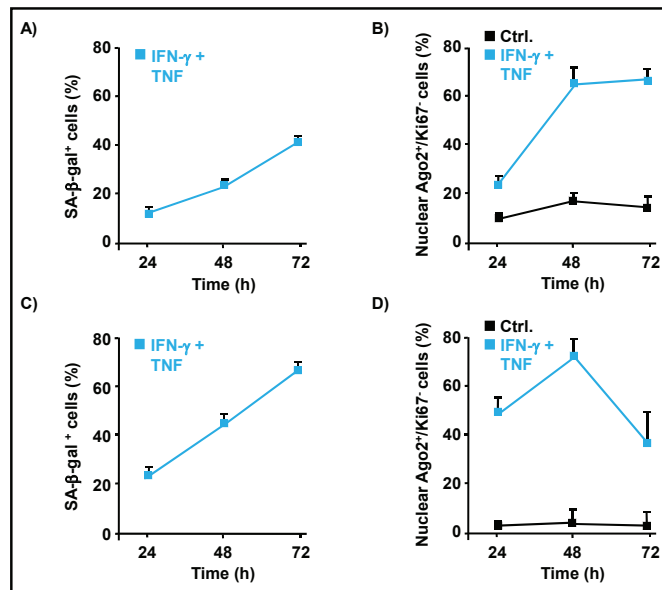


**Fig. 3.** Kinetics of cytokine-induced Ago2 translocation. A, B) Time dependency of cytokine-induced SA- $\beta$ -gal activity (A; mean  $\pm$  s.e.m., n=6-9), and cytokine-induced nuclear Ago2 translocation in % of the total population (B; mean  $\pm$  s.e.m., n=4-6) of A204 rhabdomyosarcoma cells. Medium-treated A204 cells displayed  $10.6 \pm 0.7\%$  (n=6) SA- $\beta$ -gal<sup>+</sup> cells after 72 h of incubation (A). C, D) Time dependency of cytokine-induced SA- $\beta$ -gal activity (C; mean  $\pm$  s.e.m., n=6), and cytokine-induced nuclear Ago2 translocation in % of the total population (D; mean  $\pm$  s.e.m., n=7) of MCF-7 breast cancer cells. Medium-treated MCF-7 cells displayed  $7.4 \pm 0.9\%$  (n=6) SA- $\beta$ -gal<sup>+</sup> cells after 72 h of incubation (C).

breast cancer cells (red dots) confirmed the downregulation of all five cell cycle genes after 24 h and 48 h (Fig. 5B). Thus, CIS proceeds through rapid suppression of 5 important cell cycle control genes which are known to be regulated by Ago2.

*Transient downregulation of Ago2 by siRNA impairs cytokine-induced cell growth inhibition*

To examine the functional role of Ago2 in cell cycle regulation in more detail, we downregulated Ago2 in A204 cells using siRNAs. Combined treatment of siRNAs with cytokines for 72 h strongly impacted the viability of cells in an Ago2-independent manner. The number of viable cells was  $14.9 \pm 1.9\%$  (n=6) for Ago2 siRNA plus cytokine-treated cells and  $17.0 \pm 1.2\%$  (n=6) for non-targeting control siRNA plus cytokine-treated cells as compared with transfection reagent-treated cells. We therefore reduced the siRNA treatment cycles to 24 h – 48 h in the absence (Fig. 6A) or presence of IFN- $\gamma$  + TNF (Fig. 6B). We could demonstrate that a mixture of four different Ago2 siRNAs (SMARTpool) as well as single Ago2-specific siRNAs reduced Ago2 mRNA levels by 70% – 80% as compared with control siRNAs (non-targeting pool)

(Fig. 6C), while the viability of Ago2 siRNA-treated cells was only slightly reduced ( $82.4 \pm 1.2\%$  (n=6) as compared with siCtrl.). Additionally, specific siRNAs also downregulated Ago2 expression in the presence of the cytokine cocktail (Fig. 6C) without significantly influencing the viability ( $105.3 \pm 9.7\%$  (n=6) as compared with siCtrl.). Transient knockdown of Ago2 was also confirmed on the protein level (Fig. 6D). Next, we tested the functional effects of Ago2 downregulation, and measured the proliferation of A204 cells by [ $^3$ H]-thymidine incorporation. IFN- $\gamma$  + TNF blunted proliferation of A204 cells already after 24 h. The inhibition lasted at least 96 h (Fig. 7A). Then, we asked whether Ago2- siRNAs could antagonize the cytokine-induced inhibition of proliferation. However, we realized that siRNA treatment in the absence of cytokines strongly reduced [ $^3$ H]-thymidine incorporation to a similar level (Fig. 7B). Thus, analysis of cell proliferation by this method did not show consistent effects of Ago2 knockdown on cytokine-induced inhibition of DNA synthesis, neither during the 48 h treatment phase (Fig. 7B) nor after removal of the stressors (Fig. 7C). Subsequently, we measured SA- $\beta$ -gal activity after a total incubation time of 120 h (48 h treatment cycle and 72 h removal phase). After this long incubation time, the medium-treated, siAgo2- or siCtrl.-transfected cells already showed high levels of SA- $\beta$ -gal $^+$  cells (Fig. 7D). Nevertheless, siCtrl.-treated A204 cells still responded to IFN- $\gamma$  + TNF, and the cytokine cocktail significantly increased the percentage of SA- $\beta$ -gal $^+$  cells up to approximately 86%. In contrast, the cytokine cocktail failed to further enhance SA- $\beta$ -gal activity in siAgo2-treated A204 cells (Fig. 7D). To functionally test for another feature of senescent cells, i.e. cell cycle arrest, we performed established growth assays [12] with some modifications (see also Material and Methods). In the absence of cytokines, siAgo treatment did not change the proliferative behavior of A204 cells after one 48 h treatment cycle (Fig. 7E, F). In contrast, Ago2-specific siRNAs changed

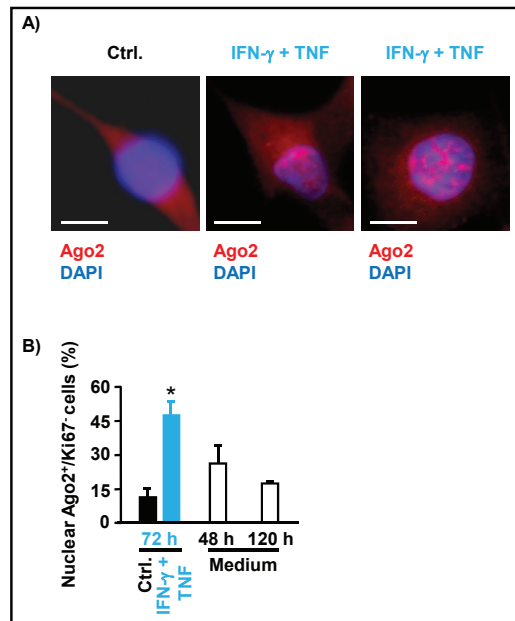
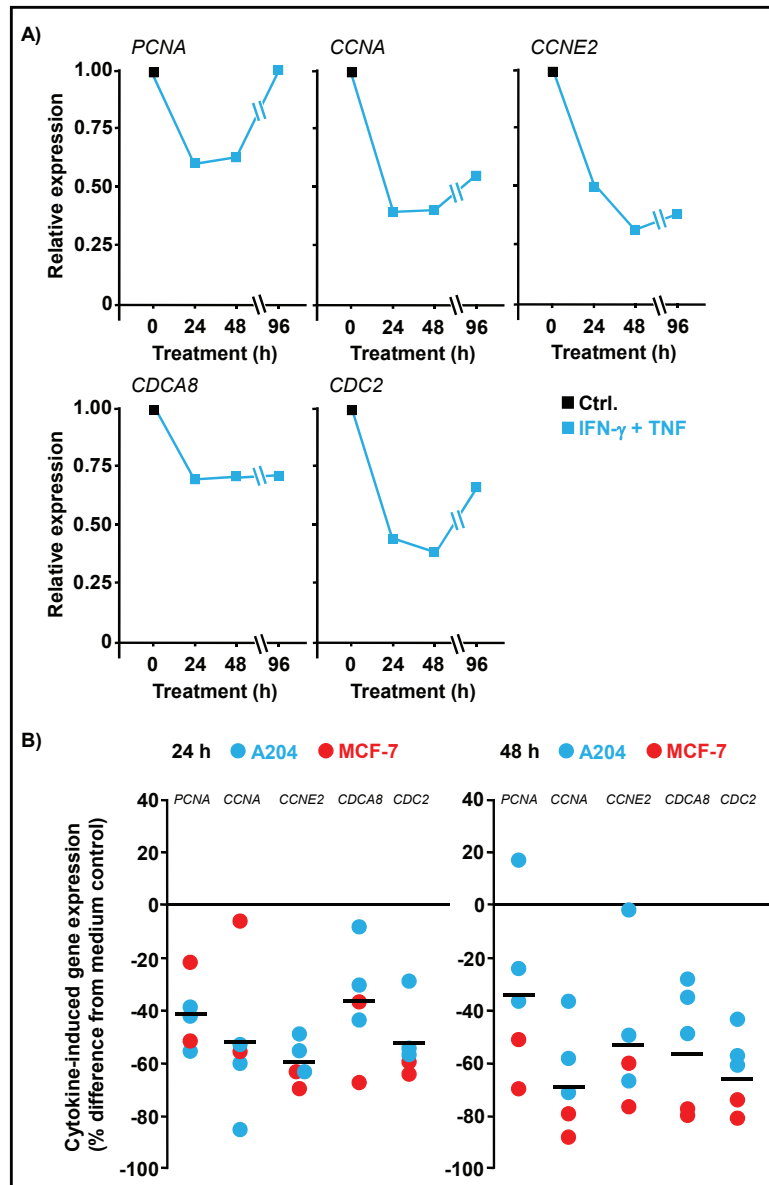


**Fig. 4.** Ago2 shuttling between the nucleus and cytosol. A) Localization of Ago2 (red) in the cytosol of medium-treated A204 cells (left), in the perinuclear region (middle) or in the nucleus (right) of IFN- $\gamma$  + TNF-treated A204 cells. Nuclei appear in blue. B) Retranslocation of Ago2 into the cytosol after cytokine removal in A204 cells (mean  $\pm$  s.e.m., n=3-6). Bar = 10  $\mu$ m (A). \*P<0.05 from medium-treated control (B).

**Fig. 5.** Repression of Ago2-regulated cell cycle control genes after cytokine treatment of cancer cells. A) Expression of cell cycle control genes in A204 cells after 24 h, 48 h or 96 h of IFN- $\gamma$  + TNF. Relative gene expression of A204 cells was assayed in duplicates and time point 0 h was set as 1. The experiment was repeated with similar results. B) Gene expression of A204 cells (blue dots) or MCF-7 cells (red dots) after treatment with IFN- $\gamma$  + TNF for 24 h (left) or 48 h (right) was assayed in duplicates. Data are given as % difference from medium-treated controls. The black bars indicate the mean value of gene downregulation of the respective cell cycle control genes. CCNA2, cyclin A2; CCNE2, cyclin E2; CDCA8, cell division cycle associated 8; CDC2, cell division control protein 2; PCNA, proliferating cell nuclear antigen.



the growth characteristics of cytokine-treated A204 cells when compared with Ctrl. siRNAs (Fig. 7G). Ago2 downregulation repeatedly led to an increase of the relative growth rate as in comparison with the Ctrl. siRNAs (Fig. 7H). Taken together, these data support the notion that Ago2 interferes with IFN- $\gamma$  + TNF-induced growth inhibition during the first 48 h of cytokine treatment.

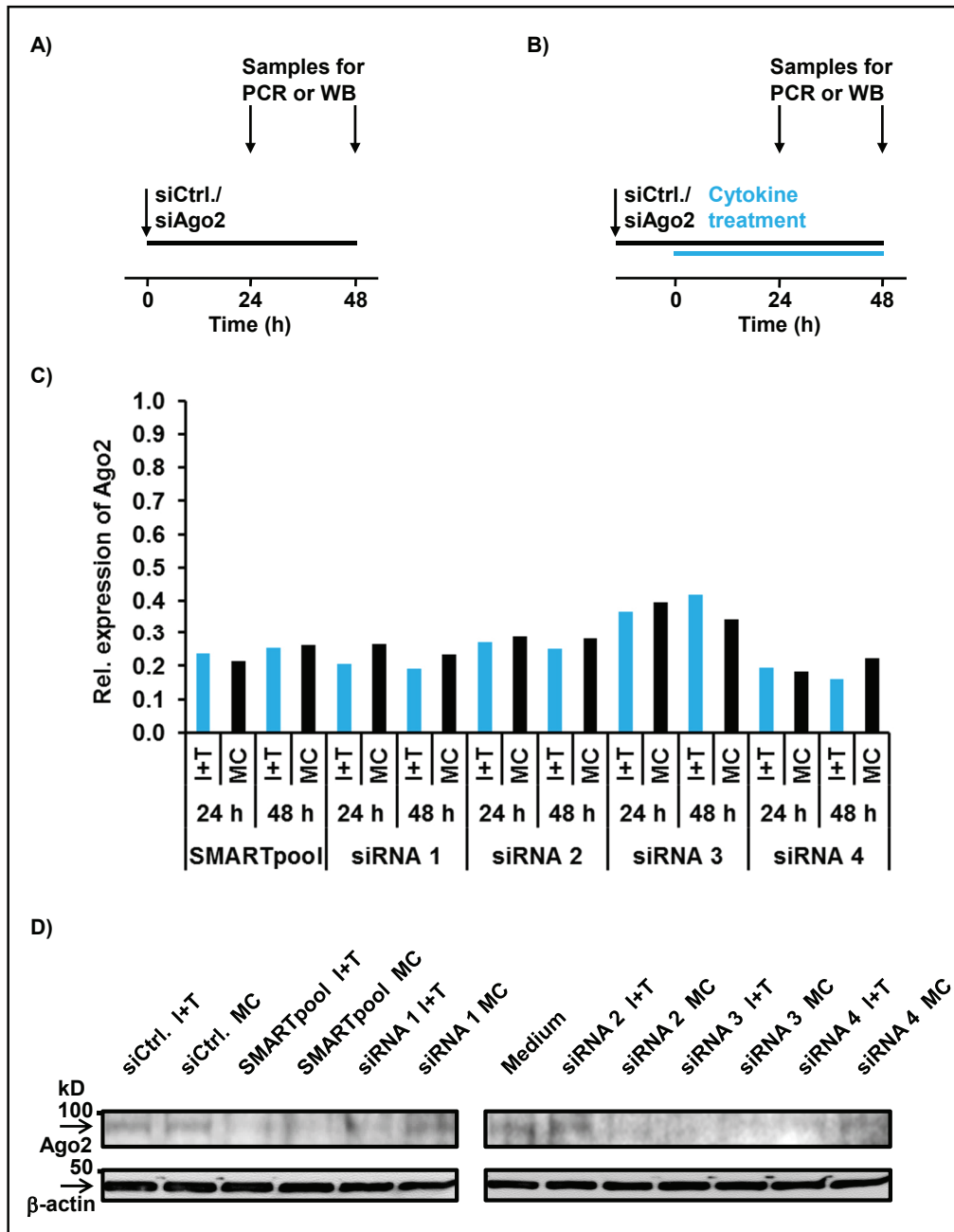
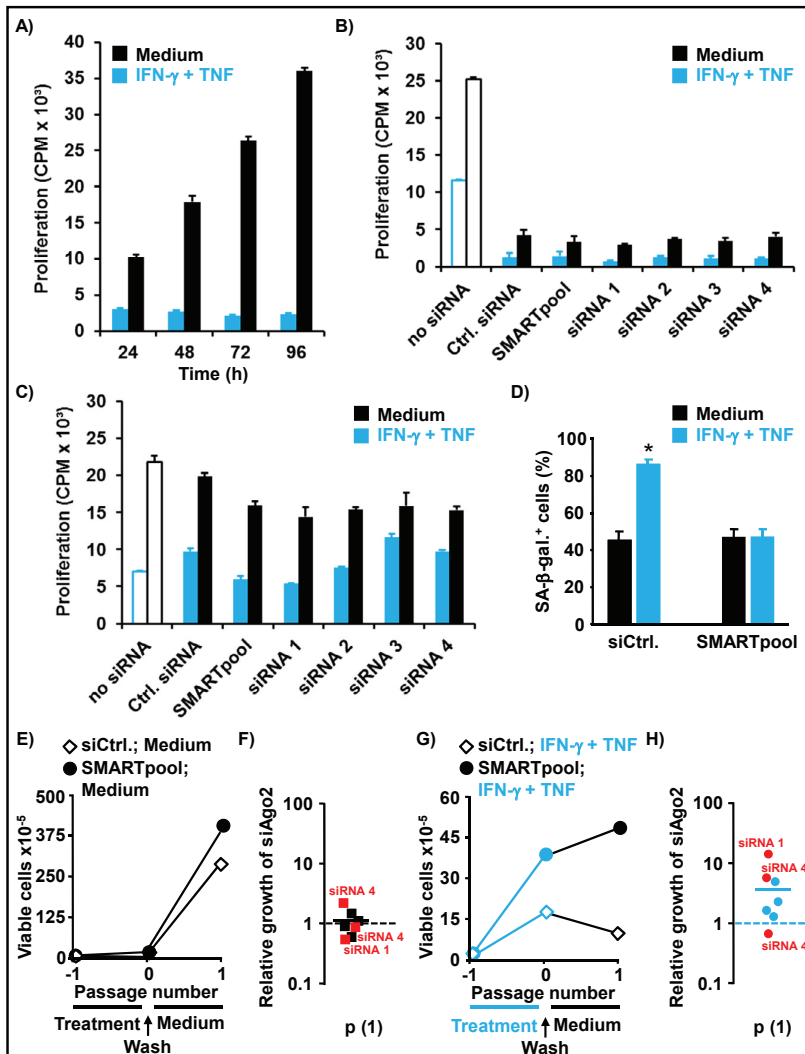


**Fig. 6.** Knockdown of Ago2 in A204 cells by the use of siRNA. A, B) Experimental set up for transient, siRNA-mediated downregulation of Ago2 either in the absence (A) or presence of IFN- $\gamma$  + TNF (B). C) Knockdown of Ago2 expression by SMARTpool Ago2-siRNA or by single Ago2-specific siRNAs as measured by qPCR after 24 h or 48 h of incubation. Ago2 expression of non-targeting siRNA controls was set as 1. Data are presented as relative expression (mean of two determinations, each). D) Downregulation of Ago2 protein levels by SMARTpool Ago2-siRNA or by single Ago2-specific siRNAs as determined by western blot after 48 h of incubation.

**Fig. 7.** Influence of Ago2 knockdown on  $\text{INF-}\gamma$  and TNF mediated growth behavior of A204 cells. A) Proliferation of cytokine-treated (blue bars) or medium-treated (black bars) A204 cells as measured by [ $^3\text{H}$ ]-thymidine incorporation (mean  $\pm$  s.e.m., n=6). B) A204 cells were treated with Ago2- or Ctrl.-siRNAs either in the absence (closed black bars) or presence (closed blue bars) of  $\text{INF-}\gamma$  + TNF. Simultaneously, A204 cells were also incubated without siRNAs in medium alone (open black bar) or with the cytokine cocktail (open blue bar). After 48 h of incubation, cellular proliferation was assessed by the uptake of [ $^3\text{H}$ ]-



thymidine (mean  $\pm$  s.e.m., n=6). C) After 48 h treatment with Ago2- or Ctrl.-siRNAs, either in the absence (closed black bars) or presence (closed blue bars) of  $\text{INF-}\gamma$  + TNF, A204 cells were reseeded without the stressors to analyze their proliferative capacity during the following 72 h using [ $^3\text{H}$ ]-thymidine. Additionally, the growth behavior of A204 cells preincubated for 48 h without siRNAs in medium alone (open black bar) or with the cytokine cocktail (open blue bar) was also measured 72 h after reseeding (mean  $\pm$  s.e.m., n=6). D) A204 cells were treated with Ctrl.-siRNA (left) or SMARTpool Ago2-siRNA (right) for 48 h, either in the absence (medium) or presence of  $\text{INF-}\gamma$  + TNF. 72 h after removal of the siRNAs and cytokines, SA- $\beta$ -gal activity was measured (mean  $\pm$  s.e.m., n=6). \*P<0.05 from medium-treated control. E, F) Growth curves of Ctrl.-siRNA- (open diamonds) or Ago2-siRNA-treated A204 cells (closed dots) in the absence of  $\text{INF-}\gamma$  + TNF for 48 h (E), and relative growth of siAgo2-treated cells at p (1) after removal of the siRNAs (n=7). Cellular growth of non-targeting siRNA controls were set as 1 (F). G, H) Growth curves of Ctrl.-siRNA- (open diamonds) or Ago2-siRNA-treated A204 cells (closed dots) in the presence of  $\text{INF-}\gamma$  + TNF for 48 h (G), and relative growth of siAgo2-treated cells at p (1) after removal of the stressors (n=7). Cellular growth of non-targeting siRNA controls was set as 1 (H). CPM = counts per minute (A-C). siCtrl.=non-targeting pool siRNA; siAgo2=Ago2 SMARTpool siRNA (A-H).

## Discussion

Ago2 is a prominent member of the argonaute protein family. The protein combines RNA binding properties with an intrinsic enzyme activity and is thus a central part of the RNA silencing machinery [2]. Besides its role as the enzymatic component of the cytosolic RISC, translocation of Ago2 into the nucleus has been described [17, 22]. In addition, detailed analysis of the subcellular localization of Ago2 revealed that the protein also associates physically with the rough endoplasmic reticulum [23]. This fits well with our high resolution immunofluorescence pictures showing a perinuclear localization of Ago2, and with our observation that Ago2 may shuttle between the cytosol and the nucleus. Whereas the molecular regulation of Ago2 as part of the RISC or as part of the nuclear gene silencing machinery has been extensively studied, not that much is known about the roles of Ago2 in superordinated cellular processes, such as apoptosis, differentiation, proliferation or permanent growth arrest. For example, it has been demonstrated that the activity of Ago2 is regulated by phosphorylation/dephosphorylation [24-26]. These data clearly show that (i) an Ago2 phosphorylation cycle regulates the interactions of miRNAs with their targets [26], (ii) the epidermal growth factor receptor (EGFR) enhances Ago2 phosphorylation which in turn inhibits miRNA processing [24] and (iii) phosphorylation of Ago2 at the amino acid residue Tyr 393 inhibits loading with miRNAs and miRNA-mediated gene silencing [25]. According to these data, phosphorylation of Ago2 correlates with a disturbed function as a gene silencer. In this line, preliminary data from our laboratory show that cytokine treatment of cancer cells leads to a rapid dephosphorylation of Ago2 thereby pointing to activation of its gene silencing function (data not shown).

As far as the role of Ago proteins in essential cellular pathways is concerned, several reports point to Ago-dependent regulation of programmed cell death or apoptosis [27-29]. For example, evidence has been provided that Ago2/miR-21 targets large tumor suppressor kinase 1 (LATS1) thereby inhibiting apoptosis in T cells [29]. This miRNA-mediated mechanism might explain the involvement of Ago2 in this process, as apoptosis is a rapidly proceeding cellular pathway with activation of the executioner enzymes, i.e. caspases, as early as 10 h to 48 h after challenge with the death-inducing substances [30, 31]. In addition, Ago2 downregulation has been associated with apoptosis induction in prostate cancer cells [28]. Thus, Ago2 seems to counteract apoptosis. On the other hand, as demonstrated in the present study for extrinsic, cytokine-induced growth inhibition, and by others for intrinsic, oncogene-induced senescence [17, 25], Ago2 nuclear translocation favors growth arrest. This is an interesting aspect as it is known that senescent cells are resistant to stimulus-specific apoptosis induction [32], but can be specifically cleared by targeted apoptosis induction using proapoptotic FOXO4-derived peptides [33].

Senescence induction in tumors is an intrinsic cellular response to oncogenic signaling that may have evolved alongside apoptosis to suppress tumorigenesis [34]. However, in contrast to apoptosis, senescent cells are viable over a long period of time. In addition, they have the potential to influence neighboring tumor cells or cells of the tumor microenvironment through secreted soluble molecules, known as the senescence-associated secretory phenotype (SASP) [35-37]. Interestingly, the transcellular regulation of senescence by soluble factors is also true vice versa: our findings that specific immune cells control cancer cells by cytokine secretion and CIS [12] demonstrate that immune surveillance of tumors [16, 38] takes advantage of extrinsic, receptor-mediated senescence pathways. CIS is now accepted as a non-cell-autonomous inducer of cellular senescence that limits tumorigenesis [15], and several different cytokines or cytokine mixtures, e.g. interleukin-6 (IL-6) [39], transforming growth factor beta (TGF- $\beta$ ) [40], or IFN- $\gamma$  and TNF [12-14], have been implicated in senescence induction.

## Conclusion

In conclusion, we show here that the small RNA-binding protein Ago2 rapidly translocates into the nucleus of senescence-prone cancer cells after stimulation with the T<sub>H</sub>1 cell cytokines IFN- $\gamma$  and TNF. Ago2 translocation in cancer cells is already observed after 24 h and reached a maximum after 48 h of treatment thereby preceding the induction of permanent growth arrest which takes at least 96 h continuous presence of IFN- $\gamma$  and TNF [12]. We also show the suppression of important Ago2-regulated cell cycle control genes as early as 24 h after cytokine challenge thereby pointing to a functional role of Ago2 in the signal transduction of CIS. In addition, the role of Ago2 during the first 48 h of cytokine treatment was supported by transient Ago2 downregulation, and subsequent measurement of the senescence marker SA- $\beta$ -gal [18] and the growth characteristics of the cells. Future studies will aim to decipher (i) the signals that mediate Ago2 translocation in CIS, e.g. phosphorylation/dephosphorylation and binding to nuclear import proteins, (ii) the binding partners of Ago2 which build up the repressor complex that leads to transcriptional silencing of the important cell cycle control genes in CIS and (iii) the role of Ago2 in the later phases of CIS, i.e. in the phase of permanent growth arrest which, at least *in vitro*, may last several weeks.

## Acknowledgements

Martin Röcken and Thomas Wieder share senior authorship. The authors would like to thank S. Weidemann and V. Galinat for expert technical assistance. This work was supported by the Wilhelm Sander Foundation (2012.056.3 to M.R.), German Cancer Aid (application numbers 109037 and 110664 to M.R.), and German Research Association (TRR-SFB 156, DFG RO 764/14-1 and DFG RO 764/15-2 to M.R. and DFG WI 1279/4-1 to T.W.). The group of O.B. is supported by grants from ANR-BMFT, Fondation ARC pour la recherche sur le Cancer, INSERM, and the National Cancer Institute of the National Institutes of Health under Award Number R01CA136533. O.B. is a CNRS Research Director DR2.

We acknowledge support by Deutsche Forschungsgemeinschaft and open Access Publishing Fund of University of Tübingen.

## Disclosure Statement

No conflicts of interest, financial or otherwise, are declared by the authors.

## References

- 1 Farazi TA, Juranek SA, Tuschl T: The growing catalog of small RNAs and their association with distinct Argonaute/Piwi family members. *Development* 2008;135:1201-1214.
- 2 Meister G, Landthaler M, Patkaniowska A, Dorsett Y, Teng G, Tuschl T: Human Argonaute2 mediates RNA cleavage targeted by miRNAs and siRNAs. *Mol Cell* 2004;15:185-197.
- 3 Castel SE, Martienssen RA: RNA interference in the nucleus: roles for small RNAs in transcription, epigenetics and beyond. *Nat Rev Genet* 2013;14:100-112.
- 4 Buckley BA, Burkhart KB, Gu SG, Spracklin G, Kershner A, Fritz H, Kimble J, Fire A, Kennedy S: A nuclear Argonaute promotes multigenerational epigenetic inheritance and germline immortality. *Nature* 2012;489:447-451.
- 5 Pérez-Mancera PA, Young AR, Narita M: Inside and out: the activities of senescence in cancer. *Nat Rev Cancer* 2014;14:547-558.
- 6 Muñoz-Espín D, Serrano M: Cellular senescence: from physiology to pathology. *Nat Rev Mol Cell Biol* 2014;15:482-496.



- 7 Michaloglou C, Vredeveld LC, Soengas MS, Denoyelle C, Kuilman T, van der Horst CM, Majoor DM, Shay JW, Mooi WJ, Peeper DS: BRAFE600-associated senescence-like cell cycle arrest of human naevi. *Nature* 2005;436:720-724.
- 8 Collado M, Gil J, Efeyan A, Guerra C, Schuhmacher AJ, Barradas M, Benguría A, Zaballos A, Flores JM, Barbacid M, Beach D, Serrano M: Tumour biology: senescence in premalignant tumours. *Nature* 2005;436:642.
- 9 Takaoka M, Harada H, Deramandt TB, Oyama K, Andl CD, Johnstone CN, Rhoades B, Enders GH, Opitz OG, Nakagawa H: Ha-Ras(G12V) induces senescence in primary and immortalized human esophageal keratinocytes with p53 dysfunction. *Oncogene* 2004;23:6760-6768.
- 10 Schmitt CA, Fridman JS, Yang M, Lee S, Baranov E, Hoffman RM, Lowe SW: A senescence program controlled by p53 and p16INK4a contributes to the outcome of cancer therapy. *Cell* 2002;109:335-346.
- 11 Haferkamp S, Borst A, Adam C, Becker TM, Motschenbacher S, Windhövel S, Hufnagel AL, Houben R, Meierjohann S: Vemurafenib induces senescence features in melanoma cells. *J Invest Dermatol* 2013;133:1601-1609.
- 12 Braumüller H, Wieder T, Brenner E, Aßmann S, Hahn M, Alkhaled M, Schilbach K, Essmann F, Kneilling M, Griessinger C, Ranta F, Ullrich S, Mocikat R, Braungart K, Mehra T, Fehrenbacher B, Berdel J, Niessner H, Meier F, van den Broek M et al.: T-helper-1-cell cytokines drive cancer into senescence. *Nature* 2013;494:361-365.
- 13 Schilbach K, Alkhaled M, Welker C, Eckert F, Blank G, Ziegler H, Sterk M, Müller F, Sonntag K, Wieder T, Braumüller H, Schmitt J, Eyrich M, Schleicher S, Seitz C, Erbacher A, Pichler BJ, Müller H, Tighe R, Lim A et al.: Cancer-targeted IL-12 controls human rhabdomyosarcoma by senescence induction and myogenic differentiation. *Oncoimmunology* 2015;4:e1014760.
- 14 Hubackova S, Kucerova A, Michlits G, Kyjacova L, Reinis M, Korolov O, Bartek J, Hodny Z: IFN $\gamma$  induces oxidative stress, DNA damage and tumor cell senescence via TGF $\beta$ /SMAD signaling-dependent induction of Nox4 and suppression of ANT2. *Oncogene* 2016;35:1236-1249.
- 15 Wieder T, Brenner E, Braumüller H, Bischof O, Röcken M: Cytokine-induced senescence for cancer surveillance. *Cancer Metastasis Rev* 2017;36:357-365.
- 16 Schreiber RD, Old LJ, Smyth MJ: Cancer immunoediting: integrating immunity's roles in cancer suppression and promotion. *Science* 2011;331:1565-1570.
- 17 Benhamed M, Herbig U, Ye T, Dejean A, Bischof O: Senescence is an endogenous trigger for microRNA-directed transcriptional gene silencing in human cells. *Nat Cell Biol* 2012;14:266-275.
- 18 Itahana K, Campisi J, Dimri GP: Methods to detect biomarkers of cellular senescence: the senescence-associated beta-galactosidase assay. *Methods Mol Biol* 2007;371:21-31.
- 19 Friedrich K, Wieder T, von Haefen C, Radetzki S, Jänicke R, Schulze-Osthoff K, Dörken B, Daniel PT: Overexpression of caspase-3 restores sensitivity for drug-induced apoptosis in breast cancer cell lines with acquired drug resistance. *Oncogene* 2001;20:2749-2760.
- 20 Ghashghaieina M, Cluitmans JC, Toulany M, Saki M, Köberle M, Lang E, Dreischer P, Biedermann T, Duszenko M, Lang F, Bosman GJ, Wieder T: Age sensitivity of NF $\kappa$ B abundance and programmed cell death in erythrocytes induced by NF $\kappa$ B inhibitors. *Cell Physiol Biochem* 2013;32:801-813.
- 21 Wieder T, Braumüller H, Brenner E, Zender L, Röcken M: Changing T-cell enigma: cancer killing or cancer control? *Cell Cycle* 2013;12:3146-3153.
- 22 Kim BS, Jung JS, Jang JH, Kang KS, Kang SK: Nuclear Argonaute 2 regulates adipose tissue-derived stem cell survival through direct control of miR10b and selenoprotein N1 expression. *Aging Cell* 2011;10:277-291.
- 23 Stalder L, Heusermann W, Sokol L, Trojer D, Wirz J, Hean J, Fritzsche A, Aeschmann F, Pfanzagl V, Basselet P, Weiler J, Hintersteiner M, Morrissey DV, Meisner-Kober NC: The rough endoplasmic reticulum is a central nucleation site of siRNA-mediated RNA silencing. *EMBO J.* 2013;32:1115-1127.
- 24 Shen J, Xia W, Khotskaya YB, Huo L, Nakanishi K, Lim SO, Du Y, Wang Y, Chang WC, Chen CH, Hsu JL, Wu Y, Lam YC, James BP, Liu X, Liu CG, Patel DJ, Hung MC: EGFR modulates microRNA maturation in response to hypoxia through phosphorylation of AGO2. *Nature* 2013;497:383-387.
- 25 Yang M, Haase AD, Huang FK, Coulis G, Rivera KD, Dickinson BC, Chang CJ, Pappin DJ, Neubert TA, Hannon GJ, Boivin B, Tonks NK: Dephosphorylation of tyrosine 393 in argonaute 2 by protein tyrosine phosphatase 1B regulates gene silencing in oncogenic RAS-induced senescence. *Mol Cell* 2014;55: 782-790.

- 26 Golden RJ, Chen B, Li T, Braun J, Manjunath H, Chen X, Wu J, Schmid V, Chang TC, Kopp F, Ramirez-Martinez A, Tagliabracci VS, Chen ZJ, Xie Y, Mendell JT: An Argonaute phosphorylation cycle promotes microRNA-mediated silencing. *Nature* 2017;542:197-202.
- 27 Parisi C, Giorgi C, Batassa EM, Braccini L, Maresca G, D'agnano I, Caputo V, Salvatore A, Pietrolati F, Cogoni C, Catalanotto C: Ago1 and Ago2 differentially affect cell proliferation, motility and apoptosis when overexpressed in SH-SY5Y neuroblastoma cells. *FEBS Lett* 2011;585:2965-2971.
- 28 Bian XJ, Zhang GM, Gu CY, Cai Y, Wang CF, Shen YJ, Zhu Y, Zhang HL, Dai B, Ye DW: Down-regulation of Dicer and Ago2 is associated with cell proliferation and apoptosis in prostate cancer. *Tumour Biol* 2014;35:11571-11578.
- 29 Teteloshvili N, Smigielska-Czepiel K, Yuan Y, Seitz A, de Jong D, Rutgers B, Jellema P, van der Lei RJ, Slezak-Prochazka I, Brouwer E, Boots AM, Kroesen BJ, van den Berg A, Kluiver J: Argonaute 2 immunoprecipitation revealed large tumor suppressor kinase 1 as a novel proapoptotic target of miR-21 in T cells. *FEBS J* 2017;284:555-567.
- 30 Prokop A, Wrasidlo W, Lode H, Herold R, Lang F, Henze G, Dörken B, Wieder T, Daniel PT: Induction of apoptosis by enediyne antibiotic calicheamicin thetaII proceeds through a caspase-mediated mitochondrial amplification loop in an entirely Bax-dependent manner. *Oncogene* 2003;22:9107-9120.
- 31 Wieder T, Eßmann F, Prokop A, Schmelz K, Schulze-Osthoff K, Beyaert R, Dörken B, Daniel, PT: Activation of caspase-8 in drug-induced apoptosis of B-lymphoid cells is independent of CD95/Fas receptor-ligand interaction and occurs downstream of caspase-3. *Blood* 2001;97:1378-1387.
- 32 Kim SY, Ryu SJ, Kang HT, Choi HR, Park SC: Defective nuclear translocation of stress-activated signaling in senescent diploid human fibroblasts: a possible explanation for aging-associated apoptosis resistance. *Apoptosis* 2011;16:795-807.
- 33 Baar MP, Brandt RMC, Putavet DA, Klein JDD, Derks KWJ, Bourgeois BRM, Stryeck S, Rijkse Y, van Willigenburg H, Feijtel DA, van der Pluijm I, Essers J, van Cappellen WA, van IJcken WF, Houtsmuller AB, Pothof J, de Bruin RWF, Madl T, Hoeijmakers JHJ, Campisi J, de Keizer PLJ: Targeted apoptosis of senescent cells restores tissue homeostasis in response to chemotoxicity and aging. *Cell* 2017;169:132-147.
- 34 Childs BG, Baker DJ, Kirkland JL, Campisi J, van Deursen JM: Senescence and apoptosis: dueling or complementary cell fates? *EMBO Rep* 2014;15:1139-1153.
- 35 Demaria M, O'Leary MN, Chang J, Shao L, Liu S, Alimirah F, Koenig K, Le C, Mitin N, Deal AM, Alston S, Academia EC, Kilmarx S, Valdovinos A, Wang B, de Bruin A, Kennedy BK, Melov S, Zhou D, Sharpless NE et al.: Cellular Senescence Promotes Adverse Effects of Chemotherapy and Cancer Relapse. *Cancer Discov* 2017;7:165-176.
- 36 McHugh D, Gil J: Senescence and aging: Causes, consequences, and therapeutic avenues. *J Cell Biol* 2018;217:65-77.
- 37 He S, Sharpless NE: Senescence in Health and Disease. *Cell* 2017;169:1000-1011.
- 38 Chow MT, Möller A, Smyth MJ: Inflammation and immune surveillance in cancer. *Semin Cancer Biol* 2012;22:23-32.
- 39 Kojima H, Inoue T, Kunimoto H, Nakajima K: IL-6-STAT3 signaling and premature senescence. *JAKSTAT* 2013;2:e25763.
- 40 Reimann M, Lee S, Loddenkemper C, Dörr JR, Tabor V, Aichele P, Stein H, Dörken B, Jenuwein T, Schmitt CA: Tumor stroma-derived TGF-beta limits myc-driven lymphomagenesis via Suv39h1-dependent senescence. *Cancer Cell* 2010;17:262-272.

## Immune checkpoint blockade therapy



Thomas Wieder, PhD, Thomas Eigentler, MD, Ellen Brenner, Dipl Biol, and Martin Röcken, MD Tübingen, Germany

Immune checkpoints are accessory molecules that either promote or inhibit T-cell activation. Two inhibitory molecules, cytotoxic T-lymphocyte antigen 4 (CTLA-4) and programmed cell death protein 1 (PD-1), got high attention, as inhibition of CTLA-4 or PD-1 signaling provides the first immune therapy that significantly improves the survival of patients with metastatic solid cancers. Inhibition of CTLA-4 or PD-1 was first studied in and approved for patients with metastatic melanoma. Blocking immune checkpoints is also efficient in non-small-cell lung cancer, renal cell cancers, hypermutated gastrointestinal cancers, and others. Immune responses, whether directed against infections or against tumors, are divided into 2 phases: an initiation phase and an activation phase, where the immune system recognizes a danger signal and becomes activated by innate signals to fight the danger. This reaction is fundamental for the control of infections and cancer, but needs to be turned off once the danger is controlled, because persistence of this activation ultimately causes severe tissue damage. Therefore, each activation of the immune system is followed by a termination phase, where endogenous immune suppressor molecules arrest immune responses to prevent harmful damage. In the case of cancer immune therapies, therapeutic approaches classically enhanced the initiation and activation of immune responses to increase the emergence and the efficacy of cytotoxic T lymphocytes (CTL) against cancers. In sharp contrast, immune checkpoint blockade focuses on the termination of

immune responses by inhibiting immune suppressor molecules. It thus prevents the termination of immune responses or even awakes those CTLs that became exhausted during an immune response. Therefore, blocking negatively regulating immune checkpoints restores the capacity of exhausted CTL to kill the cancer they infiltrate. In addition, they drive surviving cancer cells into a still poorly defined state of dormancy. As the therapy also awakes self-reactive CTL, one downside of the therapy is the induction of organ-specific autoimmune diseases. The second downside is the exorbitant drug price that withdraws patients in need from a therapy that was developed by academic research, which impairs further academic treatment development and financially charges the public health system. (J Allergy Clin Immunol 2018;142:1403-14.)

**Key words:** Cytokine-induced senescence, cytotoxic T lymphocytes, interferon, T helper cells, tumor dormancy, tumor eradication, autoimmunity

Modern cancer immune therapy developed over more than 50 years.<sup>1</sup> Bone marrow transplantation and donor T lymphocyte transfusion<sup>2</sup> showed that T-cell-dependent immune responses can control hematological malignancies. Yet, solid cancers were largely resistant to cancer immune therapy in humans. Around 2010, the 50 years of basic and clinical research then provided the rationale to investigate immune checkpoint blockade (ICB) as therapy of solid cancer. Important insights came from data showing that cancer can be killed by cytotoxic T lymphocytes (CTL) or by natural killer cells,<sup>3</sup> and from the demonstration that IFN- $\gamma$ -producing cluster of differentiation (CD) 4 T<sub>H</sub>1 can contain solid tumors.<sup>4,5</sup> Importantly, the description of tumor-associated antigens (TAAs),<sup>6</sup> which are a requirement for tailored tumor immune therapy,<sup>7</sup> paved the way for clinical use. Yet, this scientific progress did not directly result in the development of efficient immune therapy for patients with established cancers.

Cancers are less efficient in activating innate immunity than are infections by pathogens. Therefore, optimization of the immune priming with dendritic cells,<sup>8</sup> mRNA vaccination against personalized neoantigens,<sup>9-11</sup> or novel innate stimuli as adjuvants, such as Toll-like receptor ligands,<sup>12,13</sup> became an important research focus (Fig 1, A and B). Alternatively, the need of immune activation was circumvented by the transfer of TAA-reactive CTL.<sup>14</sup> All these approaches of immune activation were successful in single patients, but none of them brought significant improvement in clinical studies, with the exception of a synthetic long-peptide vaccine in patients with vulvar intraepithelial neoplasia.<sup>15</sup>

Specific T-cell activation requires permission by the trimeric complex of T-cell receptor (TCR)-antigen-MHC (TCR-antigen-MHC). Formation of this complex results in the expression of accessory molecules that subsequently control activation, migration, homing, and silencing of the T cells. Accessory molecules

From the Department of Dermatology, Eberhard Karls University.

The work of the authors is supported by the Wilhelm Sander Stiftung (grant no. 2012.056.3), the Deutsche Krebshilfe (grant no. 110664), and the Deutsche Forschungsgemeinschaft (grant nos. DFG Ro764/14-1, Ro764/15-1, WI 1279/4-1, and SFB-TR 156).

Disclosure of potential conflict of interest: T. Eigentler received consultancy fees from Bristol-Myers Squibb, Merck-Serono, and Roche and payment for lectures from MSD and Novartis. M. Röcken received a grant from Deutsche Forschungsgemeinschaft (grant no. SFB TRR 156/1 TP B06) and Deutsche Forschungsgemeinschaft (grant no. RO 764/15-1 AOBJ) for this work and from Deutsche Forschungsgemeinschaft for other works; consultancy fees from both Almirall Hermal and Biogen Idec for other works, and Regeneron; is employed with Government Baden-Württemberg; has stock options from Bristol-Myers Squibb and Merck; received travel expenses from Deutsche Dermatologische Gesellschaft e. V., the European Academy of Dermatology and Venereology, and diverse universities and public funding organizations (eg, Deutsche Krebshilfe e. V.); and holds patent DE 10 2012 024 749.4. The rest of the authors declare that they have no relevant conflicts of interest.

Received for publication July 14, 2017; revised February 9, 2018; accepted for publication February 27, 2018.

Available online March 27, 2018.

Corresponding author: Martin Röcken, MD, Department of Dermatology, Eberhard Karls University, Liebermeisterstr. 25, 72076 Tübingen, Germany. E-mail: mrocken@med.uni-tuebingen.de.

The CrossMark symbol notifies online readers when updates have been made to the article such as errata or minor corrections

0091-6749/\$36.00

© 2018 Published by Elsevier Inc. on behalf of the American Academy of Allergy, Asthma & Immunology

<https://doi.org/10.1016/j.jaci.2018.02.042>

**Abbreviations used**

BRAF:	Serine/threonine-protein kinase
BRAF <sup>V600E/K</sup> :	Serine/threonine-protein kinase B-Raf carrying the respective V600 mutation
CD:	Cluster of differentiation
CTL:	Cytotoxic T lymphocytes
CTLA-4:	Cytotoxic T-lymphocyte-associated antigen 4
ICB:	Immune checkpoint blockade
JAK1/2:	Janus kinase 1 or 2
NSCLC:	Non-small-cell lung cancer
PD-1:	Programmed cell death protein 1
PD-L1:	Programmed death-ligand 1
PD-L2:	Programmed death-ligand 2
TAA:	Tumor-associated antigen
TCR:	T-cell receptor

regulating the activation and silencing of T cells are now called immune checkpoints. While some researchers focused on the enhancement of T-cell priming (Fig 1, B; see also above), others developed immune therapies based on the inhibition of negative signals or signaling pathways, like CD25,<sup>16</sup> IL-10,<sup>17</sup> indoleamine 2,3-dioxygenase,<sup>18</sup> the TGF- $\beta$ -docking receptor glycoprotein A repetitions predominant/TGF- $\beta$  axis,<sup>19</sup> cytotoxic T-lymphocyte-associated antigen 4 (CTLA-4),<sup>20</sup> or programmed cell death protein 1 (PD-1).<sup>21</sup> Blocking such negative signals either delays or even prevents T-cell silencing (Fig 1, C). This may, on one side, induce tumor surveillance and, on the other, induce organ-specific autoimmune diseases, as expected.<sup>21</sup>

All immune therapies developed so far did not only fail as treatment of established cancers but also as treatment of chronic infections, like chronic lymphochoriomeningitis virus. Lymphochoriomeningitis virus-specific T cells become exhausted during chronic infection. Exhausted T cells originating from either chronic infections or from the cancer microenvironment both express PD-1<sup>22</sup> and are functionally indistinguishable.<sup>23</sup>

In 2006, Barber et al<sup>24</sup> found that exhausted T cells can be reactivated *in vivo* with an anti-PD-1 antibody (mAb) by studying chronic lymphochoriomeningitis virus disease. *In vivo* treatment not only restored the activity of exhausted CTL but was also the first successful immune therapy of a chronic infection. Subsequent academic work then showed that PD-1 is also expressed by T cells in the tumor microenvironment, and on tumor cells, such as melanoma<sup>25</sup> or esophageal adenocarcinoma.<sup>26</sup> The ligands of PD-1, programmed death-ligand 1 (PD-L1) and programmed death-ligand 2 (PD-L2), however, are expressed mainly by tumors and antigen-presenting cells in the microenvironment. Moreover, inhibiting the PD-1/PD-L1 interaction was highly efficient in the treatment of experimental tumors, including melanomas.<sup>22</sup> These data showed for the first time that a paralyzed immune response could be restored. Hence, they provided a rationale to further develop biologic response modifiers,<sup>27,28</sup> in this case antibodies against immune suppressor molecules, as an immune therapy for patients with either chronic infection, like chronic hepatitis, or metastatic cancer.

### T-CELL EXHAUSTION IN THE TUMOR MICROENVIRONMENT

Mouse PD-1 has originally been described in 1992 as a novel member of the immunoglobulin gene superfamily that is

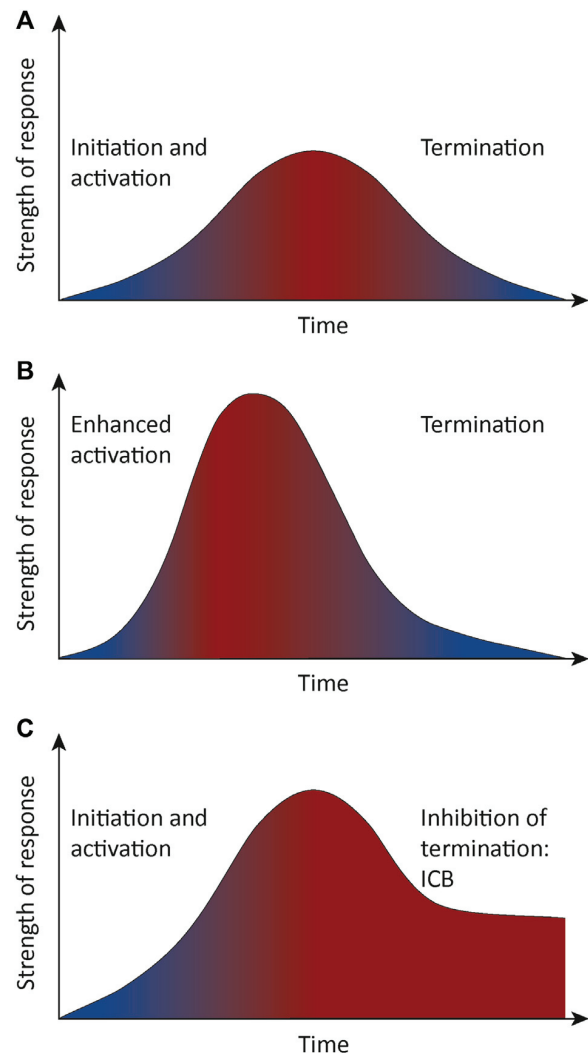


**FIG 1.** Time course of immune responses with or without immune therapy. **A**, Biphasic courses of immune responses. Directly after infection, an immune response becomes initiated and later on fully activated. After reaching the peak of immune activation, the immune response will be silenced and terminated. **B**, Classical immune therapy-induced course of immune responses. Classical immune therapies are designed to enhance the initiation and activation rate of the immune response. After reaching the peak with a steeper slope, the immune response becomes terminated at a normal rate. **C**, Novel immune therapy-induced course of immune responses during ICB. After normal initiation and activation phases of the immune response, ICB therapies (anti-CTLA-4 or anti-PD-1 or anti-PD-L1 antibodies or in combination) stop the termination and prolong the activation phase of the immune response.

selectively expressed on thymoma cells after apoptosis induction.<sup>29</sup> It took about a decade to decipher the physiological role and the signaling pathways of this immunoinhibitory receptor. The first reports that PD-1 may play a crucial role in maintaining self-tolerance came from the description of PD-1 knockout mice: depending on their genetic background, these mice developed different autoimmune diseases such as systemic lupus erythematosus<sup>30</sup> or autoimmune cardiomyopathy.<sup>31</sup> In 2000, the novel B7 family member PD-L1<sup>32</sup> and in 2001 PD-L2<sup>33</sup> were described as ligands for PD-1. Both PD-1/PD-L1 and PD-1/PD-L2 binding

inhibit T-cell activation. Detailed analyses revealed important molecular mechanisms and intracellular pathways leading to T-cell anergy, inhibition of cell growth, and attenuation of T-cell effector function (for review, see Okazaki et al<sup>21</sup>). The PD-L1/PD-1 interaction leads to the recruitment of the tyrosine phosphatase Src-homology 2 domain-containing tyrosine phosphatase,<sup>34</sup> which then in turn dephosphorylates and inactivates downstream effector signaling molecules of the T- or B-cell receptors, such as Zap70 in T cells<sup>35,36</sup> or Syk in B cells.<sup>34</sup> Thus, signaling through PD-1 mainly impairs the effector phase of an immune response through cell-intrinsic inhibition of the antigen-specific signaling (Fig 2, A). This discriminates PD-1 from CTLA-4, which has a distinct mechanism of immune suppression.<sup>37</sup> Specific T-cell activation requires at least binding of the trimolecular TCR-antigen-MHC complex and an important costimulatory molecule, namely, CD28,<sup>38</sup> binding with low affinity to CD80 or CD86 (Fig 2, B). During this T-cell activation, CTLA-4, which represents another accessory molecule that attenuates T-cell activation, starts to be expressed on the cell membrane. Because of higher affinity, CTLA-4 then captures CD80 and CD86 on the antigen-presenting cells. As a result, CD80 and CD86 are no longer able to occupy the binding sites of CD28. CTLA-4 thus not only suppresses T-cell activation but also abrogates the costimulatory effect of CD28 on effector T cells (Fig 2, C). In line with the clinical data demonstrating that combined treatment with an anti-CTLA-4 mAb and an anti-PD-1 mAb is more efficient in the acute cancer remission phase than either therapy alone,<sup>39,40</sup> recent experimental data show that the costimulatory CD28 pathway enhances the rescue of exhausted CTL by anti-PD-1 mAb. Yet, the exact molecular mechanisms underlying this effect remain to be elucidated.<sup>41</sup> In view of the fact that deeply exhausted CTL cannot be rescued because of the specific methylation status of their DNA,<sup>42</sup> the question has to be answered whether the CD28-mediated enhancement of the CTL response results from an improved T-cell recruitment, or from a direct interaction between the CD28 and the PD-1 signaling cascade *in vivo*.<sup>41</sup>

Data suggesting that the tumor or the tumor microenvironment may dampen the immunosurveillance of tumors through negatively regulating accessory molecules came from the observation that overexpression of PD-L1 on plasmacytoma cells enhances cancer growth and invasiveness by inhibition of the cytolytic, antitumor activity of CD8<sup>+</sup> T cells.<sup>43</sup> In line with this, a correlation of PD-L1 expression with the appearance of exhausted T cells in the tumor microenvironment was frequently observed. Recent characterization of such exhausted, PD-1-expressing T cells suggests a critical role for their metabolic reprogramming in the glucose-poor tumor microenvironment. The data show that activated T cells need enhanced glycolytic activity. In addition, the glycolytic metabolite phosphoenolpyruvate functions as a crucial regulator of T effector cells by repressing sarco/endoplasmic reticulum Ca<sup>2+</sup>-ATPase. This repression, in turn, sustains Ca<sup>2+</sup>-dependent nuclear factor of activated T-cell signaling.<sup>44</sup> Thus, overexpression of the gluconeogenic enzyme phosphoenolpyruvate carboxykinase 1 in tumor-specific T<sub>H</sub> or in CTL leads to enhanced phosphoenolpyruvate levels, thereby strengthening their antitumor activity.<sup>44</sup>

This is in accordance with a second report investigating the balance between anabolic and catabolic pathways and the regulatory role of the mitochondria in activated T cells.<sup>45</sup> The authors describe 2 different types of mitochondria: (1) punctuated

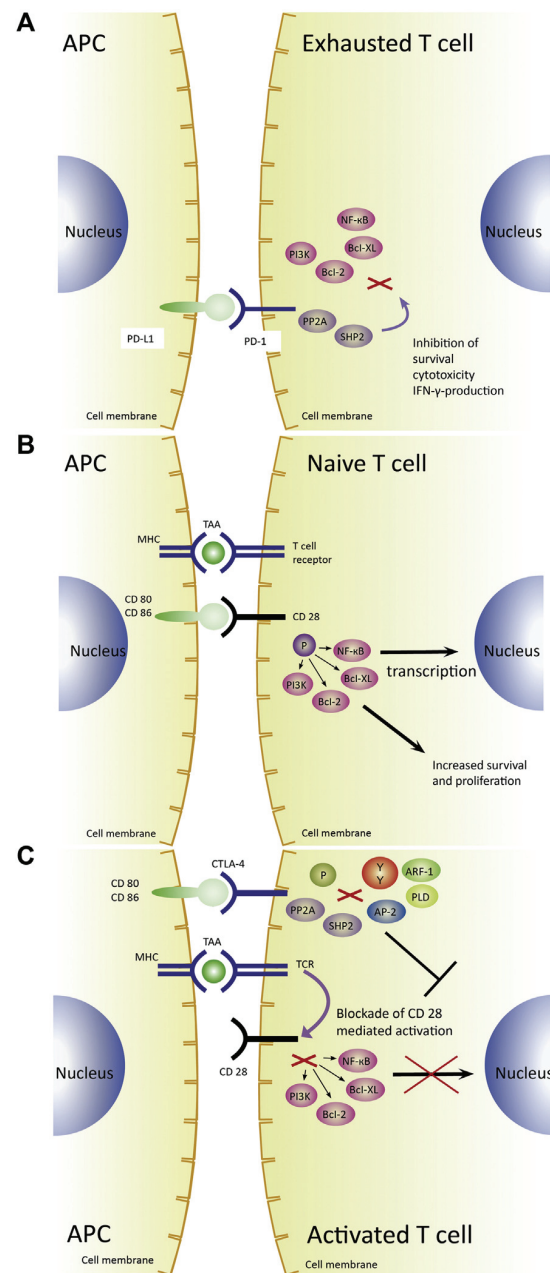


**FIG 2.** Molecular mechanisms of T-cell inhibition by immune checkpoints. **A**, PD-1 being expressed on T cells inhibits prosurvival pathways, induces cytotoxicity, and downregulates IFN- $\gamma$  production after binding to PD-L1 on APCs. Anti-PD-1 antibodies interfere with PD-1/PD-L1 interaction, thereby reactivating the T-cell functions (not shown). **B**, Activation of naive T cells proceeds via TAA-mediated T-cell receptor stimulation and costimulation of CD28 by CD80/86 expressed on APCs. This leads to increased proliferation of antigen-specific T cells. **C**, Once T cells are activated, CTLA-4 becomes expressed on T cells. Because of its higher affinity to CD80/CD86, CTLA-4 replaces CD28 and inhibits the T-cell activation. Anti-CTLA-4 antibodies interfere with CD80/CD86/CTLA-4 interactions, thereby suppressing the negative signaling and reactivating CD28-mediated T-cell signaling (not shown). *AP-2*, Activating protein 2; *APC*, antigen-presenting cell; *ARF-1*, ADP-ribosylation factor 1; *Bcl-2*, B-cell lymphoma-2; *Bcl-XL*, B-cell lymphoma-XL; *CD28*, 80, 86, cluster of differentiation 28, 80, 86; *NF- $\kappa$ B*, nuclear factor  $\kappa$ B; *PI3K*, phosphatidylinositol-4,5-bisphosphate 3-kinase; *PLD*, phospholipase D; *PP2A*, protein phosphatase 2A; *SHP-2*, Src-homology 2 domain-containing tyrosine phosphatase.

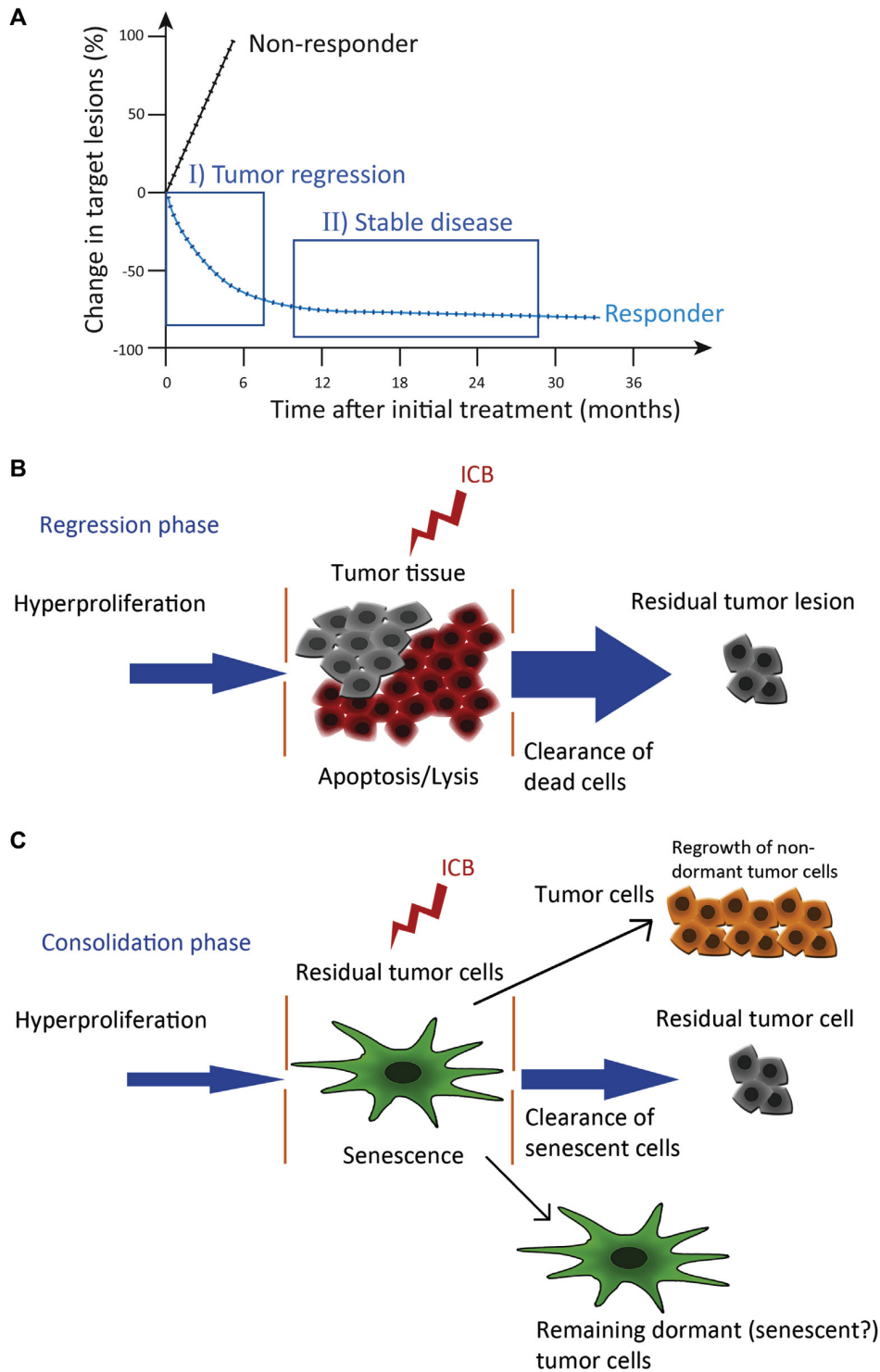


**FIG 3.** Cytotoxic tumor reduction and consolidation phase during ICB. **A**, Change in target lesions in % of the initial value at the start of ICB therapy (modified from Le et al<sup>53</sup> and Topalian et al<sup>54</sup>). Responders (blue line) show a 2-phasic response with a strong decline in the target lesions in the first phase and stable target lesions in the second phase. Nonresponders (black line) show progressive target lesions. **B**, During the first phase, efficient ICB therapy leads to activation of a cytotoxic immune response, leading to intensive tumor cell death via apoptosis and/or lysis. Because the clearance of dead cells by far outweighs hyperproliferation, the tumor regresses. **C**, During the second phase, efficient ICB therapy leads to activation of immune surveillance, leading to tumor cell control by induction of tumor cell dormancy. As dormant/senescent cells hardly proliferate, cell proliferation and cell clearance reach an equilibrium, and the target lesions stay at a constant level for years. However, some tumor cells may escape from proliferation control and start regrowing.

mitochondria in effector T cells, which favor aerobic glycolysis (ie, lactate-producing glycolysis in the presence of oxygen). This leads to enhanced utilization of the glycolytic pathway, mainly not for ATP production but presumably as supply of carbon chains for anabolic pathways. In contrast, (2) preactivated T cells show fused networks in their mitochondria, thereby configuring the electron transport chain and enabling oxidative phosphorylation, instead of aerobic glycolysis. Recently, it was therefore hypothesized that T cells might be manipulated by targeted reprogramming of metabolic pathways,<sup>46</sup> such as glycolysis or gluconeogenesis (see above), also for therapeutic purposes in the presence of immune checkpoint inhibitors.

Besides metabolic reprogramming, exhausted T cells in the tumor microenvironment show an epigenetic landscape that is distinct from that of memory CD8-positive T cells. Most importantly, those cells display functional enhancer maps leading to exhaustion-specific genome editing and altered gene expression.<sup>47</sup>

### CANCER KILLING AND INDUCTION OF CANCER DORMANCY BY REACTIVATION OF EXHAUSTED TUMOR-SPECIFIC T CELLS

The concept of reactivation of exhausted, tumor-specific T cells by ICB was extensively tested in clinical trials. The treatment was especially efficient in patients with metastatic melanoma,<sup>39,40,48,49</sup> but clinical efficacy has also been shown in a series of other advanced cancers, for example, advanced non-small-cell lung cancer (NSCLC),<sup>50</sup> Merkel cell carcinoma,<sup>51</sup> metastatic urothelial cancer,<sup>52</sup> or colon cancers.<sup>53</sup> The analysis of cancer lesions and tumor markers after initiation of ICB revealed a characteristic time course of tumor reduction.<sup>53,54</sup> Following the initiation of an immune response, tumors may first increase in size for up to 3 months,<sup>9</sup> due to the infiltration of T cells and the activation of dendritic cells and macrophages in the tumor microenvironment.<sup>55</sup> Subsequently, during the next 5 to 7 months, the target lesions of responding patients show a strong decline. During this regression phase, some tumors disappear clinically while other target lesions remain stable and can still be detected 2 years after initiation of the ICB (Fig 3, A). Even though complete cancer regression occurs only in a minority of patients, recent data suggest that metastases tend to remain growth-arrested when ICB is discontinued and a state of stable disease is achieved.<sup>56</sup> This situation is operationally best summarized under the term *tumor dormancy*, a condition in which the cancer cells are maintained in a condition of equilibrium. In proliferating tumors, however, this equilibrium is disturbed by hyperproliferation of the cancer cells. These cells sustain proliferative signaling and evade growth suppression by the gain of tumor driver genes and the loss of tumor suppressor genes.<sup>57</sup> During the first phase of ICB, cancerous hyperproliferation is counteracted by infiltration of reactivated, cytotoxic CD8<sup>+</sup> T cells and as a consequence by extensive induction of cancer cell death.<sup>58</sup> Tumor cell death occurs by apoptosis and/or lysis, and clearance of the dead cells then leads to a steep decline in the target lesions (Fig 3, B). This inflammatory and cytotoxic immune response can further be enhanced by combining cancer radiation with anti-CTLA-4 and anti-PD-L1/PD-1: anti-CTLA-4 increases the ratio of cytotoxic CD8<sup>+</sup> T cells to antiinflammatory T regulatory cells, while radiation shapes the TCR repertoire of the expanded peripheral clones, and PD-L1 blockade reverses T-cell exhaustion.<sup>59</sup>

A very similar enhancement of the anti-PD-1-mediated immune response can be achieved by combining oncolytic virotherapy with anti-PD-1 immunotherapy. Intratumoral application of oncolytic viruses followed by a treatment with an anti-PD-1 mAb increases the number of tumor-infiltrating CTL, PD-L1 gene expression, and an IFN- $\gamma$  signature on several cellular subsets inside the tumor.<sup>60</sup> As these reports support the finding that ICB-based immune therapies of larger tumors strictly require the infiltration by CTL,<sup>58</sup> improving the attraction of CTL to disseminated metastases may in the future improve their treatment.

Besides the need of infiltrating CTL, an increasing number of studies show that the efficacy of cancer immune therapies through ICB critically depends on 4 factors: (1) the mutational burden of the tumor,<sup>61,62</sup> (2) the capacity of the tumor to respond to IFN- $\gamma$ ,<sup>63-65</sup> (3) the expression of PD-L1 in the tumor,<sup>50</sup> and (4) the tumor load.<sup>66</sup>

1. The association between the mutational burden and the clinical response to immune therapies was originally suggested by the observation that ICB-sensitive melanomas comprise the tumors with the highest mutational burden.<sup>67,68</sup> This association was later confirmed by studies on colorectal cancers and NSCLC. Thus, only hypermutated colon cancers with a mismatch repair deficiency tend to respond to treatment with anti-PD-1 mAb, whereas colon cancers with a low mutational burden are largely resistant.<sup>53</sup> In NSCLC, treatment with anti-PD-1 mAb significantly improved the survival of only those patients having NSCLC with a large number of mutations, whereas no therapeutic benefit was obtained in patients with NSCLC that had a low mutational burden.<sup>61</sup> These data support the concept that efficient antitumor responses correlate directly with an increasing number of specific TAAs or neoantigens expressed by the cancer cells. It is thought that an increasing number of TAAs also recruit more T cells and a more diverse spectrum of T cells, which should strongly amplify the CTL activity against the tumors.<sup>61,62,69</sup> The expression of neoantigens is especially high in mismatch repair-deficient cancers, and in consequence the large spectrum of neoantigens renders these tumors especially sensitive to immune checkpoint inhibition.<sup>53,70</sup> A potential drawback is that such fragile cancer cells may more easily escape from tumor surveillance by losing their capacity to present TAAs or neoantigens and thus become resistant against ICB therapy.<sup>9,71</sup> To circumvent these problems, it will be necessary either to improve the expression and presentation of cancer-specific neoantigens, or to use technological innovations that are capable of guiding the immune cells to neoantigens that arise as a consequence of cancer-specific mutations.<sup>68</sup> One such approach could be the use of mAbs that preferentially bind to cells or extracellular structures of the tumor microenvironment and are capable of attracting T cells.
2. Another important area of resistance development in response to ICB therapy is related to the IFN- $\gamma$  signaling pathway. Yet, this regulation may be more complex than a simple loss of distinct signaling pathways. On the one side, metastases with defects in the Janus kinase 1 (JAK1) or the IFN- $\gamma$  signaling pathway seem to escape from cancer immune therapy with anti-PD-1 mAb.<sup>63,64</sup>

Moreover, suppression of the IFN- $\gamma$  signaling pathway in experimental tumors abrogates the cancer control with an anti-CTLA-4 mAb. On the other side, prolonged IFN- $\gamma$  signaling induces multiple alternative inhibitory pathways that are distinct from the induction of PD-1<sup>72</sup> and result in a loss of proinflammatory cytokine signaling (for details, see also “Ambiguous role of IFN signaling during ICB therapy” section). Thus, it is currently best assumed that efficient ICB in cancer therapy critically requires an intact JAK1-IFN- $\gamma$  signaling pathway. Nevertheless, persistent or aberrant IFN- $\gamma$  signaling may induce PD-L1-independent immune suppression and specific ICB resistance.

3. PD-L1 expression is induced by different cytokines, namely, IFN- $\gamma$ <sup>73</sup> and IL-27,<sup>74</sup> and can be expressed by multiple cells in the tumor environment including the tumor itself.<sup>50,75,76</sup> It is currently assumed that interruption of the PD-1/PD-L1 interaction at the tumor site is critical for an efficient therapy with anti-PD-L1 antibodies.<sup>77</sup> In line with this, treatment of NSCLC in humans with the anti-PD-1 mAb pembrolizumab improved the outcome of patients, where at least 50% of the tumor cells expressed PD-L1.<sup>50</sup> While the experimental data and the data from NSCLC are relatively clear, the role of PD-L1 expression in the microenvironment of melanomas is less clear. Thus, no treatment-limiting PD-L1 expression has been found for the responsiveness of melanomas to anti-PD-1 therapies. Moreover, no correlation was found between the PD-L1 expression and the response of metastatic melanomas to combination treatment with the PD-1 mAb nivolumab and the CTLA-4 mAb ipilimumab.<sup>78</sup> Because PD-L1 is expressed by multiple cells, including immunosuppressive plasma cells,<sup>79</sup> macrophages,<sup>76</sup> or tumor cells,<sup>50</sup> it remains to be established whether the PD-1/PD-L1 interaction suppresses CTL only in the tumor microenvironment, or whether distant PD-L1 expression, for example, in a draining lymph node, may cause the T-cell exhaustion. Because the association between the PD-L1 expression inside the tumor and the response to anti-PD-1 therapies differs between tumor entities, the exact role of the PD-L1 expression, the magnitude of the PD-L1 expression, and the site for the PD-L1 expression needed for an efficient therapy with anti-PD-1 mAb remain to be established.
4. A major parameter negatively influencing the response to ICB is a high tumor burden.<sup>66</sup> This can partly be compensated by a combined treatment with an anti-CTLA-4 mAb and an anti-PD-1 mAb, 2 agents targeting different immune-suppressive molecules. In treatment conditions in which monotherapy with an anti-PD-1 mAb induces remission in about 40% of patients, the combined application of the anti-CTLA-4 mAb ipilimumab with the anti-PD-1 mAb nivolumab can increase the response rate to about 60% for 18 months.<sup>39,40</sup> The role of the tumor burden is further highlighted by adjuvant ICB treatment for R0 resected stage III or IV melanomas. In these patients, high-dose ipilimumab (10 mg/kg body weight) improves the 5-year overall survival as compared with placebo, at the expense of a relatively high toxicity that mainly manifests as severe colitis.<sup>80</sup> In a direct comparison, treatment with nivolumab was even more efficient

and less toxic than with ipilimumab in the adjuvant setting; yet, despite treatment at the stage of minimal residual disease, about 30% of the patients still developed metastatic disease during treatment or the following 12 months.<sup>81</sup> These data underline on one side that a low tumor burden and a functioning immune system increase the efficacy of cancer immune therapy by ICB. Yet, they also show that still unknown factors interfere with the ICB-induced cancer control, even at conditions of an adjuvant immune therapy (see “nonresponders” in Fig 3, A).

As far as the consolidation phase of ICB is concerned, the situation is not as clear, and only limited information is available. Nevertheless, in this phase of immune checkpoint inhibitor therapy, the residual lesions are controlled by the immune system, most likely by T<sub>H</sub>1-mediated, cytokine-induced senescence.<sup>82-84</sup> Cytokine-induced senescence not only stops hyperproliferation of the remaining cancer cells but, especially after clearance of the senescent cells, also leads to stable disease without eradication of the tumor (Fig 3, C). Immune checkpoint inhibitor therapy thus ideally targets cancer immunoediting, which describes tumors in 3 sequential phases: the “Elimination,” the “Equilibrium,” and the “Escape” phases.<sup>71</sup> Here, the anti-PD-1 mAbs first reactivate exhausted and PD-1-expressing, cytotoxic T cells, thereby reducing large parts of the tumor mass. Later on, ICB shifts the remaining tumors from the “Escape” phase to the “Equilibrium” phase. In the “Equilibrium” phase, CD4<sup>+</sup> T cells as well as IL-12 and IFN- $\gamma$ -dominated immune responses will keep the tumors in a long-lasting dormant state.<sup>71,85</sup>

### AMBIGUOUS ROLE OF IFN SIGNALING DURING ICB THERAPY

Acute antitumor immunity can arrest tumor growth by inducing tumor dormancy. In a multistage carcinogenesis model, it has been demonstrated that T<sub>H</sub>1 stop tumor development by an IFN- $\gamma$ - and tumor necrosis factor (TNF) R1-dependent mechanism.<sup>85</sup> More detailed analyses revealed that the T<sub>H</sub>1 cytokines IFN- $\gamma$  and TNF drive tumor cells into permanent growth arrest, that is, cellular senescence.<sup>82-84,86</sup> Cellular senescence is an endogenous stress response mechanism that directly copes with the hyperproliferative properties of tumor cells.<sup>87,88</sup> On the other hand, cellular senescence<sup>89</sup> as well as chronic inflammation and TNF signaling<sup>90</sup> may also have tumor-promoting effects. Thus, it is not surprising that the role of IFN- $\gamma$  signaling in ICB therapy has been controversially discussed. In a recent report, Benci et al<sup>72</sup> provide experimental evidence for a protumoral role of chronic IFN- $\gamma$ . In this case, chronic IFN- $\gamma$  signaling in tumor cells increases resistance to ICB through induction of multiple inhibitory pathways. Upregulation of inhibitor receptor ligands on the tumor cells generates deeply exhausted T cells that can no longer be targeted by anti-PD-1 therapy. This finally leads to tumor progression (Fig 4, A). In contrast, loss of IFN- $\gamma$  signaling in tumors<sup>63</sup> and/or in T cells<sup>91</sup> has been described as a mechanism of resistance to immune checkpoint inhibitor therapy. Accordingly, ICB therapy leads to IFN- $\gamma$  signature and signaling in responding melanoma lesions and later on to tumor cell death and cancer regression (Fig 4, B, left panel). Alternatively, cytokine signaling may originate from checkpoint blockade-mediated reactivation of exhausted T<sub>H</sub>1, which secrete IFN- $\gamma$



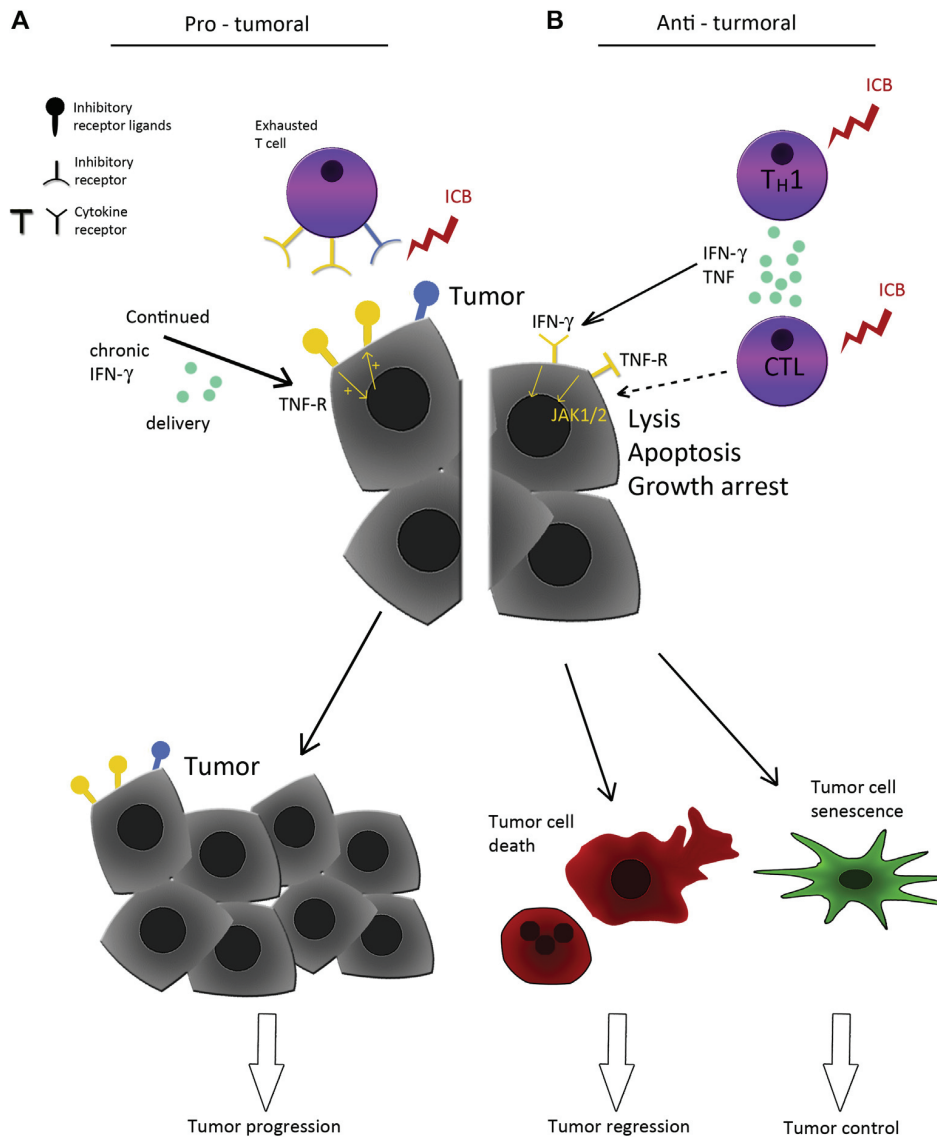


**FIG 4.** The dual role of IFN signaling during ICB: cytokine-induced regulation of PD-1 versus cytokine-induced antitumor effects. **A**, Chronic IFN- $\gamma$  signaling upregulates inhibitor receptor ligands and other negative immune regulators on tumor cells. Enhanced expression of these negative immune regulators leads to deeply exhausted T cells that cannot be reactivated by ICB therapy.<sup>72</sup> As a consequence, the tumors continue to progress during therapy. **B**, Efficient ICB leads to an acute IFN- $\gamma$  signature, and to CTL- and IFN- $\gamma$ -induced tumor cell death (*left*). ICB may also lead to reactivation of exhausted TH1. TH1 then secrete IFN- $\gamma$  and TNF, and drive the surviving tumor cells into cytokine-induced senescence (*right*). Consequently, ICB therapy leads to tumor regression by CTL and IFN- $\gamma$ -mediated apoptosis or lysis,<sup>63</sup> to control of the surviving tumor cells by IFN- $\gamma$ -induced JAK1/2 signaling,<sup>64</sup> or to cytokine-induced senescence.<sup>82</sup> Tumors may escape from this control, if the IFN- $\gamma$ -induced signaling becomes abrogated (not shown).

and TNF in the vicinity of the tumor lesions. Combined IFN- $\gamma$  and TNF then induce senescence in the tumor cells,<sup>82</sup> leading to long-lasting tumor control (Fig 4, B, right panel). In line with this, a recent report analyzed the genetic alterations that are associated with acquired resistance to anti-PD-1 therapy. They found that the cells of relapsing patients showed loss-of-function mutations in the genes encoding IFN-receptor-associated Janus kinase 1 or 2 (JAK1/2).<sup>64</sup> These mutations resulted in insensitivity to the antiproliferative effects of IFN- $\gamma$ . Interestingly, JAK1/2 losses are not rare in melanomas and predispose to IFN- $\gamma$  resistance. Thus,

JAK1/2 deficiency may also result in T-cell resistance due to HLA class I-negative tumor lesions.<sup>65</sup> Taken together, overwhelming evidence exists that IFN- $\gamma$  signaling, presumably via JAK1/2, plays a crucial role in the initial antitumor response during anti-PD-1 treatment or other immunotherapeutic regimens.

As far as the role of inflammation and IFN- $\gamma$  signaling during ICB therapy is concerned, it has to be taken into account whether (1) the cytokine signal is chronic or acute; (2) IFN- $\gamma$  is acting in the presence of additional cytokine signaling, for example, TNF signaling; (3) cells of the tumor microenvironment are also

influenced by the cytokines; and (4) the tumor cells of responders, initial nonresponders, or acquired nonresponders are analyzed.

### CLINICAL APPLICATION OF ICB

A decade ago, advanced melanoma was a tumor largely resistant to all available therapeutic approaches.<sup>92</sup> Despite worldwide efforts, especially the immunotherapeutic studies published until 2011 were restricted to highly selected patient cohorts or included only small numbers of patients with melanoma. However, in 2011, a report of a phase III trial suggested that HLA-A020.1–positive patients with melanoma treated with high-dose IL-2 combined with a gp100 peptide vaccine and incomplete Freund's adjuvant might have a small, temporary survival benefit.<sup>93</sup>

In the same year, a groundbreaking study showed for the first time that an immune therapy may slightly but significantly improve overall survival of patients with metastases of a solid cancer, in this case melanoma.<sup>94</sup> The study compared the treatment with an anti-CTLA-4 mAb (ipilimumab) at 10 mg/kg plus dacarbazine versus dacarbazine plus placebo. Dacarbazine was given for 4 cycles. Subsequently, either the anti-CTLA-4 mAb or placebo was given as maintenance therapy every 12 weeks. This was the first trial demonstrating a discrete (about 5%) but significantly improved 3-year overall survival for patients receiving an immune-based therapy for metastases from a solid cancer.<sup>94,95</sup>

An independent trial in pretreated HLA-A020.1–positive patients with melanoma compared a monotherapy with the anti-CTLA-4 mAb ipilimumab (3 mg/kg for 4 cycles), against either a combination of the anti-CTLA-4 mAb plus a gp100 peptide vaccine (in incomplete Freund's adjuvant) or the gp100 peptide vaccine alone. Monotherapy with ipilimumab resulted in a significantly higher number of patients achieving a long-term overall survival compared with the other 2 arms.<sup>96,97</sup> Thus, overall survival rates in the ipilimumab plus gp100 group, the ipilimumab-alone group, and the gp100-alone group were 21.6%, 23.5%, and 13.7% at 2 years. The therapeutic impact of ipilimumab remains, however, unclear in this study, because the gp100 peptide vaccine in incomplete Freund's adjuvant may have adversely affected patient survival due to the induction of a tumor-promoting immune response. Indeed, induction of an inappropriate antitumor immune response may not only be neutral but even promote tumor progression.<sup>1,85,98</sup>

While melanoma therapy with anti-CTLA-4 mAb paved the way, the major clinical breakthrough in melanoma immunotherapy was the introduction of PD-1 antagonists. Two such antagonists are currently approved (nivolumab and pembrolizumab), both being directed against the PD-1 molecule. Other antagonists (namely, avelumab and atezolizumab), binding the PD-1 ligand PD-L1, are likewise approved for solid cancers such as urothelial carcinoma, or Merkel cell carcinoma, or are under clinical development for a large number of cancers.<sup>51,99,100</sup>

Nivolumab (3 mg/kg every 2 weeks), the first PD-1 antagonist evaluated in a phase III trial, was compared with dacarbazine in treatment-naïve patients with serine/threonine-protein kinase (BRAF) wild-type melanoma.<sup>49</sup> The 1-year overall survival was significantly in favor of the nivolumab-treated patients (72.9% vs 42.1%). Interestingly, response to treatment was independent of the PD-L1 expression in the tumor samples. This phenomenon might be attributed to a heterogeneous expression of PD-L1 on

antigen-presenting cells of the tumor microenvironment, or to an important role of PD-L1 outside the direct tumor microenvironment, like in the tumor-draining lymph nodes (see also "Cancer killing and induction of cancer dormancy by reactivation of exhausted tumor-specific T cells" section). Pembrolizumab, the second available PD-1 antagonist, was evaluated in a phase III trial against ipilimumab.<sup>48</sup> The 1-year overall survival rate was between 74.1% and 68.4%, depending on the frequency (10 mg/kg either every 2 weeks, or every 3 weeks), and 58.2% for ipilimumab (3 mg/kg every 3 weeks for 4 doses). Updated overall survival rates of this study were shown at the ASCO 2017 meeting. At 33 months, 50% of the patients in the pooled pembrolizumab arms were alive and 39% in the ipilimumab arm.

Thus, immune therapies with mAbs against immune checkpoints not only induce a clinical improvement, but may, in line with the originally published data, even induce a stable long-term survival in those patients with stage IV melanoma who respond to the therapy. However, in about 50% to 60% of patients the tumors fail to respond to the therapy and progress continuously despite the therapy. This behavior, referred to as primary resistance, is currently under intensive evaluation (see also "Cancer killing and induction of cancer dormancy by reactivation of exhausted tumor-specific T cells" section). Despite a large number of conclusive reports, the reasons for this primary unresponsiveness are still poorly understood.<sup>101</sup>

On the other hand, 40% to 50% of the patients with melanomas respond to ICB therapy performed with either nivolumab (3 mg/kg every 2 weeks) or pembrolizumab (2 mg/kg every 3 weeks). This success rate is much lower in most other cancer entities.<sup>48-54</sup> Once melanomas are responding, ICB seems to induce a long-lasting, durable response in most tumor-bearing patients. However, a subset of patients initially responding to checkpoint inhibitor treatment relapse and develop therapy resistance—referred to as acquired resistance. The mechanisms leading to the development of this special kind of therapy resistance are the subject of current research; one reason is the loss of IFN- $\gamma$  responsiveness by the tumor cells. Most of the responders become "clinically" healthy with various degrees of residual disease, and only a minority of these patients achieves a clinically complete response. This suggests that the reactivation of the immune system by PD-1 antagonists deletes only part of the metastases.<sup>58</sup> The remaining metastases seem to be driven into a state of dormancy. A similar state of dormancy can be induced by the combined action of IFN- $\gamma$  and TNF on melanoma cells.<sup>82</sup> This mode of action may be of relevance for ICB therapy, as recent data show that the effectiveness of a therapy with either CTLA-4 or PD-1 antagonists depends on the presence of an intact IFN- $\gamma$  signaling pathway in melanoma metastases.<sup>63-65</sup>

Various approaches are currently being tested to improve the responsiveness to the immune therapy. The only approved therapy is the combined treatment of patients with melanoma with nivolumab and ipilimumab. This combination (nivolumab 1 mg/kg and ipilimumab 3 mg/kg every 3 weeks for 4 cycles followed by nivolumab 3 mg/kg every 2 weeks) was compared in a phase III trial to the individual drugs (nivolumab 3 mg/kg every 2 weeks, and ipilimumab 3 mg/kg for 4 cycles, respectively) for treatment-naïve patients.<sup>39</sup> Patients in the treatment arms containing the anti-PD-1 mAb achieved a significantly longer progression-free survival than those treated with the anti-CTLA-4 mAb only. Also, the 2-year overall survival rates

**TABLE I.** Frequently applied treatment algorithm for patients with metastatic melanoma where surgery is no longer applicable

Extent of metastases	BRAF status	General health	Treatment metastases approach
Limited	BRAF wild-type or BRAF <sup>V600E/K</sup>	Good	ICB using anti-PD-1/PD-L1 antibodies
Extended	BRAF <sup>V600E/K</sup>	Good or poor	Combined inhibition of BRAF <sup>V600E/K</sup> and MEK
Extended	BRAF wild-type	Good or poor	ICB using anti-CTLA-4 and/or anti-PD-1/PD-L1 antibodies or chemotherapy

MEK, Mitogen-activated protein kinase kinase.

The table summarizes treatment options using immune checkpoint inhibitors, kinase inhibitors or chemotherapy for patients suffering from metastatic melanoma (according to the extent of dissemination,<sup>66</sup> see text).

were 64% for the combined treatment with the anti-PD-1 mAb and the anti-CTLA-4 mAb, 59% for those treated with the anti-PD-1 mAb, and 45% for those treated with the anti-CTLA-4 mAb.<sup>40</sup> The combined therapy provided the highest benefit for both progression-free and for overall survival in patients with a low PD-L1 expression (<5%). Thus, PD-1 antagonists (and probably also PD-L1 antagonists) are superior to CTLA-4 antagonists and seem to prolong the median overall survival of patients with metastatic melanoma up to 32 months. Moreover, patients with melanoma with limited metastatic disease and a good health status seem to respond very favorably to the immune therapy with an anti-PD-1 mAb, whereas those with a poor health status and extensive metastases seem to respond rarely to an anti-PD-1 mAb therapy.<sup>66</sup>

Combining the current experience with immune therapies with the experience obtained from the treatment of metastatic melanomas bearing the serine/threonine-protein kinase B-Raf carrying the respective V600 mutation (BRAF<sup>V600E/K</sup>) mutation led to the treatment algorithm illustrated in Table I, which is currently broadly used. It is based on the following experience: anti-PD-1 mAbs are independently of the presence of a BRAF<sup>V600E/K</sup> mutation efficient in patients with a limited tumor load, especially with lung and lymph node metastases, and normal monocyte numbers in the peripheral blood. It seems that in many of those patients treatment can be terminated or interrupted after 2 years of successful therapy. In contrast, in patients with a higher tumor burden, where rapid responses are needed, the combination of targeted drug therapies using inhibitors of the serine/threonine-protein kinase BRAF and the mitogen-activated protein kinase kinase seems to be more efficient. Yet, this pharmacotherapy requires the presence of the BRAF<sup>V600E/K</sup> mutation in the metastases. It seems to be somewhat less efficient than anti-PD-1 mAb in patients with a limited tumor load (if the data from phase III studies are compared) and requires a continued therapy. For patients with more extensive melanoma metastases that are devoid of the BRAF<sup>V600E/K</sup> mutation, the approved combination therapy with ipilimumab and nivolumab is to date the treatment option with the best-reported treatment outcome. To improve the outcome, the combination of targeted drug therapies using the above-mentioned kinase inhibitors with PD-1 and PD-L1 antagonists is currently in clinical trials. The use of anti-PD-1 mAbs in combination with other immune-modulating approaches is also being investigated in clinical studies. This comprises the combination with indoleamine 2,3-dioxygenase 1 inhibitors or the intralesional use of oncolytic viruses or bacterial DNA.

Most immunotherapies are applied in the metastatic setting. However, another central question focuses on whether ICB was also efficient in the adjuvant situation to prevent the development

of metastatic disease in patients at high risk. An adjuvant phase III trial compared ipilimumab (10 mg/kg body) with placebo applied in an induction phase every 3 weeks for 4 cycles, followed by a maintenance phase of 1 anti-CTLA-4 infusion every 3 months for up to 3 years.<sup>80</sup> After a median follow-up of 5.3 years, both the 5-year recurrence-free survival and the 5-year overall survival were superior for patients treated with the anti-CTLA-4 mAb. Subsequent studies with an anti-PD-1 mAb (3 mg/kg nivolumab, every 2 weeks) showed that the anti-PD-1 treatment, given in the adjuvant setting for 1 year, is at 2 years safer and more efficient than the anti-CTLA-4 mAb (10 mg/kg ipilimumab; every 3 weeks for 4 doses and then every 12 weeks for up to 1 year). The 1-year rate of recurrence-free survival in the nivolumab arm was 70.5% compared with 60.8% in the ipilimumab arm.<sup>81</sup> Together, these 2 studies demonstrate for the first time that an immunotherapy may be efficient in the adjuvant setting when given to patients at high risk of further metastatic disease after R0 resection of melanoma metastases.

### IMMUNE CHECKPOINT INHIBITOR-INDUCED AUTOIMMUNE DISEASES

PD-1 (also CD 279) was initially recognized as a receptor inducing a downregulation of the immune system and thus preventing autoimmune diseases. Thus, PD-1 promotes self-tolerance by suppressing T-cell-driven tissue destruction.<sup>30,31</sup> As immune checkpoint inhibitors antagonize exactly this brake, treatment regimens with PD-1 or CTLA-4 antagonists may initiate the development of mainly T-cell-mediated organ-specific autoimmune diseases.<sup>102-106</sup> In principle, both CTLA-4 and PD-1 antagonists are able to induce any organ-specific autoimmune disease described; yet, CTLA-4 and PD-1 antagonists cause those diseases with different frequency and distribution.<sup>48</sup> Severe colitis is mainly caused by the anti-CTLA-4 mAb,<sup>96</sup> whereas endocrine and pulmonary side effects are more closely linked with PD-1 antagonists.<sup>48</sup> The severity of side effects is rather modest for most patients treated with PD-1 antagonists alone, whereas the severity of side effects, especially of colitis, is increased in patients receiving monotherapy with anti-CTLA-4 mAb, and most severe in those receiving PD-1 antagonists combined with anti-CTLA-4 mAb.<sup>39</sup> In those patients, severe grade 3 to 5 colitis occurs in up to two-third of the treated patients and may even be fatal.<sup>39</sup>

Albeit the time to onset of adverse events is not predictable, most events develop within the first 3 months of treatment and can normally be controlled with systemic glucocorticosteroids of 1 to 2 mg prednisolone equivalents per day. An exception is the destruction of endocrine tissue, which may require a lifelong hormone replacement therapy. The sooner side effects are

detected and the more rigorously they are treated, the better is the clinical outcome. In consequence, a close follow-up of the patients is mandatory to avoid long-lasting harm.

## SUMMARY

ICB is a novel treatment option for metastatic melanoma, which prolongs the lifespan of patients with metastatic melanoma and many different types of carcinomas. Interestingly, this very successful drug regimen seems to be based on 2 different biological mechanisms, that is, a cytotoxic immune response through reactivation of exhausted CD8-positive T cells and the induction of cytokine-mediated tumor dormancy. Besides the active role of immune cells, for example, T cells, ICB therapy needs a special cytokine milieu. Especially, intact IFN- $\gamma$  signaling in the tumor cells is necessary to obtain objective responses of the cancer patients during immune checkpoint inhibitor therapy. However, chronic inflammation and/or chronic IFN- $\gamma$  signaling might be harmful and lead to enhanced cancer progression due to the induction of additional signals that promote tumor immune evasion.






## REFERENCES

1. Rocken M. Early tumor dissemination, but late metastasis: insights into tumor dormancy. *J Clin Invest* 2010;120:1800-3.
2. Kolb HJ, Mittermuller J, Clemm C, Holler E, Ledderose G, Brehm G, et al. Donor leukocyte transfusions for treatment of recurrent chronic myelogenous leukemia in marrow transplant patients. *Blood* 1990;76:2462-5.
3. Mocikat R, Braumuller H, Gumy A, Egeter O, Ziegler H, Reusch U, et al. Natural killer cells activated by MHC class I (low) targets prime dendritic cells to induce protective CD8 T cell responses. *Immunity* 2003;19:561-9.
4. Egeter O, Mocikat R, Ghoreschi K, Dieckmann A, Rocken M. Eradication of disseminated lymphomas with CpG-DNA activated T helper type 1 cells from nontransgenic mice. *Cancer Res* 2000;60:1515-20.
5. Ziegler A, Heidenreich R, Braumuller H, Wolburg H, Weidemann S, Mocikat R, et al. EpCAM, a human tumor-associated antigen promotes Th2 development and tumor immune evasion. *Blood* 2009;113:3494-502.
6. Knuth A, Wolfel T, Klehmann E, Boon T, Meyer zum Buschenfelde KH. Cytolytic T-cell clones against an autologous human melanoma: specificity study and definition of three antigens by immunoselection. *Proc Natl Acad Sci U S A* 1989;86:2804-8.
7. Walter S, Weinschenk T, Stenzl A, Zdrojowy R, Pluzanska A, Szczylik C, et al. Multipptide immune response to cancer vaccine IMA901 after single-dose cyclophosphamide associates with longer patient survival. *Nat Med* 2012;18:1254-61.
8. Thurner B, Haendle I, Roder C, Dieckmann D, Keikavoussi P, Jonuleit H, et al. Vaccination with mage-3A1 peptide-pulsed mature, monocyte-derived dendritic cells expands specific cytotoxic T cells and induces regression of some metastases in advanced stage IV melanoma. *J Exp Med* 1999;190:1669-78.
9. Sahin U, Derhovanessian E, Miller M, Kloke BP, Simon P, Lower M, et al. Personalized RNA mutanome vaccines mobilize poly-specific therapeutic immunity against cancer. *Nature* 2017;547:222-6.
10. Kranz LM, Diken M, Haas H, Kreiter S, Loqui C, Reuter KC, et al. Systemic RNA delivery to dendritic cells exploits antiviral defence for cancer immunotherapy. *Nature* 2016;534:396-401.
11. Ott PA, Hu Z, Keskin DB, Shukla SA, Sun J, Bozym DJ, et al. An immunogenic personal neoantigen vaccine for patients with melanoma. *Nature* 2017;547:217-21.
12. Hartmann G, Weiner GJ, Krieg AM. CpG DNA: a potent signal for growth, activation, and maturation of human dendritic cells. *Proc Natl Acad Sci U S A* 1999;96:9305-10.
13. Wagner H. Endogenous TLR ligands and autoimmunity. *Adv Immunol* 2006;91:159-73.
14. Robbins PF, Lu YC, El-Gamil M, Li YF, Gross C, Gartner J, et al. Mining exomic sequencing data to identify mutated antigens recognized by adoptively transferred tumor-reactive T cells. *Nat Med* 2013;19:747-52.
15. Kenter GG, Welters MJ, Valentijn AR, Lowik MJ, Berends-van der Meer DM, Vloon AP, et al. Vaccination against HPV-16 oncoproteins for vulvar intraepithelial neoplasia. *N Engl J Med* 2009;361:1838-47.
16. Terabe M, Berzofsky JA. Immunoregulatory T cells in tumor immunity. *Curr Opin Immunol* 2004;16:157-62.
17. Ni G, Wang T, Walton S, Zhu B, Chen S, Wu X, et al. Manipulating IL-10 signaling blockade for better immunotherapy. *Cell Immunol* 2015;293:126-9.
18. Munn DH, Mellor AL. IDO in the tumor microenvironment: inflammation, counter-regulation, and tolerance. *Trends Immunol* 2016;37:193-207.
19. Rachidi S, Metelli A, Riesenberger B, Wu BX, Nelson MH, Wallace C, et al. Platelets subvert T cell immunity against cancer via GARP-TGFbeta axis. *Sci Immunol* 2017;2.
20. Leach DR, Krummel MF, Allison JP. Enhancement of antitumor immunity by CTLA-4 blockade. *Science* 1996;271:1734-6.
21. Okazaki T, Chikuma S, Iwai Y, Fagarasan S, Honjo T. A rheostat for immune responses: the unique properties of PD-1 and their advantages for clinical application. *Nat Immunol* 2013;14:1212-8.
22. Gajewski TF, Schreiber H, Fu YX. Innate and adaptive immune cells in the tumor microenvironment. *Nat Immunol* 2013;14:1014-22.
23. Moskophidis D, Lechner F, Pircher H, Zinkernagel RM. Virus persistence in acutely infected immunocompetent mice by exhaustion of antiviral cytotoxic effector T cells. *Nature* 1993;362:758-61.
24. Barber DL, Wherry EJ, Masopust D, Zhu B, Allison JP, Sharpe AH, et al. Restoring function in exhausted CD8 T cells during chronic viral infection. *Nature* 2006;439:682-7.
25. Kleffel S, Posch C, Barthel SR, Mueller H, Schlapbach C, Guenova E, et al. Melanoma cell-intrinsic PD-1 receptor functions promote tumor growth. *Cell* 2015;162:1242-56.
26. Kollmann D, Ignatova D, Jedamzik J, Chang YT, Jomrich G, Paireder M, et al. Expression of programmed cell death protein 1 by tumor-infiltrating lymphocytes and tumor cells is associated with advanced tumor stage in patients with esophageal adenocarcinoma. *Ann Surg Oncol* 2017;24:2698-706.
27. Davis BP, Ballas ZK. Biologic response modifiers: indications, implications, and insights. *J Allergy Clin Immunol* 2017;139:1445-56.
28. Veilleux MS, Shear NH. Biologics in patients with skin diseases. *J Allergy Clin Immunol* 2017;139:1423-30.
29. Ishida Y, Agata Y, Shibahara K, Honjo T. Induced expression of PD-1, a novel member of the immunoglobulin gene superfamily, upon programmed cell death. *EMBO J* 1992;11:3887-95.
30. Nishimura H, Nose M, Hiai H, Minato N, Honjo T. Development of lupus-like autoimmune diseases by disruption of the PD-1 gene encoding an ITIM motif-carrying immunoreceptor. *Immunity* 1999;11:141-51.
31. Nishimura H, Okazaki T, Tanaka Y, Nakatani K, Hara M, Matsumori A, et al. Autoimmune dilated cardiomyopathy in PD-1 receptor-deficient mice. *Science* 2001;291:319-22.
32. Freeman GJ, Long AJ, Iwai Y, Bourque K, Chernova T, Nishimura H, et al. Engagement of the PD-1 immunoinhibitory receptor by a novel B7 family member leads to negative regulation of lymphocyte activation. *J Exp Med* 2000;192:1027-34.
33. Latchman Y, Wood CR, Chernova T, Chaudhary D, Borde M, Chernova I, et al. PD-L2 is a second ligand for PD-1 and inhibits T cell activation. *Nat Immunol* 2001;2:261-8.
34. Okazaki T, Maeda A, Nishimura H, Kurosaki T, Honjo T. PD-1 immunoreceptor inhibits B cell receptor-mediated signaling by recruiting src homology 2-domain-containing tyrosine phosphatase 2 to phosphotyrosine. *Proc Natl Acad Sci U S A* 2001;98:13866-71.
35. Sheppard KA, Fitz LJ, Lee JM, Benander C, George JA, Wooters J, et al. PD-1 inhibits T-cell receptor induced phosphorylation of the ZAP70/CD3zeta signalosome and downstream signaling to PKCtheta. *FEBS Lett* 2004;574:37-41.
36. Yokosuka T, Takamatsu M, Kobayashi-Imanishi W, Hashimoto-Tane A, Azuma M, Saito T. Programmed cell death 1 forms negative costimulatory microclusters that directly inhibit T cell receptor signaling by recruiting phosphatase SHP2. *J Exp Med* 2012;209:1201-17.
37. Parry RV, Chemnitz JM, Frauwirth KA, Lanfranco AR, Braunstein I, Kobayashi SV, et al. CTLA-4 and PD-1 receptors inhibit T-cell activation by distinct mechanisms. *Mol Cell Biol* 2005;25:9543-53.
38. Harding FA, McArthur JG, Gross JA, Raulat DH, Allison JP. CD28-mediated signalling co-stimulates murine T cells and prevents induction of anergy in T-cell clones. *Nature* 1992;356:607-9.
39. Larkin J, Chiarion-Sileni V, Gonzalez R, Grob JJ, Cowey CL, Lao CD, et al. Combined nivolumab and ipilimumab or monotherapy in untreated melanoma. *N Engl J Med* 2015;373:1270-1.
40. Wolchok JD, Chiarion-Sileni V, Gonzalez R, Rutkowski P, Grob JJ, Cowey CL, et al. Overall survival with combined nivolumab and ipilimumab in advanced melanoma. *N Engl J Med* 2017;377:1345-56.
41. Kamphorst AO, Wieland A, Nasti T, Yang S, Zhang R, Barber DL, et al. Rescue of exhausted CD8 T cells by PD-1-targeted therapies is CD28-dependent. *Science* 2017;355:1423-7.

42. Ghoneim HE, Fan Y, Moustaki A, Abdelsamed HA, Dash P, Dogra P, et al. De novo epigenetic programs inhibit PD-1 blockade-mediated T cell rejuvenation. *Cell* 2017;170:142-57.e19.
43. Iwai Y, Ishida M, Tanaka Y, Okazaki T, Honjo T, Minato N. Involvement of PD-L1 on tumor cells in the escape from host immune system and tumor immunotherapy by PD-L1 blockade. *Proc Natl Acad Sci U S A* 2002;99:12293-7.
44. Ho PC, Bihuniak JD, Macintyre AN, Staron M, Liu X, Amezquita R, et al. Phosphoenolpyruvate is a metabolic checkpoint of anti-tumor T cell responses. *Cell* 2015;162:1217-28.
45. Buck MD, O'Sullivan D, Klein Geltink RI, Curtis JD, Chang CH, Sanin DE, et al. Mitochondrial dynamics controls T cell fate through metabolic programming. *Cell* 2016;166:63-76.
46. Chang CH, Pearce EL. Emerging concepts of T cell metabolism as a target of immunotherapy. *Nat Immunol* 2016;17:364-8.
47. Sen DR, Kaminski J, Barnitz RA, Kurachi M, Gerdemann U, Yates KB, et al. The epigenetic landscape of T cell exhaustion. *Science* 2016;354:1165-9.
48. Robert C, Schachter J, Long GV, Arance A, Grob JJ, Mortier L, et al. Pembrolizumab versus ipilimumab in advanced melanoma. *N Engl J Med* 2015;372:2521-32.
49. Robert C, Long GV, Brady B, Dutriaux C, Maio M, Mortier L, et al. Nivolumab in previously untreated melanoma without BRAF mutation. *N Engl J Med* 2015;372:320-30.
50. Reck M, Rodriguez-Abreu D, Robinson AG, Hui R, Czoszi T, Fulop A, et al. Pembrolizumab versus chemotherapy for PD-L1-positive non-small-cell lung cancer. *N Engl J Med* 2016;375:1823-33.
51. Kaufman HL, Russell J, Hamid O, Bhatia S, Terheyden P, D'Angelo SP, et al. Avelumab in patients with chemotherapy-refractory metastatic Merkel cell carcinoma: a multicentre, single-group, open-label, phase 2 trial. *Lancet Oncol* 2016;17:1374-85.
52. Balar AV, Castellano D, O'Donnell PH, Grivas P, Vuky J, Powles T, et al. First-line pembrolizumab in cisplatin-ineligible patients with locally advanced and unresectable or metastatic urothelial cancer (KEYNOTE-052): a multicentre, single-arm, phase 2 study. *Lancet Oncol* 2017;18:1483-92.
53. Le DT, Uram JN, Wang H, Bartlett BR, Kemberling H, Eyring AD, et al. PD-1 blockade in tumors with mismatch-repair deficiency. *N Engl J Med* 2015;372:2509-20.
54. Topalian SL, Hodi FS, Brahmer JR, Gettinger SN, Smith DC, McDermott DF, et al. Safety, activity, and immune correlates of anti-PD-1 antibody in cancer. *N Engl J Med* 2012;366:2443-54.
55. Riaz N, Havel JJ, Makarov V, Desrichard A, Urba WJ, Sims JS, et al. Tumor and microenvironment evolution during immunotherapy with nivolumab. *Cell* 2017;171:934-49.e15.
56. Schadendorf D, Wolchok JD, Hodi FS, Chiarion-Sileni V, Gonzalez R, Rutkowski P, et al. Efficacy and safety outcomes in patients with advanced melanoma who discontinued treatment with nivolumab and ipilimumab because of adverse events: a pooled analysis of randomized phase II and III trials. *J Clin Oncol* 2017;35:3807-14.
57. Hanahan D, Weinberg RA. Hallmarks of cancer: the next generation. *Cell* 2011;144:646-74.
58. Tumeh PC, Harview CL, Yearley JH, Shintaku IP, Taylor EJ, Robert L, et al. PD-1 blockade induces responses by inhibiting adaptive immune resistance. *Nature* 2014;515:568-71.
59. Twyman-Saint Victor C, Rech AJ, Maity A, Rengan R, Pauken KE, Stelekati E, et al. Radiation and dual checkpoint blockade activate non-redundant immune mechanisms in cancer. *Nature* 2015;520:373-7.
60. Ribas A, Dummer R, Puzanov I, VanderWalde A, Andtbacka RHI, Michielin O, et al. Oncolytic virotherapy promotes intratumoral T cell infiltration and improves anti-PD-1 immunotherapy. *Cell* 2017;170:1109-19.e10.
61. Rizvi NA, Hellmann MD, Snyder A, Kvistborg P, Makarov V, Havel JJ, et al. Cancer immunology. Mutational landscape determines sensitivity to PD-1 blockade in non-small cell lung cancer. *Science* 2015;348:124-8.
62. Van Allen EM, Miao D, Schilling B, Shukla SA, Blank C, Zimmer L, et al. Genomic correlates of response to CTLA-4 blockade in metastatic melanoma. *Science* 2015;350:207-11.
63. Gao J, Shi LZ, Zhao H, Chen J, Xiong L, He Q, et al. Loss of IFN-gamma pathway genes in tumor cells as a mechanism of resistance to anti-CTLA-4 therapy. *Cell* 2016;167:397-404.e9.
64. Zaretsky JM, Garcia-Diaz A, Shin DS, Escuin-Ordinas H, Hugo W, Hu-Lieskova S, et al. Mutations associated with acquired resistance to PD-1 blockade in melanoma. *N Engl J Med* 2016;375:819-29.
65. Sucker A, Zhao F, Pieper N, Heeke C, Maltaner R, Stadler N, et al. Acquired IFN-gamma resistance impairs anti-tumor immunity and gives rise to T-cell-resistant melanoma lesions. *Nat Commun* 2017;8:15440.
66. Weide B, Martens A, Hassel JC, Berking C, Postow MA, Bisschop K, et al. Baseline biomarkers for outcome of melanoma patients treated with pembrolizumab. *Clin Cancer Res* 2016;22:5487-96.
67. Alexandrov LB, Nik-Zainal S, Wedge DC, Aparicio SA, Behjati S, Biankin AV, et al. Signatures of mutational processes in human cancer. *Nature* 2013;500:415-21.
68. Schumacher TN, Schreiber RD. Neoantigens in cancer immunotherapy. *Science* 2015;348:69-74.
69. Stronen E, Toebes M, Kelderman S, van Buuren MM, Yang W, van Rooij N, et al. Targeting of cancer neoantigens with donor-derived T cell receptor repertoires. *Science* 2016;352:1337-41.
70. Le DT, Durham JN, Smith KN, Wang H, Bartlett BR, Aulakh LK, et al. Mismatch repair deficiency predicts response of solid tumors to PD-1 blockade. *Science* 2017;357:409-13.
71. Schreiber RD, Old LJ, Smyth MJ. Cancer immunoediting: integrating immunity's roles in cancer suppression and promotion. *Science* 2011;331:1565-70.
72. Benci JL, Xu B, Qiu Y, Wu TJ, Dada H, Twyman-Saint Victor C, et al. Tumor interferon signaling regulates a multigenic resistance program to immune checkpoint blockade. *Cell* 2016;167:1540-54.e12.
73. Chen J, Feng Y, Lu L, Wang H, Dai L, Li Y, et al. Interferon-gamma-induced PD-L1 surface expression on human oral squamous carcinoma via PKD2 signal pathway. *Immunobiology* 2012;217:385-93.
74. Hirahara K, Ghoreschi K, Yang XP, Takahashi H, Laurence A, Vahedi G, et al. Interleukin-27 priming of T cells controls IL-17 production in trans via induction of the ligand PD-L1. *Immunity* 2012;36:1017-30.
75. Wu Y, Cao D, Qu L, Cao X, Jia Z, Zhao T, et al. PD-1 and PD-L1 co-expression predicts favorable prognosis in gastric cancer. *Oncotarget* 2017;8:64066-82.
76. Menguy S, Prochazkova-Carlotti M, Beylot-Barry M, Saltel F, Vergier B, Merlio JP, et al. PD-L1 and PD-L2 are differentially expressed by macrophages or tumor cells in primary cutaneous diffuse large B-cell lymphoma, leg type. *Am J Surg Pathol* 2018;42:326-34.
77. Herbst RS, Soria JC, Kowanetz M, Fine GD, Hamid O, Gordon MS, et al. Predictive correlates of response to the anti-PD-L1 antibody MPDL3280A in cancer patients. *Nature* 2014;515:563-7.
78. Postow MA, Chesney J, Pavlick AC, Robert C, Grossmann K, McDermott D, et al. Nivolumab and ipilimumab versus ipilimumab in untreated melanoma. *N Engl J Med* 2015;372:2006-17.
79. Shalapour S, Font-Burgada J, Di Caro G, Zhong Z, Sanchez-Lopez E, Dhar D, et al. Immunosuppressive plasma cells impede T-cell-dependent immunogenic chemotherapy. *Nature* 2015;521:94-8.
80. Eggermont AM, Chiarion-Sileni V, Grob JJ, Dummer R, Wolchok JD, Schmidt H, et al. Prolonged survival in stage III melanoma with ipilimumab adjuvant therapy. *N Engl J Med* 2016;375:1845-55.
81. Weber J, Mandala M, Del Vecchio M, Gogas HJ, Arance AM, Cowey CL, et al. Checkmate 238 Collaborators. Adjuvant nivolumab versus ipilimumab in resected stage III or IV melanoma. *N Engl J Med* 2017;377:1824-35.
82. Braumuller H, Wieder T, Brenner E, Assmann S, Hahn M, Alkhaled M, et al. T-helper-1-cell cytokines drive cancer into senescence. *Nature* 2013;494:361-5.
83. Schilbach K, Alkhaled M, Welker C, Eckert F, Blank G, Ziegler H, et al. Cancer-targeted IL-12 controls human rhabdomyosarcoma by senescence induction and myogenic differentiation. *Oncimmunology* 2015;4:e1014760.
84. Wieder T, Brenner E, Braumuller H, Bischof O, Rocken M. Cytokine-induced senescence for cancer surveillance. *Cancer Metastasis Rev* 2017;6:357-65.
85. Muller-Hermelink N, Braumuller H, Pichler B, Wieder T, Mailhammer R, Schaak K, et al. TNFR1 signaling and IFN-gamma signaling determine whether T cells induce tumor dormancy or promote multistage carcinogenesis. *Cancer Cell* 2008;13:507-18.
86. Hubackova S, Kucerova A, Michlits G, Kyjacova L, Reinis M, Korolov O, et al. IFN-gamma induces oxidative stress, DNA damage and tumor cell senescence via TGFbeta/SMAD signaling-dependent induction of Nox4 and suppression of ANT2. *Oncogene* 2016;35:1236-49.
87. Perez-Mancera PA, Young AR, Narita M. Inside and out: the activities of senescence in cancer. *Nat Rev Cancer* 2014;14:547-58.
88. Campisi J, Andersen JK, Kapahi P, Melov S. Cellular senescence: a link between cancer and age-related degenerative disease? *Semin Cancer Biol* 2011;21:354-9.
89. Campisi J. Aging, cellular senescence, and cancer. *Annu Rev Physiol* 2013;75:685-705.
90. Landsberg J, Kohlmeyer J, Renn M, Bald T, Rogava M, Cron M, et al. Melanomas resist T-cell therapy through inflammation-induced reversible dedifferentiation. *Nature* 2012;490:412-6.
91. Shi LZ, Fu T, Guan B, Chen J, Blando JM, Allison JP, et al. Interdependent IL-7 and IFN-gamma signalling in T-cell controls tumour eradication by combined alpha-CTLA-4+alpha-PD-1 therapy. *Nat Commun* 2016;7:12335.

92. Eigentler TK, Caroli UM, Radny P, Garbe C. Palliative therapy of disseminated malignant melanoma: a systematic review of 41 randomised clinical trials. *Lancet Oncol* 2003;4:748-59.
93. Schwartzenuber DJ, Lawson DH, Richards JM, Conry RM, Miller DM, Treisman J, et al. gp100 peptide vaccine and interleukin-2 in patients with advanced melanoma. *N Engl J Med* 2011;364:2119-27.
94. Robert C, Thomas L, Bondarenko I, O'Day S, Weber J, Garbe C, et al. Ipilimumab plus dacarbazine for previously untreated metastatic melanoma. *N Engl J Med* 2011;364:2517-26.
95. Maio M, Grob JJ, Aamdal S, Bondarenko I, Robert C, Thomas L, et al. Five-year survival rates for treatment-naïve patients with advanced melanoma who received ipilimumab plus dacarbazine in a phase III trial. *J Clin Oncol* 2015;33:1191-6.
96. Hodi FS, O'Day SJ, McDermott DF, Weber RW, Sosman JA, Haanen JB, et al. Improved survival with ipilimumab in patients with metastatic melanoma. *N Engl J Med* 2010;363:711-23.
97. Schadendorf D, Hodi FS, Robert C, Weber JS, Margolin K, Hamid O, et al. Pooled analysis of long-term survival data from phase II and phase III trials of ipilimumab in unresectable or metastatic melanoma. *J Clin Oncol* 2015;33:1889-94.
98. Eggermont AM, Spatz A, Robert C. Cutaneous melanoma. *Lancet* 2014;383:816-27.
99. Gulley JL, Rajan A, Spigel DR, Iannotti N, Chandler J, Wong DJL, et al. Avelumab for patients with previously treated metastatic or recurrent non-small-cell lung cancer (JAVELIN Solid Tumor): dose-expansion cohort of a multicentre, open-label, phase 1b trial. *Lancet Oncol* 2017;18:599-610.
100. Kourie HR, Awada G, Awada A. The second wave of immune checkpoint inhibitor tsunami: advance, challenges and perspectives. *Immunotherapy* 2017;9:647-57.
101. Gide TN, Wilmott JS, Scolyer RA, Long GV. Primary and acquired resistance to immune checkpoint inhibitors in metastatic melanoma. *Clin Cancer Res* 2018;24:1260-70.
102. Voskens CJ, Goldinger SM, Loquai C, Robert C, Kaehler KC, Berking C, et al. The price of tumor control: an analysis of rare side effects of anti-CTLA-4 therapy in metastatic melanoma from the ipilimumab network. *PLoS One* 2013;8:e53745.
103. Hofmann L, Forschner A, Loquai C, Goldinger SM, Zimmer L, Ugurel S, et al. Cutaneous, gastrointestinal, hepatic, endocrine, and renal side-effects of anti-PD-1 therapy. *Eur J Cancer* 2016;60:190-209.
104. Zimmer L, Goldinger SM, Hofmann L, Loquai C, Ugurel S, Thomas I, et al. Neurological, respiratory, musculoskeletal, cardiac and ocular side-effects of anti-PD-1 therapy. *Eur J Cancer* 2016;60:210-25.
105. Eigentler TK, Hassel JC, Berking C, Aberle J, Bachmann O, Grunwald V, et al. Diagnosis, monitoring and management of immune-related adverse drug reactions of anti-PD-1 antibody therapy. *Cancer Treat Rev* 2016;45:7-18.
106. Hassel JC, Heinzerling L, Aberle J, Bahr O, Eigentler TK, Grimm MO, et al. Combined immune checkpoint blockade (anti-PD-1/anti-CTLA-4): evaluation and management of adverse drug reactions. *Cancer Treat Rev* 2017;57:36-49.

# Cancer immune control needs senescence induction by interferon-dependent cell cycle regulator pathways in tumours

Ellen Brenner<sup>1,14</sup>, Barbara F. Schörg <sup>2,14</sup>, Fatima Ahmetlić<sup>3,4,14</sup>, Thomas Wieder<sup>1</sup>, Franz Joachim Hilke<sup>5</sup>, Nadine Simon<sup>1</sup>, Christopher Schroeder<sup>5</sup>, German Demidov <sup>5</sup>, Tanja Riedel<sup>3</sup>, Birgit Fehrenbacher<sup>1</sup>, Martin Schaller<sup>1</sup>, Andrea Forschner<sup>1</sup>, Thomas Eigentler<sup>1</sup>, Heike Niessner<sup>1</sup>, Tobias Sinnberg <sup>1</sup>, Katharina S. Böhm<sup>1</sup>, Nadine Hömberg<sup>3,4</sup>, Heidi Braumüller<sup>1</sup>, Daniel Dauch<sup>6,7</sup>, Stefan Zwirner<sup>6</sup>, Lars Zender<sup>6,7,8</sup>, Dominik Sonanini<sup>2,6</sup>, Albert Geishauer<sup>3,4</sup>, Jürgen Bauer<sup>1</sup>, Martin Eichner<sup>9</sup>, Katja J. Jarick <sup>10</sup>, Andreas Beilhack<sup>10</sup>, Saskia Biskup<sup>8,11</sup>, Dennis Döcker<sup>1,11</sup>, Dirk Schadendorf <sup>7,12</sup>, Leticia Quintanilla-Martinez<sup>8,13</sup>, Bernd J. Pichler<sup>2,8</sup>, Manfred Kneilling<sup>1,2,8</sup>, Ralph Mocikat<sup>3,4</sup> & Martin Röcken<sup>1,7,8</sup>✉

Immune checkpoint blockade (ICB)-based or natural cancer immune responses largely eliminate tumours. Yet, they require additional mechanisms to arrest those cancer cells that are not rejected. Cytokine-induced senescence (CIS) can stably arrest cancer cells, suggesting that interferon-dependent induction of senescence-inducing cell cycle regulators is needed to control those cancer cells that escape from killing. Here we report in two different cancers sensitive to T cell-mediated rejection, that deletion of the senescence-inducing cell cycle regulators p16<sup>Ink4a</sup>/p19<sup>Arf</sup> (*Cdkn2a*) or p21<sup>Cip1</sup> (*Cdkn1a*) in the tumour cells abrogates both the natural and the ICB-induced cancer immune control. Also in humans, melanoma metastases that progressed rapidly during ICB have losses of senescence-inducing genes and amplifications of senescence inhibitors. Metastatic cells also resist CIS. Such genetic and functional alterations are infrequent in metastatic melanomas regressing during ICB. Thus, activation of tumour-intrinsic, senescence-inducing cell cycle regulators is required to stably arrest cancer cells that escape from eradication.

<sup>1</sup>Department of Dermatology, University of Tübingen, 72076 Tübingen, Germany. <sup>2</sup>Department of Preclinical Imaging and Radiopharmacy, Laboratory for Preclinical Imaging and Imaging Technology of the Werner Siemens-Foundation, University of Tübingen, 72076 Tübingen, Germany. <sup>3</sup>Institut für Molekulare Immunologie, Helmholtz-Zentrum München, 81377 Munich, Germany. <sup>4</sup>Eigenständige Forschungseinheit Translationale Molekulare Immunologie, Helmholtz Zentrum München, 81377 Munich, Germany. <sup>5</sup>Institute of Medical Genetics and Applied Genomics, University of Tübingen, 72076 Tübingen, Germany. <sup>6</sup>Department of Medical Oncology and Pneumology, University Hospital Tübingen, 72076 Tübingen, Germany. <sup>7</sup>German Cancer Research Consortium (DKTK), German Cancer Research Center (DKFZ), 69120 Heidelberg, Germany. <sup>8</sup>Cluster of Excellence iFIT (EXC 2180) "Image Guided and Functionally Instructed Tumor Therapies", 72076 Tübingen, Germany. <sup>9</sup>Institute of Clinical Epidemiology and Applied Biometry, University of Tübingen, 72076 Tübingen, Germany. <sup>10</sup>Department of Medicine II, Würzburg University, 97078 Würzburg, Germany. <sup>11</sup>Center for Genomics and Transcriptomics (CeGaT) GmbH and Practice for Human Genetics, 72076 Tübingen, Germany. <sup>12</sup>Department of Dermatology, University Hospital, West German Cancer Centre, University Duisburg-Essen, 45147 Essen, Germany. <sup>13</sup>Institute of Pathology, University of Tübingen, 72076 Tübingen, Germany. <sup>14</sup>These authors contributed equally: Ellen Brenner, Barbara F. Schörg, Fatima Ahmetlić. ✉email: [mrocken@med.uni-tuebingen.de](mailto:mrocken@med.uni-tuebingen.de)

Immune therapy with ICB and natural immune responses reveal that tumour-infiltrating cytotoxic T cells, natural killer cells and T<sub>H</sub>1 cells can be activated to cause cancer regression and clearance of tumour cells through cytolysis, apoptosis and by activated macrophages in mice and in humans<sup>1–10</sup>. Nonetheless, cancers are often not completely eliminated, and aggregate or single cancer cells may persist in a controlled state, called tumour dormancy<sup>2,11–17</sup>. The failure of inducing tumour dormancy is a major cause of treatment resistance that may result from inappropriate immune activation, low tumour mutation burden, resistance to lysis or apoptosis, and other mechanisms<sup>4,8,16,18–24</sup>. More recent data associate melanoma progression and treatment resistance of cancers with functional losses of the IFN-JAK1-STAT1 signalling pathway<sup>11,23,25–30</sup>. IFN- $\gamma$  has multiple effects on cancers. Previously, we have shown that the combined action of IFN- $\gamma$  and TNF is capable of inducing a stable, senescence-like growth arrest in cancer cells that is called cytokine-induced senescence (CIS)<sup>31</sup>. As the IFN-JAK1-STAT1 signalling cascade activates two key inducers of senescence<sup>14,31,32</sup>, p16<sup>Ink4a</sup> and p21<sup>Cip1</sup>, here we analyse whether cancer immune control requires the IFN- $\gamma$ -dependent induction of the tumour-intrinsic p16<sup>Ink4a</sup>-CDK4/6-Rb1 and MDM-p53-p21<sup>Cip1</sup> cell cycle regulation pathways to arrest those cancer cells that escape from cytotoxicity.

## Results

**Cancer immune control needs *Stat1*-dependent *Cdkn2a* activity.** In vitro activation of p16<sup>Ink4a</sup> and p21<sup>Cip1</sup> requires IFN- $\gamma$  signalling in the tumour cells<sup>31,32</sup>. We therefore asked whether in vivo activation of p16<sup>Ink4a</sup>, senescence induction and cancer immune control also require a functioning IFN- $\gamma$  signalling cascade in the cancer cells. To investigate the role of the IFN-*Stat1*-dependent activation of *Cdkn2a*, what encodes alternatively spliced variants, including the structurally related CDK4 kinase inhibitor isoforms p16<sup>Ink4a</sup> and p19<sup>Arf</sup>, we analysed the immune control of transplanted cancer cells isolated from RIP-Tag2 mice, where expression of the T antigen under the control of the rat insulin promoter (RIP) leads to pancreatic islet cancers (RT2-cancers)<sup>25</sup>. For this, we implanted either *Stat1*-positive or *Stat1*-negative RT2-cancer cells into syngeneic mice. Most *Stat1*-positive and *Stat1*-negative RT2-cancers (>80%) were rejected. As *Stat1*-positive and *Stat1*-negative RT2-cancers were similarly susceptible to lysis by cytotoxic CD8<sup>+</sup> T cells (Supplementary Fig. 1a), we depleted CD8 T cells with mAb before transplanting the cancer cells. Following CD8-depletion the tumours grew in vivo, and treatment was started when tumours reached >3 mm (Supplementary Fig. 1b). In sham-treated mice cancers reached a critical size within three weeks, and the tumours were analysed (Fig. 1a). The rapidly growing cancers from sham-treated mice had a proliferative Ki67<sup>+</sup>p16<sup>Ink4a</sup><sup>-</sup> phenotype (Fig. 1b, c and Fig. 2a) that was negative for phosphorylated heterochromatin protein 1 $\gamma$  (S93) (pHP1 $\gamma$ ) in senescence-associated heterochromatin foci (SAHF), H3K9me3 and senescence-associated  $\beta$ -galactosidase (SA- $\beta$ -gal) (Fig. 2b–d, Supplementary Fig. 2a, b). To determine whether the immune system can control these cancers, we treated mice with a combination of anti-PD-L1 and anti-LAG-3 mAb<sup>33</sup>. In preclinical studies and human trials, dual blockade of LAG-3 and the PD-1/PD-L1 interaction generates a more efficient anti-cancer immunity in mice and in humans than blocking either molecule alone<sup>34</sup>. The *Stat1*-positive RT2-cancers became growth arrested or regressed (Fig. 1a). The residual cancer cells displayed a senescent p16<sup>Ink4a</sup><sup>+</sup>, Ki67<sup>-</sup> phenotype with an induction of p21<sup>Cip1</sup> in single cells (Fig. 1b, c and Fig. 2a). RT2-cancers were also positive for pHP1 $\gamma$ , H3K9me3 and SA- $\beta$ -gal (Fig. 2b–d), and showed no ICB-induced double strand breaks as determined by  $\gamma$ H2AX and DNA-PK staining (Supplementary Fig. 3a, b). In contrast, ICB did

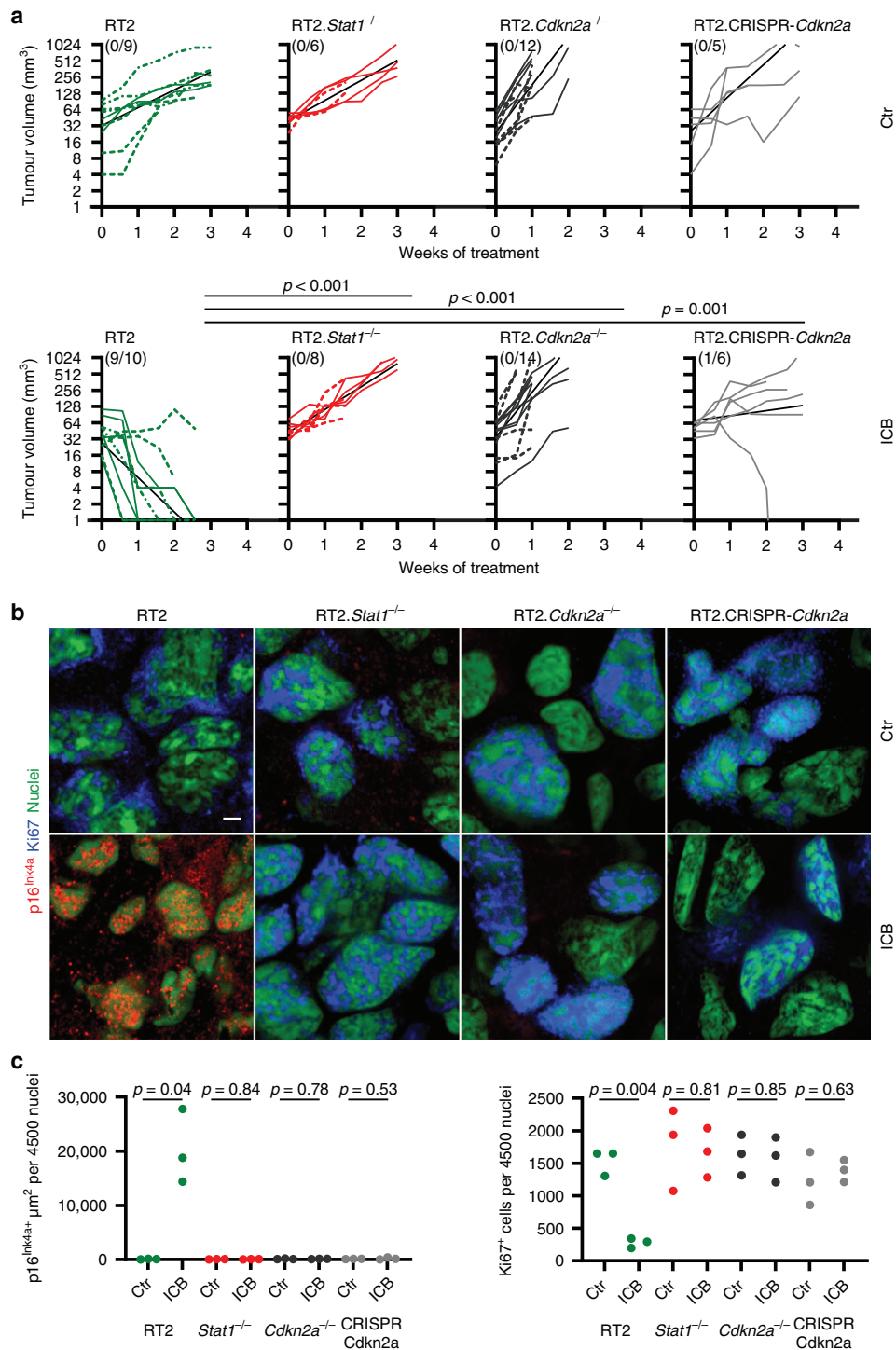
not arrest *Stat1*-negative RT2-cancers that grew rapidly even when treated with ICB (Fig. 1a). *Stat1*-negative tumour cells were p16<sup>Ink4a</sup>-negative and expressed Ki67 (Fig. 1b, c) but neither pHP1 $\gamma$ , H3K9me3, nor SA- $\beta$ -gal (Fig. 2b–d). In vitro data confirmed that RT2.*Stat1*<sup>-/-</sup>-cancers were selectively resistant to CIS but susceptible to apoptosis (Fig. 3a).

Immune activation with anti-PD-L1 and anti-LAG-3 requires the presence of PD-L1. *Stat1*-positive and *Stat1*-negative RT2-cancers expressed PD-L1 in the tumour tissue and on more than 10% of the isolated cancer cells (Supplementary Fig. 4a, b), showing that *Stat1*-negative RT2-cancers expressed the target of the anti-PD-L1 mAb. IFN- $\gamma$  strongly increased PD-L1 and  $\beta$ 2-microglobulin expression on RT2-cancer cells but not on RT2.*Stat1*<sup>-/-</sup>-cancer cells;  $\beta$ 2-microglobulin<sup>+</sup> cells were found in sections of RT2.*Stat1*<sup>-/-</sup>-cancers, showing that IFN- $\gamma$ -responsive host immune cells infiltrated the tumour microenvironment during ICB (Supplementary Fig. 4a–d).

*Stat1* was not required for tumour elimination by CD8<sup>+</sup> cells but for the induction of p16<sup>Ink4a</sup> by IFN- $\gamma$ -producing immune cells and for an efficient cancer immune control. As p16<sup>Ink4a</sup> is needed for CIS in RT2-cancer cells<sup>31</sup>, we asked whether cancer immune control needs the senescence-inducing cell cycle regulator p16<sup>Ink4a</sup> in the tumour cells. To address this question, we generated *Cdkn2a*-deficient RT2-cancer cell lines through in vitro and in vivo selection. Comparative genomic hybridisation (CGH) showed the loss of *Cdkn2a* on chromosome 4 (qC4.A) as the only genetic aberration common to all six cell lines (Supplementary Fig. 5a). PCR analysis confirmed the loss of *Cdkn2a* (Supplementary Fig. 5b); PCR also revealed that *Cdkn2a*<sup>-/-</sup>-RT2-cancer cells expressed Tag. RT2.*Cdkn2a*<sup>-/-</sup>-cancer cells also expressed PD-L1 and responded to IFN- $\gamma$  (Supplementary Fig. 4a, b, d). While the parental RT2-cancer cells were susceptible to CIS and to apoptosis, the *Cdkn2a*-loss mutant cell lines were resistant to CIS but susceptible to apoptosis in vitro (Fig. 3b). To test the role of *Cdkn2a* for tumour immune control in vivo, we injected the tumour cell lines into syngeneic mice and again started treatment with ICB once tumours reached a diameter >3 mm. As we transferred polyclonal *Cdkn2a*-loss mutant cancer cell lines, the tumours grew with slightly different dynamics (Fig. 1a). ICB did not attenuate the growth of *Cdkn2a*-deficient RT2-cancers. Immune histology showed that ICB also failed to induce senescence in *Cdkn2a*-deficient RT2-cancers as they displayed a Ki67<sup>+</sup>p16<sup>Ink4a</sup><sup>-</sup>, pHP1 $\gamma$ <sup>-</sup>, H3K9me3<sup>-</sup>, SA- $\beta$ -gal<sup>-</sup> phenotype (Fig. 1b, c and Fig. 2b–d).

To test whether the resistance to ICB specifically resulted from the p16<sup>Ink4a</sup>/p19<sup>Arf</sup> loss, and to exclude other potential confounders, we generated RT2-cancer cells from another diseased mouse and deleted p16<sup>Ink4a</sup>/p19<sup>Arf</sup> (*gCdkn2a*) using CRISPR-Cas9<sup>31</sup>. In vitro, RT2-cancer cells transfected with either a control sgGFP or the *gCdkn2a* construct grew with similar dynamics. Both cell types were sensitive to apoptosis. The CRISPR-Cas9 control cells expressed SA- $\beta$ -gal when exposed to IFN- $\gamma$ /TNF and did not restart their exponential growth following IFN- $\gamma$ /TNF withdrawal, showing that they were susceptible to CIS (Fig. 3c). In contrast, IFN- $\gamma$ /TNF did not induce SA- $\beta$ -gal in the RT2.CRISPR-*Cdkn2a*-cancer cells, and the cells restarted exponentially growing after IFN- $\gamma$ /TNF withdrawal, showing that RT2.CRISPR-*Cdkn2a*-cancer cells were resistant to CIS (Fig. 3c). To specifically analyse *Cdkn2a* in vivo, we injected the cells into the CD8-depleted mice. All CRISPR-Cas9 control cell lines were rejected, revealing that the cells were highly immunogenic. In contrast, 80% of the RT2.CRISPR-*Cdkn2a*-cancer cells grew in syngeneic mice (Supplementary Fig. 5c), demonstrating that natural immune responses required the senescence-inducing *Cdkn2a* gene to control these highly immunogenic cancer cells (Fig. 1a, upper panel). Even enhancement of the immune response with ICB did not arrest





their growth in vivo (Fig. 1a, lower panel). RT2.CRISPR-*Cdkn2a*-cancer cells expressed PD-L1,  $\beta$ 2-microglobulin (Supplementary Fig. 4a–d) and Tag. Immune histology revealed that the rapidly growing RT2.CRISPR-*Cdkn2a*-cancer cells had a Ki67<sup>+</sup>, p16<sup>Ink4a</sup><sup>-</sup>, pHP1 $\gamma$ <sup>-</sup>, SA- $\beta$ -gal<sup>-</sup> proliferative phenotype, but were positive for H3K9me3 (Fig. 1b, c and Fig. 2b–d). Even though H3K9me3 is a marker of senescence, others have shown that CRISPR-Cas9 editing itself may also induce a non-specific H3K9

methylation that persists<sup>35</sup>. Importantly, ICB treatment increased neither H3K9me3, nor DNA-PK, nor  $\gamma$ H2AX in RT2.CRISPR-*Cdkn2a*-cancer cells (Fig. 2c, Supplementary Fig. 3a, b).

CGH of 10 different cell lines revealed that the loss of the p16<sup>Ink4a</sup>/p19<sup>Arf</sup>-locus was the only common signature where the RT2.Cdkn2a<sup>-/-</sup> or the RT2.CRISPR-*Cdkn2a*-cancer cells differed from the parental or the CRISPR-Cas9 control cell lines (Supplementary Fig. 5a, b). We analysed a total of seven different

**Fig. 1** *Stat1*- and *Cdkn2a*-dependent immune control of transplanted RT2-cancers and induction of Ki67<sup>-</sup>p16<sup>Ink4a</sup><sup>+</sup> senescent cancer cells. **a** Individual follow-up of tumour volumes. CD8-depleted mice were subcutaneously (s.c.) engrafted with  $1 \times 10^6$  RT2-, RT2.*Stat1*<sup>-/-</sup>-, RT2.*Cdkn2a*<sup>-/-</sup>- or RT2.CRISPR-*Cdkn2a*-cancer cells. Treatment with isotype control mAbs (Ctr) or combined immune checkpoint inhibitors (ICB; anti-PD-L1 and anti-LAG-3) once per week was started when tumours were >3 mm in diameter. Cancer size was measured 2 times per week. Number of mice with regressing tumours and the total number of mice is given in parenthesis; RT2 Ctr *N* = 9, ICB *N* = 10, RT2.*Stat1*<sup>-/-</sup> Ctr *N* = 6, ICB *N* = 8, RT2.*Cdkn2a*<sup>-/-</sup> Ctr *N* = 12, ICB *N* = 14, RT2.CRISPR-*Cdkn2a* Ctr *N* = 5, ICB *N* = 10. Each cell line was given a different lining. Black lines summarise the results for different treatment groups (as obtained from ANCOVA). *p*-values examine the question whether the treatment effect was different between two genotypes. Mice were killed either when tumours reached the critical diameter of 15–20 mm or ulcerated, or when mice developed signs of wasting. **b** Representative triple-staining for the senescence marker p16<sup>Ink4a</sup> (red) and the proliferation marker Ki67 (blue) and for nuclei (green) of the s.c. tumour of individual mice treated as described in (a). Scale bar 2 μm. **c** Individual data points showing quantification of p16<sup>Ink4a</sup><sup>+</sup> (left) or Ki67<sup>+</sup> (right) cells. Each data point represents the total of three tumour slides measurements, tumours of three individual mice (described in a) were analysed. In a significance was tested by using unequal variances *t*-test, *p*-values examines the treatment effect, comparing the ICB-treated RT2-cancers with each ICB-treated knock-out group.

*Cdkn2a*-deficient RT2-cancer cell lines in vitro. All were resistant to CIS. Next, we analysed three of them in vivo, all were resistant to ICB. Thus, cytotoxic CD8<sup>+</sup> T cells can directly reject *Cdkn2a*-deficient RT2-cancers, but senescence-induction through IFN-γ-mediated activation of the cell cycle regulators p16<sup>Ink4a</sup>/p19<sup>Arf</sup> was strictly needed to control those cancer cells that escape from cytotoxicity.

Cancers are frequently rejected by CD8 T cells. In addition, immune clearance of senescent cancer is mediated by IFN-γ-producing T<sub>H</sub>1 cells and by IFN-γ-activated type I macrophages<sup>25,31,36–39</sup>. Indeed, the tumours controlled by ICB showed the established features of the T<sub>H</sub>1-mediated clearance mechanism, as β2-microglobulin was strongly expressed (Supplementary Fig. 4c, d) and as the tumours were infiltrated by CD3<sup>+</sup>CD8<sup>-</sup> T cells and F4/80<sup>+</sup> and MHC class II<sup>+</sup> activated macrophages (Supplementary Fig. 6a–c). We detected no CD8<sup>+</sup> T cells and no CD49b<sup>+</sup> NK cells (Supplementary Fig. 6d), what may be due to the fact that NK cells are primarily found in the spleen<sup>40,41</sup>. As ICB induced a similar immune infiltrate in RT2-cancers and in *Stat1*- and *Cdkn2a*-deficient RT2-cancers (Supplementary Fig. 6a–c), the data strongly suggest that senescence induction in the cancer cells was a prerequisite for tumour cell clearance by T<sub>H</sub>1 cells and IFN-γ-activated type I macrophages<sup>25,31,36–39</sup>.

**Cancer immune therapy and senescence induction require *Stat1*.** To determine whether IFN-γ signalling through *Stat1* is also needed for the induction of p16<sup>Ink4a</sup>, p21<sup>Cip1</sup>, senescence and the control of endogenous cancers that are destroyed by strong T cell responses, we treated RT2 mice by the combination of anti-PD-L1 and anti-LAG-3 mAbs and adoptive T cell transfer (AT), with T<sub>H</sub>1 cells specific for a tumour associated antigen (TAA) in the SV40-Tag protein<sup>31</sup> (Supplementary Fig. 7a). Combining anti-PD-L1/anti-LAG-3 mAbs with AT further enhances the therapeutic effect of ICB and largely eradicates all cancer cells<sup>33</sup>. We started the treatment once RT2 mice had a major cancer load, as documented by magnetic resonance imaging (Supplementary Fig. 7b). This immune therapy strongly decreased the islet size within 4 weeks, and functionally restored the blood glucose control (Fig. 4a–c). It largely destroyed the RT2-cancers but failed to eradicate all cancer cells (Fig. 4b, Supplementary Fig. 8a). Immune histology of residual RT2-cancers showed CD3<sup>+</sup> cells, MHC class II<sup>+</sup> and F4/80<sup>+</sup> cells following ICB/AT treatment but only very few or no Foxp3<sup>+</sup> regulatory T cells, CD8<sup>+</sup> or CD49b<sup>+</sup> cells (Fig. 5a, Supplementary Fig. 8a–c). The RT2-cancers expressed normal levels of Tag mRNA and protein (Fig. 5b, c) and expressed PD-L1 and β2-microglobulin protein (Supplementary Fig. 8d). The RT2-cancer cells showed a senescent phenotype as they expressed p16<sup>Ink4a</sup>, p21<sup>Cip1</sup>, H3K9me3, pHP1γ, and SA-β-gal but were Ki67<sup>-</sup> (Fig. 4d, e and Fig. 6a–d). Staining for γH2AX and DNA-PK, markers that mainly indicate

double strand breaks, remained largely negative, confirming that CIS caused only minor DNA damage (Supplementary Fig. 9). Electron microscopy confirmed the accumulation of SA-β-gal in the cytoplasm of senescent tumour cells (Supplementary Fig. 10a–c). These residual RT2-cancer cells were also functionally senescent. When isolated and cultured for ≥5 passages in vitro they preserved their growth-arrested, SA-β-gal<sup>+</sup> phenotype (Fig. 7a–c). RT2-cancer cells with such a senescent phenotype remain growth arrested for at least 3 months, even when transplanted into immune compromised NOD-SCIDII2ry<sup>-/-</sup> mice, demonstrating the absence of cancer initiating cells<sup>31</sup>.

Sham-treated RT2-mice, sham-treated *Stat1*<sup>-/-</sup> RT2 mice or *Stat1*<sup>-/-</sup> RT2 mice treated with ICB/AT died within 4 weeks, showed large tumours and failed to control their blood glucose levels (Fig. 4a–c). The tumours of these three groups of mice were strongly enriched in Ki67<sup>+</sup> RT2-cancer cells that were negative for p16<sup>Ink4a</sup>, p21<sup>Cip1</sup>, H3K9me3, pHP1γ, and SA-β-gal (Fig. 4d, e and Fig. 6a–d). The isolated tumour cells also proliferated strongly when cultured in vitro and did not develop a senescent phenotype (Fig. 7a–c). While treatment with ICB/AT did not induce a senescent phenotype and did not attenuate the tumour growth in the RT2.*Stat1*<sup>-/-</sup> mice, the inflammatory infiltrate was similar to that of cancers in RT2.*Stat1*<sup>+/+</sup> mice (Supplementary Fig. 8a–c). Also three-dimensional imaging and FACS analyses revealed that the adoptively transferred T cells and dendritic cells infiltrated RT2-cancers of *Stat1*<sup>-/-</sup> or *Stat1*<sup>+/+</sup> mice with similar dynamics (Supplementary Fig. 11a–e); immune histology confirmed these findings. Islet tumours of RT2 and RT2.*Stat1*<sup>-/-</sup> mice had both CD3<sup>+</sup> T-cells and MHC class II<sup>+</sup>, F4/80<sup>+</sup> macrophages (Fig. 5a and Supplementary Fig. 8a, b). In islet tumours of RT2.*Stat1*<sup>-/-</sup> mice the T cell infiltrate was variable but there was no detectable size difference between tumour areas that were strongly or poorly infiltrated. At this advanced cancer stage, the combined ICB/AT therapy was superior to either ICB or AT monotherapy that provided intermediate results (Fig. 4a–e and Fig. 6a–d).

Importantly, the tumour cells surviving the combined ICB/AT immune therapy did not result from classical immune evasion mechanisms. In vitro, all RT2-cancer cells, including the RT2.*Stat1*<sup>-/-</sup>-cancer cells were fully susceptible to T cell-mediated killing (Supplementary Fig. 1a) or apoptosis (Fig. 3a). RT2.*Stat1*<sup>+/+</sup>-cancer cells and RT2.*Stat1*<sup>-/-</sup>-cancer cells expressed normal levels of Tag (Fig. 5b, c), the antigen targeted by the immune therapy. RT2.*Stat1*<sup>+/+</sup>-cancers and RT2.*Stat1*<sup>-/-</sup>-cancers had normal baseline levels of PD-L1 and β2-microglobulin, and in RT2.*Stat1*<sup>-/-</sup>-cancers β2-microglobulin was in the tumour micro-environment (Supplementary Fig. 4a–d and Supplementary Fig. 8d). Foxp3 regulatory T cells were not increased inside the tumours (Supplementary Fig. 8b). In consequence, the RT2.*Stat1*<sup>-/-</sup>-cancers differed from RT2.*Stat1*<sup>+/+</sup>-cancers selectively by their resistance to CIS (Fig. 3a).

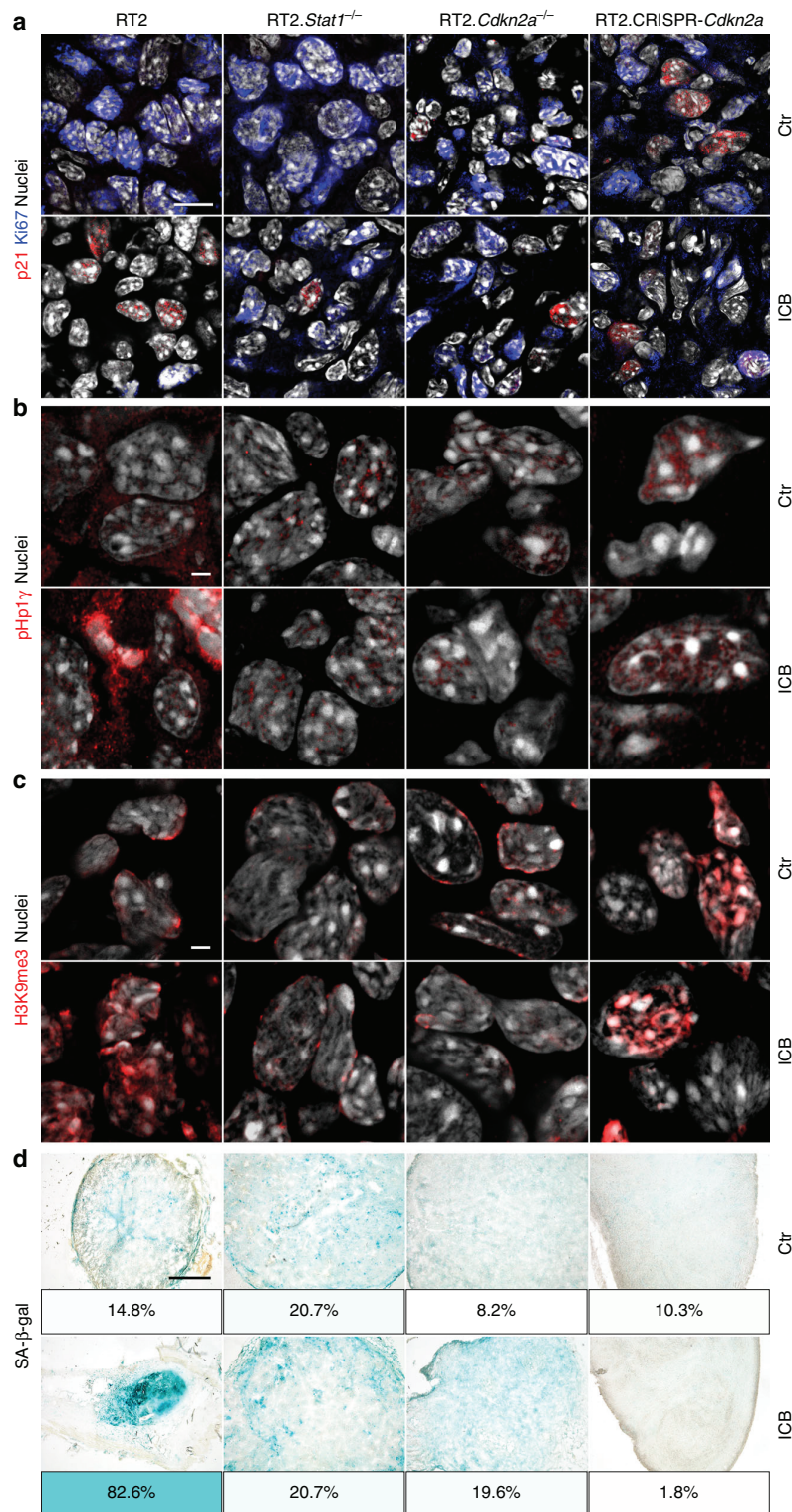


**Fig. 2** *Stat1*- and *Cdkn2a*-dependent induction of the senescence markers pHp1 $\gamma$ , H3K9me3, and of SA- $\beta$ -gal in transplanted RT2-cancers.

**a-d** Representative microscopic images of s.c. RT2-cancers from either RT2-, RT2.*Stat1*<sup>-/-</sup>-, RT2.*Cdkn2a*<sup>-/-</sup>- or from RT2.CRISPR-*Cdkn2a*-cancer cells. Mice were treated with isotype control mAbs (Ctr) or with immune checkpoint blockade (ICB, anti-PD-L1 and anti-LAG-3). Staining for the senescence marker p21<sup>Cip1</sup> (red), the proliferation marker Ki67 (blue) and for nuclei (white) (**a**), pHp1 $\gamma$  (red), nuclei (white) (**b**), H3K9me3 (red), nuclei (white) (**c**). SA- $\beta$ -gal activity at pH5.5 and percentage of SA- $\beta$ -gal positive tumour cells in each tumour (**d**). The colour evaluation and calculation of the SA- $\beta$ -gal<sup>+</sup> cells are described in Supplementary Fig. 2 and Methods (for **d**). Scale bars 10  $\mu$ m (**a**), 2  $\mu$ m (**b**, **c**), 1000  $\mu$ m (**d**). Histology was performed in one to three representative tumours from Fig. 1c.

Even though the ICB/AT combination therapy largely destroyed the tumours, the therapy failed to eradicate all cancer cells. Together the data prove that *Stat1* is needed to activate p16<sup>Ink4a</sup> in vitro and in vivo and that *Stat1*-mediated activation of *Cdkn2a* is needed to induce senescence in cancer cells. In consequence, cancer immune control required *Stat1*-mediated activation of the cell cycle regulators like p16<sup>Ink4a</sup> to stably arrest the growth of those cancer cells that are not eliminated by cytotoxicity.

**Cancer immune control needs IFN- $\gamma$ -dependent p21<sup>Cip1</sup> induction.** Following ICB *Stat1*-deficient cancers showed neither increased p16<sup>Ink4a</sup> nor p21<sup>Cip1</sup>. Thus, besides p16<sup>Ink4a</sup>, cancer immune control may also require p21<sup>Cip1</sup> activation. SV40-Tag expression impairs p53 activation<sup>42</sup>. As p53 regulates mRNA and protein production of p21<sup>Cip1</sup>, RT2-cancers are inappropriate to carefully investigate the role of p21<sup>Cip1</sup> for senescence induction in response to ICB. To test the need of senescence-inducing p21<sup>Cip1</sup> for cancer immune control and to determine whether senescence induction is also needed for tumours other than RT2-cancers, we studied the role of p21<sup>Cip1</sup> in the immune control of lymphomas. For this, we used  $\lambda$ -MYC mice, where a human *MYC* oncogene under the control of the immunoglobulin  $\lambda$  enhancer induces the development of endogenous B-cell lymphomas<sup>43</sup>. This also allows directly investigating the role of p21<sup>Cip1</sup> in the immune therapy of a naturally developing malignancy. Untreated mice died within <150 days (Fig. 8a) from Ki67<sup>+</sup>p16<sup>Ink4a</sup><sup>-</sup>, CD20<sup>low</sup> B-cell lymphomas that destroyed lymph nodes and spleen (Fig. 8b, c and Supplementary Fig. 12a). The Ki67<sup>+</sup> B cells were also negative for p21<sup>Cip1</sup>, pHP1 $\gamma$ , H3K9me3 or SA- $\beta$ -gal, showing that the tumours had a high proliferative capacity and were not senescent (Fig. 8b, c and Fig. 9a–c). Combined ICB with anti-CTLA-4 and anti-PD-1 mAb protected 18% (Fig. 8a) to 30% (Fig. 8d) of  $\lambda$ -MYC mice from lymphomas for at least 200 days. In a long-term experiment, 18% of the  $\lambda$ -MYC mice with a combined ICB therapy were still healthy at >250 days (Fig. 8a), a lifetime that has never been achieved by any other therapy in this mouse model. Treatment with either mAb alone did not rescue mice from lymphomas. Lymph nodes from healthy ICB-treated  $\lambda$ -MYC mice showed a normal architecture with normal B and T cell areas, expression of PD-L1 and  $\beta$ 2-microglobulin, no T cell infiltration, normal CD20<sup>+</sup> $\lambda$ -MYC<sup>-</sup> B cells, few CD161<sup>+</sup> cells, no signs of DNA double strand breaks and no destruction (Supplementary Fig. 12a–e). Even though we found no signs of immune destruction in the lymph nodes, depletion of pan-T cells with a mAb abrogated the ICB-mediated protection of  $\lambda$ -MYC mice, as all mice died from lymphomas by day 200 (Fig. 8d). Splenic dendritic cells of  $\lambda$ -MYC mice express the CTLA-4-targets CD80 and CD86 that are enhanced by IFN- $\gamma$ <sup>41</sup>. Lymphoma-specific, regulatory T cells are also increased in the spleen. Yet, depletion of regulatory T cells delays lymphoma development and death only for a short time<sup>40</sup>.

Nodal B cells from ICB-treated, healthy  $\lambda$ -MYC mice were Ki67<sup>-</sup> but strongly expressed nuclear p16<sup>Ink4a</sup> and p21<sup>Cip1</sup> (Fig. 8b, c), pHP1 $\gamma$ , H3K9me3 and SA- $\beta$ -gal (Fig. 9a–c), displaying a senescent phenotype<sup>24,31</sup>. This suggests that ICB-mediated protection from B-cell lymphomas included mechanisms other than cancer cell killing. To test whether ICB-mediated lymphoma prevention required the senescence-inducing p21<sup>Cip1</sup>, we generated syngeneic  $\lambda$ -MYC.p21<sup>Cip1</sup><sup>-/-</sup> mice. While ICB protected 18–30% of  $\lambda$ -MYC mice from lymphoma and death (Fig. 8a, d), all ICB-treated  $\lambda$ -MYC.p21<sup>Cip1</sup><sup>-/-</sup> mice died from lymphomas between day 100 and 210 (Fig. 8e). Histology revealed lymph node destruction by Ki67<sup>+</sup>, CD20<sup>low</sup> B cells that

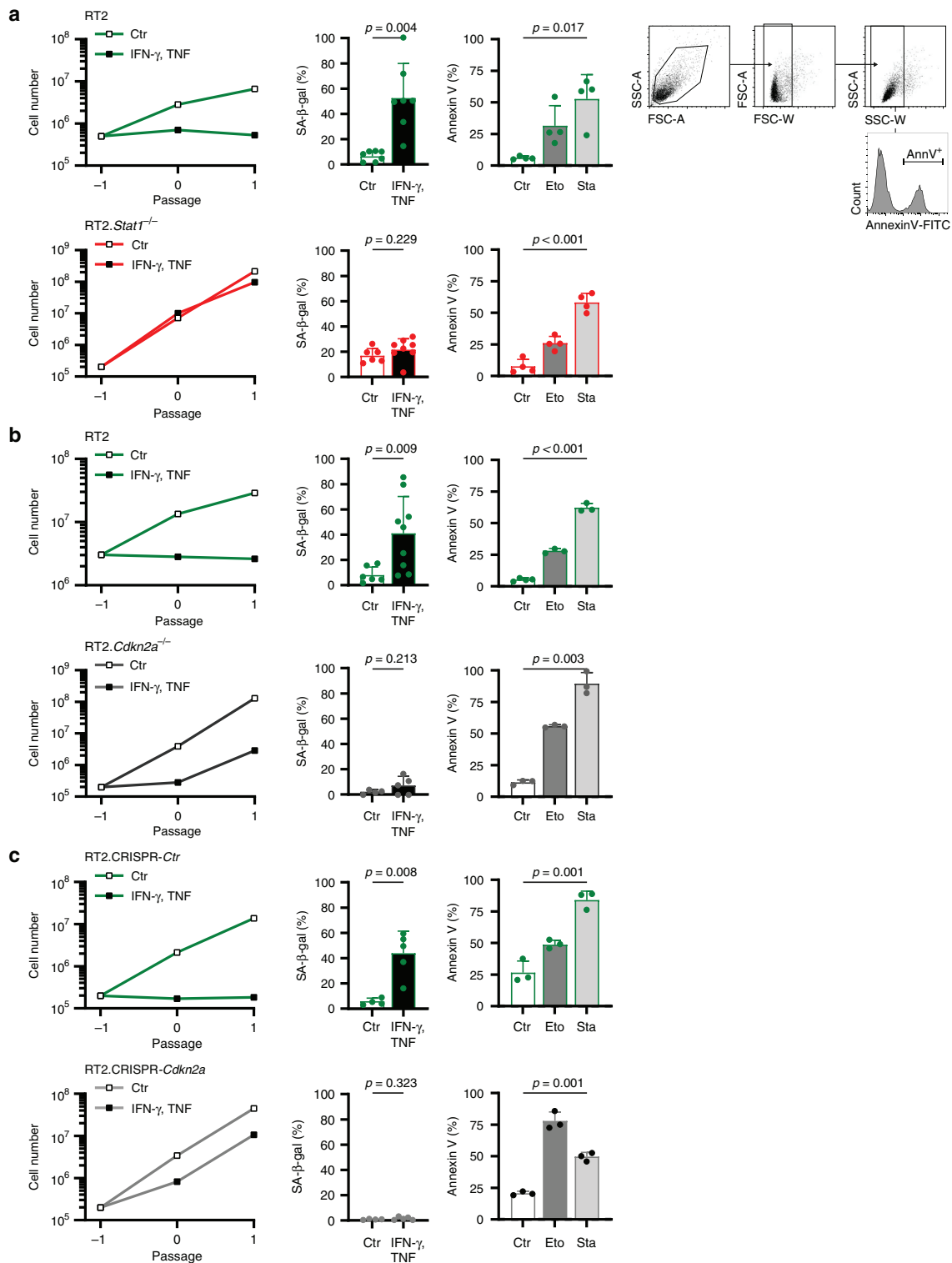
were devoid of the senescence markers p16<sup>Ink4a</sup>, p21<sup>Cip1</sup>, pHP1 $\gamma$ , H3K9me3, or SA- $\beta$ -gal (Fig. 8b, c, Fig. 9a–c and Supplementary Fig. 12a).

ICB-mediated p21<sup>Cip1</sup> induction and lymphoma prevention required IFN- $\gamma$ , as mice receiving ICB in the presence of anti-IFN- $\gamma$  mAb died from CD20<sup>low</sup> B-cell lymphomas as fast as untreated mice (Fig. 8a). B cells were Ki67<sup>+</sup> and negative for p21<sup>Cip1</sup>, p16<sup>Ink4a</sup>, pHP1 $\gamma$ , H3K9me3 and SA- $\beta$ -gal (Fig. 8b, c and Fig. 9a–c), showing that IFN- $\gamma$  was needed to activate the cell cycle regulators p16<sup>Ink4a</sup> and p21<sup>Cip1</sup> that, in turn, were required for senescence-induction in vivo. This proves that the senescence-inducing cell cycle regulator p21<sup>Cip1</sup> was strictly required to prevent the transition of pre-malignant B cells into B-cell lymphomas in ICB-treated  $\lambda$ -MYC mice, and that ICB-mediated p21<sup>Cip1</sup> activation was IFN- $\gamma$ -dependent.

### Impaired senescence pathways in melanomas resistant to ICB.

ICB is an approved standard of care therapy for metastatic melanoma and some other cancers, and efficient in about 40% of patients with metastatic melanoma. Another 40% are non-responder patients that mostly progress rapidly despite ICB therapy<sup>6,8,30,44</sup>. Based on the experimental data, we asked whether cell cycle regulator genes that control senescence induction were also needed for cancer immune control in humans. To address this, we compared the genetic alterations by targeted panel sequencing of 30 melanoma biopsies of consecutive non-responder patients, where metastases progressed within <3 months of ICB with the genetic alterations in melanoma biopsies of 12 responder patients, where metastases regressed during ICB  $\geq$ 1 year. For each patient we identified the tumour-specific alterations by paired sequencing of tumour and normal tissue. In agreement with published data, the biopsy material of responder patients had a significantly higher tumour mutational burden than that of non-responder patients<sup>8,10,45</sup> (Fig. 10a). We used a panel that includes a total of 678 established cancer-associated genes<sup>46</sup> (Supplementary Data Tables 1–3). To determine whether CIS was needed to protect from tumour progression, we explicitly focussed only on 19 genes of the panel that encode for molecules that are also involved in the IFN- $\gamma$ -mediated activation of the senescence signalling pathways that we identified in our murine experiments. This panel approach may have missed very rare fusion/translocation alterations of the genes investigated, but it would be difficult to identify such rare fusion/translocation alterations also with an exome-based approach, as the panel allowed the deep sequencing necessary to find the DNA alterations in less than 10% of all cells of the melanoma metastases.

We focused on somatic alterations, namely copy number variants (CNVs) and single nucleotide variants (SNVs) in key cell cycle control genes (*CCND1/2/3*; *CDKN2A/B/C*, *CDK4/6*, *CCNE1*, *CDKN1A/B*, *RB1*, *TP53*, *MDM2/4*), as well as *JAK1,2,3* and *MYC*. Both groups had a similar distribution of genetic aberrations in *JAK1,2,3*, *MYC* and the cell cycle control genes when all somatic alterations (SNVs and CNVs) were included (Fig. 10b). In contrast, comparing especially the number of strong amplification ( $\geq$  3fold amplification) and of fully inactivating mutations (homozygous deletions and loss of heterozygosity (LOH)), we observed significant differences between the two groups. Melanomas of non-responder patients had significantly more fully inactivating mutations of senescence-inducing cell cycle genes (*CDKN2A/B/C*; *CDKN1A/B*; *RB1*; *TP53*; *JAK1/2/3*) or  $\geq$  3fold amplifications of genes promoting cell cycle progression (*CCND1/2/3*; *CDK4/6*; *CCNE1*; *MDM2/4*; *MYC*) than the biopsy material of melanomas from responder patients (Fig. 10c, Supplementary Fig. 13 and 14a, b).



The genetic data were supported by functional analyses in vitro. Melanoma lines that we developed from biopsies of non-responder patients grew with similar dynamics as those derived from biopsies of responder patients and were susceptible to apoptosis (Fig. 10d). Yet, these cell lines were resistant to CIS. In contrast, melanoma lines that we derived from biopsy material

of responder patients were susceptible to both, CIS and drug-induced apoptosis. TNF and IFN- $\gamma$  are established inducers of annexin V and apoptosis in multiple cancer cells including melanoma cell lines<sup>47</sup>. Importantly, they induced senescence only in selected lines, such as those that could be derived from biopsy material of responder patients (Fig. 10e).

**Fig. 3** *Stat1*- and *Cdkn2a*-dependent induction of CIS in RT2-cancer cells, but *Stat1*- and *Cdkn2a*-independent induction of apoptosis. **a–c** Assays were performed with RT2-cancer cells (**a, b**), RT2.*Stat1*<sup>-/-</sup>-cancer cells (**a**), *Cdkn2a*-deficient RT2-cancer cells (**b**), or RT2.CRISPR-Ctr-control, or RT2.CRISPR-*Cdkn2a*-cancer cells (**c**). For the senescence growth assay, cells were cultured either with medium (Ctr) or with medium containing 100 ng ml<sup>-1</sup> IFN- $\gamma$  and 10 ng ml<sup>-1</sup> TNF for 96 h, washed and then cultured with medium for another 3–4 days. One representative out of 3 independent experiments was given. SA- $\beta$ -gal activity was determined after 96 h of culture with medium (Ctr) or with medium containing 100 ng ml<sup>-1</sup> IFN- $\gamma$  and 10 ng ml<sup>-1</sup> TNF, data show the mean with SD, RT2 Ctr  $n = 7$ , CIS  $n = 7$ , RT2.*Stat1*<sup>-/-</sup> Ctr  $n = 6$ , CIS  $n = 8$  (**a**), RT2 Ctr  $n = 6$ , CIS  $n = 9$ , RT2.*Cdkn2a*<sup>-/-</sup> Ctr  $n = 4$ , CIS  $n = 5$  (**b**), RT2.CRISPR-Ctr Ctr  $n = 4$ , CIS  $n = 5$ , RT2.CRISPR-*Cdkn2a* Ctr  $n = 4$ , CIS  $n = 5$  (**c**). For apoptosis induction, cells were exposed to either medium (Ctr) or etoposide (Eto, 100  $\mu$ M) or staurosporine (Sta, 0.5  $\mu$ M) for 24 h and then stained for annexin V. Positive cells were detected by flow cytometry data show the mean with SD (**a** (including gating strategy), **b, c**), RT2  $n = 4$ , RT2.*Stat1*<sup>-/-</sup>  $n = 4$  (**a**), RT2 Ctr  $n = 4$ , Eto, Stau  $n = 3$ , RT2.*Cdkn2a*<sup>-/-</sup>  $n = 3$  (**b**), RT2.CRISPR-Ctr and RT2.CRISPR-*Cdkn2a*  $n = 3$  (**c**). Significance tested by using unequal variances *t*-test.

## Discussion

Our results show that cancer control strictly requires the activation of tumour-intrinsic, senescence-inducing cell cycle regulators by the immune system to stably arrest those cancer cells that escape from eradication, in mice and in humans. Even though elimination of cancer cells is a primary therapeutic goal, cancer cell reduction by cytotoxicity is frequently incomplete and insufficient for permanent cancer control. About 90% of all cancer-related deaths result from metastases arising from reawakened, dormant cancer cells that survive chemo- or immunotherapies<sup>2,48–51</sup>, often months to decades after treatment of the primary tumour<sup>15</sup>. The data here unravel that IFN- $\gamma$ /STAT1-dependent activation of the senescence-inducing cell cycle regulators p16<sup>Ink4a</sup>/p19<sup>Arf</sup> and p21<sup>Cip1</sup> is needed to keep those cells senescent that escape from ICB-induced cell death, and that metastases resistant to immune therapies grow, when senescence-inducing signalling pathways become interrupted. This concept is supported by recent clinical data. Thus, melanoma metastases regress and may even clinically disappear upon ICB therapy, but can restart growing when mutations abrogate the IFN- $\gamma$ -signalling pathway<sup>26</sup>. Various observations suggest that immune control of cancers requires, in addition to cancer cell killing, IFN-dependent activation of cancer-intrinsic senescence-inducing cell cycle regulators<sup>13,14,31,52,53</sup>, to stably arrest those cancer cells that escape from cytotoxicity.

Even though senescence occurs following cancer therapy<sup>54</sup>, the role of senescence in the development of metastases and the response to chemo- and immune-therapy has not been resolved<sup>52,53,55</sup>. In mice, loss of p16<sup>Ink4a</sup> promotes the development of melanoma metastases in mice<sup>56</sup> and loss of the *Suv39h1* or *p53* genes in senescent cells may transform these cells in highly aggressive, cancer initiating cells<sup>24</sup>. In contrast, in humans the biallelic loss of *CDKN2A* has only been shown to promote melanoma invasion. Until now, it was not possible to identify specific gene mutations, like the loss of *CDKN2A* that promote the development of melanoma metastases in humans. This has only been demonstrated in mice<sup>56–59</sup>. The missing identification of metastases-promoting genes may be due to the fact that the IFN- $\gamma$ -mediated activation of the MDM2-p53-p21<sup>Cip1</sup> senescence pathway can in part compensate the loss of *CDKN2A*<sup>55</sup>. In line with this, we found gene amplifications of *MDM2* and *MDM4* in 26% and of *CDK4/6* in 13% of the melanoma biopsies of patients that did not respond to ICB. These amplifications were absent in melanoma biopsies of patients responding to ICB. More than half of the metastases of non-responder patients had at least one defect in the IFN-dependent senescence-signalling pathway. Both, p16<sup>Ink4a</sup> and p21<sup>Cip1</sup> induce senescence by inhibiting CDK4/6, and most genes associated with the resistance of melanoma metastases to ICB were up-stream of CDK4/6. Therefore, combining ICB with CDK4/6 inhibitors is a promising strategy to turn metastases with these types of defects in the senescence pathway from metastases not responding to ICB into metastases responding to ICB.

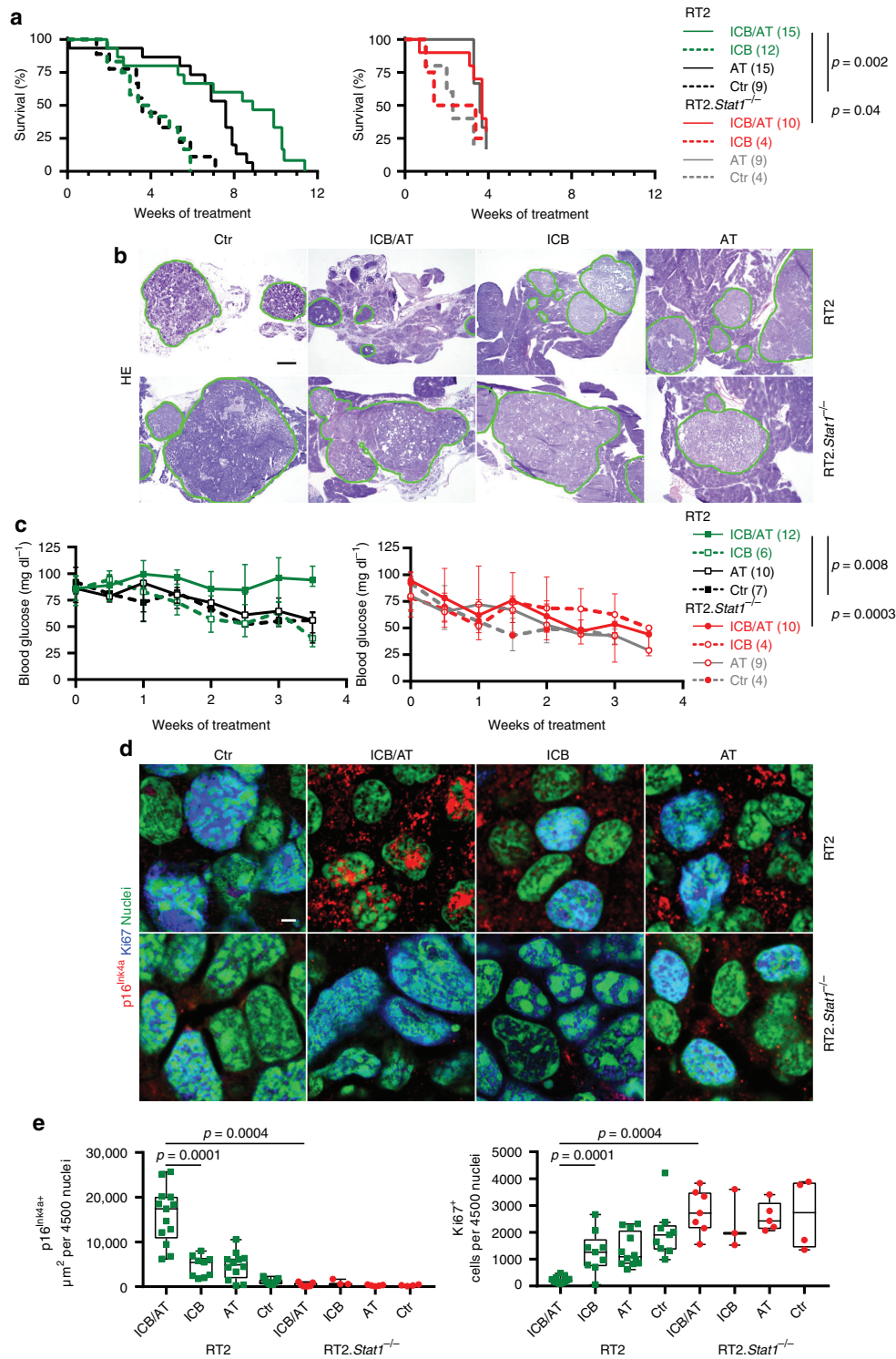
While senescence is established as a barrier against cancer development<sup>60</sup>, and while it is needed to prevent the rapid regrowth of cancers that escape from therapy- or immune-mediated lysis or apoptosis, the exact role of senescence in halting the progression of established cancers is still under debate. Some data suggest that the senescence-associated secretory phenotype (SASP) may even exert harmful effects<sup>54</sup>. Moreover, senescence induction requires subsequent clearance of the residual cancer cells by T<sub>H</sub>1 cells and macrophages to protect from cancer progression in a model of hepatocellular carcinoma<sup>36</sup>. In contrast, other data strongly suggest that senescence is a critical barrier that protects better against the progression of cancers than the attempt to clear all cancer cells<sup>61</sup>.

It remains open whether senescence in established cancers generally protects against cancer progression or whether this depends on the mode of senescence induction. TNF and IFN- $\gamma$  are major inducers of apoptosis in cancer cells but some cells escape from TNF- and IFN- $\gamma$ -induced apoptosis<sup>47</sup>. We have previously shown that TNF and IFN- $\gamma$  induced senescence in cells escaping from TNF/IFN- $\gamma$ -mediated apoptosis<sup>31</sup>, and here we showed that CIS protected from the regrowth of cancer cells resistant to the elimination by natural or ICB-enhanced cytotoxicity. In RT2-cancers, CIS establishes a stable type of senescence where the SASP does not promote cancer progression for prolonged periods of time, as the senescent RT2-cancer cells remain growth arrested for extended periods of time, even when transplanted into severely immune compromised mice<sup>31</sup>. Importantly, CIS requires the combined action of TNF and IFN- $\gamma$ , as immune therapies of cancers in the absence of either IFN- $\gamma$ , of *Stat1*- or of *Tnfr1*-signalling strongly accelerate the transformation and growth of cancer cells<sup>19,25</sup>.

This is especially relevant in the context of our data showing that melanoma metastases that fail responding to ICB therapies and that grow very fast despite ICB, frequently show functionally relevant gene aberrations in IFN- $\gamma$ -regulated, cancer-intrinsic senescence-inducing cell cycle regulators. Even though IFN- $\gamma$  induces a broad spectrum of tumour-protective mechanisms, the data here proved that IFN- $\gamma$ -dependent senescence induction is a key mechanism required to protect against those cancer cells that escape from cytotoxicity.

## Methods

**Animals.** C3HeB/FeJ mice were purchased from The Jackson Laboratory (Bar Harbor, ME, USA). Syngeneic transgenic TCR2 mice<sup>31,62</sup> express a T cell receptor (TCR) specific for Tag peptide 362–384 on CD4<sup>+</sup> T cells, RIP-Tag2 (RT2) mice express the T antigen under control of the rat insulin promoter (RIP) that leads to pancreatic islet cancers (RT2-cancers)<sup>31,62</sup> and double transgenic RT2.*Stat1*<sup>-/-</sup> mice (backcross of 129S6/SvEv-*Stat1*<sup>tm1Rds</sup> mice<sup>31</sup>) were provided by Taconic and backcrossed to C3HeB/FeJ. OT-1 mice (C57BL/6-Tg(Tcr $\alpha$ Cr $\beta$ )1100Mjb/J), and NSG (NOD.Cg-Prkdc<sup>scid</sup>Il2rg<sup>tm1Wjl</sup>/SzJ) mice were from The Jackson Laboratory.  $\lambda$ -MYC mice and double transgenic  $\lambda$ -MYC.p21<sup>-/-</sup> mice (both C57BL/6 background) express a human *MYC* oncogene under the control of the immunoglobulin  $\lambda$  enhancer and develop an endogenous B-cell lymphoma<sup>43</sup>. Mice with C3HeB/FeJ background, OT-1 mice and NSG-mice were bred in the animal facility Tübingen.  $\lambda$ -MYC and  $\lambda$ -MYC.p21<sup>-/-</sup> mice were bred in the animal facility Munich. All animals were bred under specific pathogen-free conditions. Animal



experiments were in accordance with animal welfare regulations and ethical approval was obtained by the local authorities (Regierung von Oberbayern and Regierungspräsidium Tübingen).

**Treatment of RT2-cancers in C3HeB/FeJ mice.** A total of  $1 \times 10^6$  cells (in 100  $\mu$ l NaCl) RT2-, RT2.Stat1<sup>-/-</sup>-, RT2.Cdkn2a<sup>-/-</sup>- or RT2.CRISPR-Cdkn2a-cancer cells were s.c. transplanted, three days after depletion of CD8 cells with 100  $\mu$ g anti-CD8

mAb<sup>39</sup> (Rm-CD8-2 AK, Core Facility mAb, Helmholtz-Zentrum München). CD8 depletion was repeated every ten days till the tumour lesion became palpable. Once tumours were  $\geq 3$  mm, mice were treated with anti-PD-L1 mAb and anti-LAG-3 mAb once per week (initially 500  $\mu$ g, then 200  $\mu$ g). Ctr mice received isotype-control mAbs (clone LTF-2 and HRPN, Bio X Cell). Tumour growth was monitored two times per week using a calliper and blood glucose was measured twice a week using an Accu-Check sensor for up to 8 weeks. Cancer size was measured two times per week. Mice were sacrificed after 4 treatment cycles, when the tumour

**Fig. 4** *Stat1*-dependent immune control of endogenous RT2-cancers and induction of Ki67<sup>+</sup>p16<sup>Ink4a</sup><sup>+</sup> senescent cancer cells. **a** Survival curves of RT2 or RT2.*Stat1*<sup>-/-</sup> mice treated with either isotype control mAbs (Ctr, RT2 *N* = 9, RT2.*Stat1*<sup>-/-</sup> *N* = 4), with adoptive transfer of T antigen-specific CD4<sup>+</sup> T<sub>H</sub>1 cells (AT, RT2 *N* = 15, RT2.*Stat1*<sup>-/-</sup> *N* = 9), with immune checkpoint inhibitors (ICB, RT2 *N* = 12, RT2.*Stat1*<sup>-/-</sup> *N* = 4; anti-PD-L1 and anti-LAG-3) or with ICB/AT (RT2 *N* = 15, RT2.*Stat1*<sup>-/-</sup> *N* = 10). For each AT experiment we generated a non-cytotoxic Tag-specific T<sub>H</sub>1 cell line. **b** Cancer size shown by representative hematoxylin and eosin staining of pancreas of RT2 (upper panel) or RT2.*Stat1*<sup>-/-</sup> mice (lower panel) after four weeks of treatment. Mice were treated as described in **a**. Green lines depict the size of RT2-cancers after treatment. After 4 weeks of treatment ICB/AT-treated mice (*N* = 6) had a two-fold smaller islet size than Ctr (*N* = 7). **c** Time course of blood glucose levels as surrogate marker for the growth of the insulin-producing tumours of RT2 or RT2.*Stat1*<sup>-/-</sup> mice (median ± interquartile range) treated as described in **a** (Ctr, RT2 *N* = 7, RT2.*Stat1*<sup>-/-</sup> *N* = 4; AT, RT2 *N* = 10, RT2.*Stat1*<sup>-/-</sup> *N* = 9; ICB, RT2 *N* = 6, RT2.*Stat1*<sup>-/-</sup> *N* = 4, ICB/AT, RT2 *N* = 12, RT2.*Stat1*<sup>-/-</sup> *N* = 10). The mice were sacrificed after 4 weeks of treatment for ex vivo analysis. **d, e** Representative triple-staining for the senescence marker p16<sup>Ink4a</sup> (red) and the proliferation marker Ki67 (blue) and for nuclei (green) (**d**), **e** showing quantification of p16<sup>Ink4a</sup><sup>+</sup> (left) or Ki67<sup>+</sup> (right) cancer cells of individual mice, treated as described in **a**, each data point represents the total of three tumour slides measurements (Ctr, RT2 *N* = 9, RT2.*Stat1*<sup>-/-</sup> *N* = 4; AT, RT2 *N* = 12, RT2.*Stat1*<sup>-/-</sup> *N* = 5; ICB, RT2 *N* = 9, RT2.*Stat1*<sup>-/-</sup> *N* = 3, ICB/AT, RT2 *N* = 13, RT2.*Stat1*<sup>-/-</sup> *N* = 7), box plots show the median with 25th and 75th interquartile range (IQR), and whiskers indicate 1.5 × IQR. Significance tested by using Log Rank test (**a**, left), Fishers exact test (**a**, right), or two-tailed Mann-Whitney test (**c**, **e**). RT2.*Stat1*<sup>-/-</sup> mice have been censored after 3.7 weeks of treatment. Scale bars 200 μm (**b**) or 2 μm (**d**). Number of mice is given in parenthesis.

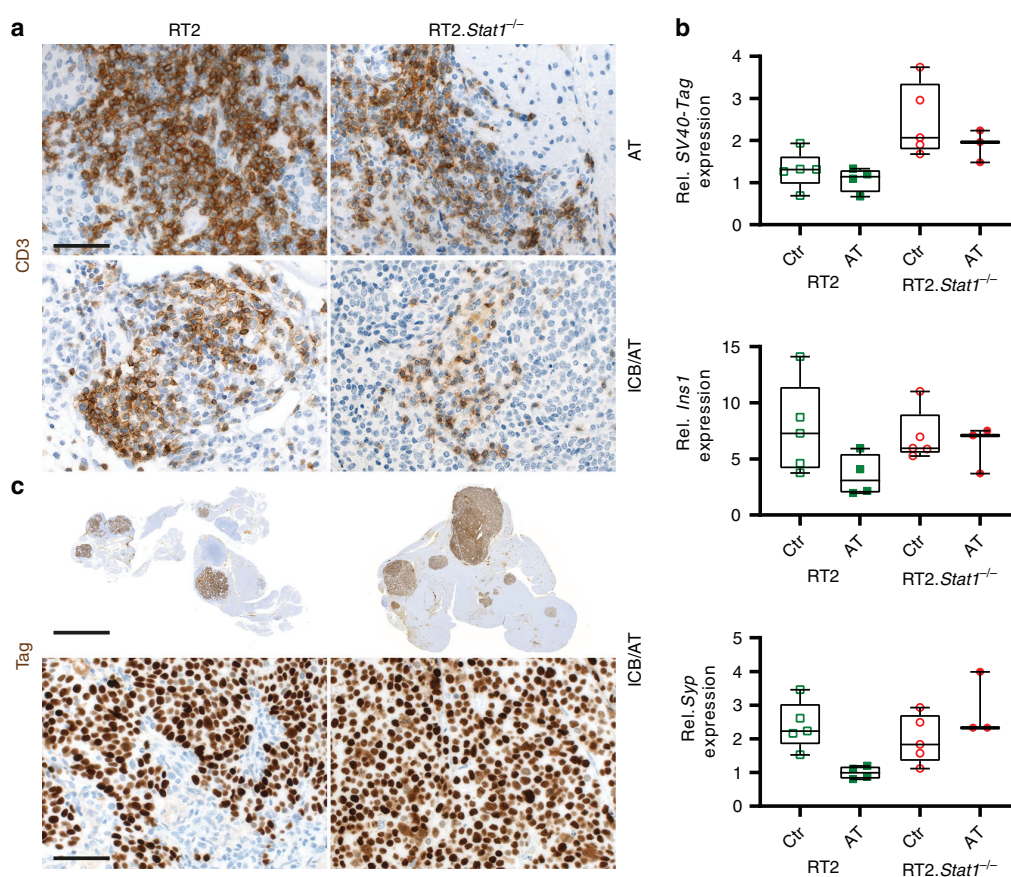
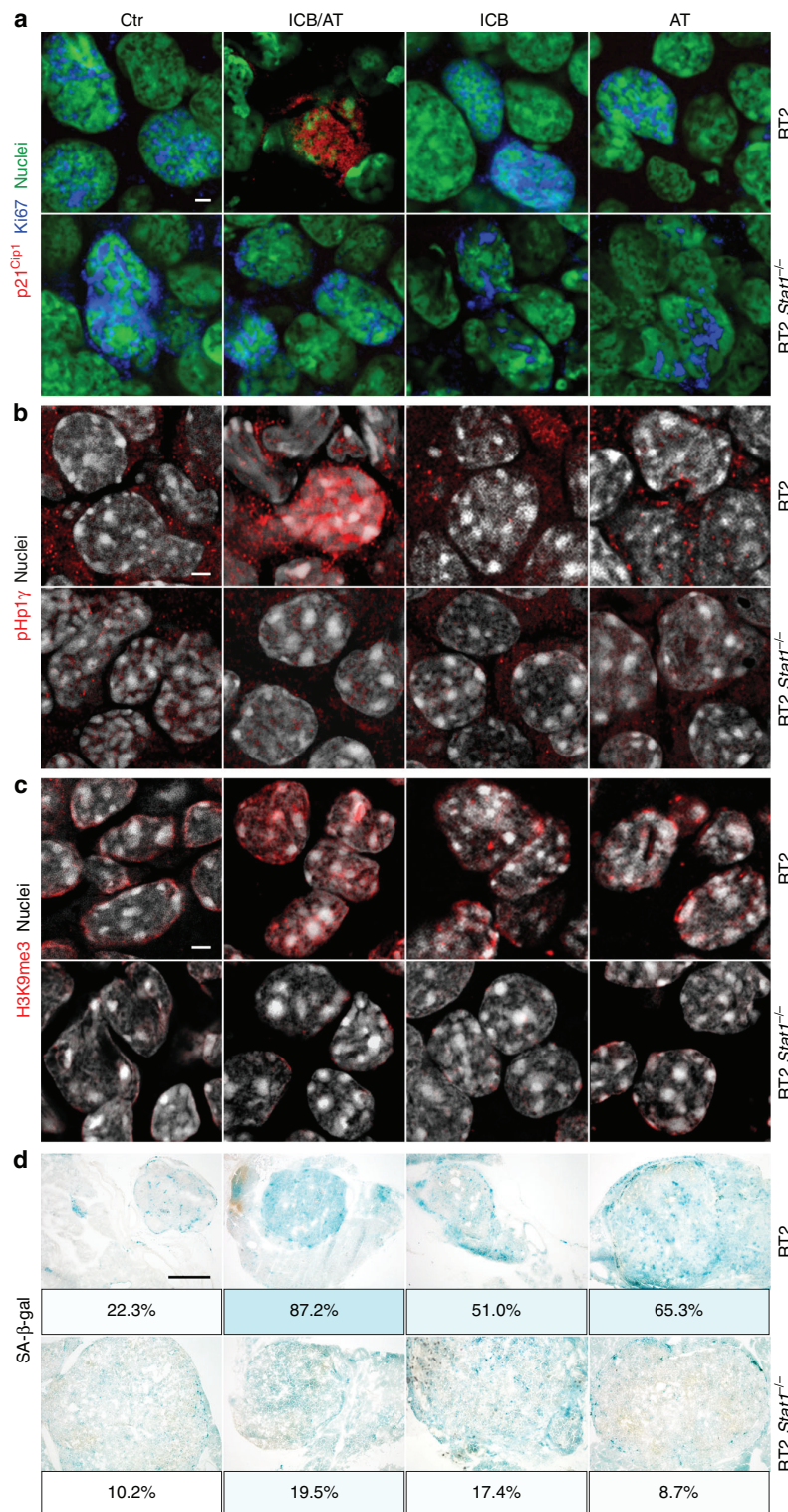


**Fig. 5** Infiltration of either RT2 or RT2.*Stat1*<sup>-/-</sup> cancers by CD3<sup>+</sup> T cells, mRNA expression of tumour associated antigens (TAA) and protein expression of the SV40-Tag tumour antigen recognised by the transferred TAA-specific T<sub>H</sub>1 cells. **a** Representative CD3 immune histochemistry images of RT2-cancers from either RT2 or RT2.*Stat1*<sup>-/-</sup> mice treated with adoptive transfer of T antigen-specific CD4<sup>+</sup> T<sub>H</sub>1 cells (AT) or immune checkpoint blockade combined with AT (ICB/AT), scale bar 20 μm. **b** Relative expression of SV40-Tag, insulin (*Ins1*) or of synaptophysin (*Syp*) in single tumours isolated from RT2 or RT2.*Stat1*<sup>-/-</sup> mice after control (Ctr) treatment with NaCl or AT. Gene expression was analysed using *Actb* and *Eef1a1* as references. Each point represents one tumour from one mouse (Ctr, RT2 *N* = 5, RT2.*Stat1*<sup>-/-</sup> *N* = 5; AT, RT2 *N* = 4, RT2.*Stat1*<sup>-/-</sup> *N* = 3), box plots show the median with 25th and 75th interquartile range (IQR), and whiskers indicate 1.5 × IQR. **c** SV40-Tag immunohistochemistry images of RT2-cancers were from either RT2 or RT2.*Stat1*<sup>-/-</sup> mice after ICB/AT therapy. Scale bar upper panel 400 μm, lower panel 20 μm.

diameter reached >15 mm, or ulcerated or when blood glucose dropped the second time below 30 mg dl<sup>-1</sup>. Tumours were collected for ex vivo analysis. The tumour volume was calculated as ellipsoid  $V = \frac{4}{3}\pi abc$ ; *a*, *b*, *c* are the semi-major axis ( $\frac{\text{length}}{2}$ ), ( $\frac{\text{width}}{2}$ ), with the assumption that the tumour height is equal to the short tumour side, defined as width *b* = *c*.

**Treatment of RT2 or RT2.*Stat1*<sup>-/-</sup> mice.** Ten- to eleven-week-old old female RIP-Tag2 (RT2)<sup>31,62</sup> or RT2.*Stat1*<sup>-/-</sup> mice were irradiated with 2 Gy one day before the first i.p. transfer of  $1 \times 10^7$  tumour antigen-specific T<sub>H</sub>1 cells. Tag-specific T<sub>H</sub>1 cells were generated from spleen and lymph node cells of TCR2 mice. CD4<sup>+</sup> T cells were enriched by positive selection over magnetic microbeads. To generate Tag-T<sub>H</sub>1 cells CD4<sup>+</sup> T cells were stimulated with Tag





peptide 362–384 (EMC Microcollections), CpG-DNA 1668 (Eurofins MWG Operon) and 11B11 mAb (anti-IL-4; in-house production) and cultured in the presence of irradiated (30 Gy), syngeneic, T-cell-depleted antigen presenting cells (APC)<sup>39</sup>. After 3–4 days, Tag-T<sub>H</sub>1 cells were expanded in the presence of 50 U IL-2 (hrIL-2). After cultivation for another 8 days, the Tag-T<sub>H</sub>1 cells were used for adoptive transfer<sup>31</sup>. Cell transfer was applied once weekly. Anti-PD-L1 mAb (clone 10F.9G2, Bio X Cell) and anti-LAG-3 mAb (clone C9B7W, Bio X

Cell) were i.p. injected twice per week (initially 500 µg each, afterwards 200 µg). Ctr mice received isotype-matched control antibodies (clone LTF-2 and HRPN, Bio X Cell) and PBS. Blood glucose was measured twice per week using the HemoCue Glucose 201+ System (HemoCue). Treatment was ended either after 4 treatment cycles for ex vivo analysis of tumour tissue, or when the blood glucose of the mice dropped twice below 30 mg dl<sup>-1</sup> or when disease reached evidence; mice had no food restriction.

**Fig. 6** *Stat1*-dependent induction of the nuclear senescence markers p21<sup>Cip1</sup>, HP1 $\gamma$ , H3K9me3, and SA- $\beta$ -gal in RT2-cancers by combined ICB/AT therapy. Representative fresh frozen cryostat sections of RT2-cancers from either RT2 or RT2.*Stat1*<sup>-/-</sup> mice with established cancers were treated with either isotype control mAbs (Ctr), with adoptive transfer of TAA-specific T<sub>H</sub>1 cells (AT), with immune checkpoint inhibitors (ICB; anti-PD-L1 and anti-LAG-3), or with ICB/AT. **a** p21<sup>Cip1</sup> (red), Ki67 (blue), nuclei (green). **b** HP1 $\gamma$  (red), nuclei (white). **c** H3K9me3 (red), nuclei (white). **d** Representative microscopic images of SA- $\beta$ -gal activity at pH5.5 and percentage of SA- $\beta$ -gal positive tumour cells in each tumour. The colour evaluation and calculation of the SA- $\beta$ -gal<sup>+</sup> cells are described in Supplementary Fig. 2 and Methods. Scale bars 2  $\mu$ m (**a-c**), 1000  $\mu$ m (**d**). Histology was performed in one to three representative tumours from Fig. 4e.

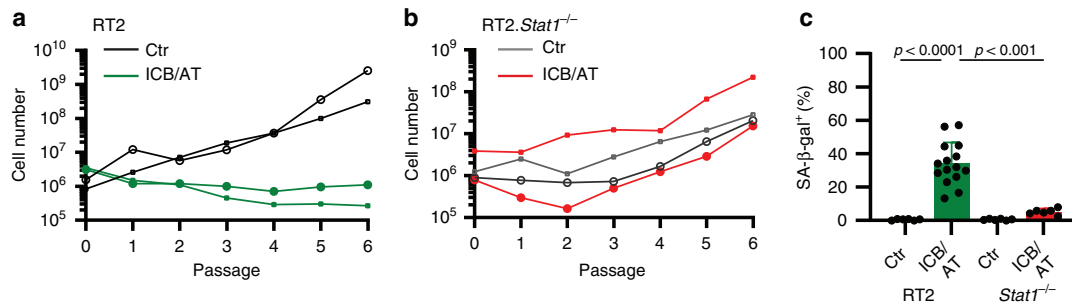


**Fig. 7** *Stat1*-dependent induction of senescence in RT2-cancers by combined ICB/AT therapy. **a**, **b** Either RT2 mice (**a**) or RT2.*Stat1*<sup>-/-</sup> mice (**b**) with established cancers were either treated with isotype control mAbs (Ctr) or treated with immune checkpoint blockade (anti-PD-L1 and anti-LAG-3) and adoptive transfer of TAA-specific T<sub>H</sub>1 cells (ICB/AT). After four weeks of treatment cells were isolated from the RT2-cancers and cultured in medium. Cells were counted at each passage. **c** After the passage  $\geq 5$ , we determined the percentage of the SA- $\beta$ -gal<sup>+</sup> cells. Data show the mean with SD; Ctr, RT2  $n = 6$ , RT2.*Stat1*<sup>-/-</sup>  $n = 6$ ; ICB/AT, RT2  $n = 15$ , RT2.*Stat1*<sup>-/-</sup>  $n = 6$ . Staining for synaptophysin confirmed that the cultured cells were RT2-cancer cells. Significance was tested by using unequal variances t-test.

**Treatment of  $\lambda$ -MYC mice.**  $\lambda$ -MYC mice and double transgenic  $\lambda$ -MYC.p21<sup>-/-</sup> mice received intraperitoneal (i.p.) injections of 100  $\mu$ g anti-CTLA-4 mAb (clone UC10-4B9, BioLegend) and 100  $\mu$ g anti-PD-1 mAb (clone J43, Bio X Cell) (ICB) two to four times every ten days, starting at day 55 after birth. Control mice (Ctr) received no treatment. For IFN- $\gamma$  neutralisation (ICB/anti-IFN- $\gamma$  mAb), mice were additionally treated with an initial dose of 500  $\mu$ g on day 54 and later with 300  $\mu$ g anti-IFN- $\gamma$  mAb (clone XMGI.2<sup>25</sup>, Core Facility mAb, Helmholtz-Zentrum München) 6 h prior to the anti-CTLA-4/ PD-1 mAbs injection. Administration of 100  $\mu$ g of the IFN- $\gamma$ -neutralising mAb was continued at ten day intervals until the mice developed lymphomas. T cells were depleted by i.p. injection of 1 mg anti-pan-T-cell mAb MmTC<sup>53</sup> at day 54. Treatment was repeated every 3 to 4 days using doses of 400  $\mu$ g. Mice were sacrificed as soon as tumours became clinically visible.

**Immunofluorescence staining.** Fresh frozen 5  $\mu$ m serial cryosections of lymph nodes from  $\lambda$ -MYC mice, whole pancreas from RT2 and RT2.*Stat1*<sup>-/-</sup> mice or isolated RT2-, *Stat1*<sup>-/-</sup>, or p16<sup>Ink4a</sup>-deficient RT2-cancer cells were fixed with periodate-lysine-paraformaldehyde. Sections were blocked using donkey serum and stained with primary antibodies using rabbit-anti-p16<sup>Ink4a</sup> (clone CDKN2A, catalogue number AHP1488, dilution 1:100 Bio-Rad/Serotec), rat-anti-Ki67 (clone SolA15, catalogue number 14-5698-82, dilution 1:100, Thermo Fisher Scientific/eBioscience), rat-anti-p21<sup>Cip1</sup> (clone HUGO291, catalogue number, dilution 1:100, Abcam), goat-anti-CD20 (clone M-20, catalogue number sc-7735, dilution 1:50, Santa Cruz), rabbit-anti-CD3 (clone SP7, catalogue number C1597R06, dilution 1:100, DCS), rabbit-anti-pHP1 $\gamma$  phospho S93 (aa 50-150, catalogue number ab45270, dilution 1:50, Abcam), rabbit-anti-H3K9me3 (aa 1-100, catalogue number ab8898, dilution 1:100, Abcam), rat-anti-PD-L1 (clone MIH6, catalogue number ab80276, dilution 1:50, Abcam) to use a mAb that recognises a different PD-L1 epitope than the applied in vivo mAb from clone 10F.9G2, rabbit-anti-beta 2 microglobulin antibody (clone EP2978Y, catalogue number ab75853, dilution 1:50, Abcam), goat-anti-CD3 $\epsilon$  (clone M-20, catalogue number sc-1127, dilution 1:20, Santa Cruz), rat-anti-CD8a (clone 53-6.7, catalogue number 14-0081, dilution 1:1000, eBioscience), rat-anti-F4/80 (clone BM8, catalogue number 14-4801-82, dilution 1:50, eBioscience), rat-anti-MHC Class II antigen I Ak,d,b,q,r (ER-TR3) (catalogue number NB100-64961, dilution 1:200 Novusbio), armenian hamster-anti-CD49b (Integrin alpha 2) (catalogue number 14-0491 dilution 1:50, eBioscience), rabbit-anti-gamma H2A.X (phospho S139) (aa 100-200, catalogue number ab2893, dilution 1:200, abcam), goat-anti-DNA PKcs (aa 4078-4128, catalogue number ab168854, dilution 1:500, abcam), rabbit-anti-synaptophysin (aa 41-62, catalogue number NB300-653, dilution 1:200, Novusbio), rabbit-anti-CD161 antibody (clone ERP21236, catalogue number ab234107, dilution 1:100, abcam), rabbit-anti-Foxp3 (aa 43-100, catalogue number NB 100-39002, dilution 1:200, Novusbio). Bound antibodies were visualised using donkey-anti-rabbit-Cy3 (catalogue number 711-166-152, dilution 1:500 Dianova), donkey-anti-rat-Alexa 647 (catalogue number 712-606-153, dilution 1:500 Dianova), donkey-anti-rat-Cy3

(catalogue number 712-166-153, dilution 1:500, Dianova), donkey-anti-goat-Cy3 (catalogue number 705-166-147, dilution 1:500, Dianova) and donkey-anti-rabbit-Alexa 488 catalogue number 711-546-152, dilution 1:500, Dianova). For nuclear staining, Yopro (catalogue number Y 3603, dilution 1:1000, Invitrogen) or DAPI (catalogue number D9542, dilution 1:2000 Sigma) was used. Sections were analysed using a LSM 800 confocal laser scanning microscope (Zeiss Oberkochen). Images were processed with the software ZEN 2.3 (blue edition) and the Image Analysis Module.

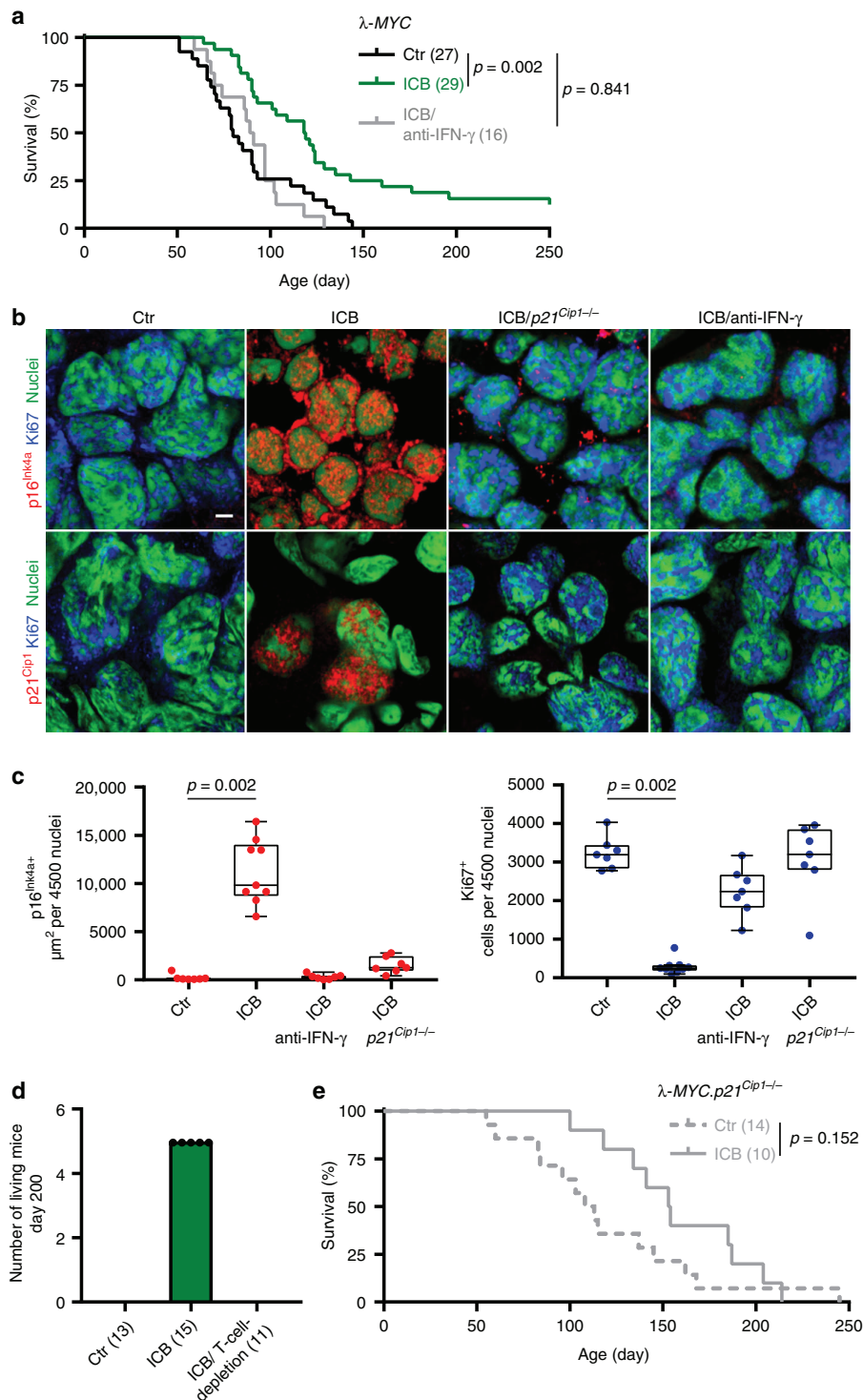
**Quantification of immunofluorescence.** Tumour areas of images derived from three individual stained cryosections per tissue sample were analysed. For quantification of the Ki67 staining, 4500 Yopro stained nuclei were counted for Ki67<sup>+</sup> cells (1500 per slide, three serial slides per mouse). For quantification of p16<sup>Ink4a</sup>, the area ( $\mu$ m<sup>2</sup>) of the nuclear p16<sup>Ink4a</sup> signal derived from 4500 Yopro stained nuclei (1500 per slide three serial slides per mouse) was measured.

**Hematoxylin and eosin staining.** Hematoxylin and eosin staining of the serial cryosections was performed according to standard procedures.

**Immunohistochemistry staining.** Immunohistochemistry was performed on an automated immunostainer (Ventana Medical Systems) according to the company's protocols for open procedures with slight modifications. 5  $\mu$ m sections were stained with rabbit-anti-human/mouse-CD3 (clone SP7, catalogue number CI597C01, dilution 1:50, DCS-diagnostics) and PAB101 (Tag-specific mouse IgG2a mAb; dilution 1:200; in-house production).

**SA- $\beta$ -gal detection.** 20  $\mu$ m serial cryosections were fixed in 2% formaldehyde/0.25% glutaraldehyde and washed in PBS/MgCl<sub>2</sub>. Slides were incubated in X-gal (5-bromo-4-chloro-3-indolyl-beta-D-galactopyranoside) staining solution (1 mg/mL X-Gal, 1 mM MgCl<sub>2</sub>, 5 mM K3Fe(CN)<sub>6</sub>, 5 mM K4Fe(CN)<sub>6</sub> in PBS, pH 4.0, 5.5, and 7.0) up to 10 h at 37  $^{\circ}$ C<sup>64</sup>. The stained slides were rinsed in PBS/MgCl<sub>2</sub> and analysed using a Nikon Eclipse 80i microscope; magnification  $\times 4$ .

**SA- $\beta$ -gal positive percentage quotation with Adobe Photoshop CS6.** All images were analysed with the "White Balance Tool" to obtain the same white background, followed by "Quick Mask Mode" to identify only the tumour area. Using this area the arithmetic mean of the blue-green values was obtained by the filter "Blur Average Tool". The "Eye Dropper Tool" was used to identify the red, green and blue (RGB) colour code to get the corresponding colour field (Supplementary Fig. 2a). Afterwards the tumour area was reselected using the previous created "Quick Mask Mode Layer". The pixels outside the tumour area were deleted by inverting the selection. The number of pixels in the histogram correlates with the tumour area. "The Posterize Tool" separated the different tonal values, in



our case blue-green. “The Magic Wand Tool” was used to select and delete the white pixels (Supplementary Fig. 2b). The number of pixels correlates with the area of SA- $\beta$ -gal stained tumour cells. The SA- $\beta$ -gal stained tumour cells in Fig. 2d, Fig. 6d and Fig. 9c were calculated and given in percent (blue pixel of total pixels of the tumour area).

**SA- $\beta$ -gal activity for electron microscopy.** Small tissue samples (semi-thin 0.5  $\mu\text{m}$  and for electron microscopy ultra-thin 20 nm, respectively) were fixed in fixation solution (0.25% Glutaraldehyde in 2% PFA) and washed in PBS/MgCl<sub>2</sub>

solution. X-gal staining solution was added for 12 h. Samples were washed in PBS/MgCl<sub>2</sub> solution afterwards followed by Karnovsky fixation. Samples were embedded in glycid ether for electron microscopic analysis<sup>64</sup>.

**Electron microscopy.** SA- $\beta$ -gal stained cryosections were fixed with Karnovsky’s fixative for 24 h. Post-fixation was based on 1% osmium tetroxide containing 1.5% K-ferrocyanide in cacodylate buffer. After following the standard methods, blocks were embedded in glycid ether and cut using an ultra-microtome (Ultracut, Reichert, Vienna, Austria). Ultra-thin sections (30 nm) were mounted on copper

**Fig. 8 IFN- $\gamma$  and p21<sup>Cip1</sup>-dependent immune control of  $\lambda$ -MYC-induced lymphomas by ICB therapy.** **a** Survival curves of control (Ctr  $N = 27$ ), or immune checkpoint inhibitor (ICB; anti-CTLA-4 and anti-PD-1  $N = 29$ ) treated  $\lambda$ -MYC mice, or of  $\lambda$ -MYC mice treated with ICB and anti-IFN- $\gamma$  ( $N = 16$ ). **b, c** Triple-staining for the senescence marker p16<sup>Ink4a</sup> (red, upper panel) or p21<sup>Cip1</sup> (red, lower panel), the proliferation marker Ki67 (blue), and for nuclei (green); scale bar 2  $\mu$ m; representative pictures from Fig. 8c (**b**). Box plots with individual data points representing p16<sup>Ink4a</sup> (**c**, left) or Ki67<sup>+</sup> nuclei (**c**, right) of B cells from Ctr- ( $N = 7$ ), ICB- ( $N = 9$ ), ICB and anti-IFN- $\gamma$ -treated  $\lambda$ -MYC mice ( $N = 7$ ), or ICB-treated  $\lambda$ -MYC.p21<sup>Cip1</sup><sup>-/-</sup> mice ( $N = 7$ ). Lymph nodes were isolated at similar ages. Each point represents triplicates from one mouse, box plot show the median with 25th and 75th interquartile range (IQR), and whiskers indicate 1.5  $\times$  IQR. **d**  $\lambda$ -MYC mice from the individual treatment groups living at day 200, Ctr  $N = 13$ , ICB  $N = 15$ , ICB and T-cell-depletion  $N = 11$ . **e** Survival curves of either control (Ctr,  $N = 14$ ) or ICB-treated  $\lambda$ -MYC.p21<sup>Cip1</sup><sup>-/-</sup> mice ( $N = 10$ ). Significance tested by using Log Rank test (**a**, **e**), two-tailed Mann-Whitney test (**c**).

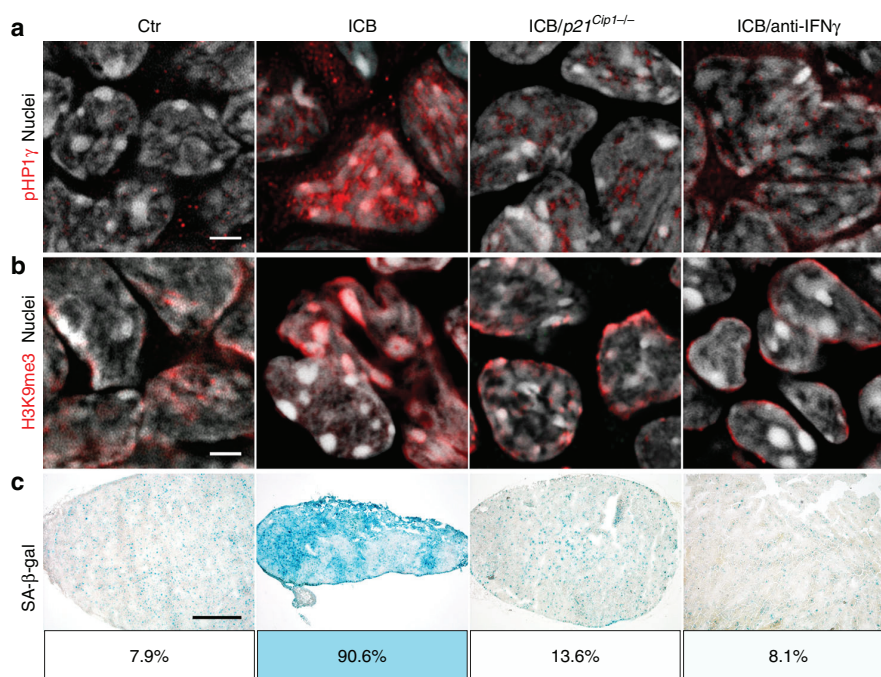


**Fig. 9 IFN- $\gamma$  and p21<sup>Cip1</sup>-dependent senescence induction in B cells of  $\lambda$ -MYC mice during ICB.** **a–c** Fresh frozen cryostat sections of representative lymph nodes of  $\lambda$ -MYC or  $\lambda$ -MYC.p21<sup>Cip1</sup><sup>-/-</sup> mice.  $\lambda$ -MYC mice were controls (Ctr) or treated with anti-CTLA-4 and anti-PD-1 mAbs (ICB) or anti-CTLA-4, anti-PD-1 and anti-IFN- $\gamma$  mAbs (ICB/anti-IFN- $\gamma$ ), or  $\lambda$ -MYC.p21<sup>Cip1</sup><sup>-/-</sup> mice were treated with ICB (ICB/p21<sup>Cip1</sup><sup>-/-</sup>). pHP1 $\gamma$  (red), nuclei (white) (**a**). H3K9me3 (red), nuclei (white) (**b**). Representative microscopic images of SA- $\beta$ -gal activity at pH5.5 and percentage of SA- $\beta$ -gal positive tumour cells in each tumour (**c**). The colour evaluation and calculation of the SA- $\beta$ -gal<sup>+</sup> cells are described in Supplementary Fig. 2 and Methods. Scale bars 2  $\mu$ m (**a**, **b**), 1000  $\mu$ m (**c**). The SA- $\beta$ -gal data are representative for three individual tumours. Immune fluorescence was performed in one to two representative tumours from Fig. 8c.

grids and analysed using a Zeiss LIBRA 120 transmission electron microscope (Carl Zeiss, Oberkochen, Germany) operating at 120 kV.

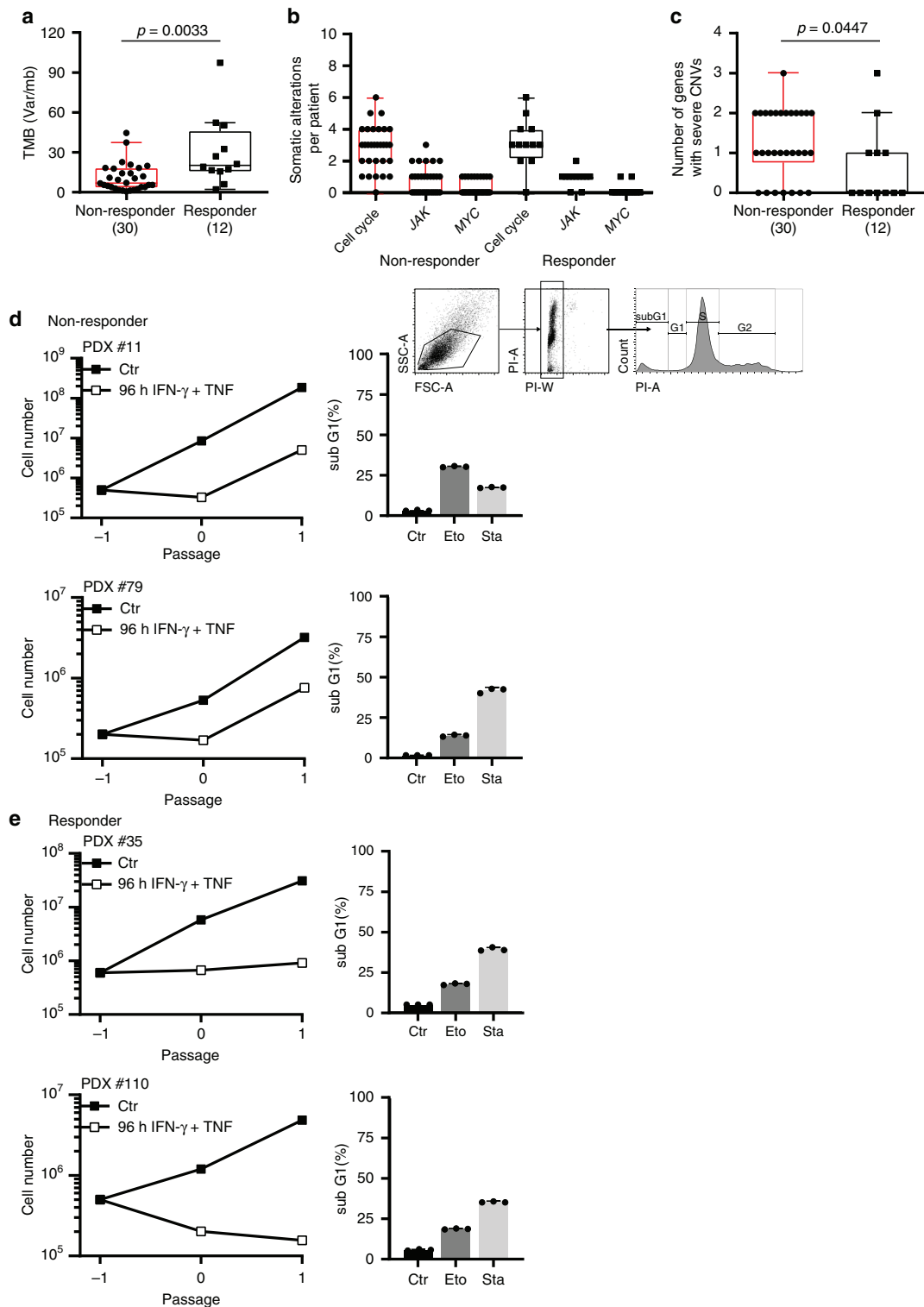
**Cell culture.** Adherent primary murine RT2-cancer cells (described above), B16-F10 melanoma cells (catalogue number CRL-6475, ATCC) and B16-OVA melanoma cells (gift from R. Dutton, Trudeau Institute, New York, USA) were cultured in Dulbecco's Modified Eagle's Medium (DMEM) supplemented with 10% foetal calf serum (FCS), nonessential amino acids, sodium pyruvate, antibiotics, and 50  $\mu$ M 2-mercaptoethanol at 37  $^{\circ}$ C and 7.5% CO<sub>2</sub>. The murine melanoma cell lines B16 and B16-OVA were cultured in DMEM medium, containing 10% FCS and penicillin/streptomycin (100 U ml<sup>-1</sup>; all from Biochrom AG), at 37  $^{\circ}$ C and 5% CO<sub>2</sub>. The human patient-derived xenograft (PDX) cell lines were cultured in RPMI-1640 medium supplemented with 10% FCS, nonessential amino acids, sodium pyruvate, antibiotics, and 5  $\mu$ g ml<sup>-1</sup> Plasmocin (Invitrogen) to treat infections of clinical samples, at 37  $^{\circ}$ C and 5.0% CO<sub>2</sub>. Cell line supernatants were tested with a mycoplasma detection PCR Venor GeM (Minerva Biolabs GmbH) regularly every 4 weeks.

**Generation of primary murine RT2- or RT2.Stat1<sup>-/-</sup>-cell lines.** RT2-cancers were isolated from the pancreas of female RT2 or RT2.Stat1<sup>-/-</sup> mice by intraductal injection of collagenase (1 mg ml<sup>-1</sup>, Serva, Heidelberg, Germany)<sup>25,31</sup>. After injection, the pancreata were harvested, digested in collagenase solution at 37  $^{\circ}$ C for 10 min, and then mechanically disrupted. Whole encapsulated tumours were separated under a dissection microscope (Leica Microsystems) and further

processed for immunofluorescence microscopy, immunohistochemistry or gene expression analysis. Alternatively, single tumour cells were obtained by incubation of the tumours in 0.05% trypsin/EDTA solution (Invitrogen) at 37  $^{\circ}$ C for 10 min. After incubation, RT2-cancer cells were seeded onto tissue culture plates.

**Generation of primary p16<sup>Ink4a</sup>-deficient RT2-cell lines.** CDKN2a-loss variants on chromosome 4, qC4.a were generated by random selection from CIS- or ICB-resistant RT2-cancer cells.

**Generation of CRISPR-mediated deletion of Cdkn2a in primary RT2-cell lines.** gRNAs targeting Exon 2 (position 120–142 and 125–157) of murine *Cdkn2a* (sequence from Ensembl genome browser 97) were designed using CRISPRdirect<sup>65</sup> (*gCdkn2a\_1*: 5'-gcgtcgtggtggtgcacagg-3', *gCdkn2a\_2*: 5'-gacacgctggtggtgctgcac-3'). As a control a previously described gRNA targeting GFP (sgRNA target site sequence: 5'-ggcgaggagctgtaccg-3')<sup>66</sup> was used. The DNA oligos were ordered from Sigma Aldrich. Equimolar amounts of complementary DNA oligos were annealed and phosphorylated in T4 ligation buffer (NEB). The reaction was performed at 37  $^{\circ}$ C for 30 min, 95  $^{\circ}$ C for 5 min, followed by a gradual temperature reduction to 25  $^{\circ}$ C (5  $^{\circ}$ C/min). The vector pSpCas9(BB)-2A-GFP (pX458; Addgene plasmid ID: 48138) was digested with the *BbsI* restriction enzyme (NEB) and dephosphorylated using Calf Intestinal Alkaline Phosphatase (NEB). The ligation reaction (NEB) was performed overnight. The plasmids were sequenced (Microsynth Seqlab) with a hU6 sequencing primer (LKO.1 5'-gactatcatatgcttaccgt). For transfection, plasmid DNA was generated by using the Qiagen



EndoFreeMaxi Kit.<sup>66</sup> The primary RT2-cell lines were transfected using the QuiaGene Effectene Transfection Reagent.

**Generation of primary human melanoma cell lines.** Melanoma tissue was cut into small pieces, digested in HBBS (w/o  $\text{Ca}^{2+}$  and  $\text{Mg}^{2+}$ ) with 0.05% collagenase, 0.1% hyaluronidase and 0.15% dispase, at 37 °C for 1 h and filtered through a cell strainer

(100  $\mu\text{m}$  mesh). The melanoma cell suspension was implanted with Matrigel (Corning Life Sciences) subcutaneously in NSG (NOD.Cg-Prkdc<sup>scid</sup> Il2rg<sup>tm1Wjl/SzJ</sup>) mice, patient derived xenografts (PDX). Tumour grafts were harvested when they reached a diameter of 10 to 15 mm, digested as above and the single cells were taken into culture using RPMI1640 with Heps and L-Glutamine, containing 10% foetal bovine serum, 1% penicillin-streptomycin at 37 °C with 5%  $\text{CO}_2$  and 95% humidity. For cryo-preservation cell pellets were resuspended in Biofreeze medium (Biochrom/Merck)

**Fig. 10 Loss of senescence-inducing and amplification of senescence-inhibiting cell cycle regulator genes in melanoma metastases of patients resistant to ICB.**

**a–c** Sequencing data from metastases of non-responder patients ( $N = 30$ ) versus metastases of responder patients ( $N = 12$ ). In non-responder patients disease progressed within 3 months of ICB therapy. In responder patients metastases regressed  $\geq 1$  year of ICB therapy. Tumour mutational burden (TMB, copy number variations) (**a**). Number of tumour-specific alterations in 19 genes of the cell cycle, *JAK* or *MYC* pathway (**b**). Number of genes with homozygous deletions in cycle inhibitors or amplifications  $\geq 3$  fold in cell cycle promoters. Genes analysed: *CDKN2A/B/C*, *CDKN1A/B*, *RBI*, *TP53*, *JAK1/2/3*, *CCND1/2/3*, *CDK4/6*, *CCNE1*, *MDM2/4*, *MYC*. We performed paired panel sequencing of the tumour DNA and of normal DNA to identify tumour-specific alterations. Box plots show the median with 25th and 75th interquartile range (IQR), and whiskers indicate  $1.5 \times$  IQR (**c**). **d, e** Growth curves of patient derived melanoma lines from two metastases of non-responder patients (**d**) or from two metastases of responder patients (**e**). Cells were cultured for the senescence assay either with medium (Ctr) or with medium containing  $100 \text{ ng ml}^{-1}$  IFN- $\gamma$  and  $10 \text{ ng ml}^{-1}$  TNF for 96 h, washed and then cultured with medium for another 4–6 days. **d, e** Apoptosis assay with melanoma cells derived from two non-responder (**d**, including gating strategy) or two responder patients (**e**) were exposed to either medium (Ctr) or etoposide (Eto,  $100 \mu\text{M}$ ) or staurosporine (Sta,  $0.5 \mu\text{M}$ ) for 24 h for apoptosis induction and then stained with propidium iodide. SubG<sub>1</sub> cells were detected by flow cytometry analysis; data show the geometric mean with geometric SD,  $n = 3$ . Significance tested by using two-tailed Mann-Whitney test (**a–c**).

and  $1 \text{ ml}$  per cryotube of the cell suspension was frozen for short-term storage at  $-80^\circ\text{C}$  and for long-term storage in liquid nitrogen.

**Senescence assay.** RT2-, RT2.*Stat1*<sup>-/-</sup>-, RT2.*p16*<sup>Ink4a</sup>-, RT2-CRISPER-control- or RT-CRISPER-*p16*<sup>Ink4a</sup>-cancer cells or human melanoma-derived (PDX) cells were cultured with medium containing  $100 \text{ ng ml}^{-1}$  IFN- $\gamma$  and  $10 \text{ ng ml}^{-1}$  TNF or exclusively with medium (Ctr) for 96 h, washed, then cultured with medium for another 3–4 days (till the Ctr cells reach confluence) and counted<sup>31</sup>.

**SA- $\beta$ -galactosidase activity assay in vitro.** After treatment with IFN- $\gamma$  and TNF, RT2-cancer cells were fixed for 15 min at room temperature, and then stained for 16 h at  $37^\circ\text{C}$  using the  $\beta$ -galactosidase staining kit (United States Biological)<sup>31</sup>. In addition, cell nuclei were stained with 4',6-diamidin-2-phenylindole (DAPI; Invitrogen). SA- $\beta$ -gal-positive and -negative cells were counted using a Zeiss Axiovert 200 microscope equipped with Visiview software and analysed by using ImageJ software (NIH).

**Apoptosis assay.** For apoptosis assay, cancer cells were exposed to etoposide (Eto,  $100 \mu\text{M}$ , Bristol-Meyers-Squibb, ETOPOPHOS), staurosporine (Sta,  $0.5 \mu\text{M}$ , Bio-Vision) or medium (Ctr) for 24 h and stained for propidium iodide and annexin V. Annexin V-positive and subG<sub>1</sub> cells were detected and quantified by flow cytometry. Analysis was performed on a LSRII cytometer (BD Bioscience) and analysed by FlowJo software version 10.

**Chromium release assay.** CD8<sup>+</sup> cytotoxic T cells (CTL) were generated from spleen and lymph node cells of OT I-transgenic mice. CD8<sup>+</sup> T cells were enriched by positive selection over magnetic microbeads. To generate CTL cells CD8<sup>+</sup> T cells were cultured in the presence of irradiated (30 Gy), syngeneic, T-cell-depleted antigen presenting cells (APC)<sup>39</sup> in the presence of IL-2 ( $10 \text{ U ml}^{-1}$ ), IL-12 ( $5 \text{ ng ml}^{-1}$ ), and anti-IL-4 Ab ( $10 \mu\text{g ml}^{-1}$ ).<sup>31</sup>  $2.5 \times 10^6$  target cells were labelled with  $250 \mu\text{Ci}$  ( $9.25 \text{ MBq}$ )<sup>51</sup>NaCr (Hartmann Analytic) at  $37^\circ\text{C}$  for 1.5 h, washed and plated into microtitre round bottom plates at  $1 \times 10^4$  cells per well. CD8<sup>+</sup> effector cells were added to target cells in the ratio 40 to 1 and incubated at  $37^\circ\text{C}$  for 4 h. B16-OVA cells were used as positive controls, B16-F10 melanoma cells were used as negative controls. Spontaneous release in the absence of effector cells was  $<30\%$  of the maximal release induced by 1% Triton X-100. After incubation,  $50 \mu\text{l}$  supernatant per well was mixed with  $200 \mu\text{l}$  scintillation cocktail (Ultima Gold, PerkinElmer) and measured in a liquid scintillation counter (MicroBeta, PerkinElmer).

**Patients and specimen collection.** Patients with metastatic melanoma were treated with either anti-PD-1 mAb or combined anti-CTLA-4 and anti-PD-1 mAbs. Non-responder patients were 30 patients (43.3% female, 61.5 median age, 22–89 age range) that progressed during the first 3 month of therapy. Responder patients were 12 patients (33.3% female, 56.5 median age, 27–75 age range) that had either a partial ( $>30\%$ ) or complete tumour regression over more than 1 year. Tumour biopsies were compared to healthy tissue from the safety margins as control tissue. Ethical approval was obtained from the Ethics Committee Tübingen. All patients had signed the written informed consent form for research analyses. The study was carried out in accordance with the Declaration of Helsinki and good clinical practice.

**Sequencing.** All patient samples were analysed using a hybridisation-based custom gene panel. Since the patient samples were collected in clinical routine, three different versions of the panel were used (ssSCv2, ssSCv3 and ssSCv4). The number of target genes was increased from one version to the next starting from 337 genes on ssSCv2, to 678 genes on version ssSCv3 and 693 on the current version ssSCv4. The panels were designed to detect somatic mutations (SNVs), small insertions and deletions (INDELs), copy number alterations (CNAs)

and selected structural rearrangements Supplementary Data Tables 1–3 (custom gene panel ssSCv2 ssSCv3 ssSCv4). The library preparation and in solution capture of the target region was performed using the Agilent SureSelectXT and SureSelectXT<sup>HS</sup> reagent kit (Agilent, Santa Clara, CA). DNA from tumour (FFPE) and matched normal controls (blood) were sequenced in parallel on an Illumina NextSeq500 using 75 bp paired-end reads. The tumour samples were sequenced to an average sequencing depth of coverage of 511x and the normal control samples to 521x, respectively. An in-house developed pipeline, called “megSAP” was used for data analysis [<https://github.com/imgag/megSAP>, version: 0.1-733-g19bde95 and 0.1-751-g1c381e5]. The sequencing reads were aligned to the human genome reference sequence (GRCh37) using BWA (vers. 0.7.15)<sup>67</sup>. Variants were called using Strelka2 (vers. 2.7.1) and annotated with SnpEff/SnpSift (vers. 4.3i)<sup>68,69</sup>. The overall mutational rate was as calculated using the formula:

$$\left[ \frac{\text{Somatic} - \text{Known} - \text{Tumorigen} \times \text{Genome size} + \text{Tumorigenes}}{\text{Target size} \times \text{Genome size}} \right]$$

For validity and clinical relevance, an allele fraction of  $\geq 5\%$  (i.e.  $\geq 10\%$  affected tumour cell fraction) was required for reported mutations (SNVs, INDELs). Copy number alterations (CNAs) were identified using ClinCNV [<https://doi.org/10.1101/837971>, <https://doi.org/10.1101/837971v1>], a method for multi-sample CNV detection using targeted or whole-genome NGS data. The method consists of four steps: (i) quantification of reads per target region, (ii) normalisation by GC-content, library size and median-coverage within a cohort of samples sequenced with the same NGS panel, (iii) calculation of log<sub>2</sub>-fold changes between tumour and normal sample, (iv) segmentation and CNV calling. Using log<sub>2</sub>-fold changes ClinCNV estimates statistical models for different copy number states per region (conditioned by tumour sample purity) and reports an likelihood for each statistical model, assuming that the majority of samples are diploid at a focal region. The log-likelihood of the diploid model is subtracted from alternative models, resulting in positive likelihoods for true alternative copy number states. Finally, maximum segments of contiguous regions with positive log-likelihood ratios are identified in an iterative manner. Segments consisting of at least three regions with log-likelihood ratio  $\geq 40$  and CN state  $\leq 1.5$  or  $\geq 3$  are reported as CNVs. Quality control (QC) parameters were collected during all analysis steps<sup>70</sup>.

**Comparative genomic hybridisation (CGH) array.** DNA was isolated from RT2-cancer cells or reference spleen (wildtype male) tissue with the DNeasy Blood & Tissue Kit (Qiagen) according to the manufacturer's instructions. DNA was labelled using the SureTag Complete DNA Labelling Kit (Agilent Technologies) and hybridised on an Agilent Mouse Genome CGH Microarray,  $2 \times 105 \text{ K}$  (Agilent Technologies), and the image was analysed using Feature Extraction 10.5.1.1 and Agilent Genomic Workbench Lite Edition 6.5 with Genome Reference Consortium Mouse Build 38.

**Quantitative PCR.** RT2-cancer cells were harvested by trypsin digestion and snap frozen in liquid nitrogen. RNA was prepared using the Nucleospin RNA Mini kit (Macherey-Nagel); cells were lysed using Tris(2-carboxyethyl)phosphine (TCEP)-containing RL1 buffer, followed by DNase digestion (Invitrogen). RNA quality was controlled by agarose gel electrophoresis and by OD600 measurements using a photometer (Eppendorf AG). Complementary DNA was prepared using the iScript cDNA synthesis kit (Bio-Rad Laboratories). Quantitative PCR was performed with SybrGreen using a LightCycler 480 (Roche). Gene expression was analysed using qbase software (Biogazelle) based on the delta-delta-CT-method and reference genes were evaluated using geNorm (feature of the q base software, Biogazelle). The following primers were used: *SV40-Tag* sense 5'-tcc act cca caa ttc tgc tct-3', antisense 5'-ttg ctt ctt atg tta att tgg tac aga-3'; *Cdkn2a* sense 5'-ttg ccc atc atc act-3', antisense 5'-ggg ttt tct tgg tga agt tgc-3'; *Actb* sense 5'-cta agg cca acc gtc aaa ag-3', antisense 5'-acc aga ggc ata cag gga ca 3'; *Eef1a1* sense 5'-aca cgt aga ttc cgg caa gt 3', antisense 5'-agg agc cct ttc cca tctc 3'.

**Magnetic resonance imaging.** Magnetic resonance imaging (MRI) was performed with ten-week-old RT2 mice under 1.5% isoflurane anaesthesia using a 7 T small animal magnetic resonance scanner (ClinScan, Bruker Biospin MRI, Ettlingen, Germany) equipped with quadrature mouse whole-body coil with an inner diameter of 35 mm. For detection of the  $\beta$ -cancers and general anatomic information, a T2-weighted 3D turbo spin-echo-sequence (TE/TR 205/3,000 ms, image matrix of 160 × 256, slice thickness 0.22 mm) was used. Respiration was monitored and used for triggering MRI data acquisition. The acquired MRI data was visualised using Inveon Research Workplace software (Siemens Preclinical Solutions, Knoxville, TN, USA).

**Light sheet fluorescence microscopy.** Five-week-old RT2 or RT2.*Stat1*<sup>-/-</sup> mice were treated with TAA-T<sub>H</sub>1 cells or NaCl as described. Mice were injected i.v. with 50  $\mu$ g of Alexa Fluor 700 anti-mouse CD4 mAb clone GK1.5 and Alexa Fluor 647 anti-mouse CD11b mAb clone M1/70 (BioLegend), 48 h after the second treatment. After 2 h, organs were harvested and fixed in 4% paraformaldehyde/PBS solution at 4 °C for 8 h. Tissue was dehydrated at room temperature using increasing concentrations of ethanol (30, 50, 70, 80, 90%) for 2 h each and in 100% ethanol at 4 °C overnight. Tissues were incubated in n-hexane for 2 h and then cleared using two parts benzyl benzoate and one part benzyl alcohol (Sigma-Aldrich) three times for 30 min. Air exposure was strictly avoided during this step. The samples were then visualised and analysed using a custom-built laser scanning light sheet microscope using a high NA 20× magnification and reconstructed using the IMARIS software (Bitplane).

**Flow cytometry.** Five-week-old RT2 or RT2.*Stat1*<sup>-/-</sup> mice were irradiated with 2 Gy one day before the first i.p. transfer of  $1 \times 10^7$  TAA-T<sub>H</sub>1 cells or NaCl<sup>25</sup>. 48 h after the second treatment mice were sacrificed. The pancreatic lymph node was separated from the pancreas tissue of each mouse, the pancreas was homogenised via a 200  $\mu$ m cell strainer in DMEM media containing 20% FCS at 4 °C, erythrocytes were lysed with ACK lysis buffer (Cambrex), and samples were stained for 30 min at 8 °C with fluorochrome-conjugated antibodies (anti-mouse CD4-Pacific Blue, clone GK1.5, catalogue number 100428; anti-mouse CD8a-PE-Cy7, clone 53-6.7, catalogue number 100722; anti-mouse CD45.2-APC-Cy7, clone 104 catalogue number 101224; anti-mouse-CD11c-APC, clone N418, catalogue number 117310; anti-mouse CD11b-Pacific blue, clone M1/70, catalogue number 101224; or corresponding isotype controls (dilution 1:150, BioLegend)). Cells were separated again via a 50  $\mu$ m cell strainer. Flow cytometry was performed using a FACS Aria and analysed with DIVA software (Becton Dickinson). Alternatively, flow cytometry analyses with T<sub>H</sub>1 cells or RT2-cancer cells which have been stained with fluorochrome-conjugated antibodies (anti-mouse-PE-IFN- $\gamma$ , clone XMG1.2, catalogue number 505807; anti-mouse-PE-TNF- $\alpha$ , clone MP6-XT22, catalogue number 506306; anti-mouse-PE IL-4, clone 11B11, catalogue number 504104; anti-mouse-PE  $\beta$ 2-microglobulin, clone A16041A, catalogue number 154503; anti-mouse PE/Cy7 CD274 (B7-H1, PD-L1), clone 10F.9G2, catalogue number 124313 (dilution 1:250, BioLegend)) were performed on a LSRII cytometer (BD Bioscience) and analysed by FlowJo software version 10.

**Statistical analysis.** The experiments were not randomised. The investigators were not blinded to allocation during the experiments or outcome assessment. No power calculations were used, but sample sizes were selected on the basis of previous experiments; in vitro results were based on three independent experiments to guarantee reproducibility of findings. The statistics software JMP version 12.2.0 (SAS Institute) and GraphPad Prism version 6 (GraphPadSoftware, California, USA) were used for statistical analyses and for the generation of diagrams. To address the question whether the treatment effect was different between two genotypes, the decadic logarithms of tumour volumes were analysed in ANCOVAs, using the nominal factors “mouseID” (nested under “treatment” and “genotype”), “treatment” and “genotype” as well as the combination “treatment” and “genotype”; “time” was used as continuous factor; finally, the combinations of “mouse ID” and “time”, “treatment” and “time”, “genotype” and “time” and the most important combination “treatment” and “genotype” and “time” were used. For purpose of normalisation, decadic logarithms of tumour volume were used in the analyses; zero observations were replaced by half the minimum of positive values before calculating the logarithms. Group comparisons were made with non-parametric, unpaired, two-tailed Mann-Whitney (Wilcoxon) tests or parametric, unpaired, two-tailed t test with Welch’s correction for unequal variances. Log-rank test was used for the comparison of survival from  $\lambda$ -MYC mice, RT2 mice and tumour latency curves. Because of disparate censoring between RT2 mice and RT2.*Stat1*<sup>-/-</sup> mice Fisher’s exact tests was used to compare the survival (as indicated in the text). N refers to the number of patients, mice or samples and cell lines from different mice, respectively.

#### Data availability

Primary generated cancer cells are available from the authors. The sequencing data from patient samples have been deposited in the EGA database under the accession code EGAS00001004151. Comparative genome hybridisation array data have been deposited in the NCBI GEO database under the accession code GSE142192. All the other data supporting the findings of this study are available within the article and its supplementary information files and from the corresponding author upon request.

Source data for Fig. 1a, c and 3a–c and 4a, c, e and 5b and 7a–c and 8a, c, d, e and 10a–e and Supplementary Figs. 1a and 11c–e are available as a source data file. A reporting summary for this article is available as a Supplementary Information file.

Received: 26 November 2018; Accepted: 7 February 2020;

Published online: 12 March 2020

#### References

- Leach, D. R., Krummel, M. F. & Allison, J. P. Enhancement of antitumor immunity by CTLA-4 blockade. *Science* **271**, 1734–1736 (1996).
- Koebel, C. M. et al. Adaptive immunity maintains occult cancer in an equilibrium state. *Nature* **450**, 903–907 (2007).
- Okazaki, T., Chikuma, S., Iwai, Y., Fagarasan, S. & Honjo, T. A rheostat for immune responses: the unique properties of PD-1 and their advantages for clinical application. *Nat. Immunol.* **14**, 1212–1218 (2013).
- Tumeh, P. C. et al. PD-1 blockade induces responses by inhibiting adaptive immune resistance. *Nature* **515**, 568–571 (2014).
- Twyman-Saint Victor, C. et al. Radiation and dual checkpoint blockade activate non-redundant immune mechanisms in cancer. *Nature* **520**, 373–377 (2015).
- Topalian, S. L., Drake, C. G. & Pardoll, D. M. Immune checkpoint blockade: a common denominator approach to cancer therapy. *Cancer Cell* **27**, 450–461 (2015).
- Kroemer, G., Senovilla, L., Galluzzi, L., Andre, F. & Zitvogel, L. Natural and therapy-induced immunosurveillance in breast cancer. *Nat. Med.* **21**, 1128–1138 (2015).
- Blank, C. U., Haanen, J. B., Ribas, A. & Schumacher, T. N. Cancer immunology. The “cancer immunogram”. *Science* **352**, 658–660 (2016).
- Tran, E., Robbins, P. F. & Rosenberg, S. A. ‘Final common pathway’ of human cancer immunotherapy: targeting random somatic mutations. *Nat. Immunol.* **18**, 255–262 (2017).
- Ribas, A. & Wolchok, J. D. Cancer immunotherapy using checkpoint blockade. *Science* **359**, 1350–1355 (2018).
- Galon, J. et al. Type, density, and location of immune cells within human colorectal tumors predict clinical outcome. *Science* **313**, 1960–1964 (2006).
- Rocken, M. Early tumor dissemination, but late metastasis: insights into tumor dormancy. *J. Clin. Invest.* **120**, 1800–1803 (2010).
- Sosa, M. S., Bragado, P. & Aguirre-Ghiso, J. A. Mechanisms of disseminated cancer cell dormancy: an awakening field. *Nat. Rev. Cancer* **14**, 611–622 (2014).
- Perez-Mancera, P. A., Young, A. R. & Narita, M. Inside and out: the activities of senescence in cancer. *Nat. Rev. Cancer* **14**, 547–558 (2014).
- Pollard, J. W. Defining metastatic cell latency. *N. Engl. J. Med.* **375**, 280–282 (2016).
- Massague, J. & Obenauf, A. C. Metastatic colonization by circulating tumour cells. *Nature* **529**, 298–306 (2016).
- Aguirre-Ghiso, J. A. How dormant cancer persists and reawakens. *Science* **361**, 1314–1315 (2018).
- Schreiber, R. D., Old, L. J. & Smyth, M. J. Cancer immunoediting: integrating immunity’s roles in cancer suppression and promotion. *Science* **331**, 1565–1570 (2011).
- Landsberg, J. et al. Melanomas resist T-cell therapy through inflammation-induced reversible dedifferentiation. *Nature* **490**, 412–416 (2012).
- Baumeister, S. H., Freeman, G. J., Dranoff, G. & Sharpe, A. H. Coinhibitory Pathways in Immunotherapy for Cancer. *Annu. Rev. Immunol.* **34**, 539–573 (2016).
- Patel, S. J. et al. Identification of essential genes for cancer immunotherapy. *Nature* **548**, 537–542 (2017).
- Pan D. et al. A major chromatin regulator determines resistance of tumor cells to T cell-mediated killing. *Science* **359**, 770–775 (2018).
- Ferrari de Andrade, L. et al. Antibody-mediated inhibition of MICA and MICB shedding promotes NK cell-driven tumor immunity. *Science* **359**, 1537–1542 (2018).
- Milanovic, M. et al. Senescence-associated reprogramming promotes cancer stemness. *Nature* **553**, 96–100 (2018).
- Muller-Hermelink, N. et al. TNFR1 signaling and IFN-gamma signaling determine whether T cells induce tumor dormancy or promote multistage carcinogenesis. *Cancer Cell* **13**, 507–518 (2008).
- Zaretsky, J. M. et al. Mutations Associated with Acquired Resistance to PD-1 Blockade in Melanoma. *N. Engl. J. Med.* **375**, 819–829 (2016).
- Manguo, R. T. et al. In vivo CRISPR screening identifies Ptpn2 as a cancer immunotherapy target. *Nature* **547**, 413–418 (2017).
- Kammertoens, T. et al. Tumour ischaemia by interferon-gamma resembles physiological blood vessel regression. *Nature* **545**, 98–102 (2017).

29. Ayers M., et al. IFN-gamma-related mRNA profile predicts clinical response to PD-1 blockade. *J. Clin. Invest.* **127**, 2930–2940 (2017).
30. Wieder T., Eigentler T., Brenner E., Rocken M. Immune checkpoint blockade therapy. *J. Allergy Clin. Immunol.* **142**, 1403–1414 (2018).
31. Braumuller, H. et al. T-helper-1-cell cytokines drive cancer into senescence. *Nature* **494**, 361–365 (2013).
32. Sun, R. & Gao, B. Negative regulation of liver regeneration by innate immunity (natural killer cells/interferon-gamma). *Gastroenterology* **127**, 1525–1539 (2004).
33. Goding, S. R. et al. Restoring immune function of tumor-specific CD4+ T cells during recurrence of melanoma. *J. Immunol.* **190**, 4899–4909 (2013).
34. Nguyen, L. T. & Ohashi, P. S. Clinical blockade of PD1 and LAG3—potential mechanisms of action. *Nat. Rev. Immunol.* **15**, 45–56 (2015).
35. Braun, S. M. G. et al. Rapid and reversible epigenome editing by endogenous chromatin regulators. *Nat. Commun.* **8**, 560 (2017).
36. Kang, T.-W. et al. Senescence surveillance of pre-malignant hepatocytes limits liver cancer development. *Nature* **479**, 547–551 (2011).
37. Speiser, D. E. et al. Self antigens expressed by solid tumors Do not efficiently stimulate naive or activated T cells: implications for immunotherapy. *J. Exp. Med.* **186**, 645–653 (1997).
38. van den Broek, M. E. et al. Decreased tumor surveillance in perforin-deficient mice. *J. Exp. Med.* **184**, 1781–1790 (1996).
39. Egeter, O., Mocikat, R., Ghoreschi, K., Dieckmann, A. & Rocken, M. Eradication of disseminated lymphomas with CpG-DNA activated T helper type 1 cells from nontransgenic mice. *Cancer Res.* **60**, 1515–1520 (2000).
40. Ahmetlic, F. et al. Regulatory T cells in an endogenous mouse lymphoma recognize specific antigen peptides and contribute to immune escape. *Cancer Immunol. Res.* **7**, 600–608 (2019).
41. Naujoks, M. et al. Alterations of costimulatory molecules and instructive cytokines expressed by dendritic cells in the microenvironment of an endogenous mouse lymphoma. *Cancer Immunol. Immunother.* **63**, 491–499 (2014).
42. Casanovas, O., Hager, J. H., Chun, M. G. & Hanahan, D. Incomplete inhibition of the Rb tumor suppressor pathway in the context of inactivated p53 is sufficient for pancreatic islet tumorigenesis. *Oncogene* **24**, 6597–6604 (2005).
43. Kovalchuk, A. L. et al. Burkitt lymphoma in the mouse. *J. Exp. Med.* **192**, 1183–1190 (2000).
44. Chen, D. S. & Mellman, I. Elements of cancer immunity and the cancer-immune set point. *Nature* **541**, 321–330 (2017).
45. Cristescu R. et al. Pan-tumor genomic biomarkers for PD-1 checkpoint blockade-based immunotherapy. *Science* **362** (2018).
46. Wang, Z. L. et al. Comprehensive genomic characterization of RNA-binding proteins across human cancers. *Cell Rep.* **22**, 286–298 (2018).
47. Kroemer, G., Galluzzi, L., Kepp, O. & Zitvogel, L. Immunogenic cell death in cancer therapy. *Annu. Rev. Immunol.* **31**, 51–72 (2013).
48. Pitt, J. M. et al. Resistance mechanisms to immune-checkpoint blockade in cancer: tumor-intrinsic and -extrinsic factors. *Immunity* **44**, 1255–1269 (2016).
49. Willimsky, G. & Blankenstein, T. Sporadic immunogenic tumours avoid destruction by inducing T-cell tolerance. *Nature* **437**, 141–146 (2005).
50. Le, D. T. et al. PD-1 blockade in tumors with mismatch-repair deficiency. *N. Engl. J. Med.* **372**, 2509–2520 (2015).
51. Topalian, S. L. et al. Safety, activity, and immune correlates of anti-PD-1 antibody in cancer. *N. Engl. J. Med.* **366**, 2443–2454 (2012).
52. Campisi, J. Aging, cellular senescence, and cancer. *Annu. Rev. Physiol.* **75**, 685–705 (2013).
53. Serrano, M., Lin, A. W., McCurrach, M. E., Beach, D. & Lowe, S. W. Oncogenic ras provokes premature cell senescence associated with accumulation of p53 and p16INK4a. *Cell* **88**, 593–602 (1997).
54. Demaria, M. et al. Cellular senescence promotes adverse effects of chemotherapy and cancer relapse. *Cancer Disco.* **7**, 165–176 (2017).
55. Lee, S. & Schmitt, C. A. The dynamic nature of senescence in cancer. *Nat. Cell Biol.* **21**, 94–101 (2019).
56. Krimpenfort, P., Quon, K. C., Mooi, W. J., Loonstra, A. & Berns, A. Loss of p16Ink4a confers susceptibility to metastatic melanoma in mice. *Nature* **413**, 83–86 (2001).
57. Damsky, W. et al. mTORC1 activation blocks BrafV600E-induced growth arrest but is insufficient for melanoma formation. *Cancer Cell* **27**, 41–56 (2015).
58. Zeng, H. et al. Bi-allelic loss of CDKN2A initiates melanoma invasion via BRN2 activation. *Cancer Cell* **34**, 56–68.e59 (2018).
59. Shain, A. H. et al. Genomic and transcriptomic analysis reveals incremental disruption of key signaling pathways during melanoma evolution. *Cancer Cell* **34**, 45–55.e44 (2018).
60. Mooi, W. J. & Peeper, D. S. Oncogene-induced cell senescence—halting on the road to cancer. *N. Engl. J. Med.* **355**, 1037–1046 (2006).
61. Pencik, J. et al. STAT3 regulated ARF expression suppresses prostate cancer metastasis. *Nat. Commun.* **6**, 7736 (2015).
62. Forster, I., Hirose, R., Arbeit, J. M., Clausen, B. E. & Hanahan, D. Limited capacity for tolerization of CD4+ T cells specific for a pancreatic beta cell neo-antigen. *Immunity* **2**, 573–585 (1995).
63. Homberg, N. et al. CD40-independent natural killer-cell help promotes dendritic cell vaccine-induced T-cell immunity against endogenous B-cell lymphoma. *Int. J. Cancer* **135**, 2825–2833 (2014).
64. Feil, S. et al. Transdifferentiation of vascular smooth muscle cells to macrophage-like cells during atherosclerosis. *Circ. Res.* **115**, 662–667 (2014).
65. Naito, Y., Hino, K., Bono, H. & Ui-Tei, K. CRISPRdirect: software for designing CRISPR/Cas guide RNA with reduced off-target sites. *Bioinformatics* **31**, 1120–1123 (2015).
66. Xue, W. et al. CRISPR-mediated direct mutation of cancer genes in the mouse liver. *Nature* **514**, 380–384 (2014).
67. Li, H. & Durbin, R. Fast and accurate short read alignment with Burrows-Wheeler transform. *Bioinformatics* **25**, 1754–1760 (2009).
68. Kim, S. et al. Strelka2: fast and accurate calling of germline and somatic variants. *Nat. Methods* **15**, 591–594 (2018).
69. Cingolani, P. et al. A program for annotating and predicting the effects of single nucleotide polymorphisms, SnpEff: SNPs in the genome of *Drosophila melanogaster* strain w1118; iso-2; iso-3. *Fly. (Austin)* **6**, 80–92 (2012).
70. Schroeder, C. M. et al. A comprehensive quality control workflow for paired tumor-normal NGS experiments. *Bioinformatics* **33**, 1721–1722 (2017).

### Acknowledgements

The excellent technical assistance of S. Weidemann, V. Galinat, E. Müller-Hermelink, A. Odon, R. Nordin, S. Riel and T. Schneider, C. Grimm is gratefully acknowledged. The authors thank H.G. Rammensee, O. Rieß, K. Ghoreschi, J. Brück, B. Bauer, M. Rentschler for helpful discussions, and T. Haug for technical support in the chromium release assay. Furthermore, the authors thank M. Hagemann, F. Liebel, J. Teutsch and M. Möschter for help in animal experiments. S. Kaesler for providing B16-OVA cells. This work is part of the doctoral thesis of E.B., B.F.S., F.A., T.R., F.J.H., G.D. and N.S. Wilhelm Sander-Stiftung (2012.056.3), Deutsche Krebshilfe (application numbers 109037, 110662, 110664, 70112332 and 70112337), Werner Reichenbach Stiftung and the Deutsche Forschungsgemeinschaft (SFB 685, SFB TRR 156/2, RO 764/14-1; RO 764/15-1, SFB 773, Wi 1279/4-1). Cluster of Excellence iFIT (EXC 2180) “Image-Guided and Functionally Instructed Tumor Therapies”, University of Tübingen, Germany, funded by the Deutsche Forschungsgemeinschaft (DFG, German Research Foundation) under Germany’s Excellence Strategy - EXC 2180 - 390900677.

### Author contributions

M.R. developed the concept, together with E.B., T.W., and with R.M., F.A., T.R. (Fig. 8) and M.K., B.F.S. (Fig. 4) M.R. planned and designed the experiments. E.B. performed or experimentally supported most experiments and analysed most data with the help of T.W. or B.F. (except Fig. 8a, c, d, e; Fig. 10a–c; Supplementary Fig. 7b and Supplementary Fig. 13a); B.F.S. and D.S. performed the experiments Fig. 4a–c. F.A., T.R., N.H., and A. G. performed the experiments Fig. 8a, d, e. F.J.H., C.S., and G.D. did the genomic analysis of melanoma patients, initiated by S.B. and D.D. B.F. and M.Scha. established and carried out fluorescence and electron microscopy. A.F. and T.E. recruited patients and provided patient material. H.N. and T.S. isolated primary melanoma cells. N.S. and J.B. performed and interpreted comparative genomic hybridisation arrays. L.Z., D.Dau. and S.Z. generated gRNAs against Cdkn2a for CRISPR gene-editing technology and supervised the knock-out experiments. H.B. did the chromium release assay. L.Q.-M. the immunohistochemistry, K.S.B. provided cell lines and data for reviewers. B.F.S. and B.J.P. established and carried out magnetic resonance imaging. M.E. did the statistical analyses (Fig. 1a, 4a and c). K.J.J. and A.B. performed two-dimensional light sheet fluorescence microscopy. E.B., T.W., L.Z., B.P., D.Sch., R.M., M.K. and M.R. discussed and interpreted the data. M.R. wrote the paper. All authors discussed the results and commented on the manuscript, and agreed with its content.

### Competing interests

M.R., E.B. and T.W. are inventors of an European pending patent Number 13 826 993.1: “Use of active substance combinations for tumour senescence” and an United States patent Number US 10,046,029 B2: “Method of inducing senescence in tumour cells by administering TNF-A in combination with IFN-γ”. As chairperson M.R. has to sign all contracts of the department. M.R. receives grants for research projects or travel support and has the indicated shares. The authors B.P. and M.K. have research contracts with Imaging modality suppliers, and are members of the “ImmunelImage” consortium within the Horizon2020 IMI programme of the European Union. F.J.H. reports institutional research support from Novartis. C.S. reports research support from Illumina and institutional research support from Novartis. All remaining authors declare no competing interests.



**Additional information**

**Supplementary information** is available for this paper at <https://doi.org/10.1038/s41467-020-14987-6>.

**Correspondence** and requests for materials should be addressed to M.Röc.

**Peer review information** *Nature Communications* thanks Raffaella Di Micco, Antoni Ribas and the other, anonymous, reviewer(s) for their contribution to the peer review of this work. Peer reviewer reports are available.

**Reprints and permission information** is available at <http://www.nature.com/reprints>

**Publisher's note** Springer Nature remains neutral with regard to jurisdictional claims in published maps and institutional affiliations.



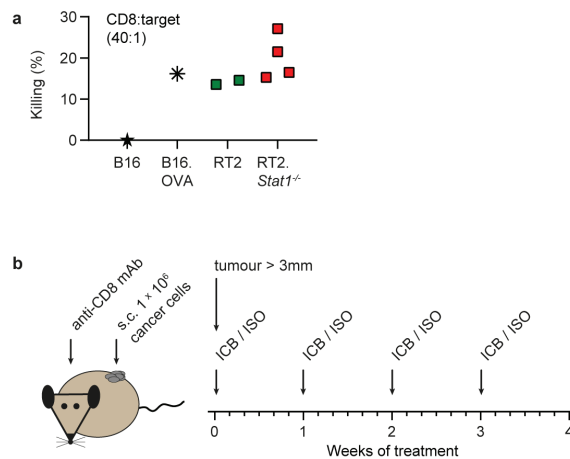
**Open Access** This article is licensed under a Creative Commons Attribution 4.0 International License, which permits use, sharing, adaptation, distribution and reproduction in any medium or format, as long as you give appropriate credit to the original author(s) and the source, provide a link to the Creative Commons license, and indicate if changes were made. The images or other third party material in this article are included in the article's Creative Commons license, unless indicated otherwise in a credit line to the material. If material is not included in the article's Creative Commons license and your intended use is not permitted by statutory regulation or exceeds the permitted use, you will need to obtain permission directly from the copyright holder. To view a copy of this license, visit <http://creativecommons.org/licenses/by/4.0/>.

© The Author(s) 2020

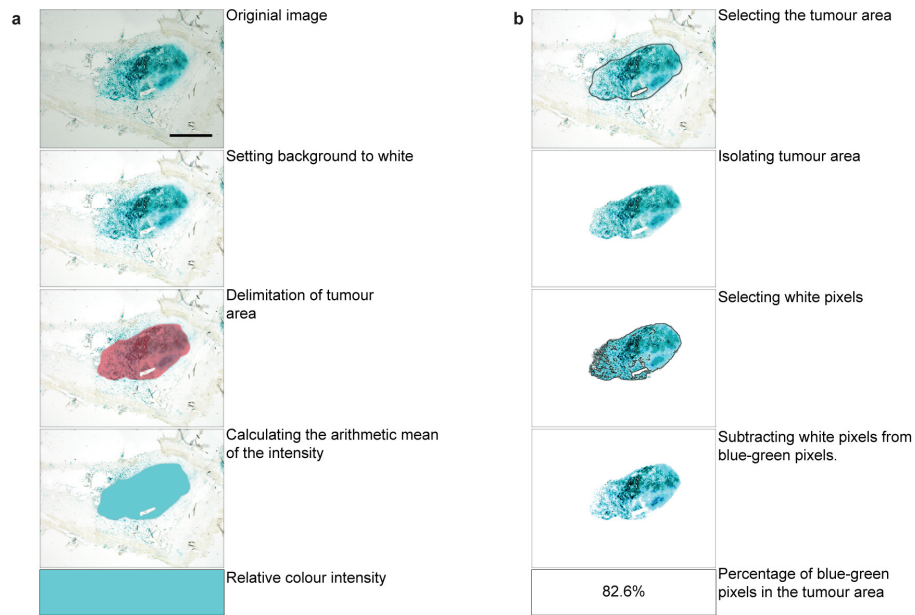
## Supplementary Information

Cancer immune control needs senescence induction by  
interferon-dependent cell cycle regulator pathways in tumours

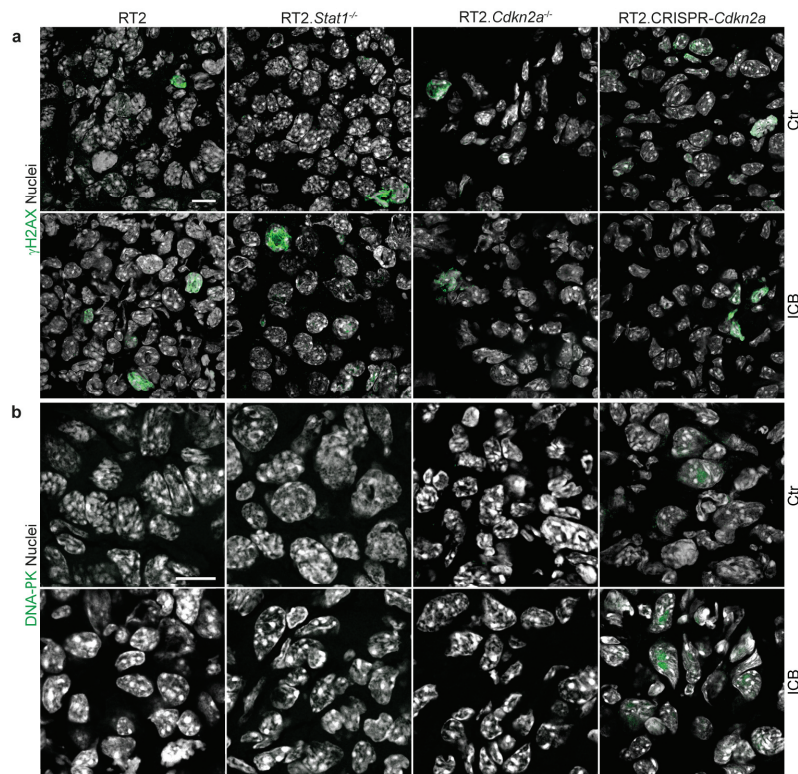
Brenner et al.



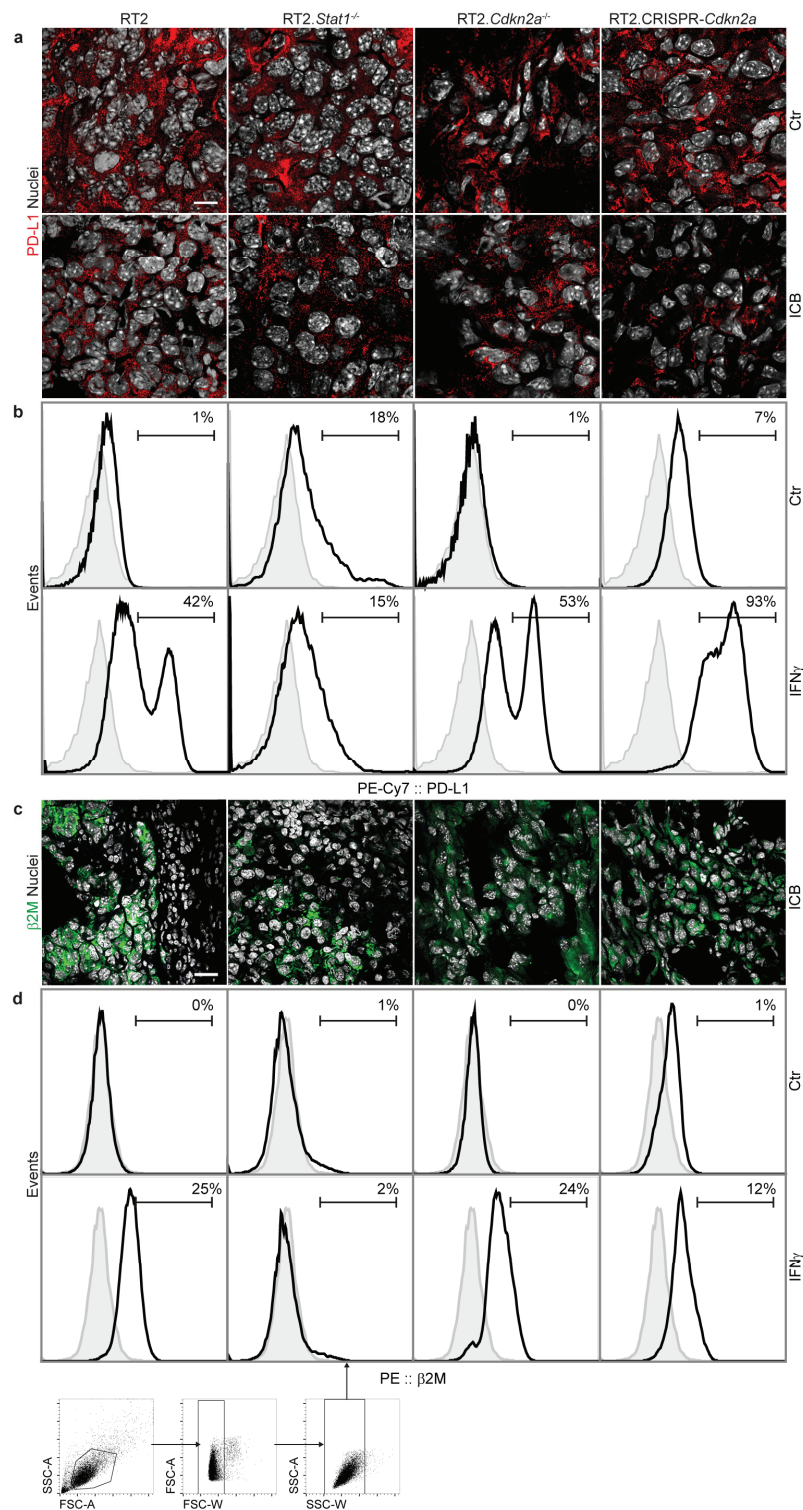
**Supplementary Figure 1** Treatment protocol depicting the immune therapy of transplanted RT2-cancers and the ability for CD8 T cell-mediated killing of RT2 and of RT2.*Stat1*<sup>-/-</sup> cancer cells *in vitro*. **a** B16-F10 ( $n=1$ ) or OVA-expressing B16 melanoma cells ( $n=1$ ) (C57BL/6), or RT2 ( $n=2$ ) or *Stat1*<sup>-/-</sup> RT2-cancer cells ( $n=4$ ) (C3HeB/FeJ) were cultured with OVA-reactive C57BL/6 CD8<sup>+</sup> cytotoxic T cells (what recognize the allogeneic RT2-cancers on the C3HeB/FeJ background) and specific chromium release was determined after 1.5 h. **b**, C3HeB/FeJ mice were CD8<sup>+</sup> T cell depleted with rat anti-mouse-CD8 mAb<sup>40</sup>. After three days  $1 \times 10^6$  RT2-, RT2.*Stat1*<sup>-/-</sup>, RT2.*Cdkn2a*<sup>-/-</sup> or RT2.CRISPR-*Cdkn2a*-cancer cells were subcutaneously (s.c.) injected. Treatment was started with either isotype control mAbs (Ctr) or immune checkpoint inhibitors (ICB; anti-PD-L1 and anti-LAG-3) once per week was started when tumours were > 3 mm in diameter. CD8 T cells did not recover during the time of the experiment. Cancer size was measured 2 times per week.



**Supplementary Figure 2** Illustration of the digital image-processing, and of the calculation of the percentage of SA- $\beta$ -gal positive tumour cells within a tumour area. **a, b** Image analysis of the field of an ICB/AT treated RT2-cancer stained with SA- $\beta$ -galactosidase at pH 5.5. **a** Calculation of the SA- $\beta$ -gal intensity within a given tumour area. **b** Calculation of the percentage of SA- $\beta$ -gal positive cells within the tumour area. The technique is described in the section Methods. Scale bar 1000  $\mu$ m.

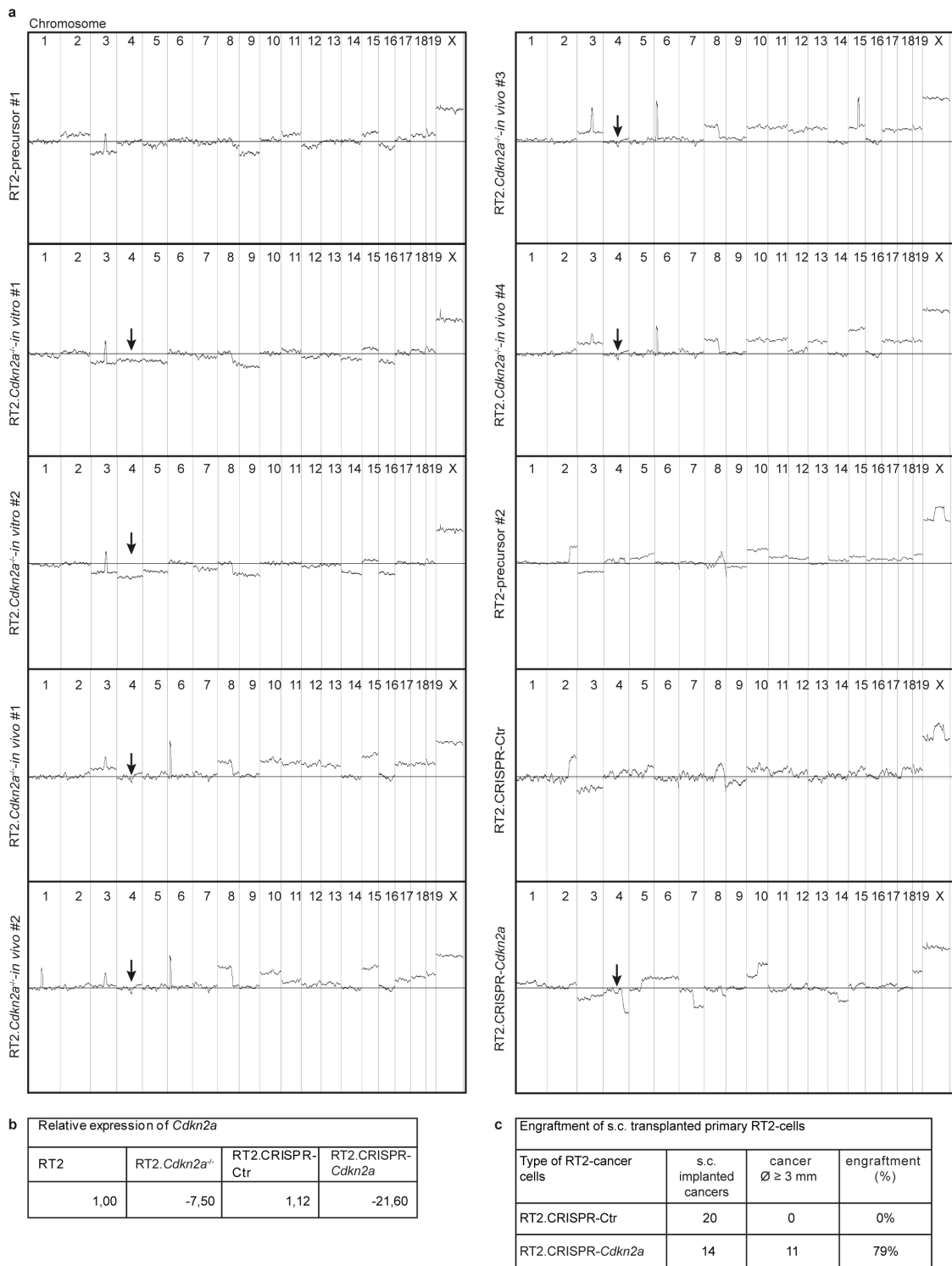


**Supplementary Figure 3** Absence of ICB-induced DNA double-strand break-associated  $\gamma$ H2AX or DNA-PK expression. **a, b** Representative immune fluorescence microscopic images of transplanted pancreatic islet cancers from either RT2-, RT2.*Stat1*<sup>-/-</sup> or RT2.*Cdkn2a*<sup>-/-</sup> or from RT2.CRISPR-*Cdkn2a*-cancer cells. Mice were treated with isotype control mAbs (Ctr) or with immune checkpoint blockade (ICB; anti-PD-L1 and anti-LAG-3). **a** Staining for the DNA double-strand break marker  $\gamma$ H2AX (green) and for nuclei (white). **b** Staining for DNA damage response kinase DNA-PK (green) and for nuclei (white). Scale bars 10  $\mu$ m. Histology was performed in one to three representative tumours from Fig. 1c.



**Supplementary Figure 4** PD-L1 or  $\beta$ 2-microglobulin protein expression. **a, c** Representative immune fluorescence microscopic images of cancers derived from either transplanted RT2-cancer cells, or from transplanted RT2.*Stat1*<sup>-/-</sup> or RT2.*Cdkn2a*<sup>-/-</sup> or RT2.CRISPER-*Cdkn2a*-cancer cells. Mice were treated with isotype control mAbs (Ctr) or with immune checkpoint blockade (ICB; anti-PD-L1 and anti-LAG-3). Staining of tumour tissue for the inhibitory

membrane protein PD-L1 (red) and for nuclei (white) (**a**) and for  $\beta$ 2-microglobulin ( $\beta$ 2M, green) and for nuclei (white) (**c**). To detect the PD-L1 molecules also on cancers of mice treated *in vivo* with mAb PD-L1 (clone 10F.9G2), sections were stained with another unlabelled anti-PD-L1 mAb clone MIH6. To detect both unlabelled anti-PD-L1 mAbs, sections were counterstained with a fluorescence labelled anti-rat antibody. Scale bars 20  $\mu$ m (**a**), 10  $\mu$ m (**c**). **b**, **d** FACS analysis of surface expression of PD-L1 (**b**) or of  $\beta$ 2-microglobulin ( $\beta$ 2M) (**d**) on RT2-cancer cells, RT2.*Stat1*<sup>-/-</sup> or RT2.*Cdkn2a*<sup>-/-</sup> or from RT2.CRISPR-*Cdkn2a*-cancer cells, cultured with medium or with medium containing 100 ng ml<sup>-1</sup> IFN- $\gamma$  (including gating strategy).

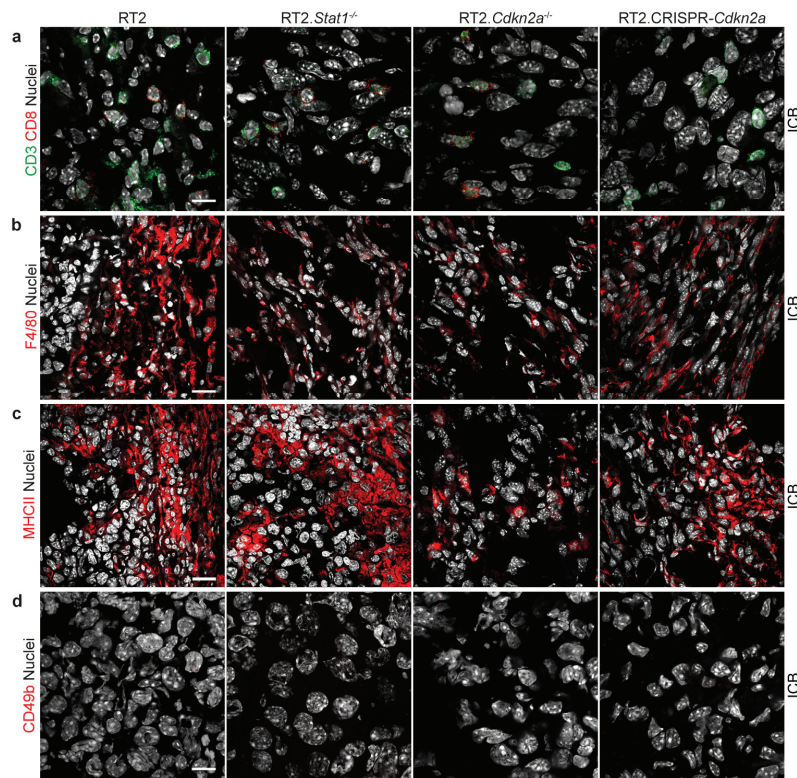


**Supplementary Figure 5** Genomic profiles of *Cdkn2a*-deficient variants of RT2-cancer cells and their parental RT2-cancer cells, expression of *Cdkn2a* mRNA and their engraftment *in vivo*. **a** Comparative genomic hybridization (CGH) arrays of RT2-cancer cells compared with the chromosome ideogram of wildtype C3HeB/FeJ mice, genome of interest from female mice (XX) compared to reference DNA of male mice (XY). The *Cdkn2a*-loss variants on

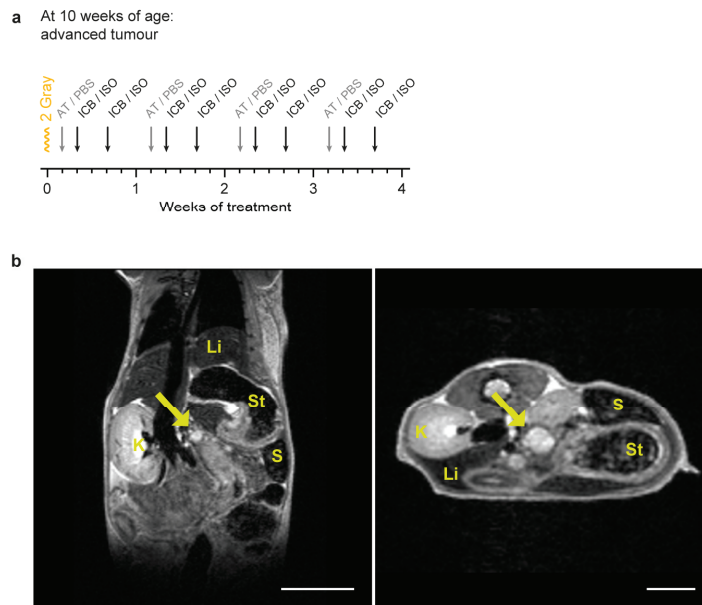


chromosome 4, qC4.A were generated by selection of cells resistant to immune therapy (by *in vitro* or *in vivo* selection) from the RT2-precursor cancer line#1. The RT2.CRISPR-Ctr or RT2.CRISPR-*Cdkn2a* were generated from the RT2-precursor cancer line#2, using a published construct<sup>33</sup> that targets *p16<sup>Ink4a</sup>p19<sup>Arf</sup>*. Arrows point towards the *Cdkn2a* locus.

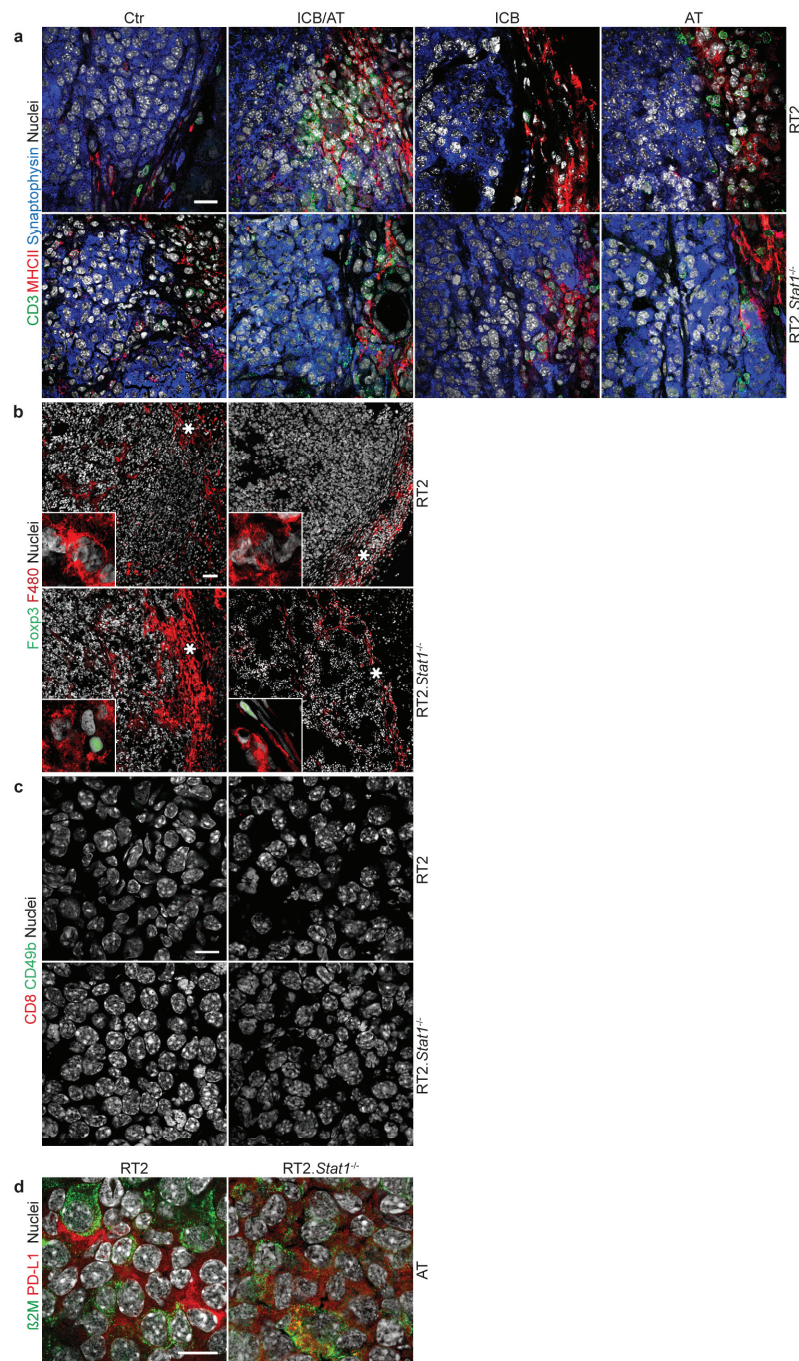
**b** Table showing the relative expression levels of *Cdkn2a* in RT2-cancers (set as 1), RT2.*Stat1*<sup>-/-</sup>, RT2.*Cdkn2a*<sup>-/-</sup>, RT2.CRISPR-Ctr- or RT2.CRISPR-*Cdkn2a*-cancer cells. Gene expression of *Cdkn2a* was analysed using *Actb* and *Eef1a1* as references. **c** Number of mice that were subcutaneously (s.c.) engrafted with  $1 \times 10^6$  cancer cells and engraftment efficacy of either RT2.CRISPR-Ctr- or RT2.CRISPR-*Cdkn2a*-cancer cells. All RT2-cancer lines expressed *SV40-Tag*, see also Fig. 5.



**Supplementary Figure 6** Infiltration of CD3<sup>+</sup>CD8<sup>+</sup> T cells and of F4/80<sup>+</sup> macrophages but absence of CD49b<sup>+</sup> NK cells in transplanted tumours after immune checkpoint blockade therapy. Representative immune fluorescence microscopic images from cancers growing after transplantation of RT2-, from RT2.*Stat1*<sup>-/-</sup>-, from RT2.*Cdkn2a*<sup>-/-</sup>- or from RT2.CRISPR-*Cdkn2a*-cancer cells into CD8-depleted C3H mice. Mice were treated with immune checkpoint blockade (ICB) as shown in Supplementary Figure 1. **a** Staining for CD8 (red) and CD3 (green) T cells and for nuclei (white), scale bar 10 μm. **b** Staining for F4/80 macrophages (red) and for nuclei (white), **c** for MHC class II (red) and for nuclei (white), and **d** for CD49b (red) and for nuclei (white), scale bar 20 μm. Immune histology was performed in one to two representative tumours from Fig. 1c.

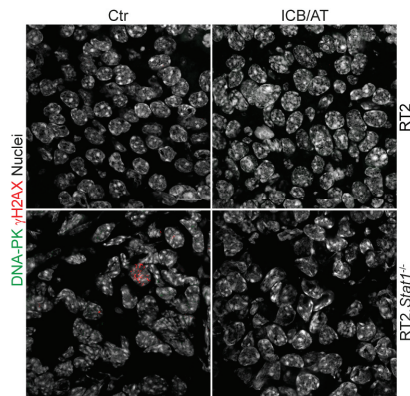


**Supplementary Figure 7** Treatment protocol depicting the immune therapy of either RT2 mice or RT2.*Stat1*<sup>-/-</sup> mice with advanced RT2-cancers. **a** At 10 weeks of age four weeks prior to the expected death RT2 mice or RT2.*Stat1*<sup>-/-</sup> mice were irradiated with 2 Gy one day before the first i.p. transfer of  $1 \times 10^7$  T antigen-specific T<sub>H</sub>1 cells. T<sub>H</sub>1 cells were prepared as described in Methods. Cell transfer was applied once weekly. ICB (anti-PD-L1/ anti-LAG-3) were i.p. injected twice per week. Ctr mice received isotype control mAbs. Blood glucose was measured twice per week. **b** Representative magnetic resonance images of a RT2 mouse at 10 weeks of age. Coronal view (left), transversal view (right). Arrows point towards RT2-cancers. Spleen (S), stomach (St), kidney (K), liver (L), scale bars 10 mm.

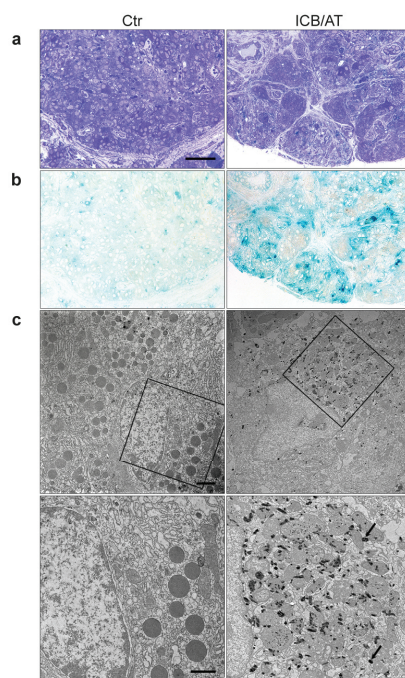


**Supplementary Figure 8** Immune infiltration and PD-L1 expression in cancers from RT2 mice or RT2.*Stat1*<sup>-/-</sup> mice. **a** MHC class II<sup>+</sup> antigen-presenting cells and CD3<sup>+</sup> cells in the microenvironment of RT2-cancers of either RT2 mice or RT2.*Stat1*<sup>-/-</sup> mice after treatment with either isotype control mAbs (Ctr) or with immune checkpoint blockade and adoptive T cell transfer (ICB/AT) or with either ICB or AT. Staining for MHC class II<sup>+</sup> APCs (in red) and the CD3ε chain on T cells (in green) and for the tumour specific neuroendocrine marker synaptophysin (in blue) and for nuclei (in white), **b** Staining for F480<sup>+</sup> on macrophages (red) or Foxp3<sup>+</sup> regulatory T cells (green) and for nuclei (white), **c** for CD8 (red) and CD49b

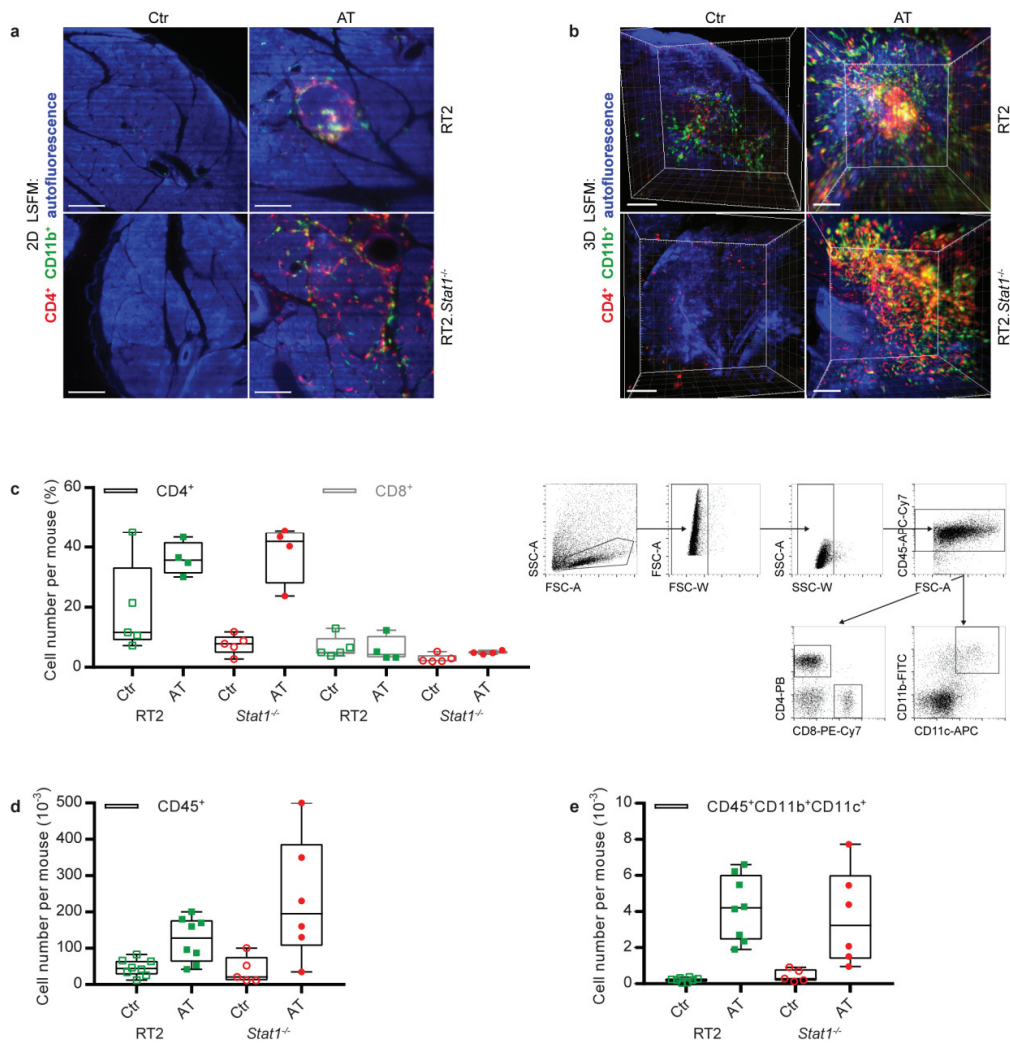
(green) and for nuclei (white). **d** Expression of the ICB target PD-L1 and of the  $\beta$ 2-microglobulin ( $\beta$ 2M) in the microenvironment of *Stat1*<sup>+/+</sup> and *Stat1*<sup>-/-</sup> RT2-cancers after AT with *Stat1*<sup>+/+</sup> T<sub>H</sub>1 cells. Staining for PD-L1 (red) and  $\beta$ 2M (green) and for nuclei (white). **a-d** Immune histology was performed in one to two representative tumours from Fig. 4e. Scale bars 20  $\mu$ m (**a**), 50  $\mu$ m (**b**) 10  $\mu$ m (**c**, **d**).



**Supplementary Figure 9** Absence of DNA double-strand break-associated  $\gamma$ H2AX or DNA-PK expression following immune therapy of RT2-cancers. Representative immune fluorescence microscopic images of pancreatic islet cancers from RT2 or RT2.*Stat1*<sup>-/-</sup> mice treated either with isotype control mAbs (Ctr) or with immune checkpoint blockade and adoptive T cell transfer (ICB/AT). Remaining tumour cells were stained for the DNA double-strand break marker  $\gamma$ H2AX (red), the DNA damage response kinase DNA-PK (green) and for nuclei (white). Immune histology was performed in one to two representative tumours from Fig. 4e. Scale bar 10  $\mu$ m.

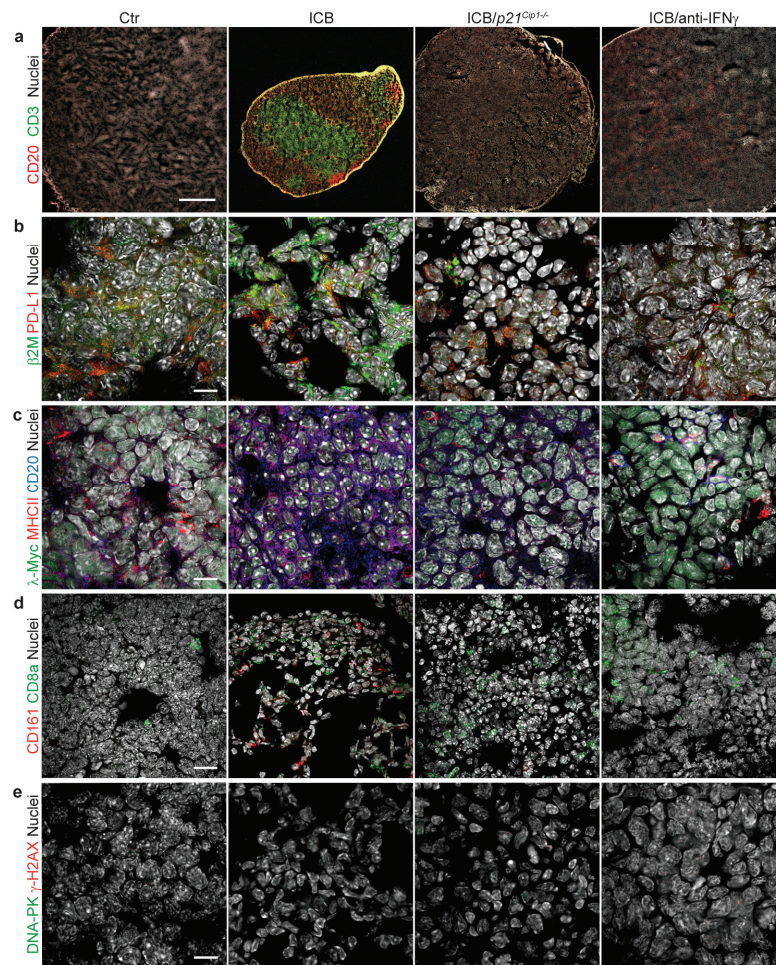


**Supplementary Figure 10** Cytoplasmic localisation of SA- $\beta$ -gal in ultrathin sections. **a** Overview image of RT2-cancers from mice treated either with isotype control mAbs (Ctr) or immune therapy (ICB/AT). Tissues were stained with toluidin blue. **b** Corresponding SA- $\beta$ -gal-staining of RT2-cancers at pH 5.5. **c** Corresponding electron microscopy (EM) of ultrathin sections of SA- $\beta$ -gal-stained RT2-cancers, overview of upper panel detail lower panel. Note the black electron-dense dots in the cytoplasm (arrows). Scale bars 100  $\mu$ m (**a**), 2  $\mu$ m (**c** upper panel), 1  $\mu$ m (**c** lower panel).

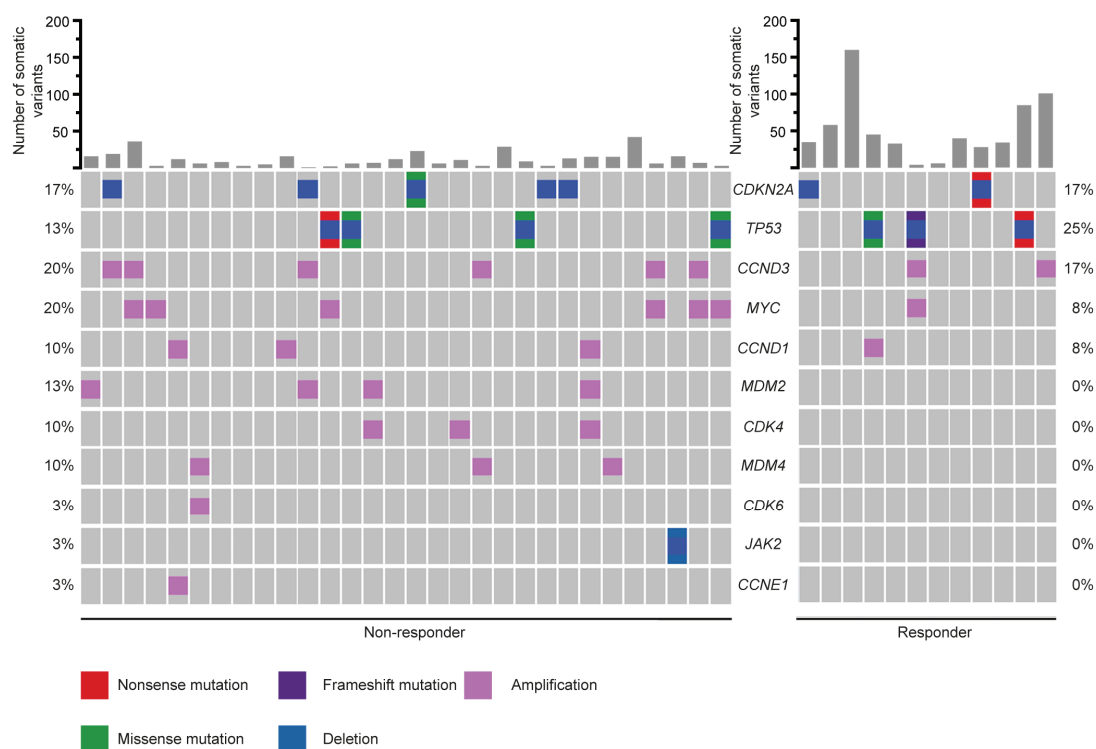


**Supplementary Figure 11** Presence of  $CD4^+$  T cells,  $CD11c^+$ - and  $CD11b^+$  leukocytes in the tumour microenvironment of RT2-cancers from either RT2 mice or RT2.Stat1<sup>-/-</sup> mice following the injection of Tag-specific T<sub>H</sub>1 cells (AT). **a** *In vivo* 2D light sheet fluorescence microscopy images (LSFM); **b** 3D LSFM,  $CD4^+$  (red),  $CD11b^+$  (green), autofluorescence (blue). Labelled mAbs were injected 2 h prior before organs were harvested. The pancreas from either RT2 mice or from RT2.Stat1<sup>-/-</sup> mice was isolated 2 days after the second treatment with either NaCl control (Ctr) or adoptive T cell transfer (AT), scale bars 100  $\mu$ m. **c-e** Flow cytometry analysis of tumour-infiltrating mononuclear leucocytes in the pancreas of RT2 or RT2.Stat1<sup>-/-</sup> mice 2 days after the second AT; percentage of  $CD4^+$  and  $CD8^+$  T cells (including gating strategy) (c); number of  $CD45^+$  immune cells (d); number of  $CD45^+CD11b^+CD11c^+$  dendritic cells (e). Each data point represents one mouse (Ctr, RT2  $N=5$ , RT2.Stat1<sup>-/-</sup>  $N=5$ ; AT, RT2  $N=4$ , RT2.Stat1<sup>-/-</sup>  $N=4$ ), box plots show the median, and whiskers indicate the 25th and 75th percentiles.

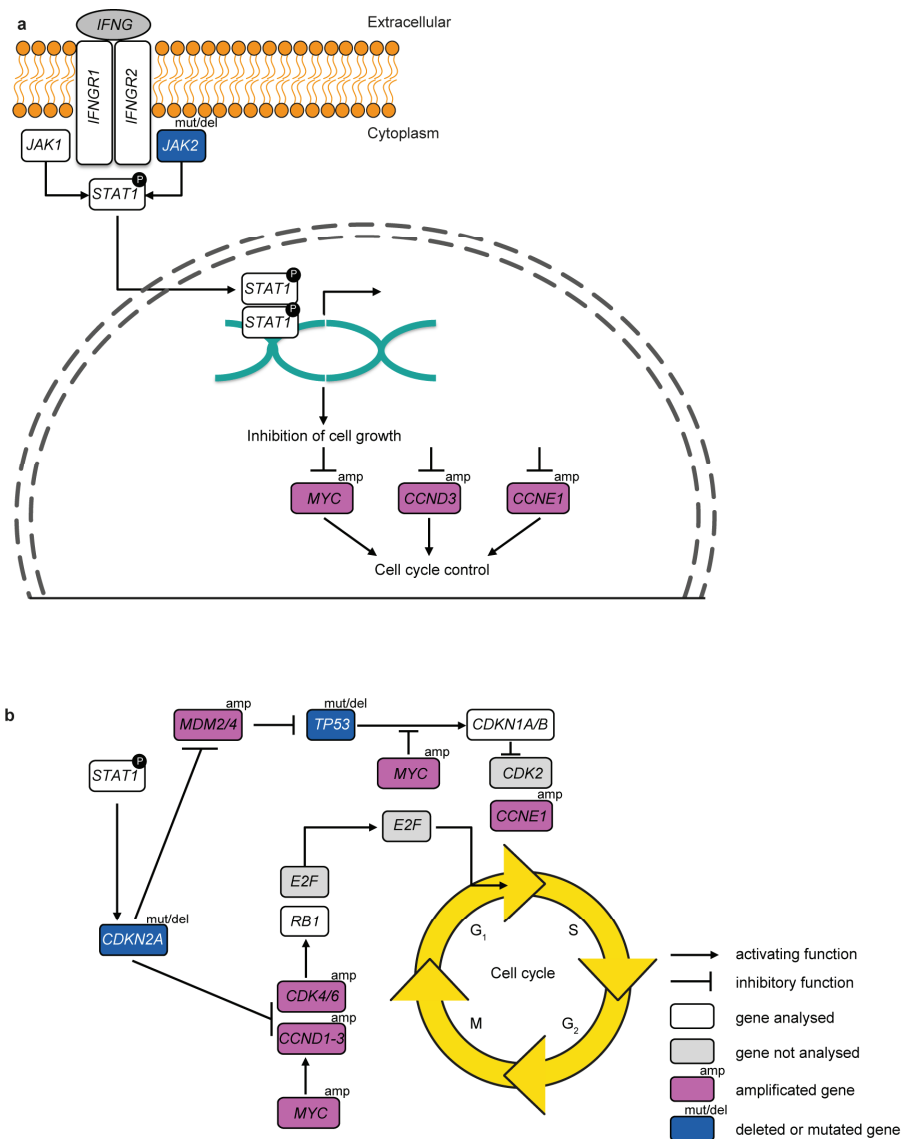




**Supplementary Figure 12** Immune therapy with anti-CTLA-4 mAb and anti-PD-1 mAb of  $\lambda$ -MYC mice preserves the normal lymph node structure without inducing DNA-double strand breaks. **a-e** Representative lymph nodes of  $\lambda$ -MYC or  $\lambda$ -MYC.*p21<sup>Cip1</sup><sup>-/-</sup>* mice.  $\lambda$ -MYC mice were controls (Ctr) or mice treated with anti-CTLA-4 and anti-PD-1 mAbs (ICB) or anti-CTLA-4, anti-PD-1 and anti-IFN- $\gamma$  mAbs (ICB/anti-IFN- $\gamma$ ).  $\lambda$ -MYC.*p21<sup>Cip1</sup><sup>-/-</sup>* mice were treated with ICB (group labelled ICB/*p21<sup>Cip1</sup><sup>-/-</sup>*). **a** CD20 (red), CD3 (green), nuclei (white). **b** Staining for PD-L1 (red),  $\beta$ 2-microglobulin ( $\beta$ 2M, green) and for nuclei (white). **c** Staining for CD20 B-cells (blue;  $\lambda$ -MYC lymphoma cells are CD20<sup>+</sup>), MHC class II (red),  $\lambda$ -MYC (green) and for nuclei (white). **d** Staining for CD161 NK cells (red) and CD8a T cells (green) and for nuclei (white). **e** Staining for the DNA double-strand break marker  $\gamma$ H2AX (red), the DNA damage response kinase DNA-PK (green) and for nuclei (white). Immune histology was performed in one to two representative tumours from Fig. 8c. Scale bars, 500  $\mu$ m (**a**), 10  $\mu$ m (**b-e**).



**Supplementary Figure 13** Function-determining aberrations of IFN- $\gamma$ -dependent cell cycle regulator genes are increased in melanoma metastases not responding to ICB therapy. Mutation Oncoplot with loss of function and gain of function alterations of cell cycle control genes leading to severe, function altering mutations. The mutation frequency alternates for each gene in metastases of the non-responder patients (progression within 3 months of ICB) is shown on the left and for each gene in metastases of the responder patients (melanoma regression  $\geq 1$  year) on the right. No changes in *CCND2*, *CDKN2B*, *CDKN2C*, *CDKN1a*, *CDKN1B*, *RBI*, *JAK1* or *JAK3* were detected.



**Supplementary Figure 14** Schematic overview of the cell cycle control genes and their functional gains and losses in metastases of non-responder patients. **a** IFN-receptor signalling. **b** Senescence regulating cell cycle control genes. Abbreviation: IFN- $\gamma$ , interferon gamma; *IFNGR1/2*, interferon gamma receptor 1/2; *JAK1/2/3*; Janus kinase 1/2/3; *STAT1*, signal transducer and activator of transcription protein family 1; *MYC*, MYC proto-oncogene; *CCND1-3*, cyclin-D1-3; *CCNE1*, cyclin-E1; *MDM2*, MDM2 proto-oncogene; *MDM4*, MDM4, p53 regulator; *TP53*, tumour protein p53; *CDKN1A/B*, cyclin dependent kinase inhibitor 1A/B (p21<sup>Cip1</sup>/p27<sup>Kip1</sup>); *CDKN2A*, cyclin-dependent kinase inhibitor 2A/2B/2C (p16<sup>Ink4a</sup>/p14<sup>Arf</sup>/p18<sup>Ink4c</sup>); *CDK2/4/6*, cyclin dependent kinase 2/4/6; *E2F*, transcription factor E2F; *RB1*, retinoblastoma protein 1. Cell cycle phases: G<sub>1</sub>/G<sub>2</sub>, Gap1/2 checkpoint control; S, synthesis; M, Mitosis.